

POLSKIE TOWARZYSTWO MIKROBIOLOGÓW
POLISH SOCIETY OF MICROBIOLOGISTS

Polish Journal of Microbiology

2019

CONTENTS

ORIGINAL PAPERS

Antibiotic susceptibility of <i>Cronobacter</i> spp. isolated from clinical samples HOLÝ O., ALSONOSI A., HOCHÉL I., RÖDEROVÁ M., ZATLOUKALOVÁ S., MLYNÁRČIK P., KOLÁŘ M., PETRŽELOVÁ J., ALAZRAQ A., CHMELAŘ D., FORSYTHE S.	5
Interferon gamma release assays in patients with respiratory isolates of non-tuberculous mycobacteria – a preliminary study AUGUSTYNOWICZ-KOPEĆ E., SIEMION-SZCZEŚNIAK I., ZABOST A., WYROSTKIEWICZ D., FILIPCZAK D., ONISZK K., GAWRYLUK D., RADZIKOWSKA E., KORZYBSKI D., SZTURMOWICZ M.	15
Bioactive compounds of <i>Pseudoalteromonas</i> sp. IBRL PD4.8 inhibit growth of fouling bacteria and attenuate biofilms of <i>Vibrio</i> <i>alginolyticus</i> FB3 SUPARDY N.A., IBRAHIM D., MAT NOR S.R., MD NOORDIN W.N.	21
Mycosynthesis of size-controlled silver nanoparticles through optimization of process variables by response surface methodology SHAHZAD A., IQTEDAR M., SAEED H., HUSSAIN S.Z., CHAUDHARY A., ABDULLAH R., KALEEM A.	35
Thermoregulation of prodigiosin biosynthesis by <i>Serratia marcescens</i> is controlled at the transcriptional level and requires HexS ROMANOWSKI E.G., LEHNER K.M., MARTIN N.C., PATEL K.R., CALLAGHAN J.D., STELLA N.A., SHANKS R.M.Q.	43
Clinical interpretation of detection of IgM anti- <i>Brucella</i> antibody in the absence of IgG and <i>vice versa</i> ; a diagnostic challenge for clinicians JINDAN R.A., SALEEM N., SHAFI A., AMJAD S.M.	51
<i>In vitro</i> and <i>in vivo</i> activity of zafloxacin and other fluoroquinolones against MRSA isolates from a University Hospital in Egypt MOHAMED N.M., ZAKARIA A.S., EDWARD E.A., ABDEL-BARY A.	59
Biodiversity of bacteria associated with eight <i>Pleurotus ostreatus</i> (Fr.) P. Kumm. Strains from Poland, Japan and the USA ADAMSKI M., PIETR S.J.	71
Microbiota and chemical compounds in fermented <i>Pinelliae Rhizoma</i> (Banxiaqu) from different areas in the Sichuan Province, China SHU B., YING J., WANG T., XIA M., ZHAO W., YOU L.	83
New insight into genotypic and phenotypic relatedness of <i>Staphylococcus aureus</i> strains from human infections or animal reservoirs LISOWSKA-ŁYSIAK K., KOSECKA-STROJEK M., BIAŁECKA J., KASPROWICZ A., GARBACZ K., PIECHOWICZ L., KMET V., SAVINI V., MIĘDZOBRODZKI J.	93
The influence of temperature and nitrogen source on cellulolytic potential of microbiota isolated from natural environment WITA A., BIAŁAS W., WILK R., SZYCHOWSKA K., CZACZYK K.	105
Dengue outbreaks in Khyber Pakhtunkhwa (KPK), Pakistan in 2017: an integrated disease surveillance and response system (IDSRS)-based report ABDULLAH, ALI S., SALMAN M., DIN M., KHAN K., AHMAD M., KHAN F.H., ARIF M.	115
Dependence of colonization of the large intestine by <i>Candida</i> on the treatment of crohn's disease KOWALSKA-DUPLAGA K., KRAWCZYK A., SROKA-OLEKSIK A., SALAMON D., WĘDRYCHOWICZ A., FYDEREK K., GOSIEWSKI T.	121
Predominance of <i>Lactobacillus plantarum</i> strains in Peruvian Amazonian fruits SÁNCHEZ J., VEGAS C., ZAVALETA A.I., ESTEVE-ZARZOSO B.	127

SHORT COMMUNICATIONS

Comparison of performance characteristics of DxN VERIS system versus Qiagen PCR for HBV genotype D and HCV genotype 1b quantification SAYAN M., ARIKAN A., SANLIDAG T.	139
---	-----

INSTRUCTIONS FOR AUTHORS

Instructions for authors: <http://www.pjmonline.org>



**Ministry of Science
and Higher Education**

Republic of Poland

Purchase of DOI numbers for articles and implementation
of a modern publication platform
for the Polish Journal of Microbiology are funded with the financial support
of the Ministry of Science and Higher Education
under agreement No. 659/P-DUN/2018 for science dissemination activities.

Antibiotic Susceptibility of *Cronobacter* spp. Isolated from Clinical Samples

ONDŘEJ HOLÝ^{1*}, ABDLRHMAN ALSONOSI², IGOR HOCHÉL³, MAGDALÉNA RÖDEROVÁ⁴, SIMONA ZATLOUKALOVÁ¹, PATRIK MLYNÁRČIK⁴, MILAN KOLÁŘ⁴, JANA PETRŽELOVÁ⁴, AIYDA ALAZRAQ⁵, DITTMAR CHMELAR⁶ and STEPHEN FORSYTHE⁷

¹Department of Public Health, Faculty of Medicine and Dentistry, Palacký University Olomouc, Olomouc, Czech Republic

²Microbiology Department, Faculty of Biomedical Sciences, Sabha University, Sabha, Libya

³Department of Biochemistry and Microbiology, University of Chemistry and Technology, Prague, Czech Republic

⁴Department of Microbiology, Faculty of Medicine and Dentistry, Palacký University Olomouc, Olomouc, Czech Republic

⁵Department of Pharmacology, Faculty of Pharmacy, Sabha University, Sabha, Libya

⁶Department of Biomedical Sciences, Institute of Microbiology and Immunology, Faculty of Medicine, University of Ostrava, Ostrava, Czech Republic

⁷foodmicrobe.com, Adams Hill, Keyworth, Nottinghamshire, United Kingdom

Submitted 20 August 2018, revised 22 October 2018, accepted 24 October 2018

Abstract

Cronobacter spp. have been recognized as causative agents of various severe infections in pre-term or full-term infants as well as elderly adults suffering from serious underlying disease or malignancy. A surveillance study was designed to identify antibiotic resistance among clinical *Cronobacter* spp. strains, which were isolated from patients of two hospitals between May 2007 and August 2013. Altogether, 52 *Cronobacter* spp. isolates were analyzed. Although MALDI-TOF mass spectrometry recognized all *Cronobacter sakazakii* and *Cronobacter malonaticus* strains, it could not identify *Cronobacter muytjensii* strain. Nevertheless, all strains were identified as *Cronobacter* spp. using multilocus sequence typing (MLST). Strains were tested against 17 types of antibiotics, using the standard microdilution method according to the 2018 European Committee on Antimicrobial Susceptibility Testing criteria. Three *Cronobacter* species were identified as *C. sakazakii* (n = 33), *C. malonaticus* (n = 18), and *C. muytjensii* (n = 1); all isolates were susceptible to all tested antibiotics. All strains were PCR-negative for *bla*_{TEM}, *bla*_{SHV}, and *bla*_{CTX-M} β-lactamase genes, as well. Even though the results of this study showed that *Cronobacter* spp. isolates were pan-susceptible, continued antibiotic resistance surveillance is warranted.

Key words: antibiotics, antimicrobial susceptibility, *Cronobacter* spp., MALDI-TOF mass spectrometry, multilocus sequence typing

Introduction

Cronobacter is a genus of Gram-negative, facultative-anaerobic, nonspore-forming, motile bacteria belonging to the *Enterobacteriaceae* family. At present, seven species are known: *Cronobacter sakazakii*, *C. malonaticus*, *C. dublinensis*, *C. muytjensii*, *C. turicensis*, *C. condimentii*, and *C. universalis* (Iversen et al. 2007; Iversen et al. 2008; Joseph et al. 2012; Stephan et al. 2014). Except for *C. condimentii*, all species of *Cronobacter* have been isolated from clinical specimens. The *Cronobacter* species of serious clinical significance are as follows: *C. sakazakii*,

C. malonaticus, *C. turicensis*, and *C. universalis*. Other members of the genus (*C. dublinensis*, *C. muytjensii*, and *C. condimentii*) are primarily environmental commensals with low clinical significance (Iversen et al. 2007; Kucerova et al. 2010; Holy et al. 2011; Holy et al. 2014; Holy and Forsythe 2014; Forsythe 2018). *Cronobacter* spp. are opportunistic pathogens that cause rare but life-threatening diseases such as meningitis, necrotizing enterocolitis, and bloodstream infections in neonates and infants. The infections caused by these bacteria are often severe with fatal health consequences. The lethality rate of meningitis in infants was estimated to be 41.9%

* Corresponding author: O. Holý, Department of Public Health, Faculty of Medicine and Dentistry, Palacký University Olomouc, Olomouc, Czech Republic; e-mail: holy.ondrej@seznam.cz

© 2019 Ondřej Holý et al.

This work is licensed under the Creative Commons Attribution-NonCommercial-NoDerivatives 4.0 License (<https://creativecommons.org/licenses/by-nc-nd/4.0/>)

with death occurring within hours after the manifestation of symptoms (Willis et al. 1988; Friedemann 2009; Holy and Forsythe 2014). The surviving individuals usually develop irreversible sequelae including serious neurological complications such as quadriplegia and impaired mental development (Bowen and Braden 2006). Infants up to two months of age, premature with low birth weight or immunocompromised newborns are at the highest risk for infection. *Cronobacter* spp. have also been recognized as causative agents of various infections in elderly adults suffering from serious underlying disease or malignancy (Dennison and Morris 2002; See et al. 2007).

Cronobacter spp. are naturally resistant to all macrolides, lincomycin, clindamycin, streptogramins, rifampicin, fusidic acid, and fosfomycin. Infections caused by these bacteria are usually treated with various combinations of ampicillin, gentamicin, cefotaxime, and chloramphenicol (Muytjens et al. 1983; Biering et al. 1989; Bar-Oz et al. 2001; Block et al. 2002). *Cronobacter* spp. tend to be more sensitive to most antibiotics that are being used clinically to treat infections caused by *Enterobacteriaceae*, although resistance to ampicillin has developed (Muytjens and van der Ros-van de Repe 1986). In 1980, all tested strains were susceptible to ampicillin, whereas in 2001, five cases of *Cronobacter* infection in which one or more of the isolates were resistant to ampicillin and first- and second-generation cephalosporins were described (Farmer et al. 1980; Lai 2011). Similarly, Block et al. (2002) reported that all *Cronobacter* isolates tested were β -lactamase positive. Caubilla-Barron et al. (2007) previously reported two neonatal deaths from extended-spectrum β -lactamase (ESBL)-encoding *C. sakazakii* strains in a retrospective study of the *Cronobacter* necrotizing enterocolitis and meningitis outbreak in the neonatal intensive care unit. Then, Stock and Weidemann (2002) studied some *Cronobacter* strains and found that all strains were susceptible to the tested β -lactams.

The β -lactamase activity in *Cronobacter* has been frequently reported by others (Pitout et al. 1997; Caubilla-Barron et al. 2007; Baldwin et al. 2009). In 1997, a low-level β -lactamase production in *Cronobacter* was detected by Pitout et al. (1997). In addition, Lai (2001) also reported that *Cronobacter* strains were resistant to ampicillin, cefazolin, and extended-spectrum penicillin. Moreover, a recent study showed that about 10.2% of the *Cronobacter* strains were resistant to cefotaxime, which is one of the third-generation cephalosporins related to penicillin (Pan et al. 2014). Rising antimicrobial resistance is generally a public health concern, potentially leading to prolonged illness and a higher risk of mortality.

The aim of this study was to examine over time the changes in antibiotic resistance of different *Crono-*

bacter spp. strains and to determine the susceptibility of *Cronobacter* isolates from clinical samples to 17 types of antibiotics.

Experimental

Materials and Methods

Bacterial strains and cultivation. The 52 isolates were collected during a survey of *Cronobacter* spp. carriage in patients of two hospitals over the 6-year period from May 2007 to August 2013. All strains were isolated from clinical samples (Table I). Microorganisms were routinely cultivated on blood agar (Oxoid, UK) at temperature of 37°C overnight.

Identification of *Cronobacter* spp. by MALDI-TOF MS. *Sample preparation.* For the protein extraction three colonies of each microorganism grown overnight on blood agar plates at 37°C under aerobic conditions were picked and resuspended in 300 μ l of water (Sigma-Aldrich, USA) in 1.5 ml tube (Eppendorf, Germany). Then, 900 μ l of absolute ethanol were added and mixed. The tubes were centrifuged twice at 13 000 rpm for 2 min and the supernatant was removed. The pellet was kept for 15 min at room temperature. The pellet was then dissolved in 50 μ l of 70% formic acid. Finally, an equal volume of acetonitrile was added to the mixture and the mixture was stirred and centrifuged at 13 000 rpm for 2 min. The mixture was then vortexed for 15 seconds. After this, 1 μ l of the supernatant was spotted eight times onto a MALDI target, followed by the addition of 1 μ l of HCCA (alpha-cyano-4-hydroxy-cinnamic acid made as saturated solution in 30% acetonitrile/0.1% trifluoroacetic acid) and allowed to dry at room temperature before MALDI-TOF MS analysis. Immediately after drying, the spot was overlaid with 1 μ l of matrix (Schulthess et al. 2016). MALDI-TOF MS measurements were performed with a microflex LT (Bruker Daltonics, Bremen, Germany). Each spot was analysed in triplicate (24 spectra in total). Each generated spectrum resulted from 240 laser shots (40 laser shots at six multiple positions on the target spot). All investigations were performed in triplicate.

Data analysis. The resulting 72 spectra were carefully analysed using the Flex Analysis (version 3.0, Bruker Daltonics, Germany) and subjected to smoothing and baseline subtraction. Furthermore, at least 24 spectra of each strain were used to create a single standard mass spectrum (MSP) with the default setting of the BioTyper MSP creation method. To visualize the difference between the strains, MSP dendrogram clustering was constructed using the standard settings in MALDI BioTyper™ software.

Table I
Identification and genotyping of *Cronobacter* spp. isolated from clinical samples.

Strain	Strain No.	Log (score)*	Sequence type	Origin
<i>C. sakazakii</i>	1836	2.354	4	Wound swab
<i>C. sakazakii</i>	1837	2.432	4	Wound swab
<i>C. sakazakii</i>	1839	2.503	4	Smear from area of percutaneous endoscopic gastrostomy
<i>C. sakazakii</i>	1840	2.452	4	Sputum
<i>C. sakazakii</i>	1841	2.444	4	Sputum
<i>C. sakazakii</i>	1842	2.409	4	Sputum
<i>C. sakazakii</i>	1901	2.467	4	Sputum
<i>C. sakazakii</i>	1902	2.421	4	Sputum
<i>C. sakazakii</i>	1903	2.487	4	Sputum
<i>C. sakazakii</i>	1915	2.509	4	Sputum
<i>C. sakazakii</i>	1916	2.464	4	Sputum
<i>C. sakazakii</i>	1996	2.484	4	Sputum
<i>C. sakazakii</i>	1997	2.505	4	Sputum
<i>C. sakazakii</i>	1998	2.485	4	Sputum
<i>C. sakazakii</i>	2000	2.479	4	Rectal swab
<i>C. sakazakii</i>	2001	2.473	4	Swab of the oral cavity
<i>C. sakazakii</i>	2002	2.476	4	Sputum
<i>C. sakazakii</i>	2003	2.423	4	Sputum
<i>C. sakazakii</i>	2005	2.457	4	Sputum
<i>C. sakazakii</i>	2006	2.357	4	Sputum
<i>C. sakazakii</i>	2007	2.438	4	Sputum
<i>C. sakazakii</i>	2008	2.416	4	Sputum
<i>C. sakazakii</i>	2009	2.459	4	Tongue swab
<i>C. sakazakii</i>	2010	2.388	4	Throat swab
<i>C. sakazakii</i>	2011	2.417	4	Suction catheter
<i>C. sakazakii</i>	2012	2.494	4	Sputum
<i>C. sakazakii</i>	2013	2.451	4	Sputum
<i>C. sakazakii</i>	2021	2.446	4	Sputum
<i>C. sakazakii</i>	2016	2.448	4	Sputum
<i>C. sakazakii</i>	2017	2.510	4	Sputum
<i>C. sakazakii</i>	2019	2.367	4	Sputum
<i>C. sakazakii</i>	2022	2.426	4	Sputum
<i>C. sakazakii</i>	1995	2.508	64	Sputum
<i>C. malonaticus</i>	1826	2.313	7	Cannula
<i>C. malonaticus</i>	1827	2.293	7	Cannula
<i>C. malonaticus</i>	1828	2.419	7	Nose swab
<i>C. malonaticus</i>	1829	2.329	7	Throat swab
<i>C. malonaticus</i>	1830	2.429	7	Throat swab
<i>C. malonaticus</i>	1831	2.415	7	Throat swab
<i>C. malonaticus</i>	1832	2.373	7	Throat swab
<i>C. malonaticus</i>	1833	2.398	7	Stool - dissection
<i>C. malonaticus</i>	1834	2.345	7	Throat swab
<i>C. malonaticus</i>	1835	2.336	7	Throat swab
<i>C. malonaticus</i>	1914	2.426	7	Sputum
<i>C. malonaticus</i>	1917	2.387	7	Throat swab
<i>C. malonaticus</i>	1999	2.361	7	Throat swab
<i>C. malonaticus</i>	2004	2.343	7	Throat swab

Table I. Continued.

Strain	Strain No.	Log (score)*	Sequence type	Origin
<i>C. malonaticus</i>	2014	2.388	7	Throat swab
<i>C. malonaticus</i>	2015	2.353	7	Throat swab
<i>C. malonaticus</i>	2018	2.339	7	Sputum
<i>C. malonaticus</i>	2020	2.173	7	Stool
<i>P. agglomerans</i> / <i>C. muytjensii</i>	1838	2.358	28	Sputum

* Log (score) according to MALDI-TOF identification. According to the MALDI-TOF MS strain No. 1838 was identified as *P. agglomerans*.

This strain was subsequently reclassified as *C. muytjensii* according to results of the MLST

The linkage function was normalised according to the distance between 0 (perfect match) and 1 000 (no match). Species with distance levels under 500 have been described as reliably classified species (Sauer et al. 2008).

Following the creation of MSPs of strains, each MSP was identified. All spectra were imported into the Biotyper software and analyzed against the Bruker library. Identification scores of ≥ 2.0 have been declared by manufacturer as a reliable identification to the species level and scores of ≥ 1.7 but < 2.0 to the genus level if the conditions of species and genus consistency are fulfilled, respectively. Isolates with log-score above 2.3 were used for dendrogram generation if the best three matches indicated the same species.

Multilocus sequence typing (MLST). The MLST scheme for the strains investigated was performed previously by Alsonosi et al. (2015) and published in the curated *Cronobacter* PubMLST open access database (<http://www.pubmlst.org/cronobacter>). The seven housekeeping genes *atpD* (ATP synthase beta chain), *fusA* (elongation factor G), *glnS* (glutamyl-tRNA synthetase), *gltB* (glutamate synthase large subunit), *gyrB* (gyrase subunit B), *infB* (translation initiation factor IF-2), and *ppsA* (phosphoenolpyruvate synthase) were sequenced. The results obtained were compared with data at the *Cronobacter* PubMLST database.

Antimicrobial susceptibility testing. All *Cronobacter* strains were tested for susceptibility against 17 types of antibiotics, that were: ampicillin, aztreonam, ampicillin/sulbactam, gentamicin, piperacillin, tobramycin, piperacillin/tazobactam, amikacin, cefuroxime, ciprofloxacin, cefotaxime, tigecycline, ceftazidime, colistin, cefepime, trimethoprim/sulfamethoxazole, and meropenem. The susceptibility to antibiotics was assessed by a standard microdilution method according to the European Committee on Antimicrobial Susceptibility Testing criteria 2018 (EUCAST 2018).

Detection of *blaTEM*, *blaSHV*, and *blaCTX-M* genes. The detection of *blaTEM*, *blaSHV*, and *blaCTX-M* genes (encoding TEM, SHV, and CTX-M types of β -lactamases) was performed by PCR in all *Cronobac-*

ter spp. isolates examined. As positive controls, the following strains were used: *Escherichia coli* NCTC 13400 (*blaCTX-M*₋₁₅), *E. coli* NCTC 13351 (*blaTEM*₋₃) and *Klebsiella pneumoniae* NCTC 13368 (*blaSHV*₋₁₈). Total bacterial DNA was isolated from an overnight culture of the isolates (16 h, 37°C) grown on meat-peptone agar. Two colonies were suspended in 100 μ l of water and heated at 95°C for 10 min. After removing of cellular debris by centrifugation at 13 000 \times g for 2 min, the supernatant was used as a template DNA for amplification. Polymerase chain reaction with a specific set of primers was performed for the detection of genes that encode relevant beta-lactamases (Arlet et al. 1995; Chanawong et al. 2000; Pagani et al. 2003).

Results

Identification and typing of *Cronobacter* isolates.

Bacterial strains were identified by the MALDI-TOF mass spectrometry and genotyped by MLST. The protein spectra of 52 isolates were compared with those included in MALDI BioTyper™ reference database. The matching of an unknown spectrum with that in reference database was quantified by the log-score. The protein spectra of 52 isolates were obtained from three independent assays. The logarithms of score values ≥ 2 were required for reliable identification of the unknown strains at the species level. The average values of the log-score fall within limits of 2.173 to 2.510 (Table I). The most prevalent species recovered from clinical samples were *C. sakazakii* (n = 33; 63.5%) and *C. malonaticus* (n = 18; 34.6%). Only one strain was identified as *Pantoea agglomerans* (1.9%) – the strain No. 1838. However, this strain was subsequently reclassified as *C. muytjensii* according to results of the MLST.

As we previously published, based on the MLST results for clinical strains, the intra-species diversity was poor. A majority of *C. sakazakii* strains (n = 32) belonged to the dominant sequence type 4, whereas only one *C. sakazakii* strain isolated from sputum was

determined as ST64. All *C. malonaticus* isolates were classified as ST7. Only *C. muytjensii* was assigned to ST28 (Alsonosi et al. 2015).

Antibiotic susceptibility. Antibiotic resistance profiling revealed that all 52 isolates were sensitive to ampicillin, aztreonam, ampicillin/sulbactam, gentamicin, piperacillin, tobramycin, piperacillin/tazobactam, amikacin, cefuroxime, ciprofloxacin, cefotaxime, tigecycline, ceftazidime, colistin, cefepime, trimethoprim/sulfamethoxazole, and meropenem. No resistant strains were found. The minimal inhibitory concentrations of the antimicrobial mentioned above were given in Table II. The *bla*_{TEM}, *bla*_{SHV}, and *bla*_{CTX-M} β -lactamase genes in the genome of our isolates were not found in any *Cronobacter* species, as well.

Discussion

The *Enterobacteriaceae* family are often associated with hospital-acquired infections. The most vulnerable population consists of immunocompromised patients (Holy et al. 2012; Matouskova et al. 2012; Matouskova and Holy 2013; Matouskova and Holy 2014). Antimicrobial resistance is a public health concern because it may cause failure of conventional treatment, resulting in prolonged illness and a higher risk of mortality. Resistance among human pathogens of *Enterobacteriaceae* has direct clinical impact on patients due to longer treatment and hospitalization, need for more expensive drugs, and often fatal consequences. Thus, infections due to resistant *Klebsiella* spp., *E. coli*, and *Enterobacter* spp. are now known as a major problem associated with health-care associated infections. The *Cronobacter* genus has undergone an extensive diversification during the course of its evolution, with some species clearly pathogenic for humans and other species still with unknown or uncertain impact on human health. Unfortunately, information on the diversity, pathogenicity, and virulence of *Cronobacter* species obtained from various sources is still relatively scarce and fragmentary. Applying the MLST scheme on clinical *C. sakazakii* strains revealed that the strains associated with meningitis, bacteremia, undefined infection, or necrotizing enterocolitis in neonates, infants, and children belong to the predominant sequence type profile 4 (Joseph and Forsythe 2011; Hariri et al. 2013). Virulence-related traits have also been found through draft and complete genome sequencing of *Cronobacter* spp. (Bar-Oz et al. 2001; Stephan et al. 2014). In some studies, up to 50% of *Cronobacter* spp. infection in adults had underlying malignancy (Lai 2001).

Two distinct identification systems, MALDI-TOF mass spectrometry and MLST, were compared in this study. MALDI-TOF MS protein profiling, based on

the protein spectra obtained from intact whole cells, cell lysates, or bacterial extracts, is now widely used as an instrumental technique for bacterial identification. The main advantage of this analytical method, compared with other typing procedures, is its rapidity, low-cost requirements, and ease of use. Although the method usually provides the reliable discrimination of the common human pathogens (Barbuddhe et al. 2008; Mellmann et al. 2008; Davies et al. 2012; Kuhns et al. 2012), the correct identification of unknown protein profiles depends on the size and precision of the default database. In our case, the majority of isolates was reliably discriminated at the species level in congruence with results obtained via MLST. Only isolate 1838 was misidentified as *Pantoea agglomerans* by MALDI-TOF MS. Further analysis by MLST resulted in a re-classification of this microorganism as *C. muytjensii*, sequencing type 28 (Table I). An application of at least two independent identification methods is therefore recommended to minimize the number of misidentified strains.

Multilocus sequence typing divided 52 clinical strains into three species and five sequencing types (Alsonosi et al. 2015, Table I). Nearly all of the 33 *C. sakazakii* were typed as neonatal ST4, and only one was classified as a neonatal ST64. The 18 *C. malonaticus* strains belonged to ST7, which is usually isolated and causes serious infections in neonates or adults. The spectrum of *Cronobacter* spp. and types is quite similar to those reported in previous studies (Joseph and Forsythe 2011; Kadlicekova et al. 2018). Poor species and intra-species diversity of the strains obtained from the clinical samples indicates that mucosa of human beings may be colonized by only limited *Cronobacter* sequence types.

Antimicrobial susceptibility was performed against 17 antibacterial agents. It is known that the extensive use of antimicrobials in agriculture and health-care facilities has led to the emergence of resistant bacterial strains. Nonetheless, the present study has shown that all used clinical strains of *Cronobacter* were susceptible to 17 antimicrobial agents, which represent a broad spectrum of typical antibiotics for enterobacteria. Similarly to these study findings, other studies have reported the susceptibility of *Cronobacter* strains to all antibiotics that were used in these studies (Terragno et al. 2009; Hochel et al. 2012; Vojkovska et al. 2016; Brandão et al. 2017). In these studies, all *Cronobacter* strains were isolated from food sources or powdered infant formula and mainly *C. sakazakii* was investigated. Therefore, our study is a unique one since it shows a susceptibility of clinical isolates of both species *C. sakazakii* and *C. malonaticus*. These two species have been found to be associated with several serious neonatal and adult infections (See et al. 2007; Healy et al. 2010; Asato et al. 2013; Hariri et al. 2013; Brandão et al. 2017; Alsonosi

Table II
Minimum inhibitory concentration (MIC) of *Cronobacter* spp. isolated from clinical samples.

Strain	Strain No.	Minimum inhibitory concentration – MIC (mg · l ⁻¹)																
		AMP	AMS	PIP	PPT	CRX	CTX	CTZ	CPM	MER	AZT	GEN	TOB	AMI	CIP	TIG	COL	COT
<i>C. sakazakii</i>	1836	1	2	1	1	4	0.1	0.1	0.1	0.1	0.2	0.2	0.2	1	0.03	0.06	0.5	1
<i>C. sakazakii</i>	1837	0.5	0.5	1	1	1	0.1	0.1	0.1	0.1	0.2	0.2	0.5	2	0.1	0.06	0.5	1
<i>C. sakazakii</i>	1839	1	1	1	1	2	0.1	0.1	0.1	0.2	0.2	0.2	0.2	1	0.03	0.06	0.5	1
<i>C. sakazakii</i>	1840	1	1	1	1	4	0.1	0.1	0.1	0.2	0.2	0.2	0.2	1	0.03	0.06	1	1
<i>C. sakazakii</i>	1841	1	2	1	1	2	0.1	0.1	0.1	0.2	0.2	0.2	0.2	1	0.03	0.06	0.5	1
<i>C. sakazakii</i>	1842	1	2	1	1	4	0.1	0.1	0.1	0.2	0.2	0.2	0.2	1	0.03	0.06	0.5	1
<i>C. sakazakii</i>	1901	0.5	0.5	2	1	1	0.1	0.1	0.2	0.1	0.2	0.2	0.5	0.5	0.1	0.2	0.5	1
<i>C. sakazakii</i>	1902	0.5	0.5	2	1	1	0.1	0.1	0.2	0.1	0.2	0.2	0.5	0.5	0.1	0.1	0.5	1
<i>C. sakazakii</i>	1903	1	0.5	2	1	2	0.1	0.1	0.2	0.1	0.2	0.2	0.5	0.5	0.1	0.1	0.5	2
<i>C. sakazakii</i>	1915	0.5	0.5	2	1	0.5	0.1	0.1	0.2	0.1	0.2	0.2	0.5	0.5	0.1	0.1	0.5	1
<i>C. sakazakii</i>	1916	8	2	8	4	4	0.1	0.5	0.1	0.2	0.2	0.2	0.5	1	0.1	0.1	0.5	1
<i>C. sakazakii</i>	1996	4	1	4	1	1	0.1	0.1	0.1	0.5	0.2	0.2	0.5	2	0.06	0.2	0.5	1
<i>C. sakazakii</i>	1997	1	0.5	2	1	1	0.1	0.1	0.2	0.1	0.2	0.2	0.5	0.5	0.1	0.06	0.5	1
<i>C. sakazakii</i>	1998	0.5	0.5	2	1	1	0.1	0.1	0.2	0.1	0.2	0.2	0.5	0.5	0.1	0.1	0.5	1
<i>C. sakazakii</i>	2000	1	1	1	1	1	0.1	0.1	0.1	0.1	0.2	0.2	0.5	2	0.2	0.06	0.5	0.2
<i>C. sakazakii</i>	2001	2	1	2	1	4	0.1	0.1	0.1	0.5	0.1	1	0.2	1	0.06	0.03	0.1	0.2
<i>C. sakazakii</i>	2002	1	1	1	1	0.5	0.1	0.1	0.1	0.1	0.2	0.2	0.5	2	0.2	0.06	0.5	0.2
<i>C. sakazakii</i>	2003	2	1	2	1	4	0.1	0.1	0.1	0.5	0.1	1	0.2	2	0.06	0.06	0.1	0.2
<i>C. sakazakii</i>	2005	2	1	2	1	4	0.1	0.1	0.1	0.5	0.1	1	0.2	1	0.06	0.03	0.1	0.2
<i>C. sakazakii</i>	2006	2	0.5	2	1	4	0.1	0.1	0.1	0.5	0.1	1	0.5	1	0.06	0.03	0.1	0.2
<i>C. sakazakii</i>	2007	2	1	2	1	4	0.1	0.1	0.1	0.5	0.1	1	0.2	1	0.06	0.03	0.1	0.5
<i>C. sakazakii</i>	2008	2	1	2	1	4	0.1	0.1	0.1	0.5	0.1	1	0.5	1	0.06	0.03	0.1	0.2
<i>C. sakazakii</i>	2009	0.5	0.5	2	1	1	0.1	0.1	0.2	0.1	0.2	0.2	0.5	0.5	0.1	0.1	0.5	0.2
<i>C. sakazakii</i>	2010	2	1	2	1	2	0.1	0.2	0.1	0.5	0.2	0.5	0.5	1	0.1	0.06	1	2
<i>C. sakazakii</i>	2011	2	1	2	1	2	0.1	0.2	0.1	0.5	0.2	0.5	0.5	1	0.1	0.06	0.2	2
<i>C. sakazakii</i>	2012	1	0.5	2	1	1	0.1	0.2	0.1	0.5	0.2	0.5	0.5	1	0.1	0.06	0.2	2
<i>C. sakazakii</i>	2013	1	1	2	1	2	0.1	0.2	0.1	0.5	0.2	0.5	0.5	1	0.1	0.06	0.5	2
<i>C. sakazakii</i>	2021	2	1	2	1	2	0.1	0.2	0.1	0.5	0.2	0.5	0.5	1	0.1	0.06	1	2
<i>C. sakazakii</i>	2016	2	1	2	1	1	0.1	0.2	0.1	0.5	0.2	0.5	0.5	1	0.1	0.06	0.5	2
<i>C. sakazakii</i>	2017	2	1	2	1	2	0.1	0.2	0.1	0.5	0.2	0.5	0.5	1	0.1	0.06	1	2

Table II. Continued.

Strain	Strain No.	Minimum inhibitory concentration – MIC (mg · l ⁻¹)																
		AMP	AMS	PIP	PPT	CRX	CTX	CTZ	CPM	MER	AZT	GEN	TOB	AMI	CIP	TIG	COL	COT
<i>C. sakazakii</i>	2019	2	1	2	1	2	0.1	0.2	0.1	0.5	0.2	0.5	0.5	1	0.1	0.06	1	2
<i>C. sakazakii</i>	2022	2	1	2	1	4	0.1	0.1	0.1	0.5	0.1	1	0.2	1	0.06	0.03	0.1	0.5
<i>C. sakazakii</i>	1995	4	2	2	1	4	0.1	0.1	0.1	0.5	0.2	0.2	0.5	1	0.06	0.2	1	1
<i>C. malonaticus</i>	1826	0.5	1	1	1	2	0.1	0.1	0.1	0.2	0.2	0.2	0.2	1	0.03	0.06	1	1
<i>C. malonaticus</i>	1827	0.5	1	1	1	2	0.1	0.1	0.1	0.2	0.2	0.2	0.2	1	0.03	0.06	1	1
<i>C. malonaticus</i>	1828	0.5	1	1	1	1	0.1	0.1	0.1	0.2	0.2	0.2	0.2	0.5	0.03	0.06	1	1
<i>C. malonaticus</i>	1829	0.5	1	1	1	2	0.1	0.1	0.1	0.2	0.2	0.2	0.2	1	0.03	0.06	1	1
<i>C. malonaticus</i>	1830	1	2	1	1	2	0.1	0.1	0.1	0.2	0.2	0.2	0.2	1	0.03	0.06	1	1
<i>C. malonaticus</i>	1831	1	1	1	1	2	0.1	0.1	0.1	0.2	0.2	0.2	0.2	1	0.03	0.06	0.1	1
<i>C. malonaticus</i>	1832	0.5	1	1	1	2	0.1	0.1	0.1	0.2	0.2	0.2	0.2	1	0.03	0.06	1	1
<i>C. malonaticus</i>	1833	0.5	1	1	1	2	0.1	0.1	0.1	0.2	0.2	0.2	0.2	1	0.03	0.06	1	1
<i>C. malonaticus</i>	1834	0.5	1	1	1	1	0.1	0.1	0.1	0.2	0.2	0.2	0.2	1	0.03	0.06	1	1
<i>C. malonaticus</i>	1835	0.2	1	1	1	1	0.1	0.1	0.2	0.2	0.2	0.2	0.2	1	0.03	0.06	1	1
<i>C. malonaticus</i>	1914	2	2	1	1	4	0.1	0.1	0.1	0.5	0.1	0.2	0.5	1	0.06	0.5	0.2	1
<i>C. malonaticus</i>	1917	1	1	1	1	1	0.1	0.1	0.1	0.5	0.1	0.2	0.2	0.5	0.06	0.2	0.2	1
<i>C. malonaticus</i>	1999	1	0.5	2	1	1	0.1	0.1	0.1	0.5	0.2	0.2	0.2	1	0.06	0.2	1	1
<i>C. malonaticus</i>	2004	0.5	0.5	2	1	1	0.1	0.1	0.1	0.1	0.2	0.2	0.5	0.5	0.1	0.1	0.5	0.2
<i>C. malonaticus</i>	2014	1	0.5	2	0.5	2	0.1	0.1	0.1	0.2	0.2	0.2	0.2	1	0.06	0.2	2	2
<i>C. malonaticus</i>	2015	1	0.5	2	1	1	0.1	0.2	0.1	0.5	0.2	0.5	0.5	1	0.1	0.06	1	2
<i>C. malonaticus</i>	2018	1	1	2	1	2	0.1	0.2	0.1	0.5	0.2	0.5	0.5	1	0.1	0.06	1	2
<i>C. malonaticus</i>	2020	1	0.5	2	1	0.5	0.1	0.2	0.1	0.5	0.2	0.5	0.5	1	0.1	0.06	1	2
<i>P. agglomerans</i> / <i>C. mytjensii</i>	1838	1	2	1	1	1	0.1	0.1	0.1	0.2	0.2	0.2	0.2	1	0.03	0.06	0.2	1

AMP – ampicillin; AZT – aztreonam; AMS – ampicillin/sulbactam; GEN – gentamicin; PIP – piperacillin; TOB – tobramycin; PPT – piperacillin/tazobactam; AMI – amikacin; CRX – cefuroxime; CIP – ciprofloxacin; CTX cefotaxime; TIG – tigecycline; CTZ – tigecycline; COL – colistin; CPM – ceftazidime; COL – colistin; CPM – ceftazidime; COT – trimethoprim/sulfamethoxazole; MER – meropenem
MIC (Minimum inhibitory concentration) – the lowest concentration of the antibiotics that can inhibit effectively growth of the tested microorganism

et al. 2018). As a part of the present study, β -lactamase genes, *bla*_{TEM}, *bla*_{SHV} and *bla*_{CTX-M} were screened among *Cronobacter* isolates. The results were consistent with the results of susceptibility assays, as all strains were negative for β -lactamase genes. However, other studies have shown emergence of resistance to penicillin and extended-spectrum β -lactamases (Block et al. 2002; Caubilla-Barron et al. 2007). Recently, two studies have shown that multi-drug resistance in *Cronobacter* is emerging through horizontal gene transfer mechanisms (Cui et al. 2015; Shi et al. 2016). In addition, the excessive use of antibiotics in the hospital environment facilitates the possibility of emerging of a high level of antimicrobial resistance among clinical strains. Therefore, the surveillance studies would assist in prevention of the developing this phenomenon and in keeping *Cronobacter* susceptible to the majority of the available clinical antimicrobial agents.

Conclusions

A low level of antibiotic resistance among *Cronobacter* spp. in our region is due to a good antibiotic usage policy. The minimizing of the occurrence of encephalitis, necrotizing enterocolitis, and septicemia among infants in the Czech Republic caused by *Cronobacter* spp. is also due to the excellent hospital care. We were able to isolate only 52 strains during the 6-year period of our study, and the majority of them were isolated from adults.

This study shows that although antimicrobial resistance among *Cronobacter* spp. is not a big issue nowadays, many resistant cases among *Cronobacter* spp. have been reported worldwide. Increasing antimicrobial resistance is not only a clinical problem associated with health-care facilities, but it is also a big public health issue. Selection pressure plays a crucial role in their spreading not only in health care facilities but also in the environment (e.g., food chains and waste waters).

The authors are aware of the limitations associated with this study, especially of the low number of samples. On the other hand, the advantage is that these samples were collected over quite a long period of time.

No official breakpoints by EUCAST were established for *Cronobacter* spp., only for *Enterobacteriaceae* in general, which is not sufficient. The epidemiological cut-off value (ECOFF) for *Cronobacter* spp. should be established in the near future.

Author's contributions

OH, AA, IH, MK, AA, SF participated in the study design, coordination and carried out data analyses. MR, SZ, PM, JP, DC participated and performed measurements, laboratory testing's and data collection. All authors read and approved the final manuscript.

All authors contributed to the draft of the manuscript and discussed results. All authors gave final approval for publication.

Acknowledgements

This work was supported by Research Support Foundation, Vaduz (991100531/39), IGA_LF_2016_022 and IGA_LF_2016_025.

Conflict of interest

Author does not report any financial or personal connections with other persons or organizations, which might negatively affect the contents of this publication and/or claim authorship rights to this publication.

Literature

- Alsonosi A, Hariri S, Kajsík M, Orišková M, Hanulík V, Röderová M, Petrželová J, Kollárová H, Drahovská H, Forsythe S, et al.** The speciation and genotyping of *Cronobacter* isolates from hospitalised patients. *Eur J Clin Microbiol Infect Dis*. 2015;34(10):1979–1988. doi:10.1007/s10096-015-2440-8 [Medline](#)
- Alsonosi AM, Holy O, Forsythe SJ.** Characterization of the pathogenicity of clinical *Cronobacter malonaticus* strains based on the tissue culture investigations. *Antonie van Leeuwenhoek*. 2018. doi:10.1007/s10482-018-1178-6 [Medline](#)
- Arlet G, Bami G, Décrè D, Flippo A, Gaillot O, Lagrange PH, Philippon A.** Molecular characterisation by PCR-restriction fragment length polymorphism of TEM beta-lactamases. *FEMS Microbiol Lett*. 1995;134(2–3):203–208. [Medline](#)
- Asato VC, Vilches VE, Pineda MG, Casanueva E, Cane A, Moroni MP, Brengi SP, Pichel MG.** First clinical isolates of *Cronobacter* spp. (*Enterobacter sakazakii*) in Argentina: characterization and subtyping by pulsed-field gel electrophoresis. *Rev Argent Microbiol*. 2013;45(3):160–164. doi:10.1016/S0325-7541(13)70018-X [Medline](#)
- Baldwin A, Loughlin M, Caubilla-Barron J, Kucerova E, Manning G, Dowson C, Forsythe S.** Multilocus sequence typing of *Cronobacter sakazakii* and *Cronobacter malonaticus* reveals stable clonal structures with clinical significance which do not correlate with biotypes. *BMC Microbiol*. 2009;9(1):223. doi:10.1186/1471-2180-9-223 [Medline](#)
- Barbuddhe SB, Maier T, Schwarz G, Kostrzewa M, Hof H, Domann E, Chakraborty T, Hain T.** Rapid identification and typing of *Listeria* species by matrix-assisted laser desorption ionization-time of flight mass spectrometry. *Appl Environ Microbiol*. 2008;74(17):5402–5407. doi:10.1128/AEM.02689-07 [Medline](#)
- Bar-Oz B, Preminger A, Peleg O, Block C, Arad I.** *Enterobacter sakazakii* infection in the newborn. *Acta Paediatr*. 2001; 90(3): 356–358. doi:10.1111/j.1651-2227.2001.tb00319.x [Medline](#)
- Biering G, Karlsson S, Clark NC, Jónsdóttir KE, Lúdvígsson P, Steingrímsson O.** Three cases of neonatal meningitis caused by *Enterobacter sakazakii* in powdered milk. *J Clin Microbiol*. 1989; 27(9):2054–2056. [Medline](#)
- Block C, Peleg O, Minster N, Bar-Oz B, Simhon A, Arad I, Shapiro M.** Cluster of neonatal infections in Jerusalem due to unusual biochemical variant of *Enterobacter sakazakii*. *Eur J Clin Microbiol Infect Dis*. 2002;21(8):613–616. doi:10.1007/s10096-002-0774-5 [Medline](#)
- Bowen AB, Braden CR.** Invasive *Enterobacter sakazakii* disease in infants. *Emerg Infect Dis*. 2006;12(8):1185–1189. doi:10.3201/eid1208.051509 [Medline](#)
- Brandão MLL, Umeda NS, Jackson E, Forsythe SJ, de Filippis I.** Isolation, molecular and phenotypic characterization, and antibiotic susceptibility of *Cronobacter* spp. from Brazilian retail foods. *Food Microbiol*. 2017;63:129–138. doi:10.1016/j.fm.2016.11.011 [Medline](#)

- Caubilla-Barron J, Hurrell E, Townsend S, Cheetham P, Loc-Carillo C, Fayet O, Prère MF, Forsythe SJ.** Genotypic and phenotypic analysis of *Enterobacter sakazakii* strains from an outbreak resulting in fatalities in a neonatal intensive care unit in France. *J Clin Microbiol.* 2007;45(12):3979–3985. doi:10.1128/JCM.01075-07 Medline
- Chanawong A, M'Zali FH, Heritage J, Lulitanond A, Hawkey PM.** Characterisation of extended-spectrum beta-lactamases of the SHV family using a combination of PCR-single strand conformational polymorphism (PCR-SSCP) and PCR-restriction fragment length polymorphism (PCR-RFLP). *FEMS Microbiol Lett.* 2000;184(1): 85–89. Medline
- Cui JH, Du XL, Wei RJ, Zhou HJ, Li W, Forsythe S, Cui ZG.** Multi-locus sequence typing analysis of *Cronobacter* spp. isolated from China. *Arch Microbiol.* 2015;197(5):665–672. doi:10.1007/s00203-015-1097-0 Medline
- Davies AP, Reid M, Hadfield SJ, Johnston S, Mikhail J, Harris LG, Jenkinson HF, Berry N, Lewis AM, El-Bouri K, et al.** Identification of clinical isolates of α -hemolytic streptococci by 16S rRNA gene sequencing, matrix-assisted laser desorption ionization-time of flight mass spectrometry using MALDI Biotyper, and conventional phenotypic methods: a comparison. *J Clin Microbiol.* 2012;50(12): 4087–4090. doi:10.1128/JCM.02387-12 Medline
- Dennison SK, Morris J.** Multiresistant *Enterobacter sakazakii* wound infection in an adult. *Infect Med.* 2002;19(11):533–535.
- EUCAST.** Breakpoint tables for interpretation of MICs and zone diameters. Version 8.0. The European Committee on Antimicrobial Susceptibility Testing. 2018.
- Farmer JJ 3rd, Asbury MA, Hickman FW, Brenner DJ.** The *Enterobacteriaceae* Study Group. *Enterobacter sakazakii*: a new species of “*Enterobacteriaceae*” isolated from clinical specimens. *Int J Syst Bacteriol.* 1980;30(3):569–584. doi:10.1099/00207713-30-3-569
- Forsythe SJ.** Updates on the *Cronobacter* Genus. *Annu Rev Food Sci Technol.* 2018;9(1):23–44. doi:10.1146/annurev-food-030117-012246 Medline
- Friedemann M.** Epidemiology of invasive neonatal *Cronobacter* (*Enterobacter sakazakii*) infections. *Eur J Clin Microbiol Infect Dis.* 2009;28(11):1297–1304. doi:10.1007/s10096-009-0779-4 Medline
- Hariri S, Joseph S, Forsythe SJ.** *Cronobacter sakazakii* ST4 strains and neonatal meningitis, United States. *Emerg Infect Dis.* 2013; 19(1):175–177. doi:10.3201/eid1901.120649 Medline
- Healy B, Cooney S, O'Brien S, Iversen C, Whyte P, Nally J, Callanan JJ, Fanning S.** *Cronobacter* (*Enterobacter sakazakii*): an opportunistic foodborne pathogen. *Foodborne Pathog Dis.* 2010;7(4): 339–350. doi:10.1089/fpd.2009.0379 Medline
- Hochel I, Růžičková H, Krásný L, Demnerová K.** Occurrence of *Cronobacter* spp. in retail foods. *J Appl Microbiol.* 2012;112(6): 1257–1265. doi:10.1111/j.1365-2672.2012.05292.x Medline
- Holý O, Forsythe S.** *Cronobacter* spp. as emerging causes of healthcare-associated infection. *J Hosp Infect.* 2014;86(3):169–177. doi:10.1016/j.jhin.2013.09.011 Medline
- Holý O, Matoušková I, Holý V, Koukalová D, Chmelar D.** Isolation of *Cronobacter* spp. (formerly *Enterobacter sakazakii*) from nostrils of healthy stable horse – short communication. *Epidemiol Mikrobiol Imunol.* 2011;60(4):167–169. Medline
- Holý O, Matoušková I, Raida L.** [The incidence of gram-negative bacteria in the environment of the Transplant Unit, Department of Hemato-oncology, University Hospital - Olomouc]. (in Czech). *Epidemiol Mikrobiol Imunol.* 2012;61(4):103–109. Medline
- Holý O, Petrželová J, Hanulík V, Chromá M, Matoušková I, Forsythe SJ.** Epidemiology of *Cronobacter* spp. isolates from patients admitted to the Olomouc University Hospital (Czech Republic). *Epidemiol Mikrobiol Imunol.* 2014;63(1):69–72. Medline
- Iversen C, Lehner A, Mullane N, Bidlas E, Cleenwerck I, Marugg J, Fanning S, Stephan R, Joosten H.** The taxonomy of *Enterobacter sakazakii*: proposal of a new genus *Cronobacter* gen. nov. and descriptions of *Cronobacter sakazakii* comb. nov., *Cronobacter sakazakii* subsp. *sakazakii*, comb. nov., *Cronobacter sakazakii* subsp. *malonaticus* subsp. nov., *Cronobacter turicensis* sp. nov., *Cronobacter myuvtjensii* sp. nov., *Cronobacter dublinensis* sp. nov. and *Cronobacter* genomospecies 1. *BMC Evol Biol.* 2007;7(1):64. doi:10.1186/1471-2148-7-64 Medline
- Iversen C, Mullane N, McCardell B, Tall BD, Lehner A, Fanning S, Stephan R, Joosten H.** *Cronobacter* gen. nov., a new genus to accommodate the biogroups of *Enterobacter sakazakii*, and proposal of *Cronobacter sakazakii* gen. nov., comb. nov., *Cronobacter malonaticus* sp. nov., *Cronobacter turicensis* sp. nov., *Cronobacter myuvtjensii* sp. nov., *Cronobacter dublinensis* sp. nov., *Cronobacter* genomospecies 1, and of three subspecies, *Cronobacter dublinensis* subsp. *dublinensis* subsp. nov., *Cronobacter dublinensis* subsp. *lausannensis* subsp. nov. and *Cronobacter dublinensis* subsp. *lactaridi* subsp. nov. *Int J Syst Evol Microbiol.* 2008;58(6):1442–1447. doi:10.1099/ijs.0.65577-0 Medline
- Joseph S, Cetinkaya E, Drahovska H, Levican A, Figueras MJ, Forsythe SJ.** *Cronobacter condimentii* sp. nov., isolated from spiced meat, and *Cronobacter universalis* sp. nov., a species designation for *Cronobacter* sp. genomospecies 1, recovered from a leg infection, water and food ingredients. *Int J Syst Evol Microbiol.* 2012;62 (Pt 6):1277–1283. doi:10.1099/ijs.0.032292-0 Medline
- Joseph S, Forsythe SJ.** Predominance of *Cronobacter sakazakii* sequence type 4 in neonatal infections. *Emerg Infect Dis.* 2011;17(9):1713–1715. doi:10.3201/eid1709.110260 Medline
- Kadliceckova V, Kajsik M, Soltys K, Szemes T, Slobodnikova L, Janosikova L, Hubenakova Z, Ogrodzki P, Forsythe S, Turna J, et al.** Characterisation of *Cronobacter* strains isolated from hospitalised adult patients. *Antonie van Leeuwenhoek.* 2018;111(7):1073–1085. doi:10.1007/s10482-017-1008-2 Medline
- Kucerova E, Clifton SW, Xia XQ, Long F, Porwollik S, Fulton L, Fronick C, Minx P, Kyung K, Warren W, et al.** Genome sequence of *Cronobacter sakazakii* BAA-894 and comparative genomic hybridization analysis with other *Cronobacter* species. *PLoS One.* 2010;5(3):e9556. doi:10.1371/journal.pone.0009556 Medline
- Kuhns M, Zautner AE, Rabsch W, Zimmermann O, Weig M, Bader O, Groß U.** Rapid discrimination of *Salmonella enterica* serovar *Typhi* from other serovars by MALDI-TOF mass spectrometry. *PLoS One.* 2012;7(6):e40004. doi:10.1371/journal.pone.0040004 Medline
- Lai KK.** *Enterobacter sakazakii* infections among neonates, infants, children, and adults. Case reports and a review of the literature. *Medicine.* 2001;80(2):113–122. doi:10.1097/00005792-200103000-00004 Medline
- Matoušková I, Holý O.** [Bacterial contamination of the indoor air in a transplant unit]. (in Czech). *Epidemiol Mikrobiol Imunol.* 2013;62(4):153–159. Medline
- Matoušková I, Holý O.** Monitoring of the environment at the transplant unit-hemato-oncology clinic. *Int J Environ Res Public Health.* 2014;11(9):9480–9490. doi:10.3390/ijerph110909480 Medline
- Matoušková I, Raida L, Holý O.** [The incidence of nonfermentative gram-negative bacilli in the environment of the transplant unit, department of hemato-oncology, university hospital Olomouc]. (in Czech). *Epidemiol Mikrobiol Imunol.* 2012;61(4):110–115. Medline
- Mellmann A, Cloud J, Maier T, Keckevoet U, Ramminger I, Iwen P, Dunn J, Hall G, Wilson D, LaSala P, et al.** Evaluation of matrix-assisted laser desorption ionization-time-of-flight mass spectrometry in comparison to 16S rRNA gene sequencing for species identification of nonfermenting bacteria. *J Clin Microbiol.* 2008;46(6):1946–1954. doi:10.1128/JCM.00157-08 Medline
- Muytjens HL, van der Ros-van de Repe J.** Comparative in vitro susceptibilities of eight *Enterobacter* species, with special reference to *Enterobacter sakazakii*. *Antimicrob Agents Chemother.* 1986;29(2): 367–370. doi:10.1128/AAC.29.2.367 Medline

- Muytjens HL, Zanen HC, Sonderkamp HJ, Kollée LA, Wachsmuth IK, Farmer JJ 3rd. Analysis of eight cases of neonatal meningitis and sepsis due to *Enterobacter sakazakii*. J Clin Microbiol. 1983;18(1):115–120. [Medline](#)
- Pagani L, Dell'Amico E, Migliavacca R, D'Andrea MM, Giacobone E, Amicosante G, Romero E, Rossolini GM. Multiple CTX-M-type extended-spectrum beta-lactamases in nosocomial isolates of *Enterobacteriaceae* from a hospital in northern Italy. J Clin Microbiol. 2003;41(9):4264–4269. [doi:10.1128/JCM.41.9.4264-4269.2003](#) [Medline](#)
- Pan Z, Cui J, Lyu G, Du X, Qin L, Guo Y, Xu B, Li W, Cui Z, Zhao C. Isolation and molecular typing of *Cronobacter* spp. in commercial powdered infant formula and follow-up formula. Foodborne Pathog Dis. 2014;11(6):456–461. [doi:10.1089/fpd.2013.1691](#) [Medline](#)
- Pitout JD, Moland ES, Sanders CC, Thomson KS, Fitzsimmons SR. Beta-lactamases and detection of beta-lactam resistance in *Enterobacter* spp. Antimicrob Agents Chemother. 1997;41(1):35–39. [doi:10.1128/AAC.41.1.35](#) [Medline](#)
- Sauer S, Freiwald A, Maier T, Kube M, Reinhardt R, Kostrzewa M, Geider K. Classification and identification of bacteria by mass spectrometry and computational analysis. PLoS One. 2008;3(7):e2843. [doi:10.1371/journal.pone.0002843](#) [Medline](#)
- Schulthess B, Bloemberg GV, Zbinden A, Mouttet F, Zbinden R, Böttger EC, Hombach M. Evaluation of the Bruker MALDI Biolyser for identification of fastidious Gram-negative rods. J Clin Microbiol. 2016;54(3):543–548. [doi:10.1128/JCM.03107-15](#) [Medline](#)
- See KC, Than HA, Tang T. *Enterobacter sakazakii* bacteraemia with multiple splenic abscesses in a 75-year-old woman: a case report. Age Ageing. 2007;36(5):595–596. [doi:10.1093/ageing/afm092](#) [Medline](#)
- Shi C, Song K, Zhang X, Sun Y, Sui Y, Chen Y, Jia Z, Sun H, Sun Z, Xia X. Antimicrobial activity and possible mechanism of action of citral against *Cronobacter sakazakii*. PLoS One. 2016;11(7):e0159006. [doi:10.1371/journal.pone.0159006](#) [Medline](#)
- Stephan R, Grim CJ, Gopinath GR, Mammel MK, Sathyamoorthy V, Trach LH, Chase HR, Fanning S, Tall BD. Re-examination of the taxonomic status of *Enterobacter helveticus*, *Enterobacter pulveris* and *Enterobacter turicensis* as members of the genus *Cronobacter* and their reclassification in the genera *Franconibacter* gen. nov. and *Siccibacter* gen. nov. as *Franconibacter helveticus* comb. nov., *Franconibacter pulveris* comb. nov. and *Siccibacter turicensis* comb. nov., respectively. Int J Syst Evol Microbiol. 2014;64(Pt10):3402–3410. [doi:10.1099/ijs.0.059832-0](#) [Medline](#)
- Stock I, Wiedemann B. Natural antibiotic susceptibility of *Enterobacter amnigenus*, *Enterobacter cancerogenus*, *Enterobacter gergoviae* and *Enterobacter sakazakii* strains. Clin Microbiol Infect. 2002;8(9):564–578. [doi:10.1046/j.1469-0691.2002.00413.x](#) [Medline](#)
- Terragno R, Salve A, Pichel M, Epsztejn S, Brengi S, Binsztein N. Characterization and subtyping of *Cronobacter* spp. from imported powdered infant formulae in Argentina. Int J Food Microbiol. 2009;136(2):193–197. [doi:10.1016/j.ijfoodmicro.2009.10.013](#) [Medline](#)
- Vojtkovska H, Karpiskova R, Orieskova M, Drahovska H. Characterization of *Cronobacter* spp. isolated from food of plant origin and environmental samples collected from farms and from supermarkets in the Czech Republic. Int J Food Microbiol. 2016;217:130–136. [doi:10.1016/j.ijfoodmicro.2015.10.017](#) [Medline](#)
- Willis J, Robinson J. *Enterobacter sakazakii* meningitis in neonates. Pediatr Infect Dis J. 1988;7(3):196–199. [doi:10.1097/00006454-198803000-00012](#) [Medline](#)

Interferon Gamma Release Assays in Patients with Respiratory Isolates of Non-Tuberculous Mycobacteria – a Preliminary Study

EWA AUGUSTYNOWICZ-KOPEĆ¹, IZABELA SIEMION-SZCZEŚNIAK², ANNA ZABOST¹,
DOROTA WYROSTKIEWICZ², DOROTA FILIPCZAK¹, KARINA ONISZH³, DARIUSZ GAWRYLUK⁴,
ELŻBIETA RADZIKOWSKA⁴, DAMIAN KORZYBSKI⁵ and MONIKA SZTURMOWICZ^{2*}

¹Department of Microbiology, National Research Institute of Tuberculosis and Lung Diseases, Warsaw, Poland

²The First Department of Lung Diseases, National Research Institute of Tuberculosis and Lung Diseases, Warsaw, Poland

³Department of Radiology and Diagnostic Imaging, National Institute of Tuberculosis and Lung Diseases, Warsaw, Poland

⁴The Third Department of Lung Diseases, National Research Institute of Tuberculosis and Lung Diseases, Warsaw, Poland

⁵The Second Department of Lung Diseases, National Research Institute of Tuberculosis and Lung Diseases, Warsaw, Poland

Submitted 7 August 2018, revised 24 October 2018, accepted 25 October 2018

Abstract

Interferon gamma releasing assays (IGRAs) are extensively used in the diagnosis of latent tuberculosis infections. Comparing to tuberculin skin test (TST) they lack false positive results in the populations vaccinated with BCG, and in most non-tuberculous mycobacteria (NTM) infections. Nevertheless, *Mycobacterium kansasii*, *Mycobacterium marinum*, and *Mycobacterium szulgai* may induce positive IGRAs due to RD1 homology with *Mycobacterium tuberculosis*. The aim of the study was to investigate the possible influence of NTM respiratory isolates on the results of IGRAs. 39 patients (23 females and 16 males) of median age 61 years, with negative medical history concerning tuberculosis, entered the study. Identification of NTM was performed using the niacin test and molecular method GenoType CM test (Hain Lifescience). QFT-Plus was performed in 17 patients, T-SPOT-Tb – in 23 patients. Chest X-rays and a high-resolution computed tomography of the chest have been reviewed by the experienced radiologist blinded to the results of IGRAs, in search of past tuberculosis signs. Positive IGRAs results were obtained in three out of 39 patients (8%): 22% of patients with *M. kansasii* isolates and 18% of patients with radiological signs on HRCT that might be suggestive of past tuberculosis. Positive IGRAs correlated with radiological signs suggestive of past tuberculosis ($r=0.32$, $p=0.04$), and on the borderline with isolation of *M. kansasii* ($r=0.29$, $p=0.06$). These findings may suggest that a positive IGRAs result, in our material, could depend mostly on asymptomatic past Tb infection. The cross-reactivity of *M. kansasii* isolates with IGRAs was less probable; nevertheless, it requires further investigations.

Key words: interferon gamma release, non-tuberculous mycobacteria, *Mycobacterium kansasii*, latent tuberculosis infection

Introduction

The introduction of IGRAs to clinical practice enabled to improve the diagnostic accuracy of latent tuberculosis infection (LTBI). The assessment of LTBI by IGRAs is based on response to specific antigens: early secreted antigenic target 6 kDa (ESAT-6) and culture filtrate protein 10 kDa (CFP-10), localized in a specific genomic area of *Mycobacterium tuberculosis*, called the region of difference (RD1) (Borkowska 2011; Demkow 2011).

Subsequently, IGRAs have been extensively used to diagnose LTBI in susceptible populations, among others, persons after active tuberculosis contact, immunocompromised hosts, and the candidates to immunosuppressive therapy, especially to anti-TNF alfa treatment (Borkowska et al. 2011; Demkow 2011).

The overall prevalence of LTBI in different countries is closely related to tuberculosis (Tb) burden; thus, the countries with high Tb burden would have more LTBI cases diagnosed with IGRAs and those with low Tb burden – less such cases (Kuś et al. 2011).

* Corresponding author: M. Szturmowicz, The First Department of Lung Diseases, National Research Institute of Tuberculosis and Lung Diseases, Warsaw, Poland; e-mail: monika.szturmowicz@gmail.com

© 2019 Ewa Augustynowicz-Kopeć et al.

This work is licensed under the Creative Commons Attribution-NonCommercial-NoDerivatives 4.0 License (<https://creativecommons.org/licenses/by-nc-nd/4.0/>)

The superiority of IGRAs over tuberculin skin test (TST) in LTBI diagnostic pathway, is related to its higher specificity, e.g. lack of false positive results in the populations vaccinated against *M. tuberculosis* and those infected with most of non-tuberculous mycobacteria (NTM) (Demkow 2011; Kuś et al. 2011; Mancuso et al. 2012). Nevertheless, some NTM, such as *Mycobacterium kansasii*, *Mycobacterium marinum* and *Mycobacterium szulgai* share RD1 with *M. tuberculosis* and could induce false positive immunological response assessed by IGRAs (Demkow 2011). This observation may be important, especially in the countries with low Tb burden, defined by European Centre for Disease Prevention and Control experts as notification rate lower than 20 per 100 000 population (ECDC/WHO 2018), and with increased incidence of diseases caused by NTM (Prevots et al. 2010). In Poland, as well as in Slovakia and in the United Kingdom, a large proportion of NTM infections have been caused by *M. kansasii*, possibly influencing the specificity of IGRAs in LTBI diagnostics (Ślupek et al. 1997; Hoefsloot et al. 2013; van der Werf et al. 2014; Wilińska et al. 2014; Bakula et al. 2018).

Thus, the aim of the present study was to investigate the influence of NTM isolation from respiratory specimens on the results of IGRAs in patients with no medical history of tuberculosis.

Experimental

Materials and Methods

Patients. Overall, 39 patients (23 females and 16 males) of median age 61 years (27–85 years), from whom NTM was cultured from respiratory specimens (sputum and/or bronchial washings) in the period of 2010–2017, and IGRA test was performed simultaneously, entered the study. Patients, who had been diagnosed and treated for tuberculosis, were excluded from the study.

Non-tuberculous mycobacterial lung disease (NTMLD) was recognized in 16 patients according to

American Thoracic Society/Infectious Diseases Society of America (ATS/IDSA) and recent British Thoracic Society recommendations (Griffith et al. 2007; Haworth et al. 2017). In 23 patients, respiratory isolates did not cause the disease. The characteristic of the population is summarized in Table I.

Chest X-rays and high resolution computed tomography (HRCT) of the chest were reviewed by the experienced radiologist blinded to the results of IGRAs in search of fibrotic foci localized in the upper lobes or upper parts of lower lobes, as well as parenchymal and lymph nodes' calcifications.

Methods of NTM culture and identification. The specimens were digested with the sodium hydroxide and N-acetyl-L-cysteine (NaOH/NALC) method. After decontamination, the sample was neutralized with sterile phosphate buffer (pH 6.8) and centrifuged at 3000 × g for 15 min. The pellet was suspended in 2 ml of phosphate buffer. The strains were cultured on solid media: egg-based L-J medium, Stonebrink medium and in automated system MGIT (Becton Dickinson) (Klatt et al. 2015).

Identification of culture was performed using the niacin test and a molecular method GenoType CM test (Hain Lifescience). The GenoType CM test, using the DNA-STRIP method allowed the identification of *M. tuberculosis* complex strains and 14 clinically relevant NTM within a single procedure. The procedure for identifying strains consists of three steps: isolation of DNA, amplification using primers labeled with biotin and a reverse hybridization. This hybridization reaction includes the consecutive steps: chemical denaturation of the amplification products, hybridization of single-stranded amplicons labeled with biotin on a membrane coated with probes, washing, adding streptavidin/alkaline phosphatase conjugate, staining reaction using alkaline phosphatase (Zabost and Augustynowicz-Kopec 2015).

Molecular detection of *M. tuberculosis*. Identification using the BD ProbeTec ET system (Becton Dickinson Diagnostic Instruments) was performed according to the manufacturer's instructions. The instrument

Table I

Characteristics of the population of patients, from whom NTM was isolated from respiratory specimens.

Sex	No of pts	Age Median (range)	BMI Median (range)	Number of patients with certain coexisting disease					
				COPD	ILD or GPA	CTD	CF	Npl	Others*
Males	16	58.5 (28–75)	24.9 (19.5–38.9)	5	3	0	0	3	5
Females	23	62 (29–85)	23.8 (16.2–37.3)	5	6	4	2	2	4
Total	39	61 (27–85)	24.3 (15–38.9)	10	9	4	2	5	9

COPD – chronic obstructive pulmonary disease; ILD – interstitial lung disease; GPA – granulomatosis with polyangiitis;

CTD – connective tissue disease; CF – cystic fibrosis; npl – neoplasm; BMI – body mass index

* Diabetes (2), hypothyreosis (1), lung aspergilloma (1), renal insufficiency (1), bronchiectasis (2), actinomycosis (1), lung cirrhosis (1), lobar pulmonary artery agenesis (1), trombofilia (1)

reported amplification signals > 3 500 method-other-than-acceleration (MOTA) units as positive (Klatt 2015). It was performed in all cases with a positive result of direct bacterioscopy.

Interferon gamma release assays. The IGRAs assays identified cellular immune responses to *M. tuberculosis* by measuring interferon-gamma (IFN- γ) after stimulation of T cells with *M. tuberculosis*-specific antigens. Two tests were available: T-SPOT.TB based on the Elispot-enzyme-linked immuno spot and Quanti-Feron TB Gold Plus (QFT-Plus) based on the enzyme-linked immunosorbent assays (ELISA) technique. The T-SPOT.TB test is based on measurement of the number of peripheral mononuclear cells that produce IFN- γ after stimulation with two antigens: ESAT-6 and CFP 10. The antigens used in QFT-Plus consisted of a peptide cocktail simulating the ESAT-6 and CFP 10 (Borkowska et al. 2017).

QFT-Plus was performed in 17 patients, T-SPOT-Tb – in 23 (including one patient, in whom both IGRAs have been performed).

Statistical analysis. The data were presented as medians and ranges or as number and percentage of positive cases. The differences between categorical variables were analyzed with the *chi*-square test, for quantitative variables – ANOVA test was used. The correlation was assessed with Spearman rank order test. $P < 0.05$ was considered statistically significant.

Results

Positive IGRAs results were obtained in three out of 39 patients (8%): positive QFT Plus – in two cases, T-SPOT-TB – in one case. In one patient, in whom both tests were performed, T-SPOT-Tb was negative but QFT was positive.

IGRAs results according to the identified type of NTM were shown in Table II. Positive results were obtained in 2/9 (22%) of patients with *M. kansasii* and one patient with *M. fortuitum* isolate. IGRAs positivity was thus found in 2/10 (20%) of NTM sharing the RD1 region with *M. tuberculosis* (*M. kansasii*, *M. szulgai*) and 1/29 (3%) of those without RD1 sharing ($p = 0.31$).

Positive IGRAs were obtained in 2/23 females (9%) and 1/16 males (6%), ($p = 0.91$).

IGRAs results according to the patients' age (Table III) revealed that positive results were found only in the patients above 60 years of age; nevertheless, the age-related differences were not significant ($p = 0.49$).

HRCT analysis revealed the presence of lesions suggesting the possibility of the previous infection with *M. tuberculosis* in 17/39 (44%) of patients.

The results of IGRAs according to the results of radiological analysis are shown in Table IV. Positive

Table II
IGRAs results according to the NTM species.

Species	IGRA (+)	IGRA (-)	Total
<i>M. kansasii</i>	2 (22%)	7	9
<i>M. avium</i>	0	7	7
<i>M. goodnae</i>	0	6	6
<i>M. chimaera</i>	0	5	5
<i>M. xenopi</i>	0	5	5
<i>M. fortuitum</i>	1 (33%)	2	3
<i>M. szulgai</i>	0	1	1
<i>M. abscessus</i>	0	1	1
<i>M. mucogenicum</i>	0	1	1
<i>M. smegmatis</i>	0	1	1
Total	3 (8%)	36	39

Table III
IGRAs result according to patients' age.

Age (years)	≤24	25–44	45–59	≥60	Total
IGRAs (+)	0	0	0	3 (14%)	3
IGRAs (-)	0	11	8	17	36
Total	0	11	8	20	39

Table IV
The IGRAs results according to radiologic signs of past tuberculosis.

Chest CT	IGRA (+)	IGRA (-)	Total
Past tb signs	3 (18%)	14 (82%)	17
No past tb signs	0 (0%)	22	22
Total	3	36	39

CT – computed tomography, tb – tuberculosis

IGRAs were found in 3/17 (18%) patients with the above-mentioned radiological signs and none of the remaining patients ($p = 0.15$).

Positive IGRAs results correlated with radiological signs suggestive of possibility of infection with *M. tuberculosis* in the past ($r = 0.32$, $p = 0.04$); the correlation of positive IGRA with the isolation of *M. kansasii* was borderline ($r = 0.29$, $p = 0.06$).

Discussion

Positive IGRAs have been found in three (8%) of patients with NTM cultured from respiratory specimens. Two positive IGRAs results concerned the patients with *M. kansasii* isolates (22%), the species sharing RD1 with *M. tuberculosis*, one – the patient with *M. fortuitum* isolate, the species not sharing RD1. The Japanese studies revealed IGRAs positivity in 19–52% of *M. kansasii* isolates (Kobashi et al. 2009; Sato et al.

2016). The European experience is scarce; nevertheless, Hermansen et al. (2014) found positive IGRAs results in 2/2 *M. kansasii* isolates (100%).

The discrepancies concerning IGRAs positivity were found also in *M. avium/M. intracellulare* (MAC) infection: from 0–8% positive results in the studies conducted in Northern Europe and Japan (Adams et al. 2008; Kobashi et al. 2009; Hermansen et al. 2014) to 34% in the study conducted in South Korea (Ra et al. 2011). In our study, all seven cases of *M. avium* isolates were IGRAs negative. As MAC doesn't share the RD1 region with *M. tuberculosis*, positive IGRAs obtained for the patients with MAC isolates by other authors might reflect the background influence of past tuberculosis, especially in countries with high Tb burden (Ra et al. 2011; Wang et al. 2016).

Poland belongs to low Tb burden countries, with the incidence rate of tuberculosis calculated as 19.7/100 000 in 2010 and 15.1/100 000 in 2017 (Korzeniewska-Koseła 2017, 2018). The analysis of LTBI prevalence assessed with QFT, performed in 2010 on 621 healthy subjects from Mazowieckie province, revealed the positive results in 23.3% of them, more frequently in older people compared to younger ones (Kuś et al. 2011). Positive IGRAs in the present study were found exclusively in patients > 60 years of age, indicating possible influence of background non-recognized Tb infection in the past on the results obtained.

Retrospective analysis of HRCT scans by an experienced radiologist blinded to IGRAs results, revealed the lesions suggestive of possibility of infection with *M. tuberculosis* in the past in 17 out of 39 patients (44%), despite lack of Tb in anamnesis. Positive IGRAs were noted in three out of 17 patients with radiological signs suggestive of past tuberculosis (18%) and none of the patients without such findings on chest CT scan.

These findings may suggest that positive IGRAs result, in our material, could depend mostly on asymptomatic past Tb infection. The cross-reactivity of *M. kansasii* isolates with IGRAs is less probable, because it was present only in two out of nine patients with *M. kansasii* isolates.

The same type of analysis has been performed by Sato et al. who found T-SPOT positivity in 33% of patients with *M. kansasii* isolates, but after exclusion of those with a history of tuberculosis (defined as either Tb diagnosis and treatment in the past or chest X-ray features suggesting previous tuberculosis), the percentage of T-SPOT positive cases decreased to 19%. They concluded that features of previous Tb are the only risk factor for positive IGRAs in the patients with *M. kansasii* respiratory isolates.

Since the group of patients was small in the current study, further studies are required to answer the question, whether the positive IGRAs in patients with

M. kansasii isolates is caused by RD1 cross-reactivity or rather the background of asymptomatic tuberculosis in the past.

Conflict of interest

Author does not report any financial or personal connections with other persons or organizations, which might negatively affect the contents of this publication and/or claim authorship rights to this publication.

Literature

- Adams LV, Waddell RD, Fordham Von Reyn C. T-SPOT. TB Test® results in adults with *Mycobacterium avium* complex pulmonary disease. Scand J Infect Dis. 2008;40(3):196–203. doi:10.1080/00365540701642179 Medline
- Adzic-Vukicevic T, Barac A, Blanka-Protic A, Laban-Lazovic M, Lukovic B, Skodric-Trifunovic V, Rubino S. Clinical features of infection caused by non-tuberculous mycobacteria: 7 years' experience. Infection. 2018;46(3):357–363. doi:10.1007/s15010-018-1128-2 Medline
- Bakuła Z, Kościuch J, Safianowska A, Proboszcz M, Bielecki J, van Ingen J, Krenke R, Jagielski T. Clinical, radiological and molecular features of *Mycobacterium kansasii* pulmonary disease. Respir Med. 2018;139:91–100. doi:10.1016/j.rmed.2018.05.007 Medline
- Borkowska D, Zwolska Z, Michałowska-Mitczuk D, Korzeniewska-Koseła M, Zabost A, Napiórkowska A, Kozłowska M, Brzezińska S, Augustynowicz-Kopec E. [Interferon-gamma assays T-SPOT.TB for the diagnosis of latent tuberculosis infection] (in Polish). Pneumonol Alergol Pol. 2011;79(4):264–271. Medline
- Borkowska DI, Napiórkowska AM, Brzezińska SA, Kozłowska M, Zabost AT, Augustynowicz-Kopec EM. From latent tuberculosis infection to tuberculosis. News in diagnostics (QuantiferON-Plus). Pol J Microbiol. 2017;66(1):5–8. doi:10.5604/17331331.1234987 Medline
- Demkow U. [Interferon gamma based tests as a new tool in diagnosis of latent tuberculosis] (in Polish). Pneumonol Alergol Pol. 2011;79(4):261–263. Medline
- European Centre for Disease Prevention and Control/WHO Regional Office for Europe. Tuberculosis surveillance and monitoring in Europe 2016–2018. Stockholm (Sweden): European Centre for Disease Prevention and Control. 2018.
- Griffith DE, Aksamit T, Brown-Elliott BA, Catanzaro A, Daley C, Gordin F, Holland SM, Horsburgh R, Huit G, Iademarco MF, et al.; ATS Mycobacterial Diseases Subcommittee; American Thoracic Society; Infectious Disease Society of America. An official ATS/IDSA statement: diagnosis, treatment, and prevention of nontuberculous mycobacterial diseases. Am J Respir Crit Care Med. 2007;175(4):367–416. doi:10.1164/rccm.200604-571ST Medline
- Korzeniewska-Koseła M (editor). Gruźlica i choroby układu oddechowego w Polsce w 2017 roku. Warszawa (Poland): Instytut Gruźlicy i Chorób Płuc. 2018.
- Haworth CS, Banks J, Capstick T, Fisher AJ, Gorsuch T, Laursen IF, Leitch A, Loebinger MR, Milburn HJ, Nightingale M, et al. British Thoracic Society guidelines for the management of non-tuberculous mycobacterial pulmonary disease (NTM-PD). Thorax. 2017;72 Suppl 2:ii1–ii64. doi:10.1136/thoraxjnl-2017-210927 Medline
- Hermansen TS, Thomsen VØ, Lillebaek T, Ravn P. Non-tuberculous mycobacteria and the performance of interferon gamma release assays in Denmark. PLoS One. 2014;9(4):e93986. doi:10.1371/journal.pone.0093986 Medline

- Hoefsloot W, van Ingen J, Andrejak C, Ängeby K, Bauriaud R, Bemer P, Beylis N, Boeree MJ, Cacho J, Chihota V, et al.; **Non-tuberculous Mycobacteria Network European Trials Group**. The geographic diversity of nontuberculous mycobacteria isolated from pulmonary samples: an NTM-NET collaborative study. *Eur Respir J*. 2013;42(6):1604–1613. doi:10.1183/09031936.00149212 [Medline](#)
- Klatt M, Zabost A, Augustynowicz-Kopeć E. Diagnostyka mikrobiologiczna gruźlicy z zastosowaniem testów genetycznych XPERT MTB/RIF. *Zakażenia*. 2015;15(6):85–92.
- Kobashi Y, Mouri K, Yagi S, Obase Y, Miyashita N, Okimoto N, Matsushima T, Kageoka T, Oka M. Clinical evaluation of the QuantiFERON-TB Gold test in patients with non-tuberculous mycobacterial disease. *Int J Tuberc Lung Dis*. 2009;13(11):1422–1426. [Medline](#)
- Korzeniewska-Koseła M. Tuberculosis in Poland in 2015. *Przegl Epidemiol*. 2017;71(3):391–403. [Medline](#)
- Kuś J, Demkow U, Lewandowska K, Korzeniewska-Koseła M, Rabczenko D, Siemion-Szcześniak I, Białas-Chromiec B, Bychawska M, Sapigórski P, Maciejewski J. [Prevalence of latent infection with *Mycobacterium tuberculosis* in Mazovia Region using interferon gamma release assay after stimulation with specific antigens ESAT-6 and CFP-10]. *Pneumonol Alergol Pol*. 2011;79(6):407–418. [Medline](#)
- Mancuso JD, Mazurek GH, Tribble D, Olsen C, Aronson NE, Geiter L, Goodwin D, Keep LW. Discordance among commercially available diagnostics for latent tuberculosis infection. *Am J Respir Crit Care Med*. 2012;185(4):427–434. doi:10.1164/rccm.201107-1244OC [Medline](#)
- Prevots DR, Shaw PA, Strickland D, Jackson LA, Raebel MA, Blosky MA, Montes de Oca R, Shea YR, Seitz AE, Holland SM, et al. Nontuberculous mycobacterial lung disease prevalence at four integrated health care delivery systems. *Am J Respir Crit Care Med*. 2010;182(7):970–976. doi:10.1164/rccm.201002-0310OC [Medline](#)
- Ra SW, Lyu J, Choi C-M, Oh Y-M, Lee S-D, Kim WS, Kim DS, Shim TS. Distinguishing tuberculosis from *Mycobacterium avium* complex disease using an interferon-gamma release assay. *Int J Tuberc Lung Dis*. 2011;15(5):635–640. doi:10.5588/ijtld.10.0485 [Medline](#)
- Sato R, Nagai H, Matsui H, Kawabe Y, Takeda K, Kawashima M, Suzuki J, Ohshima N, Masuda K, Yamane A, et al. Interferon-gamma release assays in patients with *Mycobacterium kansasii* pulmonary infection: A retrospective survey. *J Infect*. 2016;72(6):706–712. doi:10.1016/j.jinf.2016.03.011 [Medline](#)
- Słupek A, Zwolska Z, Miller M, Rowińska-Zakrzewska E. [Pulmonary mycobacteriosis-diagnostic problem and prevalence in Poland (a retrospective study)]. (in Polish). *Pneumonol Alergol Pol*. 1997;65(5–6):326–332. [Medline](#)
- van der Werf MJ, Ködmön C, Katalinić-Janković V, Kummik T, Soini H, Richter E, Papaventsis D, Tortoli E, Perrin M, van Soolingen D, et al. Inventory study of non-tuberculous mycobacteria in the European Union. *BMC Infect Dis*. 2014;14(1):62–70. doi:10.1186/1471-2334-14-62 [Medline](#)
- Wang MS, Wang JL, Wang XF. The performance of interferon-gamma release assay in nontuberculous mycobacterial diseases: a retrospective study in China. *BMC Pulm Med*. 2016;16(1):163. doi:10.1186/s12890-016-0320-3 [Medline](#)
- Wilińska E, Oniszh K, Augustynowicz-Kopeć E, Zabost A, Fijałkowska A, Kurzyna M, Wieteska M, Torbicki A, Kuś J, Szturmowicz M. Non-tuberculous mycobacterial lung disease (NTMLD) in patients with chronic thromboembolic pulmonary hypertension and idiopathic pulmonary arterial hypertension. *Pneumonol Alergol Pol*. 2014;82(6):495–502. doi:10.5603/PiAP.2014.0066 [Medline](#)
- Zabost A, Augustynowicz-Kopeć E. Use of GenoType MTBDR plus assay for the detection of mycobacteria molecular rifampicin and isoniazid resistance. *Post Nauk Med*. 2015;4:249–254.

Bioactive Compounds of *Pseudoalteromonas* sp. IBRL PD4.8 Inhibit Growth of Fouling Bacteria and Attenuate Biofilms of *Vibrio alginolyticus* FB3

NOR AFIFAH SUPARDY^{1*}, DARAH IBRAHIM¹, SHARIFAH RADZIAH MAT NOR¹
and WAN NORHANA MD NOORDIN²

¹Industrial Biotechnology Research Laboratory (IBRL), School of Biological Sciences,
Universiti Sains Malaysia, Penang, Malaysia

²Fisheries Research Institute (FRI), Penang, Malaysia

Submitted 12 August 2018, revised 11 October 2018, accepted 29 October 2018

Abstract

Biofouling is a phenomenon that describes the fouling organisms attached to man-made surfaces immersed in water over a period of time. It has emerged as a chronic problem to the oceanic industries, especially the shipping and aquaculture fields. The metal-containing coatings that have been used for many years to prevent and destroy biofouling are damaging to the ocean and many organisms. Therefore, this calls for the critical need of natural product-based antifoulants as a substitute for its toxic counterparts. In this study, the antibacterial and antibiofilm activities of the bioactive compounds of *Pseudoalteromonas* sp. IBRL PD4.8 have been investigated against selected fouling bacteria. The crude extract has shown strong antibacterial activity against five fouling bacteria, with inhibition zones ranging from 9.8 to 13.7 mm and minimal inhibitory concentrations of 0.13 to 8.0 mg/ml. Meanwhile, the antibiofilm study has indicated that the extract has attenuated the initial and pre-formed biofilms of *Vibrio alginolyticus* FB3 by $45.37 \pm 4.88\%$ and $29.85 \pm 2.56\%$, respectively. Moreover, micrographs from light and scanning electron microscope have revealed extensive structural damages on the treated biofilms. The active fraction was fractionated with chromatographic methods and liquid chromatography-mass spectroscopy analyses has further disclosed the presence of a polyunsaturated fatty acid 4,7,10,13-hexadecatetraenoic acid ($C_{16}H_{24}O_2$). Therefore, this compound was suggested as a potential bioactive compound contributing to the antibacterial property. In conclusion, *Pseudoalteromonas* sp. IBRL PD4.8 is a promising source as a natural antifouling agent that can suppress the growth of five fouling bacteria and biofilms of *V. alginolyticus* FB3.

Key words: *Pseudoalteromonas* sp., antibiofilm, biofouling, liquid chromatography-mass spectroscopy, scanning electron microscope

Introduction

The aquaculture farm of the fishing industry is a severe victim from biofouling and its damaging impact. Other than the various economic consequences that had to be overcome with the cleaning, maintenance, and replacement of damaged nets, pressing focus is placed upon their detrimental effects of the cultured fishes. Colonization of bryozoans, gastropod, oyster, barnacles, and macroalgae on the pen- or cage-nets have been known to implicate the fishes by causing serious water quality problems, reducing the oxygen supply, and increasing food and space competition (Fitridge et al. 2012). Furthermore, abrasion injuries, high-stress levels, and exposure to pathogenic microbes harbored by the fouling organisms have also amplified

the risk of diseases to the cultured fishes (Floerl et al. 2016). Another on-going issue related to biofouling is linked to the underwater hulls of ships, where macroalgae and barnacles attach to these structures and reduce the ship's speed due to extra drag (Townsin 2003). As a result, it increases engine stress and fuel consumption.

Nowadays, metal-containing paints like tributyltin (TBT) and copper oxide (Cu_2O) have been widely utilized in the war against biofouling due to their effectiveness (Braddy 2000). However, tin and copper are released into the seawater and do not decompose rapidly, thus causing bio-accumulation in the food chain and intoxicating many lower and higher-level animals (Iwata et al. 1995; Guardiola 2012). Regardless, the most significant risk can be expected to be seen in human beings through the ingestion of contaminated seafood.

* Corresponding author: N.A. Supardy, Centre for Chemical Biology (CCB), Sains@USM, Universiti Sains Malaysia, Penang, Malaysia;
e-mail: afifahsupardy@gmail.com

© 2019 Nor Afifah Supardy et al.

This work is licensed under the Creative Commons Attribution-NonCommercial-NoDerivatives 4.0 License (<https://creativecommons.org/licenses/by-nc-nd/4.0/>)

Therefore, the high toxicity effect of metal-based antifoulants on non-target organisms have spurred researchers to search for the biological extracts of secondary metabolites and enzymes as a sustainable alternative (Burgess et al. 2003; Acevedo 2013). This is supplemented by the knowledge of marine organisms like corals and macroalgae that maintain their clean and foul-free surfaces by synthesizing secondary metabolites, which act as refuge mechanisms against their predators (Limna Mol et al. 2009). Nonetheless, the protection is also apparently derived by secondary metabolites produced by epiphytic bacteria that symbiotically inhabit host surfaces (Jiang et al. 2011).

According to Davey and O'Toole (2000), biofilm formation plays various roles, including environmental signaling between cells, protection from the environment, mediating in nutrient availability and metabolic activity, and attainment of gene transfer for genetic diversity. In biofouling control, biofilm, in particular, has served to be a huge hindrance as it prevents antifouling compounds from penetrating its layer and performing their inhibitory action. It has been previously discovered that a minimal inhibitory concentration (MIC) of an antimicrobial agent against biofilms increase by 1000-fold in comparison with defenseless planktonic cells (Olson et al. 2002). Therefore, the importance of getting to the root of the problem is undeniable, triggering the search for a more sustainable antifouling compound that possesses both antibacterial and antibiofilm properties.

Pseudoalteromonas sp. is a Gram-negative bacterium from the class of Gammaproteobacteria. This particular genus dominates the marine microbiome, as it is linked with bacteriolytic and algicidal properties that reveal host-protective elements (Rao et al. 2007). Hitherto, members of *Pseudoalteromonas* have been discovered to produce a variety of secondary metabolites boasting a broad range of bioactivities, which includes antibacterial (Isnansetyo and Kamei 2003), antifungal (Franks et al. 2006), anticancer, antimalarial, and antioxidant (Mitova et al. 2005; Martinez-Luis et al. 2011) benefits. Additionally, a brownish pigment called pyomelanin has been recently extracted from *Pseudoalteromonas lipolytica*, whereby its biofilms have displayed anti-larval activity against the settlement and metamorphosis of mussel *Mytilus coruscus* (Zeng et al. 2015; Zeng et al. 2017).

Thus, the objective of this study was to investigate the inhibitory activity of ethyl acetate extract of *Pseudoalteromonas* sp. IBRL PD4.8 against the fouling bacteria and biofilms of *V. alginolyticus* FB3. The present study, therefore, suggests the existence of bioactive compounds within the ethyl acetate extract, which are responsible for their inherent antimicrobial and antibiofilm activities.

Experimental

Materials and Methods

Bacterial strains and molecular identifications.

Isolate PD4.8 was isolated from the surface of a green macroalgae, *Caulerpa racemosa* at Port Dickson, Malaysia. Meanwhile, the fouling bacteria (FB) were isolated from the slime layer of a fouled fish net in an aquaculture farm located in Jerejak Island, Malaysia. All strains were then grown on marine agar (MA) for 24 h at 30°C.

An analysis of 16S ribosomal DNA (rDNA) sequence were carried out to identify all strains present. The bacteria were grown in marine broth (MB) for 20 h at 150 rpm and 30°C, whereas the culture was centrifuged at 4000 rpm and a temperature of 4°C for 30 min before a pellet was extracted according to the modified phenol-chloroform extraction method (Cheng and Jiang 2006). The extracted DNA was then amplified by polymerase chain reaction (PCR) using primer 27F (5'-AGA GTT TGA TCM TGG CTC AG-3') and reverse primer 1429R (5'-CGG TTA CCT TGT TAC GAC TT-3'). The PCR mixture was primarily consisting of 0.5 µl 27F, 0.5 µl 1429R, 0.5 µl DNA, 12.5 µl Ho Taq and 11.0 µl double distilled water (ddH₂O), which was vortexed and subjected to the following PCR cycles accordingly: 94°C for 30 sec, 30 cycles of 94°C for 30 sec, 60°C for 60 seconds, 68°C for 1 min, and finally, final extension at 68°C for 5 min. Next, the DNA was semi-quantified in 0.7% (w/v) agarose gel in Tris-acetate-EDTA (TAE) buffer and visualized under ultraviolet (UV) transilluminator (BioRad) after staining with ethidium bromide. To ensure accurate sizing and approximate quantification of the DNA, a gene ruler 1 kb Plus DNA ladder was used. The PCR products were subsequently purified using the Gel Extraction Kit (Real Biotech Corporation) and sent to First Base Laboratories Sdn. Bhd. for sequencing. Afterward, the 16S rDNA sequences obtained were aligned using ClustalW of Mega Software 5.2 and then compared with sequences available in the gene bank database of National Centre for Biotechnology Information (NCBI) using Basic Local Alignment Search Tool (BLAST). A phylogenetic tree was constructed using Maximum Parsimony Method with 1000 bootstrap replications in Mega Ver.6.0 software (Tamura et al. 2013).

Fermentation and extraction. The seed culture of PD4.8 was prepared in 100 ml MB, agitated at 150 rpm and a temperature of 30°C for 24 h. Then, 10 ml of the culture with optical density (OD) 600 of 1.0 was inoculated into sterilized MB (10% v/v) and incubated at 150 rpm at a temperature of 30°C for 5 days (Bavya et al. 2011). The fermented broth was then centrifuged at 4000 rpm and a temperature of 4°C for 30 min. Next, the filtrate was extracted with ethyl acetate (EtOAc) in

a separating funnel (1:1.3 v/v), whereby the resulting extract was concentrated using a rotary evaporator and kept at 4°C until further use.

Disc diffusion and minimal inhibitory concentration (MIC) assays. Twenty μl of the extract was prepared in 98% methanol (MeOH) at a concentration of 100 mg/ml and impregnated on sterilized 6 mm disc (Nor Afifah et al. 2017). Meanwhile, the FB bacteria (approx. 1×10^6 cells/ml) were prepared in 0.9% saline and swabbed evenly on the MA. The discs were then placed on the MA surface and incubated at 30°C for 24 h. Copper omadine (CuPT) (0.002 mg/disc) and 98% methanol were utilized as positive and negative controls, respectively. The resulting zones of inhibition produced around the discs were then measured in millimeter (mm).

The MIC assay of extract was undertaken according to the modified microdilution method (Yu et al. 2012). The extract, in particular, was prepared at 16.0 mg/ml (10% MeOH) and serially diluted with MB to obtain the concentrations of 8.0 mg/ml to 0.031 mg/ml. In the well, 100 μl of an extract was mixed together with 100 μl of FB, with an additional set of color control (100 μl of extract added with 100 μl MB). Two negative controls consisting of 100 μl 10% MeOH and 100 μl FB and 200 μl MB respectively were also prepared. The plate was incubated at 90 rpm at a temperature of 30°C for 24 h, whereby the well with the lowest extract concentration that showed no turbidity when compared with color control (100 μl of extract added with 100 μl MB) was taken as the MIC. All tests were done in triplicate.

Thin layer chromatography (TLC) agar-overlay assay. The crude extract was spotted at the bottom part of the TLC plate (aluminum, 2 cm \times 10 cm). The plate was developed with a mixture of dichloromethane (DCM): EtOAc: MeOH (5:5:1 v/v), and subsequently observed under visible and UV lights (254 nm and 366 nm, respectively). Each spot that appeared on the TLC plate was then identified and its retention factor (R_f) calculated accordingly. Then, the TLC plate was sterilized under the UV light for 30 min and placed on the MA, with the silica surface facing upwards. Next, 10 ml of molten MA (45°C) containing 1×10^6 cells/ml of the FB was poured evenly on the TLC plate and allowed to solidify. The plate was incubated at 30°C for 24 h, and the MA surface was sprayed with 5 mg/ml ethanolic solution of *p*-iodonitrotetrazolium chloride (INT) post-incubation before being incubated in the dark at room temperature ($28 \pm 2^\circ\text{C}$) for 30 min. The bioactive spot was consequently identified via the clear zones that form against the purple background. A negative control was also used, specifically the non-spotted TLC plate.

Column chromatography and preparative TLC. To purify and collect the target bioactive fraction, a normal phase column chromatography was carried

out with the isocratic elution of DCM: EtOAc: MeOH (5:5:1 v/v). The partially purified bioactive fraction was then re-tested in the MIC assay and subjected to further purification via preparative TLC using a mixture of hexane (Hex): EtOAc (1:9 v/v). The developed TLC plate was next visualized under long UV light and all sub-fractions were marked, scraped off, and soaked in 98% MeOH (HPLC) grade overnight. Then, the solutions were centrifuged at 10 000 rpm and a temperature of 4°C for 15 min, with the resulting supernatants, collected, dried, and tested in the disc diffusion assay to identify the active sub-fraction. Finally, the identified active sub-fraction was re-developed with Hex: EtOAc (1:9 v/v) so as to screen for purity.

Liquid chromatography-mass spectroscopy (LC-MS). The identified bioactive sub-fraction was dissolved in 98% MeOH (HPLC grade) and filtered through a Sartorius polytetrafluoroethylene (PTFE) membrane filter (47 mm in diameter, 0.22 μm pore size). The filtered sample was then analyzed by LC coupled with the quadrupole-time-of-flight mass spectrometer (Q-TOF MS) system (Agilent Technologies). Further reverse-phase chromatography was also conducted in a Luna C18(2) column (4.6 mm \times 150 mm, 5 μm , 100 \AA) at a flow rate of 0.40 ml/min, with the eluent of 0.001% ammonia in deionized water (pH 7.37) and acetonitrile (6:4 v/v) over 20 min. The separated peaks were then analyzed by TOF-MS (20–2000 Da) via electrospray ionization (ESI-negative ion mode) and the consequent *m/z* interpreted using the MS spectra libraries (Agilent METLIN Personal Metabolite Database).

Quantitative biofilm inhibition assay. In the biofilm inhibition assay, *V. alginolyticus* FB3 was only tested as it produced the highest level of biofilm in comparison with other strains (data not shown). The bacterial suspension was prepared by inoculating the bacteria into 50 ml MB and incubated at 150 rpm and 30°C for 24 h. Next, the pellet was collected after centrifugation at 4000 rpm for 30 min at 4°C, and re-suspended in MB (Burmølle et al. 2006). In the initial biofilm inhibition assay, 100 μl of the bacterial suspension ($\text{OD}_{600} = 0.15$) was inoculated together with 100 μl of extract into the wells of sterilized flat bottom 96-well microtiter plate. The final concentrations of the extract are 0.03, 0.06, 0.13, 0.25, 0.5, 1.0, 2.0, 4.0, 8.0, and 16.0 mg/ml respectively. Three negative controls that comprised of 200 μl MB, 100 μl inoculum with 100 μl 5% dimethyl sulfoxide (DMSO) (v/v) in MB, and 100 μl MB with 100 μl extract, were also prepared accordingly.

The plate was incubated in a static condition for 24 h at 30°C, whereby the content of the wells after 24 hours was decanted by gently flipping the microtiter plate in a sterile container. Then, the wells were gently washed twice with the sterilized phosphate-buffer solution (PBS). The biofilms were next heat-fixed for 1 h at 60°C

and stained with 210 μ l of 0.06% crystal violet for 15 min. Next, the crystal violet was discarded by gently flipping the microtiter plate in a sterile container before the wells were rinsed twice with sterilized dH₂O. Subsequently, the wells were flooded with 210 μ l of 30% acetic acid for 10 min, following which the absorbance of the crystal violet solution was measured at 570 nm with a microtiter plate reader (Thermo Scientific).

In the pre-formed biofilm inhibition assay, the biofilm was grown by adding 100 μ l of the bacterial suspension with 100 μ l MB and incubated in static for 24 h. The wells were then washed with sterilized PBS before 100 μ l of extract and 100 μ l of fresh MB was added into them and re-incubated for 24 h at 30°C. The percentage of biofilm inhibition in comparison with the untreated control biofilms was then calculated accordingly (Nikolić et al. 2014). Meanwhile, statistical analysis was undertaken using the data obtained via Tukey's posthoc test after one-way analysis of variance (ANOVA) was conducted using SPSS software (IBM software, version 22.0, USA). A *p* value of <0.05 between the means was considered as statistically different, and all experiments were performed in four replicates accordingly:

$$\% \text{ biofilm inhibition} = \frac{\text{OD growth control} - \text{OD sample}}{\text{OD growth control}} \times 100\%$$

Light microscope (LM) study. The method was undertaken as per Abu Sayem et al. (2011), with some additional modifications. Sterilized glass coverslips were placed in a tilting manner in the wells of flat-bottom 96-well microtiter plates. Then, an aliquot of 100 μ l of bacterial suspension and 100 μ l of extract (final concentration of 8.0 mg/ml) was added into the wells. Next, the plate was incubated in the static condition at 30°C for 24 h. For control, the extract was substituted with 5% DMSO (v/v). After the incubation process, a non-adherent biofilm was washed with PBS and the coverslip heat-fixed at 60°C for 1 h, followed with staining using 0.06% crystal violet for 15 min, and subsequent re-washing and air-drying. Finally, the stained coverslips were examined under the LM attached with a digital camera (Olympus U-CMAD3). In case of the pre-formed biofilm, the extract was introduced to the 24 h-old biofilm that grew on the coverslip.

Scanning electron microscopy (SEM) study. The SEM samples for initial and pre-formed biofilms were prepared according to the method in LM and continued further with biofilm fixing with 2.5% glutaraldehyde in PBS at 30°C for 24 h (Cai et al. 2013). The fixed biofilms were subjected to dehydration processes via incremental percentages of ethanol for 10 min each (50%, 75%, 95%, and 100% ethanol twice) before being air-dried. The coverslips were then immersed in the hexamethyldisilazane sputtered in gold and subsequently examined under the SEM (Leica Cambridge, S-360, UK).

Results

Bacteria identification. Table I shows the descriptions of all identified strains with their respective accession numbers from the NCBI database. The identified isolates were consequently denoted accordingly as *Pseudoalteromonas* sp. IBRL PD4.8, *V. alginolyticus* FB3, *Pseudoalteromonas* sp. FB4, *Alteromonas* sp. FB7, *Pseudoalteromonas* sp. FB9, and *Bacillus* sp. FB13 throughout the study. Based on the NCBI database, the epiphytic isolate *Pseudoalteromonas* sp. IBRL PD4.8 was closely related to *Pseudoalteromonas shioyasakiensis* with the 99% percentage of similarity (Table I). A result from the strict consensus tree (Fig. 1) has further supported that the epiphytic isolate is of *P. shioyasakiensis* with a bootstrap value of 54 %.

Disc diffusion and MIC assays. At the extract concentration of 2.0 mg/disc, the ethyl acetate extract showed various degrees of inhibitory activity on the tested FB. The most susceptible FB was *Bacillus* sp. FB13, with an inhibition zone of 13.7 \pm 2.1 mm. Meanwhile, the inhibition zones of *Pseudoalteromonas* sp. FB4 and *Pseudoalteromonas* sp. FB9 were 10.3 \pm 1.5 mm and 9.0 \pm 1.0 mm, respectively, whereas that of *V. alginolyticus* FB3 and *Alteromonas* sp. were 9.8 \pm 1.4 mm and 11.8 \pm 2.4 mm, respectively. In contrast, the extract concentration of 0.002 mg/disc was the positive control CuPT that inhibited all FB with different sizes of inhibition zones between 9.0 to 16.7 mm.

In the MIC assays, the results indicated a concentration-dependent pattern for the extract against the

Table I
Details of BLAST result, % similarity, and accession numbers of all isolates.

Isolate	Sequence length (bp)	BLAST result	% Similarity	Accession No.
PD4.8	1385	<i>Pseudoalteromonas shioyasakiensis</i>	99	LC131142.1
FB3	1349	<i>Vibrio alginolyticus</i>	97	KC884661.1
FB4	1256	<i>Pseudoalteromonas</i> sp.	96	JX0705058.1
FB7	1439	<i>Alteromonas</i> sp.	93	EF061415.1
FB9	1398	<i>Pseudoalteromonas</i> sp.	94	JX075059.1
FB13	1446	<i>Bacillus</i> sp.	93	DQ448746.1

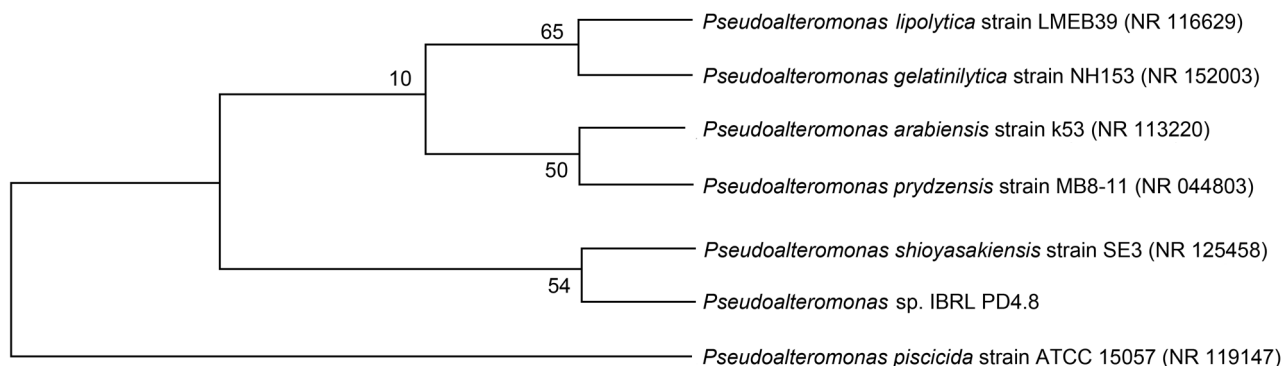


Fig. 1. Phylogenetic tree of *Pseudoalteromonas* sp. IBRL PD4.8 isolated from the surface of *C. racemosa*.

FB tested, whereby increased extract concentrations caused greater bacterial inhibition. This was evidenced by the clearer broth that was observed as the extract concentrations increased higher. The lowest MIC was noticed at 0.13 mg/ml against *Bacillus* sp. FB13. Meanwhile, for the remaining four FB (*V. alginolyticus* FB3, *Pseudoalteromonas* sp. FB4, and *Alteromonas* sp. FB7, *Pseudoalteromonas* sp. FB9) a MIC value was equal to 8.0 mg/ml (Table II).

Table II
MIC values for crude extract and fraction F3 against fouling bacteria.

Fouling bacteria	Crude (mg/ml), MIC	F3 (mg/ml), MIC
<i>Vibrio alginolyticus</i> FB3	8.00	8.00
<i>Pseudoalteromonas</i> sp. FB4	8.00	4.00
<i>Alteromonas</i> sp. FB7	8.00	8.00
<i>Pseudoalteromonas</i> sp. FB9	8.00	8.00
<i>Bacillus</i> sp. FB13	0.13	0.50

TLC agar-overlay assay. The separation of the ethyl acetate extract on the TLC plate demonstrated one yellow spot under visible light (R_f 0.55), three spots under short UV light (R_f 0.26–0.55), and seven spots under long UV light (R_f 0.06–0.85). In contrast, TLC agar-overlay assay revealed a significant clear zone formed around the yellow spot (fluorescent green; R_f 0.55), and two fuzzy zones (light yellow; R_f 0.06 and fluorescent blue; R_f 0.35) (Fig. 2). The compounds of interest were in the yellow spot at R_f 0.55.

Antimicrobial activity and purification of fraction. Based on the agar-overlay assay (Fig. 2), three fractions were identified as potential fractions displaying antimicrobial activity. The yellow fraction (R_f 0.55) that showed the strongest inhibition zone was collected from the column chromatography. The remaining two fractions were excluded due to poor antimicrobial activity and low yield. Overall, ten fractions have been collected from the column chromatography, with the

targeted yellow fraction denoted as F3. The subsequent MIC results of F3 against five FB displayed a variety of inhibitory effects, including static, decreased or enhanced activities in comparison to the crude extract (Table II). Fraction F3, in particular, has yielded a MIC value of 8.0 mg/ml against *V. alginolyticus* FB3, *Alteromonas* sp. FB7, and *Pseudoalteromonas* sp. FB9 similarly to the crude extract. The fraction F3 was found to be more effective towards *Pseudoalteromonas* sp. FB4, where the MIC was recorded to be equal to 4 mg/ml. In contrast, the MIC for fraction F3 against *Bacillus* sp. FB13 increased from 0.13 mg/ml to 0.50 mg/ml, indicating a reduction in antimicrobial activity.

Further separation of fraction F3 on the prepared TLC plate with the solvent system Hex: EtOAc (1:9 v/v) yielded five sub-fractions (under long UV light), namely: fluorescent green (R_f 0.55), light blue (R_f 0.71), light yellow (R_f 0.78), and light blue (R_f 0.84 and 0.90, respectively). All sub-fractions on *V. alginolyticus* FB3 were subjected to disc diffusion assay and the sub-fraction R_f 0.55 was identified as the only sub-fraction that showed inhibitory effect against the FB tested (data not

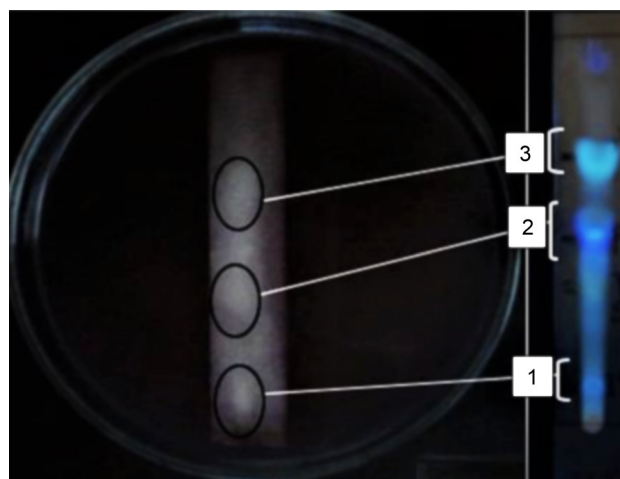


Fig. 2. Agar-overlay assay of ethyl acetate extract of *Pseudoalteromonas* sp. IBRL PD4.8 against *V. alginolyticus* FB3. Circle (1) light yellow, R_f 0.06; (2) fluorescent blue, R_f 0.35; (3) fluorescent green, R_f 0.55.

Table III
Characteristics of compounds from LC-MS analysis of sub-fraction F3a.

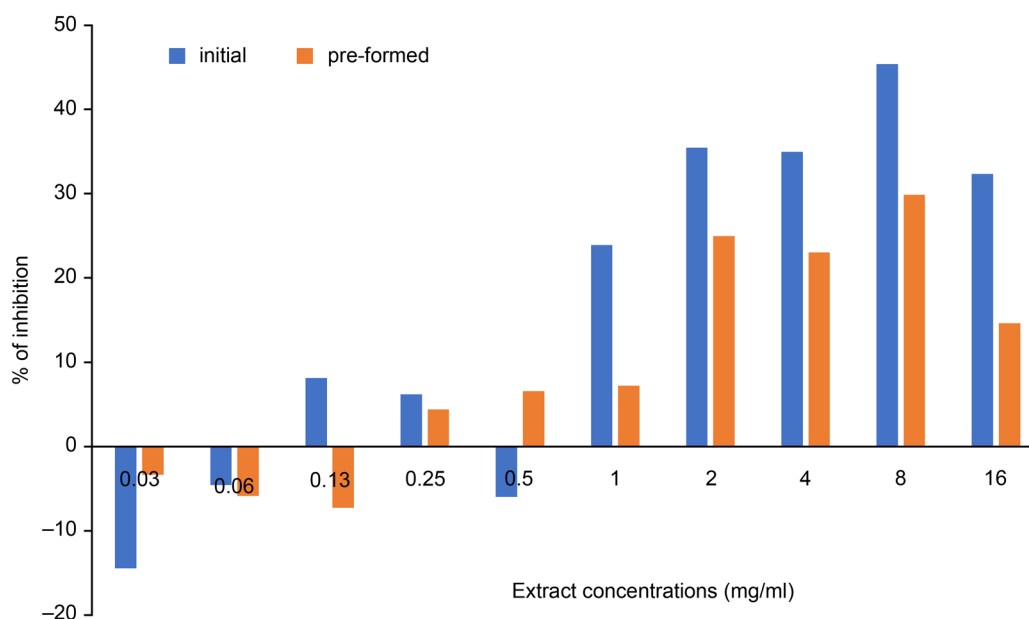
No.	R _T (min)	Compound	Mass	m/z [M-H] ⁻	Formula	Score (DB)
1	4.233	Sulfate	97.967	96.9597	H ₂ O ₄ S	98.79
2	4.906	4,7,10,13-hexadecatetraenoic acid	248.1763	293.1748	C ₁₆ H ₂₄ O ₂	84.93
3	5.662	Homoveratric acid	196.0729	241.071	C ₁₀ H ₁₂ O ₄	95.41
4	6.809	Isoacitrein	326.1891	325.1821	C ₂₁ H ₂₆ O ₃	84.11
5	6.923	Sodium tetradecyl sulfate	294.1859	293.1779	C ₁₄ H ₃₀ O ₄ S	86.66
6	7.617	D1-2-Hydroxymethylethisteron	340.2048	339.1978	C ₂₂ H ₈ O ₃	85.00

shown). It appeared as a yellow paste and was subsequently denoted as sub-fraction F3a.

LC-MS analysis. The LC-MS analysis of sub-fraction F3a identified 23 secondary metabolites within the retention times (R_T) of 4.093 to 11.838 min (in the Supplementary Material). Based on the results of the searchable MS spectra libraries (Agilent METLIN Personal Metabolite Database), only six were identifiable and matched >80% of the database search match score (score DB). The six compounds were sulfate, 4,7,10,13-hexadecatetraenoic acid, homoveratric acid, isoacitrein, sodium tetradecyl sulphate, and D1-2-Hydroxymethylethisteron. Table III summarizes the characteristics of the identified compounds. Furthermore, 12 out of the remaining 17 unidentified compounds

were found to be nitrogen-containing compounds. The compound 4,7,10,13-hexadecatetraenoic acid (C₁₆H₂₄O₂) as a type of polyunsaturated fatty acids was anticipated to be the compound responsible for the antibacterial activity of the sub-fraction F3a.

Microtiter plate biofilm inhibition assay. Figure 3 shows the percentage of the biofilm inhibition versus the extract concentrations (0.03–16 mg/ml). At the low extract concentrations of 0.03 and 0.06 mg/ml, the initial biofilm formation was stimulated by 14.44 ± 24.73% and 4.54 ± 10.54%, respectively, which is what was demonstrated by the negative values of graph bars in Fig. 3. Furthermore, inhibition of the initial biofilm was also observed when the extract concentration increased from 0.13 mg/ml (8.17 ± 8.42%) to



Extract concentrations (mg/ml)	0.03	0.06	0.13	0.25	0.50	1.00	2.00	4.00	8.00	16.00
Initial biofilm (%)	-14.44 ± 24.73	-4.54 ± 10.54	8.17 ± 8.42	6.22 ± 12.15	-5.97 ± 30.14	23.88 ± 7.54	35.44 ± 8.06	34.96 ± 3.75	45.37 ± 4.88	32.32 ± 12.24
Pre-formed biofilm (%)	-3.30 ± 17.02	-5.84 ± 13.51	-7.24 ± 4.62	4.44 ± 8.78	6.61 ± 3.88	7.24 ± 10.72	24.97 ± 9.64	23.03 ± 3.17	29.85 ± 2.56	14.61 ± 15.15

Fig. 3. Antibiofilm activity of *Pseudoalteromonas* sp. IBRL PD4.8 extract against initial and pre-formed biofilm of *V. alginolyticus* FB3. Data of inhibition percentages are presented in the table below the figure.

0.25 mg/ml ($6.22 \pm 12.15\%$). However, it was retarded at 0.50 mg/ml before the biofilm production was re-induced ($-5.97 \pm 30.14\%$). At 1.0 to 8.0 mg/ml, gradual increase of inhibition was observed from $23.88 \pm 7.54\%$ (1.0 mg/ml) to $45.37 \pm 4.88\%$ (8.0 mg/ml) accordingly. The biofilm inhibition was only reduced ($32.32 \pm 12.24\%$) at a concentration of 16.0 mg/ml.

Although inhibitory activity of the extract against the pre-formed biofilm was less effective in comparison with the initial biofilm, their inhibition patterns were comparable (Fig. 3). The pre-formed biofilm production was induced at lower extract concentrations of 0.03 mg/ml ($-3.30 \pm 17.02\%$), 0.06 mg/ml ($-5.84 \pm 13.51\%$), and 0.13 mg/ml ($-7.24 \pm 4.62\%$). Furthermore, gradual increments in the antibiofilm activity were also observed when the extract concentrations increased from 0.25 mg/ml ($4.44 \pm 8.78\%$) to 0.50 mg/ml ($6.61 \pm 3.88\%$) and 1.0 mg/ml ($7.24 \pm 10.72\%$), accordingly. Additionally, the highest inhibition of the pre-formed biofilm was detected at 8.0 mg/ml ($29.85 \pm 2.56\%$), but it was statistically not significant ($p > 0.005$).

LM study. Hypothetically, the coloration of the purple image observed under LM arised from a positively charged CV stain that bounded to the envelopes of negatively charged cells and biofilm matrix. The LM results in Fig. 4 indicated that the extract was capable of inhibiting the initial and pre-formed biofilm of *V. alginolyticus* FB3 at 8.0 mg/ml. Meanwhile, Fig. 4a and 4c depicted the untreated sets of the initial and pre-formed biofilms, respectively. The deep purple colors from both figures were suggestive of highly dense biofilms that consisted of extracellular polymeric substances (EPS) matrix that entrapped the microcolonies. In the initial biofilm set, its exposure to the extract resulted in complete eradication of the biofilm, which left unbound cells and thin strands of damaged biofilms only (Fig. 4b). However, these results also showed that the pre-formed biofilm was less disrupted when treated with the extract at 8.0 mg/ml (Fig. 4). Some small dark patches of biofilms, in particular, have been seen to crumple together into a denser form.

SEM study. The SEM observations have revealed significant destructive effects on both initial and pre-formed

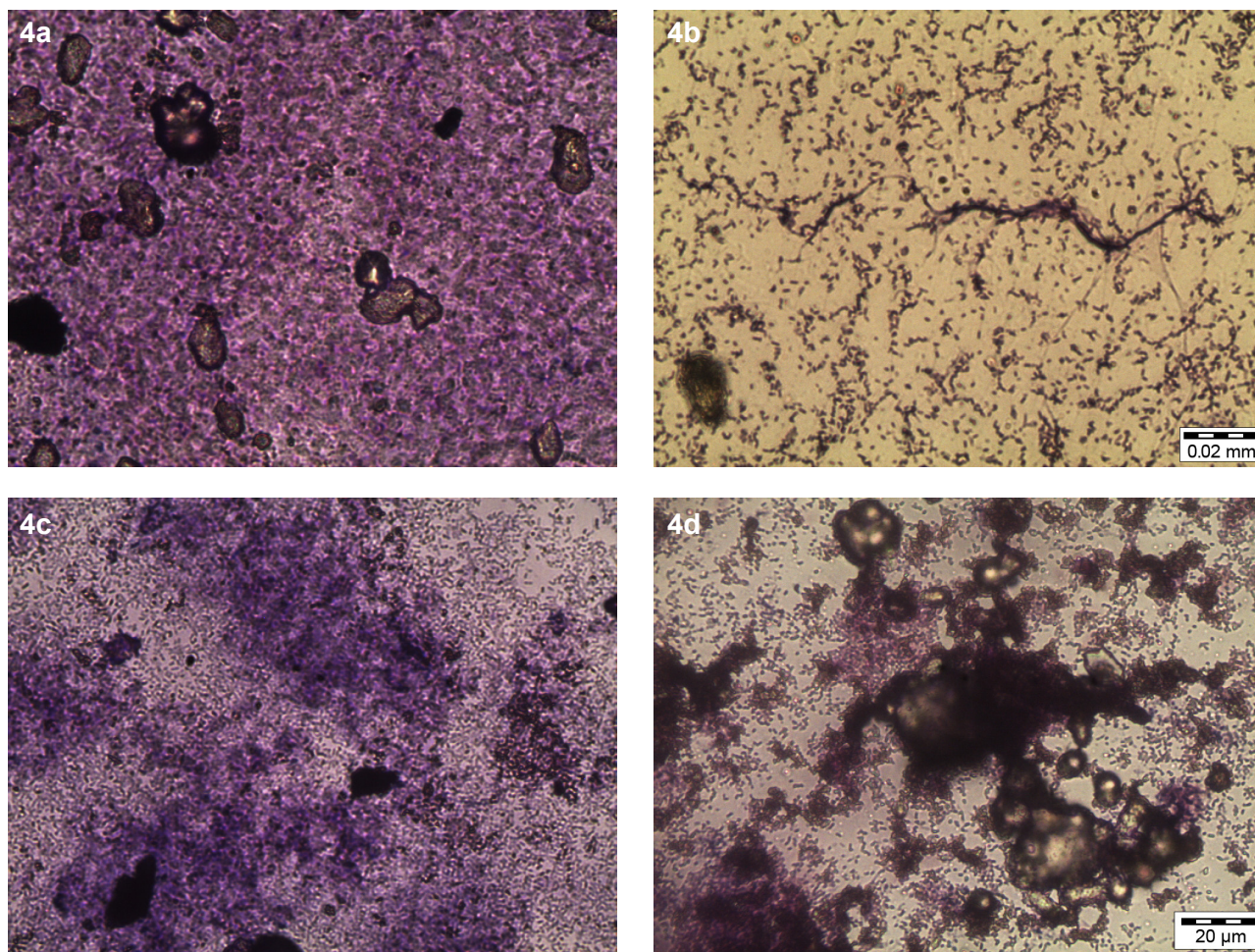


Fig. 4. The light microscopy images of *V. alginolyticus* FB3 biofilms treated with *Pseudoalteromonas* sp. IBRL PD4.8 extract.

A. Untreated initial biofilm; B. initial biofilm treated with 8.0 mg/ml; C. untreated pre-formed biofilm; D. pre-formed biofilm treated with 8.0 mg/ml; bar = 20 μ m.

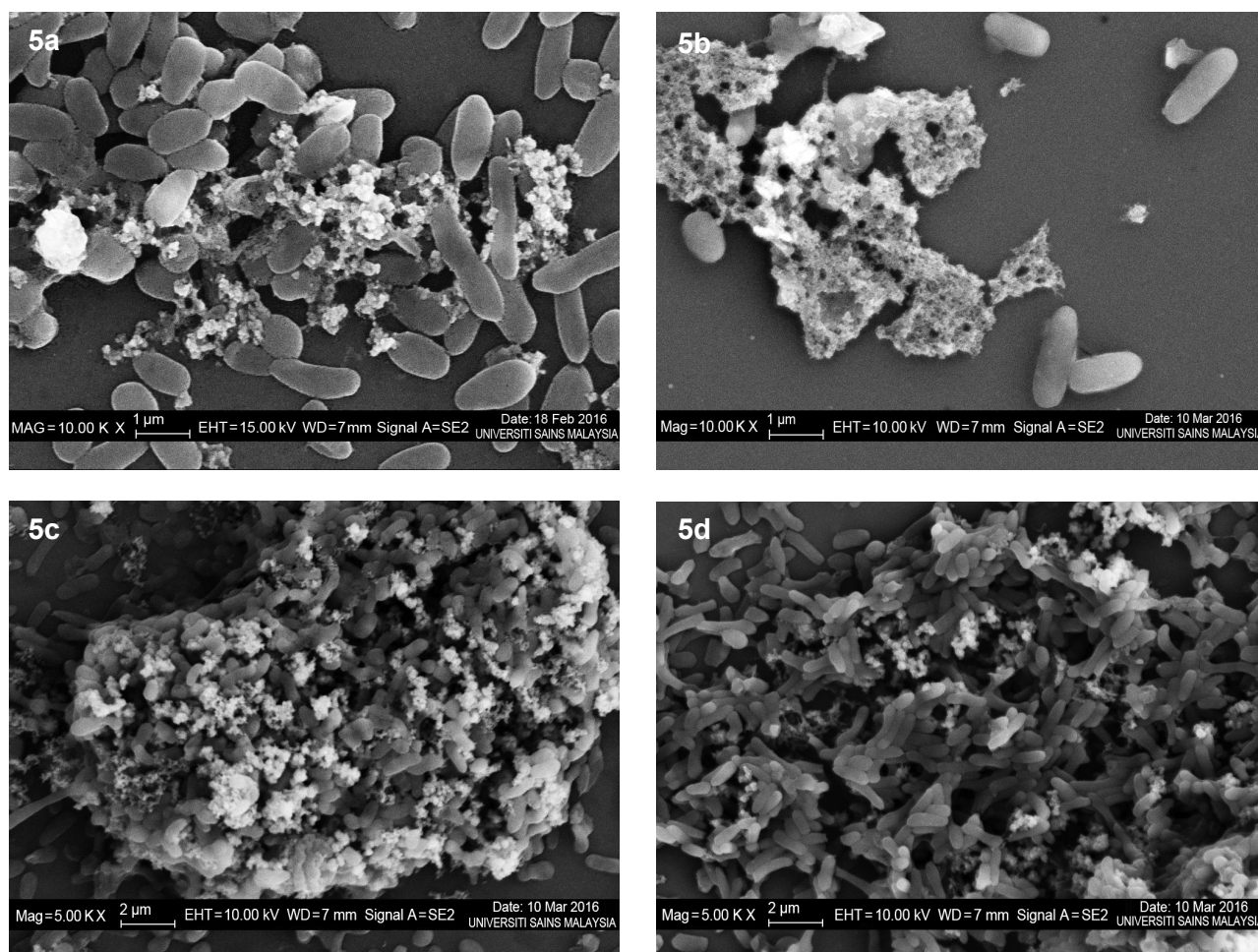


Fig. 5. The scanning electron microscopic images of *V. alginolyticus* FB3 biofilms treated with the extract at a concentration of 8.0 mg/ml. A. untreated initial biofilm (10 000 \times); B. treated initial biofilm (10 000 \times); C. untreated pre-formed biofilm (5000 \times); D. treated pre-formed biofilm (5000 \times).

biofilm architectures when treated with an extract at a concentration of 8.0 mg/ml (Fig. 5). The untreated initial biofilm shown the very low density of EPS within microcolonies that aggregated together (Fig. 5a). In contrast, the untreated pre-formed biofilm displayed more copious and non-homogenized production of EPS and microcolonies (Fig. 5c). The multilayer biofilms entrapped the microcolonies in a more complex arrangement. Moreover, the treated initial biofilm revealed that both microcolonies and EPS components alike were adversely destroyed and clumped together into unrecognised shape (Fig. 5b). Meanwhile, the treated pre-formed biofilm indicated drastic reductions with partially vanished EPS components that served to protect the cells, thereby contributing to a less compact structure (Fig. 5d).

Discussion

The present study was intended to investigate the inhibitory activity of the extract from *Pseudoalteromonas* sp. IBRL PD4.8 against fouling bacteria and

biofilm production. The results have subsequently revealed that its ethyl acetate extract possesses a wide spectrum of antimicrobial activity by inhibiting both Gram-positive and Gram-negative fouling bacteria. This is the intimation that the extract may be capable of controlling complex microbial population and preventing subsequent biofouling process (Kwon et al. 2002). Only few reports have described the microbial extracts that inhibited multiple strains of fouling bacteria, and were recognized to be potential sources for the development of non-toxic antifouling compounds. One example is the ethyl acetate extract of *Streptomyces filamentous* R1, which was isolated from the sediment sample and inhibited three fouling bacteria (*Bacillus* sp. (BB11), *Serratia* sp. (BB13), and *Alteromonas* sp. (BB14)) (Bayva et al. 2011). Besides, another study has specifically depicted the fractions of ethyl acetate extract obtained from a marine fungus, *Cladosporium* sp. 14. It showed strong inhibitory effect and influenced the growth of three larval-settlement inducing bacteria, namely *Laktonella hongkongensis*, *Micrococcus luteus*, and *Rhodovulum* sp. (Qi et al. 2009).

In the disc diffusion and MIC assays, *Bacillus* sp. FB13 has appeared to be the most susceptible FB strain towards the extract compared to other Gram-negative FB. The less virulent property of this particular strain may be attributed to its cell wall structures, whereby it is a Gram-positive bacterium with a thick cell wall in the peptidoglycan layer and lacks the outer membrane layer. The outer membrane layer of a Gram-negative bacterium typically consists of an outer membrane with lipopolysaccharides and phospholipids, which is an effective barrier and prevents the passage of foreign molecules, including antibiotics (Nikaido 2003). Furthermore, the presence of the efflux pump within the cell envelope of the Gram-negative FB may also actively functions in expelling antibiotic molecules from its cytoplasm. This subsequently results in the reduced intracellular accumulation of antibiotics, thus minimizing the antimicrobial effect (Abdallah et al. 2007).

The antibacterial activity present in the ethyl acetate extracts of *Pseudoalteromonas* sp. against marine bacteria has already been discovered (Hayashida-Soiza et al. 2008; Bernbom et al. 2011). Similarly, the ethyl acetate extract of *P. haloplanktis* INH isolated from a scallop hatchery has also shown a powerful antibacterial activity against various marine and clinical pathogens, which includes *V. alginolyticus* ATCC 17749, *Pseudomonas fluorescens* IFO 3903, *Escherichia coli* IFO 3366, and *Staphylococcus aureus* IFO 13276. The antibacterial compound has been identified as isovaleric acid (Hayashida-Soiza et al. 2008). Moreover, three ethyl acetate extracts of *Pseudoalteromonas* isolates have been isolated from the deep-sea sediment of West Pacific Ocean, which also displayed antibacterial activity against several biofilm-forming bacteria from Hong Kong waters (Xu et al. 2007). Similarly, two diketopiperazines identified as cyclo-(L-Ph-L-Pro) and cyclo-(L-Leu-L-Pro) have been isolated from *Pseudoalteromonas* sp. of octoral *Leptogorgia alba* (Martinez-Luis et al. 2011). At 100 µg/ml, both compounds have revealed a strong growth inhibitory effect on *Vibrio* sp. and *B. subtilis*, with the diameter of inhibitions of 14.5 to 25.0 mm.

From the LC-MS result, a polyunsaturated fatty acid named 4,7,10,13-hexadecatetraenoic acid (C₁₆H₂₄O₂) has been predicted to be potentially responsible for the antibacterial activity against the fouling bacteria. No antimicrobial report has been found for the remaining five identified compounds (i.e. sulphate, homoveratric acid, isoacitretin, sodium tetradecyl sulphate, and D1-2-Hydroxymethylethisteron) accordingly, thus rendering them not attributed as potentially antibacterial compounds. Therefore, fatty acids have emerged as new and promising antimicrobial agents due to a strong and broad range of activities, and low likelihood of inducing bacterial resistance (Georgel et al. 2005; Desbois 2012). Previously, two short fatty acid chains

called isovaleric acid (C₅H₁₀O₂) and 2-methylbutyric acid (C₅H₁₀O₂) have been isolated from the ethyl acetate extract of *P. haloplanktis* INH, and inhibited growth of six marine strains and eight clinical strains (Hayashida-Soiza et al. 2008). Besides, some polyunsaturated fatty acids with antibacterial activity have also been isolated from marine sources, such as, (6Z, 9Z, 12Z)-hexadecatetraenoic acid (HTA) from a marine diatom and were effective against terrestrial and marine pathogens (Desbois 2012). Other examples also include stearidonic acid and gamma-linoleic acid sourced from the dried thalli of *Enteromorpha linza*, which displayed low MIC values against some oral pathogens like *Candida albicans* and *Poryphyromonas gingivalis* (Park et al. 2013).

Several antibacterial mechanisms can be proposed in elucidating the predicted 4,7,10,13-hexadecatetraenoic acid activities against susceptible fouling bacteria. The first mechanism can involve disruption of the bacterial cell membrane. The amphipathic structure and aliphatic chains of the fatty acids serve to facilitate the compound's interaction with cell membrane components to form pores (Desbois and Smith 2010). Similarly, a toxic fatty acid like palmitoleate could create various sizes of pores at the cytoplasmic membrane of *S. aureus*, thus allowing the leakage of intracellular compounds (Parsons et al. 2012). Moreover, a significantly higher fatty acid concentration may cause a disastrous effect on the cell membrane via its solubilisation into fragmented parts (Desbois and Smith 2010). The second mechanism may be through the inhibition of bacterial enzymatic activity. It has been shown that lineolic acid inhibited the FabI enzyme, which is essential for the biosynthesis of fatty acids in bacterial cell membranes (Zheng et al. 2005). Besides, the fatty acids also aid in cell lysis (Shin et al. 2007), reducing energy production in the electron transport chain system (Cartron et al. 2014), block nutrient uptake (Galbraith and Miller 1973), and peroxidation or auto-oxidation of the cells due to degraded products of the fatty acids (Wang and Johnson 1992).

In biofouling, the presence of biofilm is important to induce the settlement of larvae and spores, while also serving as a protective barrier against the antifoulant. In this study, *V. alginolyticus* FB3 has been selected due to the high amount of biofilm produced when compared to the other FB.

Generally, the extract obtained in this study had the ability to inhibit both the initial and pre-formed biofilms of *V. alginolyticus* FB3 (Fig. 3). It also shown a biphasic effect on the biofilms, since biofilm formation was induced in low extract concentration and inhibited at a higher extract concentration (Murado and Vázquez 2010). This finding is similar to that of Kaplan (2011), who demonstrated the induction of the formation of biofilm by three MRSA strains when treated with methicillin at sub-MIC concentrations. At sub-MIC,

the methicillin triggered the extracellular (eDNA) and auto-aggregation mechanisms, subsequently aiding the formation processes, i.e., the initial attachment, early development, and stability retainment. Additionally, low concentrations (sub-MIC) of carbenicillin, cephaloridine, and ticarcillin have induced the expression of the *cps* gene, which is responsible for the synthesis of colonic acid capsular polysaccharide, and specific for mature biofilm of *E. coli* (Sailer et al. 2003).

Furthermore, some works have also reported the antibiofilm activities of *Pseudoalteromonas* species against pathogens. Strains of *P. nigrifaciens* and *P. flavipulchra* SktPp1, in particular, showed a reduction in the formation of *V. cholera* (Waturangi et al. 2011) and *Serratia marcescens* (Iqbal et al. 2015) biofilms, respectively. Meanwhile, the biofilms of *S. marcescens* treated with the crude extract of *P. flavipulchra* SktPp1 were reduced by 26.9% at a concentration of 0.1 mg/ml when compared to the control (Iqbal et al. 2015). Similarly, the filter-sterilized supernatant of *Pseudoalteromonas* sp. KS8 reduced the biofilm formation and the mass of mature biofilms of *P. aeruginosa* PAO1 by 63% and 33%, respectively (Buseti et al. 2015). The antibiofilm activity may be due to inhibition of the signaling molecule acyl-homoserine lactone (AHL) in a quorum sensing (QS) system of the *P. aeruginosa* PAO1. QS can be described as a process of cell-cell communication, allowing the bacteria to share information about cell density and secretion of a signaling molecule called auto-inducer signals (Miller and Bassler 2001). The system is particularly crucial in biofilm development as it permits a communication between cells to increase the population densities and consequently induce biofilm formation (Pearson et al. 1999; Lade et al. 2014). In the work by Ponnusamy et al. (2013), a significant reduction of initial biofilms of *A. hydrophila* has been detected under SEM and it correlated with the low amount of AHLs detected. Additionally, anti-biofilm and anti-QS activities have also been identified in the biofilm layer of *S. pyogenes*, which depicted the absence of dense biofilm layers upon treatment with the coral-associated bacterial extract (Thenmozhi et al. 2009).

In this study, the highest percentage of *V. alginolyticus* FB3 biofilm inhibition has been achieved at the concentration of the extract up to 8.0 mg/ml. Such mild inhibitory activity may be contributed to antagonistic actions of the compounds present together with the bioactive compounds. The purified compounds are generally more active than the crude extract, provided there is no synergistic enhancement within the mixture (Liu and Zhao 2016). Therefore, a bioassay-guided fractionation of the crude extract with antibiofilm activity is required to isolate the active antibiofilm compound. As it was shown in Fig. 3, the lower percentage of inhibition at a higher extract concentration (16.0 mg/ml)

when compared to inhibition at 8.0 mg/ml is presumably due to the stimulation of stress-response genes of the biofilms. At that particular concentration, the extract may have become the 'stressors' and rendered the development of protective or adaptive stress-response, promoting biofilm formation and antimicrobial resistance (Poole 2012). One example of such stress-response is the improved number of persisters that are highly tolerant to antimicrobials (Keren et al. 2004). Persisters can be described as a small subpopulation of dormant cells that survive the treatment of bactericidal antibiotic (Lewis 2010). Nonetheless, the outcomes for every antibiofilm assay is different from one another, depending on the different types of biofilms that can be formed by the microorganisms.

Moreover, the qualitative biofilm assays such as LM and SEM provided results that indicated lower disruption of the pre-formed biofilm in comparison with the initial biofilm (Fig. 4 and 5). Based on these observations, the extract may have interfered with the initial bacterial attachment on the surface, thus preventing the formation of biofilms. This is due to bacterial attachment to a surface being the initial and fundamental step in the formation of a biofilm (O'Toole et al. 2000). Moreover, the antibacterial property of the extract may have rendered some of the planktonic cells of *V. alginolyticus* FB3 to be suppressed before the coverslip surface is colonized. The attachment surface may have also been modified by the extract, thus hindering bacterial colonization and biofilm development (Lewandowski and Beyenal 2014).

The glass coverslips used as the substratum is hydrophilic in nature and display high wetting capacity, in which the conditioning layer and biofilms tend to form strong adhesion (Ben Abdallah et al. 2014). In this study, the bioactive compounds in the extract may have played a role as the biosurfactant or bioemulsifier to the surface, repelling bacterial attachment and biofilm development (Neu 1996). Additionally, microbial polyphilic (also known as amphiphilic) polymers like polysaccharides and lipoteichoic acids also contain hydrophobic substituents like methyl and acyl groups, which are structurally crucial in producing a hydrophobically modified surface (Neu 1996). Therefore, the physically modified surface might have interfered with the initial bacterial adhesion and subsequently prevented biofilm formation. This amphiphilic criterion inadvertently matched the characteristic of the identified polyunsaturated fatty acid 4,7,10,13-hexadecatetrenoic acid in sub-fraction F3a, which contains a methyl group at one of its ends. Similarly, hexadecanoic acid and lineolic acid have also depicted antibiofilm activity against *Vibrio* spp. (Santhakumari et al. 2016), and *Streptococcus mutants* (Jung et al. 2014) via their surface-active compounds properties. Microscopic

observations of the affected *Vibrio* spp. biofilms have indicated that the hexadecanoic acid reduced the initial attachment and disintegrated the mature biofilms.

In this study, SEM of the pre-formed biofilms has revealed that the biofilms were structurally thicker, hence reaffirming their function as the protective barrier that limits the entrance of antifoulants into the biofilm. Nithya and Pandian (2010) have suggested that the antibiofilm activity against the tested *V. alginolyticus*, *V. parahaemolyticus*, and *V. vulnificus* respectively was due to inhibition of the initial attachment, biofilm formation, and dispersion of the mature biofilm. Furthermore, LM results by Santhakumari et al. (2016) have also revealed the prevention of initial attachment and disruption of mature biofilms of *V. harveyi* MTCC 3438 and *V. vulnificus* MTCC 1145 with the extract of cyanobacterial *Synechococcus* sp.

In the shipping industry, the removal and prevention of biofilm attachment from different ship compartments, especially the hulls and rotating discs will reduce frictional resistance. However, only a few studies have been carried out to investigate the effects of biofilm on the drag of a ship. Watanabe et al. (1969) have specifically predicted an increase of 9–10% ship resistance when slime fouling is attached to the concentric cylinders, rotating disks and a model ship. Similarly, a whopping 18% of reduced shaft horsepower is linked with propelling a ship when microbial biofilm and slight macrofouling are removed from its hull (Haslbeck and Bohlander 1992). Additionally, the composition and thickness of the biofilms can significantly influence the friction drag of a ship (Schultz and Swain 2000), as filamentous biofilms (slime and green algae) are found to cause higher skin friction. This is upon comparison with non-filamentous biofilms, thus highlighting and attributing towards biofilm complexities. All of these studies have successfully shown that biofilms can significantly increase the drag friction of a ship and reduce its speed.

In conclusion, the ethyl acetate extract of *Pseudoalteromonas* sp. IBRL PD4.8 contains an active compound known as 4,7,10,13-hexadecatetraenoic acid which can be a potential antibacterial compound against the fouling bacteria. It may prevent biofilm formation and eradicate established biofilm of the fouling bacteria *V. alginolyticus* FB3. Regardless, further investigation should be conducted to identify the specific active antibiofilm compound. Additionally, an incorporation of the extract into paint formulation should also be considered for future application purposes.

Acknowledgements

The authors acknowledge Universiti Sains Malaysia for the Research Grant (grant no. 1001/PBIOLOGI/815098) and Ministry of Higher Education of Malaysia for the MyBrain15 scholarship awarded.

Conflict of interest

The authors do not report any financial or personal connections with other persons or organizations, which might negatively affect the contents of this publication and/or claim authorship rights to this publication.

Literature

- Abu Sayem SM, Manzo E, Ciavatta L, Tramice A, Cordone A, Zanfardino A, De Felice M, Varcamonti M.** Anti-biofilm activity of an exopolysaccharide from a sponge-associated strain of *Bacillus licheniformis*. *Microb Cell Fact.* 2011;10(1):74. doi:10.1186/1475-2859-10-74 Medline
- Acevedo MS, Puentes C, Carreño K, León JG, Stupak M, García M, Pérez M, Blustein G.** Antifouling paints based on marine natural products from Colombian Caribbean. *Int Biodeterior Biodegradation.* 2013;83:97–104. doi:10.1016/j.ibiod.2013.05.002
- Bavya M, Mohanapriya P, Pazhanimurugan R, Balagurunathan R.** Potential bioactive compound from marine actinomycetes against biofouling bacteria. *Indian J Geomarine Sci.* 2011;40(4):578–582.
- Ben Abdallah F, Lagha R, Said K, Kallel H, Gharbi J.** Detection of cell surface hydrophobicity, biofilm and fimbriae genes in *Salmonella* isolated from Tunisian clinical and poultry meat. *Iran J Public Health.* 2014;43(4):423–431. Medline
- Bernbom N, Ng YY, Kjelleberg S, Harder T, Gram L.** Marine bacteria from Danish coastal waters show antifouling activity against the marine fouling bacterium *Pseudoalteromonas* sp. strain S91 and zoospores of the green alga *Ulva australis* independent of bacteriocidal activity. *Appl Environ Microbiol.* 2011;77(24):8557–8567. doi:10.1128/AEM.06038-11 Medline
- Braddy RF Jr.** No more tin, what now for fouling control. *J Protective Coating and Linings.* 2000;5(6):42–46.
- Burgess JG, Boyd KG, Armstrong E, Jiang Z, Yan L, Berggren M, May U, Pisacane T, Granmo Å, Adams DR.** The development of a marine natural product-based antifouling paint. *Biofouling.* 2003;19(sup1) Suppl:197–205. doi:10.1080/0892701031000061778 Medline
- Burmølle M, Webb JS, Rao D, Hansen LH, Sørensen SJ, Kjelleberg S.** Enhanced biofilm formation and increased resistance to antimicrobial agents and bacterial invasion are caused by synergistic interactions in multispecies biofilms. *Appl Environ Microbiol.* 2006;72(6):3916–3923. doi:10.1128/AEM.03022-05 Medline
- Busetti A, Shaw G, Megaw J, Gorman S, Maggs C, Gilmore B.** Marine-derived quorum-sensing inhibitory activities enhance the antibacterial efficacy of tobramycin against *Pseudomonas aeruginosa*. *Mar Drugs.* 2015;13(1):1–28. doi:10.3390/md13010001 Medline
- Cai W, De La Fuente L, Arias CR.** Biofilm formation by the fish pathogen *Flavobacterium columnare*: development and parameters affecting surface attachment. *Appl Environ Microbiol.* 2013;79(18):5633–5642. doi:10.1128/AEM.01192-13 Medline
- Cartron ML, England SR, Chiriac AI, Josten M, Turner R, Rauter Y, Hurd A, Sahl HG, Jones S, Foster SJ.** Bactericidal activity of the human skin fatty acid *cis*-6-hexadecanoic acid on *Staphylococcus aureus*. *Antimicrob Agents Chemother.* 2014;58(7):3599–3609. doi:10.1128/AAC.01043-13 Medline
- Cheng HR, Jiang N.** Extremely rapid extraction of DNA from bacteria and yeasts. *Biotechnol Lett.* 2006;28(1):55–59. doi:10.1007/s10529-005-4688-z Medline
- Davey ME, O'toole GA.** Microbial biofilms: from ecology to molecular genetics. *Microbiol Mol Biol Rev.* 2000;64(4):847–867. doi:10.1128/MMBR.64.4.847-867.2000 Medline

- Desbois AP, Smith VJ.** Antibacterial free fatty acids: activities, mechanisms of action and biotechnological potential. *Appl Microbiol Biotechnol.* 2010;85(6):1629–1642. doi:10.1007/s00253-009-2355-3 Medline
- Desbois AP.** Potential applications of antimicrobial fatty acids in medicine, agriculture and other industries. *Recent Pat Antiinfect Drug Discov.* 2012;7(2):111–122. doi:10.2174/157489112801619728 Medline
- Fitridge I, Dempster T, Guenther J, de Nys R.** The impact and control of biofouling in marine aquaculture: a review. *Biofouling.* 2012;28(7):649–669. doi:10.1080/08927014.2012.700478 Medline
- Floerl O, Sunde LM, Bloecher N.** Potential environmental risks associated with biofouling management in salmon aquaculture. *Aquacult Environ Interact.* 2016;8:407–417. doi:10.3354/aei00187
- Franks A, Egan S, Holmström C, James S, Lappin-Scott H, Kjelleberg S.** Inhibition of fungal colonization by *Pseudoalteromonas tunicata* provides a competitive advantage during surface colonization. *Appl Environ Microbiol.* 2006;72(9):6079–6087. doi:10.1128/AEM.00559-06 Medline
- Galbraith H, Miller TB.** Effect of long chain fatty acids on bacterial respiration and amino acid uptake. *J Appl Bacteriol.* 1973;36(4):659–675. doi:10.1111/j.1365-2672.1973.tb04151.x Medline
- Georgel P, Crozat K, Lauth X, Makrantonaki E, Seltmann H, Sovath S, Hoebe K, Du X, Rutschmann S, Jiang Z, et al.** A toll-like receptor 2-responsive lipid effector pathway protects mammals against skin infections with Gram-positive bacteria. *Infect Immun.* 2005;73(8):4512–4521. doi:10.1128/IAI.73.8.4512-4521.2005 Medline
- Guardiola FA, Cuesta A, Meseguer J, Esteban MA.** Risks of using antifouling biocides in aquaculture. *Int J Mol Sci.* 2012;13(2):541–1560. doi:10.3390/ijms13021541 Medline
- Haslbeck EG, Bohlander G.** Microbial biofilm effects on drag-lab and field. In: *Proceedings of the 1992 Ship Production Symposium*, 2–4 September 1992. New Orleans Hyatt Regency, New Orleans, Louisiana.
- Hayashida-Soiza G, Uchida A, Mori N, Kuwahara Y, Ishida Y.** Purification and characterization of antibacterial substances produced by a marine bacterium *Pseudoalteromonas haloplanktis* strain. *J Appl Microbiol.* 2008;105(5):1672–1677. doi:10.1111/j.1365-2672.2008.03878.x Medline
- Iqbal F, Usup G, Ahmad A.** Anti-biofilm activity of *Pseudoalteromonas flavipulchra* SktPp1 against *Serratia marcescens* SMJ-11. In: *Conference Proceedings of the 2015 UKM FST Postgraduate Colloquium*, 15–16 April 2015. Universiti Kebangsaan Malaysia, Malaysia.
- Isnansetyo A, Kamei Y.** MC21-A, a bactericidal antibiotic produced by a new marine bacterium, *Pseudoalteromonas phenolica* sp. nov. O-BC30^T, against methicillin-resistant *Staphylococcus aureus*. *Antimicrob Agents Chemother.* 2003;47(2):480–488. doi:10.1128/AAC.47.2.480-488.2003 Medline
- Iwata H, Tanabe S, Mizuno T, Tatsukawa R.** High accumulation of toxic butyltins in marine mammals from Japanese coastal waters. *Environ Sci Technol.* 1995;29(12):2959–2962. doi:10.1021/es00012a011 Medline
- Jiang P, Li J, Han F, Duan G, Lu X, Gu Y, Yu W.** Antibiofilm activity of an exopolysaccharide from marine bacterium *Vibrio* sp. QY101. *PLoS One.* 2011;6(4):e18514. doi:10.1371/journal.pone.0018514 Medline
- Jung JE, Pandit S, Jeon JG.** Identification of linoleic acid, a main component of the *n*-hexane fraction from *Dryopteris crassirhizoma*, as an anti-*Streptococcus mutans* biofilm agent. *Biofouling.* 2014;30(7):789–798. doi:10.1080/08927014.2014.930446 Medline
- Kaplan JB.** Antibiotic-induced biofilm formation. *Int J Artif Organs.* 2011;34(9):737–751. doi:10.5301/ijao.5000027 Medline
- Keren I, Kaldalu N, Spoering A, Wang Y, Lewis K.** Persister cells and tolerance to antimicrobials. *FEMS Microbiol Lett.* 2004;230(1):13–18. doi:10.1016/S0378-1097(03)00856-5 Medline
- Kim W, Kim Y, Kim J, Nam BH, Kim DG, An C, Lee J, Kim P, Lee H, Oh JS, et al.** Liquid chromatography-mass spectrometry-based rapid secondary-metabolite profiling of marine *Pseudoalteromonas* sp. M2. *Mar Drugs.* 2016;14(1):24. doi:10.3390/md14010024 Medline
- Koch B, Liljefors T, Persson T, Nielsen J, Kjelleberg S, Givskov M.** The LuxR receptor: the sites of interaction with quorum-sensing signals and inhibitors. *Microbiology.* 2005;151(11):3589–3602. doi:10.1099/mic.0.27954-0 Medline
- Kwon KK, Lee HS, Jung S-Y, Yim J-H, Lee J-H, Lee HK.** Isolation and identification of biofilm-forming marine bacteria on glass surfaces in Dae-Ho, Korea. *J Microbiol.* 2002;40(4):260–266.
- Lade H, Paul D, Kweon JH.** Quorum quenching mediated approaches for control of membrane biofouling. *Int J Biol Sci.* 2014;10(5):550–565. doi:10.7150/ijbs.9028 Medline
- Lewandowski Z, Beyenal H.** *Fundamentals of biofilm research.* 2014. Boca Raton (Florida): CRC Press. p. 1–61.
- Lewis K.** Persister Cells. *Annu Rev Microbiol.* 2010;64(1):357–372. doi:10.1146/annurev.micro.112408.134306 Medline
- Limna Mol VP, Raveendran TV, Parameswaran PS.** Antifouling activity exhibited by secondary metabolites of the marine sponge, *Haliclona exigua* (Kirkpatrick). *Int Biodeterior Biodegradation.* 2009;63(1):67–72. doi:10.1016/j.ibiod.2008.07.001
- Liu Y, Zhao H.** Predicting synergistic effects between compounds through their structural similarity and effects on transcriptomes. *Bioinformatics.* 2016;32(24):3782–3789. doi:10.1093/bioinformatics/btw509 Medline
- Martínez-Luis S, Ballesteros J, Gutiérrez M.** Antibacterial constituents from the octoral associated bacterium *Pseudoalteromonas* sp. *Rev Latinoam Quím.* 2011;39(1-2):75–83.
- Miller MB, Bassler BL.** Quorum sensing in bacteria. *Annu Rev Microbiol.* 2001;55(1):165–199. doi:10.1146/annurev.micro.55.1.165 Medline
- Mitova M, Tutino ML, Infusini G, Marino G, De Rosa S.** Exocellular peptides from Antarctic psychrophile *Pseudoalteromonas haloplanktis*. *Mar Biotechnol (NY).* 2005;7(5):523–531. doi:10.1007/s10126-004-5098-2 Medline
- Murado MA, Vázquez JA.** Biphasic toxicodynamic features of some antimicrobial agents on microbial growth: a dynamic mathematical model and its implications on hormesis. *BMC Microbiol.* 2010;10:220. Medline
- Neu TR.** Significance of bacterial surface-active compounds in interaction of bacteria with interfaces. *Microbiol Rev.* 1996;60(1):151–166. Medline
- Nikaido H.** Molecular basis of bacterial outer membrane permeability revisited. *Microbiol Mol Biol Rev.* 2003;67(4):593–656. doi:10.1128/MMBR.67.4.593-656.2003 Medline
- Nikolić M, Vasić S, Djurdjević J, Stefanović O, Čomić L.** Antibacterial and anti-biofilm activity of ginger (*Zingiber officinale* (Roscoe)) ethanolic extract. *Kragujevac J Sci.* 2014;36(36):129–136. doi:10.5937/KgJSci1436129N
- Nithya C, Pandian SK.** The *in vitro* antibiofilm activity of selected marine bacterial culture supernatants against *Vibrio* spp. *Arch Microbiol.* 2010;192(10):843–854. doi:10.1007/s00203-010-0612-6 Medline
- Nor Afifah S, Darah I, Sharifah Radziah MN, Wan Norhana MN, Ahmad I.** Inhibition of fouling bacteria by the marine epiphytes from selected locations in Malaysia. *Mal J Sci.* 2017;36(1):17–21.
- O’Toole G, Kaplan HB, Kolter R.** Biofilm formation as microbial development. *Annu Rev Microbiol.* 2000;54(1):49–79. doi:10.1146/annurev.micro.54.1.49 Medline

- Olson ME, Ceri H, Morck DW, Buret AG, Read RR.** Biofilm bacteria: formation and comparative susceptibility to antibiotics. *Can J Vet Res.* 2002;66(2):86–92. [Medline](#)
- Park NH, Choi JS, Hwang SY, Kim YC, Hong YK, Cho K, Choi I, Choi IS.** Antimicrobial activities of stearidonic and gamma-linolenic acids from the green seaweed *Enteromorpha linza* against several oral pathogenic bacteria. *Bot Stud (Taipei, Taiwan).* 2013; 54(1):39. [doi:10.1186/1999-3110-54-39](#) [Medline](#)
- Parsons JB, Yao J, Frank MW, Jackson P, Rock CO.** Membrane disruption by antimicrobial fatty acids releases low-molecular-weight proteins from *Staphylococcus aureus*. *J Bacteriol.* 2012; 194(19):5294–5304. [doi:10.1128/JB.00743-12](#) [Medline](#)
- Pearson JP, Van Delden C, Iglewski BH.** Active efflux and diffusion are involved in transport of *Pseudomonas aeruginosa* cell-to-cell signals. *J Bacteriol.* 1999;181(4):1203–1210. [Medline](#)
- Ponnusamy K, Kappachery S, Thekeettle M, Song JH, Kweon JH.** Anti-biofouling property of vanillin on *Aeromonas hydrophila* initial biofilm on various membrane surfaces. *World J Microbiol Biotechnol.* 2013;29(9):1695–1703. [doi:10.1007/s11274-013-1332-2](#) [Medline](#)
- Poole K.** Stress responses as determinants of antimicrobial resistance in Gram-negative bacteria. *Trends Microbiol.* 2012;20(5): 227–234. [doi:10.1016/j.tim.2012.02.004](#) [Medline](#)
- Qi SH, Xu Y, Xiong HR, Qian PY, Zhang S.** Antifouling and anti-bacterial compounds from a marine fungus *Cladosporium* sp. F14. *World J Microbiol Biotechnol.* 2009;25(3):399–406. [doi:10.1007/s11274-008-9904-2](#)
- Rao D, Webb JS, Holmström C, Case R, Low A, Steinberg P, Kjelleberg S.** Low densities of epiphytic bacteria from the marine alga *Ulva australis* inhibit settlement of fouling organisms. *Appl Environ Microbiol.* 2007;73(24):7844–7852. [doi:10.1128/AEM.01543-07](#) [Medline](#)
- Sailer FC, Meberg BM, Young KD.** beta-Lactam induction of colanic acid gene expression in *Escherichia coli*. *FEMS Microbiol Lett.* 2003;226(2):245–249. [doi:10.1016/S0378-1097\(03\)00616-5](#) [Medline](#)
- Santhakumari S, Kannappan A, Pandian SK, Thajuddin N, Rajendran RB, Ravi AV.** Inhibitory effect of marine cyanobacterial extract on biofilm formation and virulence factor production of bacterial pathogens causing vibriosis in aquaculture. *J Appl Phycol.* 2016;28(1):313–324. [doi:10.1007/s10811-015-0554-0](#)
- Schultz MP, Swain GW.** The influence of biofilms on skin friction drag. *Biofouling.* 2000;15(1-3):129–139. [doi:10.1080/08927010009386304](#) [Medline](#)
- Shin SY, Bajpai VK, Kim HR, Kang SC.** Antibacterial activity of eicosapentaenoic acid (EPA) against foodborne and food spoilage microorganisms. *Lebensm Wiss Technol.* 2007;40(9):1515–1519. [doi:10.1016/j.lwt.2006.12.005](#)
- Tamura K, Stecher G, Peterson D, Filipinski A, Kumar S.** MEGA6: Molecular evolutionary genetics analysis version 6.0. *Mol Biol Evol.* 2013;30(12):2725–2729. [doi:10.1093/molbev/mst197](#) [Medline](#)
- Thenmozhi R, Nithyanand P, Rathna J, Karutha Pandian S.** Antibiofilm activity of coral-associated bacteria against different clinical M serotypes of *Streptococcus pyogenes*. *FEMS Immunol Med Microbiol.* 2009;57(3):284–294. [doi:10.1111/j.1574-695X.2009.00613.x](#) [Medline](#)
- Townsin RL.** The ship hull fouling penalty. *Biofouling.* 2003; 19(sup1) Suppl:9–15. [doi:10.1080/0892701031000088535](#) [Medline](#)
- Wang L-L, Johnson EA.** Inhibition of *Listeria monocytogenes* by fatty acids and monoglycerides. *Appl Environ Microbiol.* 1992 Feb; 58(2):624–629. [Medline](#)
- Watanabe S, Nagamatsu N, Yokoo K, Kawakami Y.** The augmentation in frictional resistance due to slime. *J Kansai Soc Nav Arch.* 1969;131:45–51.
- Waturangi DE, Bunardi YA, Magdalena S.** Antibiofilm activity of bacteria isolated from marine environment in Indonesia against *Vibrio cholerae*. *Res J Microbiol.* 2011;6(12):926–930. [doi:10.3923/jm.2011.926.930](#)
- Xu Y, Miao L, Li XC, Xiao X, Qian PY.** Antibacterial and anti-larval activity of deep-sea bacteria from sediments of the West Pacific Ocean. *Biofouling.* 2007;23(2):131–137. [doi:10.1080/08927010701219323](#) [Medline](#)
- Zeng Z, Guo XP, Cai X, Wang P, Li B, Yang JL, Wang X.** Pyomelanin from *Pseudoalteromonas lipolytica* reduces biofouling. *Microb Biotechnol.* 2017;10(6):1718–1731. [doi:10.1111/1751-7915.12773](#) [Medline](#)
- Zeng Z, Guo XP, Li B, Wang P, Cai X, Tian X, Zhang S, Yang JL, Wang X.** Characterization of self-generated variants in *Pseudoalteromonas lipolytica* biofilm with increased antifouling activities. *Appl Microbiol Biotechnol.* 2015;99(23):10127–10139. [doi:10.1007/s00253-015-6865-x](#) [Medline](#)
- Zheng L, Chen H, Han X, Lin W, Yan X.** Antimicrobial screening and active compound isolation from marine bacterium NJ6-3-1 associated with the sponge *Hymeniacidon perleve*. *World J Microbiol Biotechnol.* 2005;21(2):201–206. [doi:10.1007/s11274-004-3318-6](#)

Mycosynthesis of Size-Controlled Silver Nanoparticles through Optimization of Process Variables by Response Surface Methodology

ASMA SHAHZAD¹, MEHWISH IQTEDAR^{1*}, HAMID SAEED², SYED ZAJIF HUSSAIN³,
ASMA CHAUDHARY⁴, ROHEENA ABDULLAH¹ and AFSHAN KALEEM¹

¹Department of Biotechnology, Lahore College for Women University, Lahore, Pakistan

²School of Pharmacy, University of the Punjab, Lahore, Pakistan

³Department of Chemistry, Lahore University of Management Sciences,
School of Science & Engineering, Lahore, Pakistan

⁴Department of Zoology, Division of Science and Technology, University of Education, Lahore, Pakistan

Submitted 8 August 2018, revised 29 October 2018, accepted 29 October 2018

Abstract

The present study was carried out to reduce the size of silver nanoparticles (AgNPs) by optimizing physico-chemical conditions of the *Aspergillus fumigatus* BTCB10 growth based on central composite design (CCD) through response surface methodology (RSM). Variables such as a concentration of silver nitrate (mM), NaCl (%) and the wet weight of biomass (g) were controlled to produce spherical, monodispersed particles of 33.23 nm size, observing 78.7% reduction in size as compared to the initially obtained size that was equal to 356 nm. The obtained AgNPs exhibited negative zeta potential of -9.91 mV with a peak at 420 nm in the UV-Vis range whereas Fourier Transform Infrared (FT-IR) analysis identified O-H, C=C, C≡C, C-Br and C-Cl groups attached as capping agents. After conducting RSM experiments, a high nitrate reductase activity value of 179.15 nmol/h/ml was obtained; thus indicating a likely correlation between enzyme production and AgNPs synthesis. The F-value (significant at 3.91), non-significant lack of fit and determination coefficient ($R^2=0.7786$) is representative of the good relation between the predicted values of response. We conclude that CCD is an effective tool in obtaining significant results of high quality and efficiency.

Key words: *Aspergillus fumigatus* and AgNPs, Central Composite Design (CCD) for AgNPs synthesis, green synthesis of AgNPs, nitrate reductase activity for AgNPs synthesis

Introduction

Nanoparticles have gained acceptance in recent years due to their numerous applications. Metallic nanoparticles, with AgNPs in particular, become more popular due to their unique optical, electrical, and thermal properties and have been incorporated into products that range from photovoltaics to biological and chemical sensors as well as antimicrobial coatings in many textiles, keyboards, wound dressings, biomedical devices, nanoparticle-based fertilizers and insecticides (Li et al. 2010; Vijayan et al. 2016).

Numerous chemical methods have been developed in the past few years for the synthesis of nanoparticles. However, in order to enhance the yield and minimize the adverse effects of the process, environmental-friendly methods are being researched (Shanmuganathan et al. 2018). Nanoparticle synthesis is either done

by physical, chemical or biological means. The biological method takes advantage of the natural ability of microbes – referred to as nano-factories to produce nanomaterials as metabolic by-products (Mitra et al. 2016). By employing green methods for the synthesis of nanoparticles, harmful chemicals like surfactant, enhancers, and other ionic and organic compounds are used in lower amounts (Saravanan et al. 2018b). It is now known that the reduction of silver ions to form AgNPs synthesized through microbes like bacteria and fungi is associated with NADH dependent reductase (enzymatic process) (Saravanan et al. 2018a). Furthermore, peptides such as phytochelatins prevent nanoparticle aggregations and thus maintain a balanced production within the microbes (Shankar et al. 2016).

Microbial synthesis of AgNPs can be either intracellular or extracellular and has been studied in a variety of bacteria and fungi (Das et al. 2017; Banerjee et al. 2018)

* Corresponding author: M. Iqtedar, Department of Biotechnology, Lahore College for Women University, Jail road, Lahore, Pakistan;
e-mail: miqtedar@gmail.com

© 2019 Asma Shahzad et al.

This work is licensed under the Creative Commons Attribution-NonCommercial-NoDerivatives 4.0 License (<https://creativecommons.org/licenses/by-nc-nd/4.0/>)

with focus on their antibacterial activity as well (Pugazhendhi et al. 2018). With their excessive secretion of extracellular enzymes, easy culturing and upscaling, fungi are suitable candidates for nanoparticle synthesis. *Aspergillus flavus*, *Aspergillus niger*, *Aspergillus clavatus*, and *Aspergillus fumigatus* are the fungi species studied for the mycosynthesis of nanoparticles (Zomorodian et al. 2016). The major hindrance in the microbial biosynthesis of metal nanoparticles at the industrial level is the polydispersity factor (Mitrano et al. 2016). Polydispersed nanoparticles are inconsistent and inefficient, as well as irregularities in shape can delay biological experiments, e.g. drug delivery. Additionally, a purification step is also required to enhance the quality of the nanoparticles to ensure its monodispersity which is time-consuming and adds up to the end cost (Robertson et al. 2016). The ability to regulate the size, distribution, and shape of AgNPs during the biosynthesis of AgNPs is a difficult process (Hamedi et al. 2017).

To optimize the process variables, numerous strategies have been employed but achieved little success in obtaining monodispersity (Singh et al. 2014). Classical approach of altering one parameter at a time to attain optimization has many drawbacks as numerous experiments have to be designed and time-consuming yet interaction between the parameters and their effects cannot be studied. RSM, on the other hand, uses the statistical method to design experiments and study interactions between selected variables to suggest the most suitable conditions for producing the desirable nanoparticles (Othman et al. 2017). Response Surface Methodology (RSM) is preferred over the traditional one-factor method in optimizing conditions as it minimizes the number of chemicals used along with less labor (Asghar et al. 2014).

Central Composite Design (CCD) provides excellent predictions within the design space and has more centre points as compared to others like Box-Behnken design (BBD). Moreover, it is particularly used for studying extreme conditions or values both high and low resulting in a better quadratic design (Othman et al. 2017). Hence, the present study entails the use of Central Composite Design (CCD) to obtain high-quality AgNPs from *A. fumigatus* BTCB10 by optimizing different growth condition variables and to assess the interactions between them.

Experimental

Materials and Methods

Isolation of strain and biomass preparation. *A. fumigatus* BTCB10 (GenBank accession no. KY486782) (Shahzad and Iqtedar 2017) was isolated from waste

effluents of the textile industry and was grown on potato dextrose agar (PDA) at 30°C (Harrigan 1998). The media used for generating fungal biomass was according to (Mohamed et al. 2015). The pH of the media was maintained at 6.8, inoculated with fungal spores (10^5 spores/ml) and incubated at 25°C with shaking (120 rpm) for 72 hours before optimization. The biomass formed was filtered with Whatman filter paper (grade A) No. 1 (Ahlstrom, Spain) and thoroughly rinsed (three times) with sterilized distilled water to remove any traces of media. For the preparation of cell-free extract, the filtered biomass (10 g) was added to 100 ml of sterilized distilled water and incubated at 25°C with shaking (120 rpm) for 72 hours (Majeed et al. 2016).

Extracellular biosynthesis of silver nanoparticles. Cell-free extract (CFE) was prepared by filtering out the biomass and was then added to (1 mM) silver nitrate with 1:1 ratio. The mixture of CFE and AgNO₃ was incubated at 25°C with 120 rpm until the formation of AgNPs was indicated by the change in color from colorless to brown. The experiments were performed in triplicates with a control that was devoid of silver nitrate and only had CFE (Sadowski et al. 2008).

Characterization of silver nanoparticles. The AgNPs formed were characterized by the following techniques: for spectroscopic analysis (300 to 700 nm) of the colloidal silver UV-Vis spectrophotometer (ORI 4000 UV-Vis spectrophotometer, Germany) was used, for Particle size and zeta potential analysis – a Dynamic Light Scattering using Zeta sizer (Malvern Nano S, United Kingdom) was applied, the Fourier Transform infrared spectrophotometer ATR (Bruker-OPUS, USA) was used for the identification of functional groups, and the analysis of size and shape of the AgNPs was carried out by Atomic Force Microscopy AFM (Park systems, Korea) (Bordley et al. 2016).

Optimization and experimental design by response surface methodology. Response surface methodology was applied to analyze an estimated functional relationship among three factors by using Design Expert software (Ver. 10.0.3.1, Stat ease, Minneapolis, USA). All the variables were further narrowed down with the help of CCD i.e., central composite design (Dil et al. 2016). The optimized sample or “OS” had variables modified according to the experimental plan of three factors, which included substrate concentration (mM), a concentration of NaCl (%) and wet weight of biomass (g) denoted by A, B, and C, respectively (Table I).

The high and low values for CCD design were 3 and 1 mM for substrate concentration, 20 and 10% for NaCl concentration whereas 10 and 7 g for biomass (wet weight) (Table I). The size of biogenic AgNPs was the response (Y) that was also represented by the following equation:

$$Y = \beta_0 + \beta_1 X_1 + \beta_2 X_2 + \beta_3 X_3 + \beta_{11} X_{12} + \beta_{22} X_{22} + \beta_{33} X_{32} + \beta_{12} X_1 X_2 + \beta_{13} X_1 X_3 + \beta_{23} X_2 X_3 \quad (1)$$

Here, Y represents predicted responses, β_0 – the constant coefficient, β_1 , β_2 and β_3 – the linear coefficients, β_{11} , β_{22} and β_{33} – the quadratic coefficients, β_{12} , β_{13} and β_{23} – the cross products coefficients and X_1 , X_2 and X_3 were point variables. An experimental sample without RSM (i.e. without optimization), which will thereby be referred to as “WO”, was also setup besides these 20 runs to compare the size of AgNPs without optimization and to study the effectiveness of the methodology.

Nitrate reductase assay. The nitrate reductase activity of fungus during AgNPs formation was done as previously described (Hamedi et al. 2017).

Results and Discussion

Characterization of AgNPs – Preliminary observations. The production of AgNPs was at first distinguished by the color change from colorless to brown in all the samples, which occurs due to excitation of Surface Plasmon Resonance (SPR). Development of color

Table I

Central composite design (CCD) matrix of three independent variables for AgNPs biosynthesis in codes with experimental results.

Runs	Factor A: Substrate concentration (mM)	Factor B: NaCl concentration (%)	Factor C: Wet weight of biomass (g)	Response: Size of AgNPs (nm)
1	1	10	7	33.65
2	3	20	7	127.20
3	2	15	8.5	68.23
4	1	20	10	33.65
5	3	1	10	76.22
6	1	20	7	33.65
7	2	15	8.5	68.20
8	2	15	8.5	68.30
9	2	23.41	8.5	89.37
10	1	10	10	33.65
11	3	20	10	70.48
12	3.68	15	8.5	156.2
13	2	15	11.02	33.65
14	2	15	8.5	33.55
15	2	15	8.5	33.65
16	0.32	15	8.5	126.30
17	2	15	5.98	33.23
18	2	6.59	8.5	33.45
19	3	10	7	127.10
20	2	15	8.5	90.06

in CFE in WO proved nanoparticle synthesis, which was necessary before commencing optimization of the experiment (Fig. 1A). After the completion of optimization experiments under RSM, the OS also exhibited the color change to a medium-brown, verifying the synthesis of AgNPs (Fig. 2A), similarly as it was demonstrated in the studies with *Fusarium acuminatum* (Khan et al. 2018) and *A. fumigatus* (Ghanbari et al. 2018).

Characterization of AgNPs – UV-Vis spectroscopy. The UV-Vis spectra were also analyzed, and demonstrated WO peak formation at 452 nm (λ max) (Fig. 1A) and 420 nm (λ max) for OS (Fig. 2A). The result showed a significant difference between both situations, with the latter possessing a lower wavelength, which suggests the fabrication of small-sized AgNPs (Hamedi et al. 2017). Similarly, other studies on mycosynthesis have also reported the formation of AgNPs having SPR band at 420 nm with *F. acuminatum*, *A. niger* and *A. flavus* (Khan et al. 2018).

DLS analysis – Before optimization. The WO AgNPs produced larger sized nanoparticles. Their size was analyzed by zeta sizer as shown in Fig. 1B. The observed average value was 356 nm with a polydispersion index (PDI) of 0.42. Two peaks were formed of which peak one had a value of 375.0 nm with 95.8% intensity, and peak 2 presented at 5200 nm with 4.2% intensity. The sample displayed high polydispersion without the RSM. Over 100 nm-sized nanoparticles were synthesized with *A. terreus* (Rathna et al. 2013) whereas *Pleurotus sajorcaju* formed AgNPs of 5 to 50 nm (Khan et al. 2018).

DLS analysis – After optimization. The OS AgNPs were 33.23 nm with very lower PDI i.e. 0.12 having the single peak in UV-vis spectrum (Fig. 2B). Small size and less PDI both are important properties of nanoparticles that greatly influence the activity of NPs in different applications such as antimicrobial activity, increase interaction with the targeting site (Vijayan et al. 2016). The previous study on the fungal mediated synthesis of AgNPs from *Aspergillus oryzae* reported polydisperse particles; displaying size in 6–26 nm (El-Batal et al. 2017). The zeta potential (–9.91 mV) of the OS (Fig. 2C) indicated stable AgNPs formation. Zeta potential is another important property of NPs that is required for efficient performance in different applications such as long-term usage and application in the different environment without affecting the activity (Vijayan et al. 2016). A comparison with WO particle sizes and PDIs revealed that the smaller sized AgNPs were indeed produced under RSM conditions and no such polydispersity was observed.

Atomic Force Microscopy (AFM). The WO AgNPs produced were not only larger in size but also revealed triangular-shaped nanoparticles (Fig. 1C). OS AgNPs were found to be spherical under AFM (Fig. 2D).

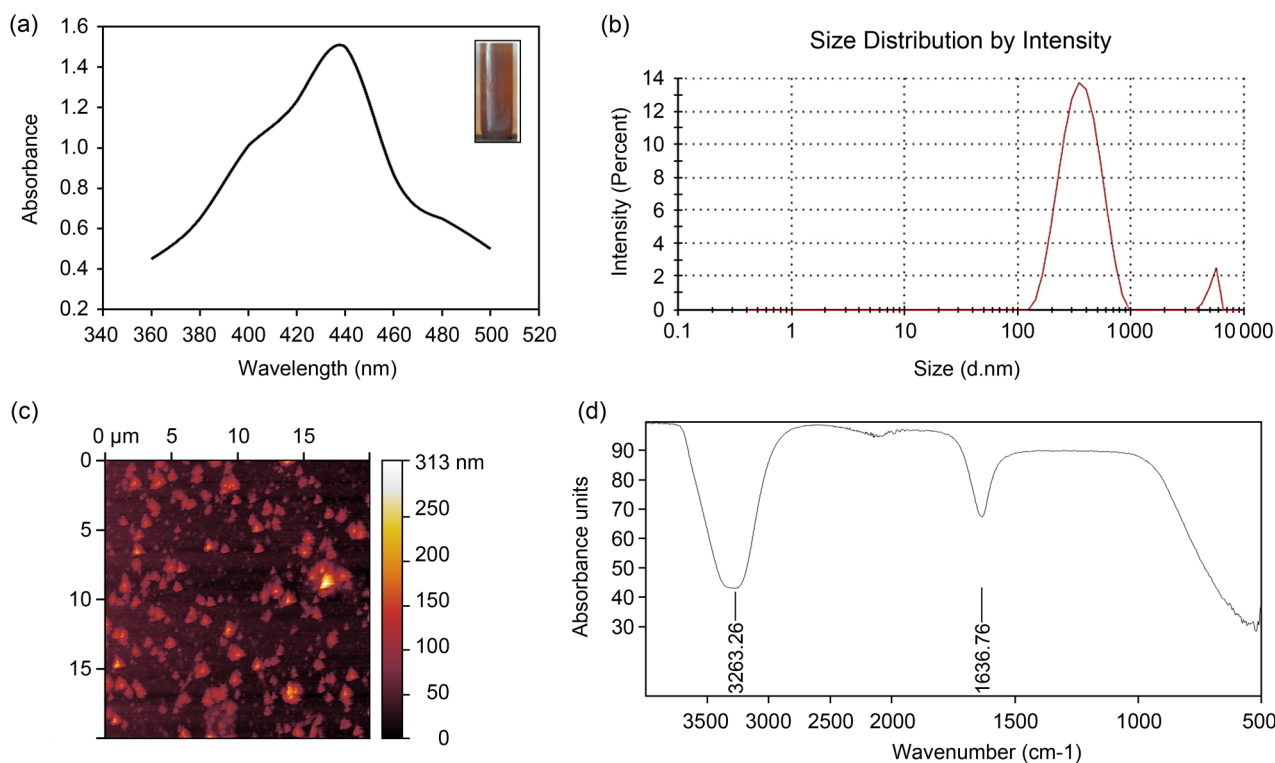


Fig. 1. Characterization of AgNPs obtained WO.

A. UV-Vis spectrophotometer analysis representing a peak of AgNPs at 452 nm and showing brown coloured nanoparticles. B. Zeta sizer (DLS) analysis representing peak at 356nm nm. C. Triangular shaped AgNPs revealed by AFM. D. Fourier transform infrared (FT-IR) analysis of AgNPs.

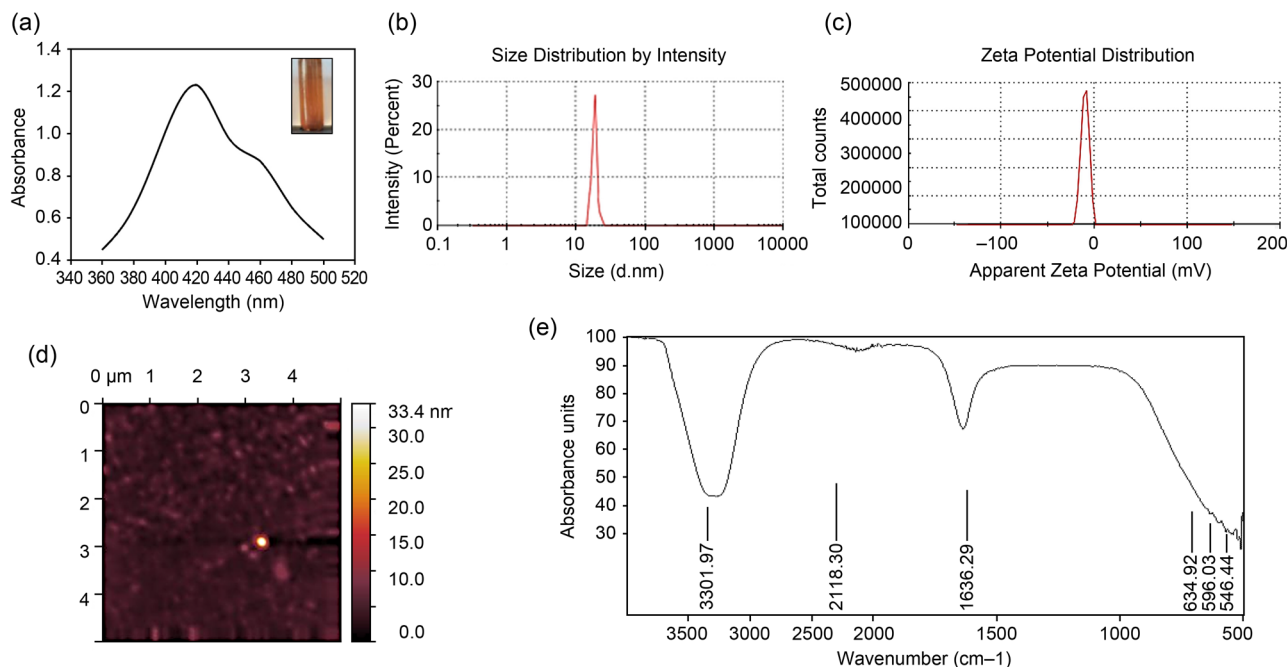


Fig. 2. Characterization of AgNPs obtained OS.

A. UV-Vis spectrophotometer analysis representing peak of AgNPs at 420 nm and showing medium brown coloured nanoparticles. B. Zeta sizer (DLS) analysis representing peak at 33.23 nm. C. Zeta potential analysis by DLS. D. Spherical shaped AgNPs revealed by AFM. E. Fourier transform infrared (FT-IR) analysis of AgNPs indicating presence of functional groups.

Othman et al. (2017) also achieved spherical shaped AgNPs using *Trichoderma viride* under RSM conditions.

FTIR spectroscopy – Before optimization. The biomolecules that are present in the cell-free extract have

the capability to bind themselves with metallic nanoparticles and act as capping agents (Gudikandula et al. 2017). Functional groups identified in WO sample were N-H (3263.26 cm^{-1}) and C=C (1636.76 cm^{-1}) (Fig. 1D).

FTIR spectroscopy – After optimization. Functional groups as capping agents involved in the stability of OS AgNPs and the prevention of their aggregation were identified as O–H, C≡C and C=C by FT-IR analysis. The FTIR spectra presented an absorption band at 3301.97 cm^{-1} , which corresponded to the stretching vibrations of alcohol (Fig. 2E). While the other absorption bands were at 2118.30 cm^{-1} and 1636.29 cm^{-1} , assigned to the stretching vibrations of alkyne and alkenes respectively. Three more bands were observed at 634.92 cm^{-1} , 596.03 cm^{-1} , and 546.44 cm^{-1} , which represented the C-Cl and C-Br groups (Fig. 2C). A similar study has also reported the presence of such groups in conferring the stability of AgNPs; C–C, –COO–, –C=C– and C–N were other functional groups found in a study with AgNPs formed by *F. oxysporum* (Hamed et al. 2017). Type of capping agents helps not only in stabilizing the NPs but also to attach them to different ligands and drugs for site-specific targeting (Majeed et al. 2016).

Nitrate reductase assay. The presence of extracellular proteins in the medium of fungi is believed to play a significant role in the synthesis and stabilization of AgNPs. NADH has been reported to be responsible for the formation of AgNPs and reduction of silver

nitrate to its colloidal state (Jogee et al. 2017) as illustrated (Fig. 3A). High enzyme activity was observed throughout the experiments, with the highest being 179.15 nmol/h/ml (Fig. 3B). All the OS experimental runs produced monodispersed AgNPs. At higher substrate and metal salt concentration, the enzyme activity seemed delayed and larger sized AgNPs were formed; which could be due to unavailability of functional groups that were responsible for carrying out reduction processes.

At comparatively lower substrate and metal concentration, the smaller-sized silver nanoparticles were produced with rapid synthesis rate possibly due to the presence of greater number of functional groups. Devi et al. (2013) has highlighted the correlation of nitrate reductase activity with nanoparticle synthesis and reported that *Trichoderma asperellum*, produced 200 (nmol/h/ml) of enzyme hence leading to the formation of stable AgNPs. According to our study sample number 13 produced $179.15\text{ (nmol/h/ml)}$ of enzyme leading to formation of small-sized AgNPs 33.65 nm , which could be due to secretion of the abundant enzyme.

The substrate concentration (mM) is defined by A, whereas the concentration of NaCl (%) by B and wet weight of biomass (g) is denoted by C, Y represents

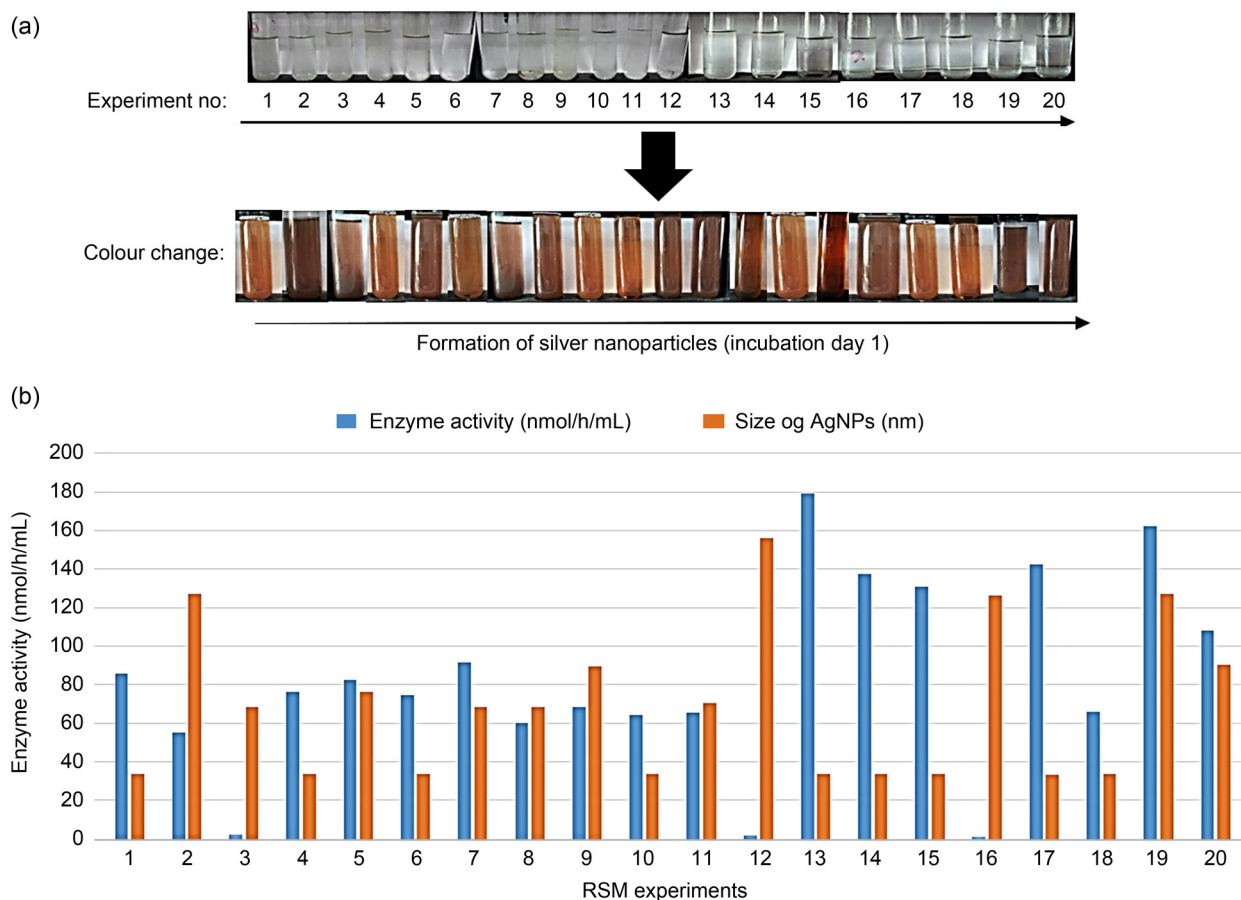


Fig. 3. A. Colour change observed during the optimization experiments (20 runs). B. Estimation of nitrate reductase activity (nmol/h/ml) and reduction in the size of AgNPs during different RSM experiments.

Table II
Analysis of Variance (ANOVA) of the Fitted Quadratic Model and regression analysis for optimization of AgNPs biosynthesis.

Source	Sum of Squares	Df	Mean Square	F-Value	p-value	Prob > F
Model	23241.50	9	2582.39	3.91	0.0224	Significant
A – Substrate concentration	7343.55	1	7343.55	11.11	0.0076	Significant
B – NaCl concentration	572.28	1	572.28	0.87	0.3740	
C – Wet weight of biomass	836.67	1	836.67	1.27	0.2868	
AB	3.98	1	3.98	0.006017	0.9397	
AC	1447.22	1	1447.22	2.19	0.1697	
BC	4.26	1	4.26	0.006451	0.9376	
A ²	9658.74	1	9658.74	14.62	0.0034	Significant
B ²	78.85	1	78.85	0.12	0.7369	
C ²	2154.83	1	2154.83	3.26	0.1011	
Residual	6608.52	10	660.85			
Lack of Fit	4113.14	5	822.63	1.65	0.2984	Not significant
Pure Error	2495.38	5	499.08			
Core Total	29850.02	19				
Std. dev	C.V	R-Squared	Adj R-Squared	Pred R-Squared	Adeq Precision	
25.71	37.53	0.7786	0.5794	0.1664	8.801	

the size of AgNPs. The analysis of variance (ANOVA) for the size of AgNPs is presented (Table II). Optimum response (33.23 nm AgNPs) was recorded with 2 mM silver nitrate concentration, 5.98 g biomass wet weight and 15% NaCl concentration. The results reflected that model was statistically significant with the confidence level of 95%, F-value of 3.91 and low probability P-value of < 0.0224. By comparing the viability of current model residuals to the variability between observations at replicate settings of the factors, the lack of fit test was performed.

The lack of fit test with F-value 1.65 and P-value 0.2984 was statistically non-significant. The insignificant lack of fit test indicated that there might be some systematic variations in the hypothesized model, which can be accounted because of replicate values of the independent variable and gave an estimate of the pure error in the model. In one of the studies with *Trichoderma viride*, RSM analysis showed a low value of 1.70 with lack of fit test, which also proved the significance of the model (Othman et al. 2017).

The values of determination coefficients R^2 and R^2_{adj} were calculated as 0.7786 and 0.5794, which measured the reliability of model. This indicated that approximately 77.86% was attributed to the variables and it indicated the significance of the model. Study with *T. viride* also illuminated coefficients R^2 (0.7246) and R^2_{adj} (0.8886) after conducting RSM experiments and indicated the reliability of model. The coefficient of variation (CV) is indicative of the degree of precision of all the compared treatments hence lower value of

CV (37.53%) approved the certainty of the model in our study. The RSM study with *T. viride* (Othman et al. 2017) also showed a lower value CV (28.67%) proving the accuracy of the model.

Analysis of 3D surface plots. A three-dimensional response surface plot illustrated the relationship between two process variables and the third one presents its optimized condition for the variables (smallest size of AgNPs). The two-dimensional contour plot specified the interaction between the dependent and independent process variables by forming different shapes like elliptical or circular depending upon the relationship between the parameters. The plots (Fig. 4A and Fig. 4B) showed a stronger interaction between metal salt (% NaCl) and substrate (mM) concentration.

It clarifies that the size of the AgNPs had increased by increasing substrate concentration (mM) while the increase in metal salt concentration would lead to the decreased size of AgNPs. The graphs (Fig. 4C) depicted the negligible interaction between metal salt concentration and weight of biomass. The increase in salt concentration caused a slight increase in the size of particles but maximum salt concentration would have resulted in smaller AgNPs. The plots further illustrated the relationship between substrate concentration and wet biomass weight. Decreased size of AgNPs was observed at minimum substrate concentration and wet biomass weight. The results corroborated the hypothesis i.e., the decreased size of AgNPs.

Conclusively, by designing experiments using Response Surface Methodology (RSM) based on Cen-

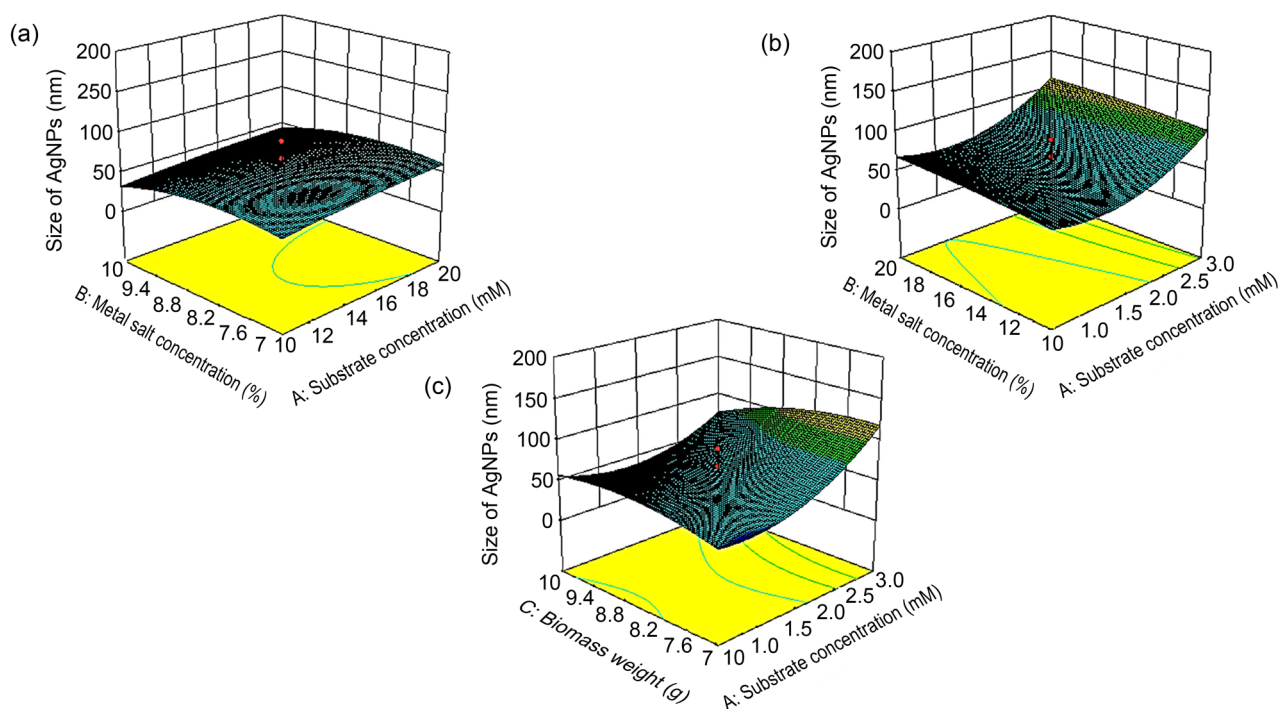


Fig. 4. 3D surface plots analysis. A. Effect of substrate concentration and metal salt concentration. B. Effect of metal salt concentration and substrate concentration. C. Effect of substrate concentration and wet weight of biomass.

tral Composite Design (CCD) about 78.7% reduction in size was observed from the sample without RSM optimization. Hence the method proved to be successful, eco-friendly and low-cost for the efficient synthesis of AgNPs with fungus *A. fumigatus* (BTCB10).

Acknowledgements

The authors greatly acknowledge the financial support provided under the Institutional Strengthening Program and Access to Scientific Instrument Program by the Higher Education Commission (HEC) Pakistan.

Conflict of interest

The authors do not report any financial or personal connections with other persons or organizations, which might negatively affect the contents of this publication and/or claim authorship rights to this publication.

Literature

- Asghar A, Abdul Raman AA, Daud WMAW. A comparison of central composite design and Taguchi method for optimizing Fenton process. *Sci World J.* 2014;2014:1–14. doi:10.1155/2014/869120 [Medline](#)
- Banerjee K, Ravishankar Rai V. A review on mycosynthesis, mechanism, and characterization of silver and gold nanoparticles. *Bionanoscience.* 2018;8(1):17–31. doi:10.1007/s12668-017-0437-8
- Bordley JA, El-Sayed MA. Enhanced electrocatalytic activity toward the oxygen reduction reaction through alloy formation: Platinum-silver alloy nanocages. *J Phys Chem C.* 2016;120(27):14643–14651. doi:10.1021/acs.jpcc.6b03032
- Das RK, Pachapur VL, Lonappan L, Naghdi M, Pulicharla R, Maiti S, Cleidon M, Dalila LMA, Sarma SJ, Brar SK. Biological synthesis of metallic nanoparticles: plants, animals and microbial aspects. *Nanotechnol Environ Eng.* 2017;2(1):18. doi:10.1007/s41204-017-0029-4
- Devi TP, Kulanthaivel S, Kamil D, Borah JL, Prabhakaran N, Srinivasa N. Biosynthesis of silver nanoparticles from *Trichoderma* species. *Indian J Exp Biol.* 2013;51(7):543–547. [Medline](#)
- Dil EA, Ghaedi M, Ghaedi A, Asfaram A, Jamshidi M, Purkait MK. Application of artificial neural network and response surface methodology for the removal of crystal violet by zinc oxide nanorods loaded on activate carbon: kinetics and equilibrium study. *J Taiwan Inst Chem Eng.* 2016;59(59):210–220. doi:10.1016/j.jtice.2015.07.023
- Ghanbari S, Vaghari H, Sayyar Z, Adibpour M, Jafarizadeh-Malmiri H. Autoclave-assisted green synthesis of silver nanoparticles using *A. fumigatus* mycelia extract and the evaluation of their physico-chemical properties and antibacterial activity. *Green Processing and Synthesis.* 2018;7(3):217–224. doi:10.1515/gps-2017-0062
- Gudikandula K, Vadapally P, Singara Charya MA. Biogenic synthesis of silver nanoparticles from white rot fungi: their characterization and antibacterial studies. *OpenNano.* 2017;2(1):64–78. doi:10.1016/j.onano.2017.07.002
- Hamed S, Ghaseminezhad M, Shokrollahzadeh S, Shojaosadati SA. Controlled biosynthesis of silver nanoparticles using nitrate reductase enzyme induction of filamentous fungus and their antibacterial evaluation. *Artif Cells Nanomed Biotechnol.* 2017;45(8):1588–1596. doi:10.1080/21691401.2016.1267011 [Medline](#)
- Hamed S, Shojaosadati SA, Shokrollahzadeh S, Hashemi-Najaf Abadi S. Controlled biosynthesis of silver nanoparticles using culture supernatant of filamentous fungus. *Iran J Chem Chem Eng.* 2017;36(5):33–42.
- Harrigan W. *Laboratory methods in food microbiology.* San Diego (USA): Academic Press. 1998;100 p.

- Jogee PS, Ingle AP, Rai M.** Isolation and identification of toxicogenic fungi from infected peanuts and efficacy of silver nanoparticles against them. *Food Control*. 2017;71:143–151. doi:10.1016/j.foodcont.2016.06.036
- Khan AU, Malik N, Khan M, Cho MH, Khan MM.** Fungi-assisted silver nanoparticle synthesis and their applications. *Bioprocess Biosyst Eng*. 2018;41(1):1–20. doi:10.1007/s00449-017-1846-3 [Medline](#)
- Li WR, Xie XB, Shi QS, Zeng HY, OU-Yang YS, Chen YB.** Antibacterial activity and mechanism of silver nanoparticles on *Escherichia coli*. *Appl Microbiol Biotechnol*. 2010;85(4):1115–1122. doi:10.1007/s00253-009-2159-5 [Medline](#)
- Majeed S, Abdullah MS, Dash GK, Ansari MT, Nanda A.** Biochemical synthesis of silver nanoparticles using filamentous fungi *Penicillium decumbens* (MTCC-2494) and its efficacy against A-549 lung cancer cell line. *Chin J Nat Med*. 2016;14(8):615–620. doi:10.1016/S1875-5364(16)30072-3 [Medline](#)
- Mitra C, Ghoshroy S, Lead J, Chanda A.** Decreased aflatoxin biosynthesis upon uptake of 20 nm-sized citrate coated silver nanoparticles by the aflatoxin producer *Aspergillus parasiticus*. *Microsc Microanal*. 2016;22 S3:1182–1183. doi:10.1017/S1431927616006759
- Mitrano DM, Lombi E, Dasilva YAR, Nowack B.** Unraveling the complexity in the aging of nanoenhanced textiles: A comprehensive sequential study on the effects of sunlight and washing on silver nanoparticles. *Environ Sci Technol*. 2016;50(11):5790–5799. doi:10.1021/acs.est.6b01478 [Medline](#)
- Mohamed YM, Azzam AM, Amin BH, Safwat NA.** Mycosynthesis of iron nanoparticles by *Alternaria alternata* and its antibacterial activity. *Afr J Biotechnol*. 2015;14(14):1234–1241. doi:10.5897/AJB2014.14286
- Othman AM, Elsayed MA, Elshafei AM, Hassan MM.** Application of response surface methodology to optimize the extracellular fungal mediated nanosilver green synthesis. *JGEB*. 2017;15(2):497–504.
- Pugazhendhi A, Prabakar D, Jacob JM, Karuppusamy I, Saratale RG.** Synthesis and characterization of silver nanoparticles using *Gelidium amansii* and its antimicrobial property against various pathogenic bacteria. *Microb Pathog*. 2018;114(114):41–45. doi:10.1016/j.micpath.2017.11.013 [Medline](#)
- Rathna GS, Elavarasi A, Peninal S, Subramanian J, Mano G, Kalaiselvam M.** Extracellular biosynthesis of silver nanoparticles by endophytic fungus *Aspergillus terreus* and its anti-dermatophytic activity. *Int J Pharm Biol Arch*. 2013;1(4):481–487.
- Robertson JD, Rizzello L, Avila-Olias M, Gaitzsch J, Contini C, Magoń MS, Renshaw SA, Battaglia G.** Purification of nanoparticles by size and shape. *Sci Rep*. 2016;6(1):27494. doi:10.1038/srep27494 [Medline](#)
- Sadowski Z, Maliszewska IH, Grochowalska B, Polowczyk I, Kozlecki T.** Synthesis of silver nanoparticles using microorganisms. *Mater Sci Pol*. 2008;26(2):419–424.
- Saravanan M, Arokiyaraj S, Lakshmi T, Pugazhendhi A.** Synthesis of silver nanoparticles from *Phenerochaete chrysosporium* (MTCC-787) and their antibacterial activity against human pathogenic bacteria. *Microb Pathog*. 2018a;117(117):68–72. doi:10.1016/j.micpath.2018.02.008 [Medline](#)
- Saravanan M, Barik SK, MubarakAli D, Prakash P, Pugazhendhi A.** Synthesis of silver nanoparticles from *Bacillus brevis* (NCIM 2533) and their antibacterial activity against pathogenic bacteria. *Microb Pathog*. 2018b;116(116):221–226. doi:10.1016/j.micpath.2018.01.038 [Medline](#)
- Shahzad A, Iqtedar M.** *Aspergillus fumigatus* isolate BTCC10 small subunit ribosomal RNA gene (KY486782) [Internet]. NCBI. 2017; [cited 2018 September 16]. Available from: <https://www.ncbi.nlm.nih.gov/nuccore/KY486782>
- Shankar PD, Shobana S, Karuppusamy I, Pugazhendhi A, Ramkumar VS, Arvindnarayan S, Kumar G.** A review on the biosynthesis of metallic nanoparticles (gold and silver) using bio-components of microalgae: formation mechanism and applications. *Enzyme Microb Technol*. 2016;95(95):28–44. doi:10.1016/j.enzymictec.2016.10.015 [Medline](#)
- Shanmuganathan R, MubarakAli D, Prabakar D, Muthukumar H, Thajuddin N, Kumar SS, Pugazhendhi A.** An enhancement of antimicrobial efficacy of biogenic and ceftriaxone-conjugated silver nanoparticles: green approach. *Environ Sci Pollut Res Int*. 2018;25(11):10362–10370. doi:10.1007/s11356-017-9367-9 [Medline](#)
- Singh D, Rathod V, Ningnanagouda S, Hiremath J, Singh AK, Mathew J.** Optimization and characterization of silver nanoparticle by endophytic fungi *Penicillium* sp. isolated from *Curcuma longa* (turmeric) and application studies against MDR *E. coli* and *S. aureus*. *Bioinorg Chem Appl*. 2014;2014:1–8. doi:10.1155/2014/408021 [Medline](#)
- Vijayan SR, Santhiyagu P, Ramasamy R, Arivalagan P, Kumar G, Ethiraj K, Ramaswamy BR.** Seaweeds: A resource for marine bionanotechnology. *Enzyme Microb Technol*. 2016;95(95):45–57. doi:10.1016/j.enzymictec.2016.06.009 [Medline](#)
- Zhao X, Zhou L, Riaz Rajoka MS, Yan L, Jiang C, Shao D, Zhu J, Shi J, Huang Q, Yang H, et al.** Fungal silver nanoparticles: synthesis, application and challenges. *Crit Rev Biotechnol*. 2018;38(6):817–835. doi:10.1080/07388551.2017.1414141 [Medline](#)
- Zomorodian K, Pourshahid S, Sadatsharifi A, Mehryar P, Pakshir K, Rahimi MJ, Arabi Monfared A.** Biosynthesis and characterization of silver nanoparticles by *Aspergillus* species. *BioMed Res Int*. 2016;2016:1–6. doi:10.1155/2016/5435397 [Medline](#)

Thermoregulation of Prodigiosin Biosynthesis by *Serratia marcescens* is Controlled at the Transcriptional Level and Requires HexS

ERIC G. ROMANOWSKI, KARA M. LEHNER, NATALIE C. MARTIN, KRIYA R. PATEL,
JAKE D. CALLAGHAN, NICHOLAS A. STELLA and ROBERT M.Q. SHANKS*^{ORCID}

Charles T. Campbell Laboratory of Ophthalmic Microbiology, Department of Ophthalmology,
University of Pittsburgh, Pittsburgh PA

Submitted 21 August 2018, revised 31 October 2018, accepted 5 November 2018

Abstract

Several biotypes of the Gram-negative bacterium *Serratia marcescens* produce the tri-pyrole pigment and secondary metabolite prodigiosin. The biological activities of this pigment have therapeutic potential. For over half a century it has been known that biosynthesis of prodigiosin is inhibited when bacteria are grown at elevated temperatures, yet the fundamental mechanism underlying this thermoregulation has not been characterized. In this study, chromosomal and plasmid-borne *luxCDABE* transcriptional reporters revealed reduced transcription of the prodigiosin biosynthetic operon at 37°C compared to 30°C indicating transcriptional control of pigment production. Moreover, induced expression of the prodigiosin biosynthetic operon at 37°C was able to produce pigmented colonies and cultures demonstrating that physiological conditions at 37°C allow prodigiosin production and indicating that post-transcriptional control is not a major contributor to the thermoregulation of prodigiosin pigmentation. Genetic experiments support the model that the HexS transcription factor is a key contributor to thermoregulation of pigmentation, whereas CRP plays a minor role, and a clear role for EepR and PigP was not observed. Together, these data indicate that thermoregulation of prodigiosin production at elevated temperatures is controlled largely, if not exclusively, at the transcriptional level.

Key words: secondary metabolite, regulation, pigment, prodigiosin, bacteria, transcription factor

Introduction

Microbial secondary metabolites include crucial medicines such as antibiotics and anti-inflammatory compounds (Vining 1990). Secondary metabolites influence microbial physiology and behaviors, for example, through regulation of outer membrane vesicle formation (Hoeffler et al. 2017), quorum sensing signaling (Waters and Bassler 2005; Barriuso et al. 2018), cellular motility (Daniels et al. 2004), metal acquisition (Demain and Fang 2000; Khan et al. 2018), and spore formation (Demain and Fang 2000).

Some of the most studied secondary metabolites are pigments such as violacein and prodigiosin (Williamson et al. 2006; Choi et al. 2017). Both of these pigments are antimicrobial and therefore likely contribute to microbe-microbe interactions (Danevcic et al. 2016a; Danevcic et al. 2016b; Im et al. 2017; Hage-

Hulsmann et al. 2018). This study focuses on the regulation of prodigiosin, a red tri-pyrole pigment made by *Serratia* species and a handful of other organisms. While the biological role for prodigiosin is not clearly elucidated, the Haddix group has provided evidence suggesting that prodigiosin is used to finely tune internal energy levels within the bacterium (Haddix et al. 2008; Haddix and Shanks 2018). With respect to mammalian cells, prodigiosin has multiple biological activities including anticancer and autophagy modulating properties (Cheng et al. 2017; Klein et al. 2017; Lin et al. 2017; Klein et al. 2018). Therefore, a thorough understanding of how this secondary metabolite is regulated can be useful for industrial prodigiosin production as well as giving insight into how the organism interacts with the environment.

A variety of transcription factors and environmental stimuli have been shown to influence prodigiosin

* Corresponding author: R.M.Q. Shanks, Department of Ophthalmology, University of Pittsburgh, Pittsburgh, PA;
e-mail: shanksrq@upmc.edu

© 2019 Eric G. Romanowski et al.

This work is licensed under the Creative Commons Attribution-NonCommercial-NoDerivatives 4.0 License (<https://creativecommons.org/licenses/by-nc-nd/4.0/>)

biosynthesis (Williamson et al. 2006). Among the earliest described is thermoregulation of prodigiosin production by *S. marcescens* (Blizzard and Peterson 1963; Williams et al. 1965; Tanaka et al. 2004). At 37°C pigment biosynthesis is strongly inhibited, whereas it is synthesized at temperatures of ~32°C and below. In this study we used a molecular genetic approach to investigate fundamental questions of whether prodigiosin is thermoregulated at the transcriptional level or at the post-transcriptional level and what transcription factors are involved in this process. We conclude that for *S. marcescens* strain PIC3611, thermoregulation is controlled primarily at the transcriptional level and this requires the HexS transcription factor.

Experimental

Materials and Methods

Bacterial strains and growth. Bacterial strains are listed in Table I. Bacteria were grown in LB broth (Bertani 1951), supplemented with antibiotics when appropriate: tetracycline (10 µg/ml), kanamycin (100 µg/ml), carbenicillin (50 µg/ml), and gentamicin (10 µg/ml) for *S. marcescens* and ampicillin (100 µg/ml) and kanamycin (50 µg/ml) for *Escherichia coli*. For liquid broth, bacteria were aerated using a TC-7 tissue culture roller (New Brunswick Inc). Conjugation was used to transform bacteria as follows. Aliquots (500 µl) of donor and acceptor overnight cultures were pelleted by centrifugation, combined, spotted on an LB agar plate, incubated for ~18 hours, and streaked for single colonies on selective medium. Macrocolonies were generated by

spotting 10 µl of culture, which was grown overnight in LB broth, on LB agar plates and incubating at 30 and 37°C for 24 hours.

Molecular biology. Plasmids were made using yeast homologous recombination as previously described (Shanks et al. 2006; Shanks et al. 2009). Primer sequences are available upon request. A marnier transposon delivery plasmid with a promoterless *luxCDABE* (*lux*) reporter was derived from pSC189 (Chiang and Rubin 2002) with yeast replication machinery from pMQ132 (Shanks et al. 2009) and the *lux* operon from pGRL1 (Benedetti et al. 2012). The resulting plasmid, pMQ690, was moved into *S. marcescens* by conjugation. Six pigmentless colonies were chosen from approximately 5000 transposon mutants and these were analyzed for *lux* operon expression using a luminometer (Perkin Elmer Wallac 1450-021). Two of the isolates generated light due to the orientation of the transposon in the genome and the mutations were mapped and the insertion junction was sequenced as previously described (Chiang and Rubin 2002). The two insertions mapped within the *pig* operon which rendered the isolates unable to make pigment, and oriented downstream of the *pig* promoter so that light can be measured as a reporter of transcription.

To make *pig* promoter reporter plasmid, pMQ713, the *pig* promoter from strain PIC3611 was cloned upstream of the *lux* operon on an ori_{pBBR1}-based low copy plasmid, pMQ670 (R. Shanks, to be described elsewhere) as noted above. This episomal plasmid was used to transform a variety of strains described herein by conjugation.

To make the *lac* promoter reporter plasmid, pMQ99, the *P_{BAD}-gfp* portion of the plasmid pMQ72 was replaced

Table I
Strains and plasmids used in this study.

Strain	Description	Source
PIC3611	Wild-type <i>Serratia marcescens</i>	Presque Isle Cultures
CMS1687	PIC3611 <i>crp-Δ4</i> mutant	(Kalivoda et al. 2010)
CMS2097	PIC3611 <i>eepR</i> mutant	(Stella et al. 2015)
CMS2922	PIC3611 <i>hexS</i> mutant	(Shanks et al. 2013)
CMS4891	PIC3611 <i>pigB::tn-lux</i> pigment operon reporter	this study
CMS4892	PIC3611 <i>pigF::tn-lux</i> pigment operon reporter	this study
Plasmid	Relevant information	Source
pMQ99	<i>P_{lac}-hcred</i> shuttle vector	this study
pMQ132	pBBR1-based shuttle vector	(Shanks et al. 2009)
pMQ200	oriR6K-based suicide plasmid with PBAD	(Shanks et al. 2009)
pMQ221	pMQ132 with <i>pigP</i> gene	(Shanks et al. 2013)
pMQ262	pMQ200 with <i>pigAB</i> ⁺	(Kadouri and Shanks, 2013)
pMQ364	pMQ132 with <i>eepR</i> gene	(Stella et al. 2015)
pMQ690	promoterless- <i>luxCDABE</i> transposon delivery plasmid	this study
pMQ713	<i>pig</i> promoter- <i>luxCDABE</i> transcriptional fusion	this study

with P_{lac} -*hcred* using homologous recombination (Shanks et al. 2006; Shanks et al. 2009).

Reporter analysis and prodigiosin assay. Bacteria were grown for 18–20 hours in LB medium with aeration and the culture density was read at 600 nm with a SpectraMax M3 spectrophotometer using a 1 cm cuvette. Luminescence was measured from 150 μ l aliquot of culture in a black, opaque, 96-well plate with a luminometer as noted above. The ratio of luminescence arbitrary units to OD_{600} was calculated as relative luminescence units (RLU). For HcRed fluorescence, a BioTek Synergy 2 plate reader was used to read fluorescence and optical density (OD_{600}) of 150 μ l samples of overnight cultures. The ratio of fluorescence to optical density was reported as relative fluorescence units (RFU).

To measure prodigiosin from macrocolonies, colonies were scraped from agar plates using a toothpick and suspended in 1.2 ml of saline. A 0.2 ml sample was used to measure OD_{600} in a 1 cm cuvette, and the remaining 1 ml was pelleted by centrifugation, prodigiosin was extracted using acidified ethanol as previously described (Slater et al. 2003), and prodigiosin was measured using a spectrophotometer at 534 nm.

Results

Transcriptional control of pigment biogenesis.

Typical of pigmented *S. marcescens* strains, strain PIC3611 does not generate prodigiosin when grown at 37°C but does so at lower temperatures, such as 30°C and below (Fig. 1A). To analyze transcription from the pigment biosynthetic operon (*pig*), we decided to make a *luxCDABE* (*lux*) reporter strain. To achieve this, we generated a promoterless *lux* mariner transposon delivery plasmid and introduced it into the chromosome of *S. marcescens* strain PIC3611. Following transposon mutagenesis, pigmentless colonies were screened with a luminometer for light production after growth at 30°C. Two isolates were found, one mapped to *pigB* (bp 1730) and another to *pigF* (bp 1074) in the *pig* operon. Cultures of these two strains were grown with aeration at 30°C and 37°C, and light production was measured (Fig. 1B). After 18 hours of growth in LB medium, there was a significantly higher level of the signal from both cultures incubated at 30°C, compared to the same strains grown at 37°C. A similar pattern was observed for both *pigB* and *pigF-lux* isolates, although there was a higher level of expression from the *pigB* insertion. This result suggests that temperature regulation of pigment production is, at least in part, controlled at the transcriptional level.

To test whether induced *pig* operon transcription at 37°C could restore prodigiosin biosynthesis, the chro-

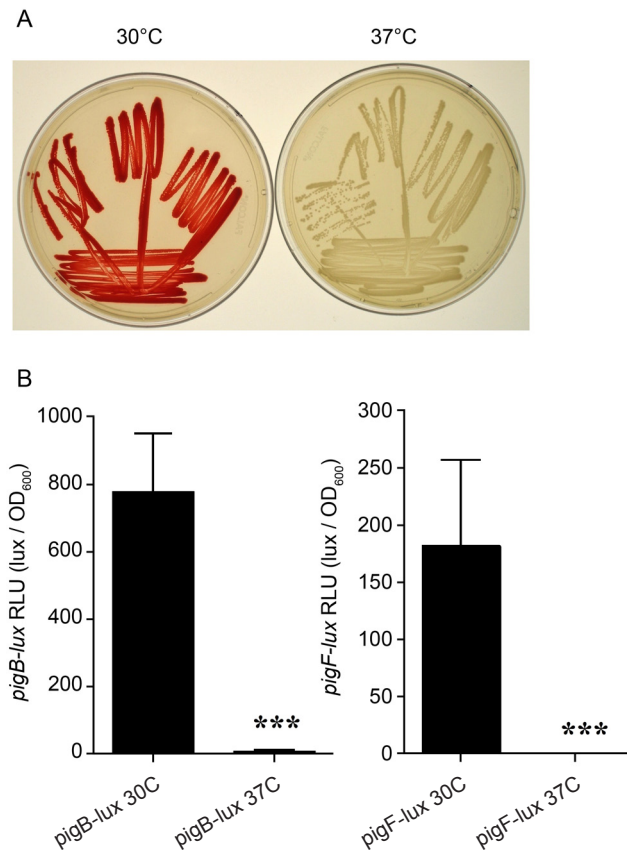


Fig. 1. Thermoregulation of pigmentation by *S. marcescens* is controlled at the transcriptional level.

A. Pigment production of the wild-type strain PIC3611 grown for 18 h at 30°C and 37°C streaked for single colonies on an LB agar plate. B. Thermoregulation of *pig* expression as measured by transposon-borne *luxCDABE* reporters integrated in *pigB* and *pigF* genes. Asterisks indicate a significant difference by Student's T-test ($p < 0.001$, $n = 6$). Means and standard deviations are shown.

mosomal *pigA-N* operon was placed under control of the inducible P_{BAD} operon of wild-type strain PIC3611 by integration of plasmid pMQ262. Prodigiosin biosynthesis of the resulting strain was tightly regulated by addition of L-arabinose to the growth medium. In the absence of L-arabinose, no visible pigmentation was observed, even at 30°C (Fig. 2A). When L-arabinose was added, pigmentation increased in a dose dependent manner at 30°C (Fig. 2A). When tested at 37°C, L-arabinose was able to induce pigmentation in the WT with P_{BAD} promoting *pig* expression (Fig. 2B). Arabinose (2 mM) added to the wild-type strain without pMQ262 did not alter pigmentation (data not shown). This result suggests that transcription of the *pigA-N* operon is sufficient to produce pigmentation even at non-permissive temperatures. This suggests that lack of *pig* operon transcription at 37°C rather than unknown mechanism(s) of post-transcriptional control are responsible for the pigmentation defect at 37°C.

HexS is necessary to inhibit pigmentation at 37°C. The CRP and HexS transcription factors are

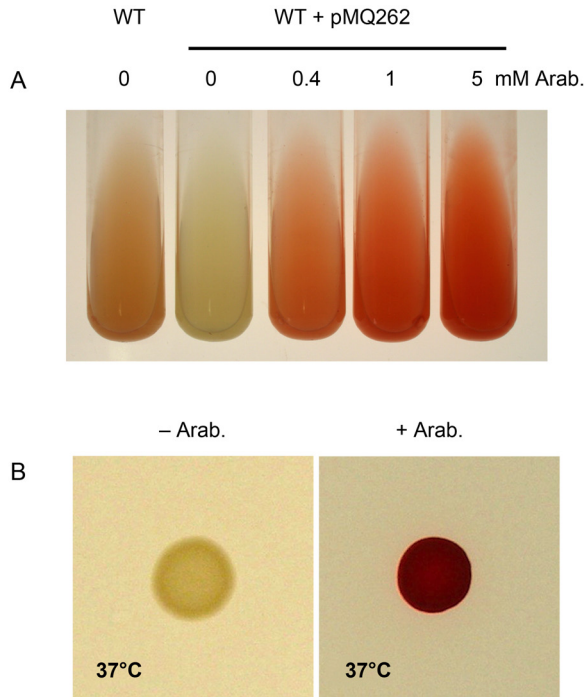


Fig. 2. Induction of *pig* operon at 37°C enables prodigiosin production.

A. Pigment production at 30°C in liquid culture after 18 h of growth at 30°C. The wild-type strain was modified by recombination of pMQ262 through which an L-arabinose-inducible promoter replaces the *pig* promoter. B. Induced expression of *pig* at 37°C enabled expression of prodigiosin demonstrates that prodigiosin can be made at 37°C when the *pig* operon is expressed using pMQ262. Images show representative macrocolonies (see materials and methods).

potent inhibitors of secondary metabolite biosynthesis in strain PIC3611 and other strains, such that *crp* and *hexS* mutants are more highly pigmented than the isogenic wild-type strains (Kalivoda et al. 2010; Stella et al. 2012; Stella and Shanks 2014; Shanks et al. 2017b). It was hypothesized that HexS and CRP were responsible for inhibiting the prodigiosin production at 37°C. To test a role for these transcription factors in thermoregulation, we used well-defined strains with *crp* and *hexS* mutations in the PIC3611 strain background. The prodigiosin phenotypes of these specific strains were previously complemented in trans with the respective genes on plasmids (Kalivoda et al. 2010; Stella and Shanks 2014). The *crp* mutant was only slightly pigmented at 37°C (Fig. 3A), whereas the *hexS* mutant was pigmented at both 30°C and 37°C (Fig. 3B). Pigment from the bacteria on agar plates was measured (Fig. 3C). The *hexS* mutant produced significantly more prodigiosin at 37°C than either wild type or the *crp* mutant. The *crp* mutant did have a ~7.5-fold increase over wild-type prodigiosin levels, but the difference was not significant. Additionally, in liquid cultures grown at 37°C, the *hexS* but not the *crp* mutant was pigmented. In this case, the wild 30°C type bacteria grown in liquid culture had an A_{534}/OD_{600} value of 0.003 ± 0.001 , the

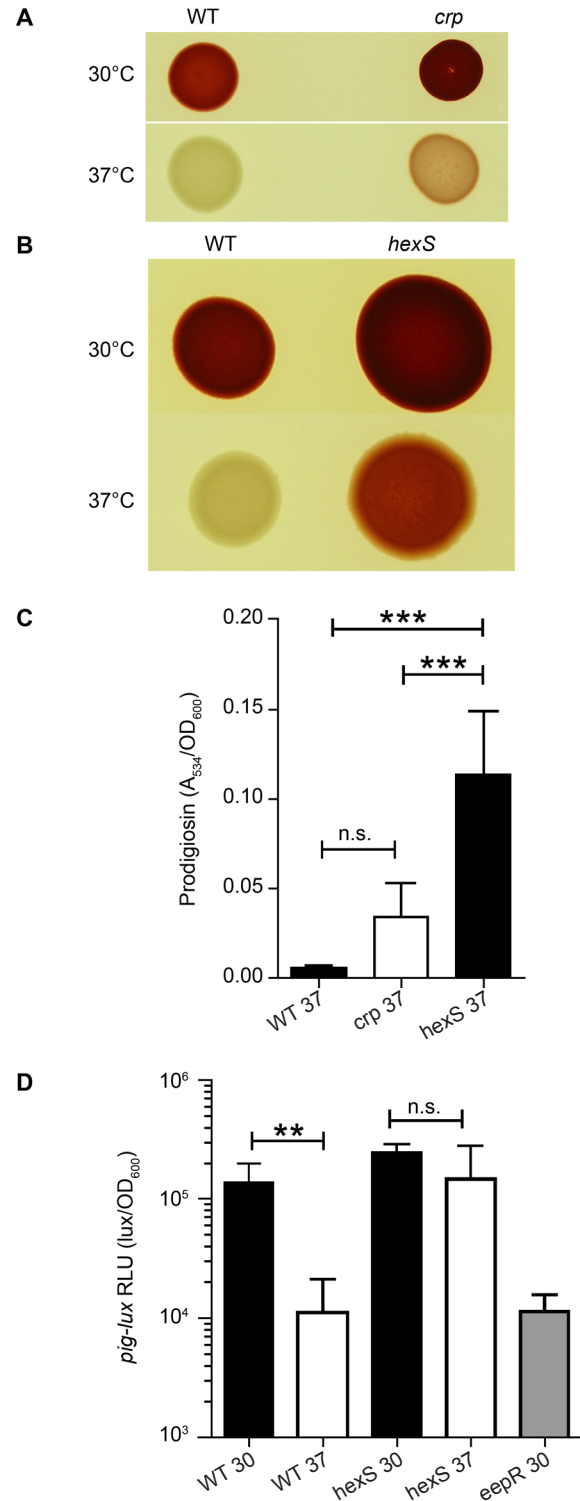


Fig. 3. The *hexS* gene contributes to pigment suppression at 37°C.

A and B. Pigment production at 30°C and 37°C after 18 h of growth at 30°C. The *hexS* mutant retains the ability to produce pigment at 37°C. The increased colony size of the *hexS* mutant reflects elevated serrawettin production. Images depict macrocolonies resulting from spotting broth from liquid culture onto an LB agar plate. C. Prodigiosin measured from macrocolonies grown at 37°C for 24 hours, normalized by OD_{600} . D. A plasmid-borne *luxCDABE* reporter for *pig* transcription was used to measure the importance of the *hexS* gene in temperature regulation. Unlike the WT, the *hexS* mutant was largely unaffected by growth at 37°C. The *eepR* mutant served as a control for low levels of *pig* transcription. Asterisks indicate significant differences by ANOVA with Tukey's post-test (** - $p < 0.01$, *** - $p < 0.001$, $n = 8$). n.s. indicates not significant.

crp mutant generated 0.004 ± 0.002 , and the *hexS* produced significantly more 0.012 ± 0.004 ($n = 6$, $p < 0.001$, ANOVA with Tukey's post-test). These results indicate that HexS has a prominent role in temperature-dependent pigment inhibition. Consistently, the *hexS* gene was found in a genetic screen in which it produced slightly pigmented colonies at 37°C in *S. marcescens* strain 274 (Tanikawa et al. 2006).

To further analyze the impact of HexS on *pig* transcription, a plasmid-borne *pig-lux* reporter was generated and used to test the prediction that *pig* transcription is increased at 37°C in the *hexS* mutant relative to the wild type. While the plasmid-borne reporter has a much higher background than the chromosomal reporters (Fig. 3D versus Fig. 1B) it was much easier to move the reporter plasmid to different strain backgrounds. A greater than 10-fold reduction in RLU measured from the *pig-lux* reporter was measured from the wild type grown at 37°C compared to 30°C. Furthermore, expression from the wild type at 37°C was indistinguishable from *pig-lux* measured from an *eepR* mutant grown at 30°C (Fig. 3D). This mutant is unable to make pigment because it lacks, EepR, a positive regulator of *pig* transcription. These data validated the reporter construct, so it was moved into the *hexS* mutant. There was no significant difference in *pig-lux* measured from the *hexS* mutant at 30°C versus 37°C ($p > 0.05$ ANOVA with Tukey's post-test), although there was a slight downward trend.

Pigment thermoregulation is EepR and PigP independent. In previous studies, it was determined that the transcription factor genes *eepR* and *pigP* were more highly expressed in *crp* and *hexS* mutants and that EepR

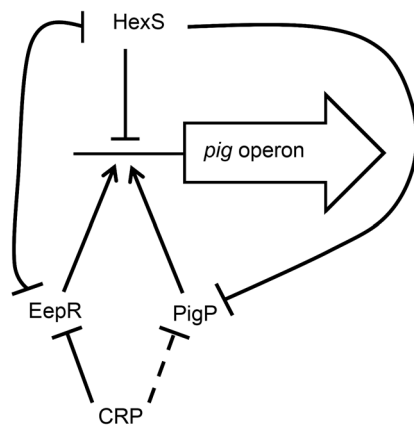


Fig. 4. Model genetic circuit used in this study. In this regulatory circuit, the role of several transcriptional regulators in control of the *pig* operon promoter and each other is depicted. Arrows indicate positive regulation and bars indicate negative regulation of transcription. All interactions have been shown to be direct except CRP inhibition of *pigP* expression (dotted line). Evidence from this study suggests that HexS inhibition of *pig* operon expression is a major reason for lack of *S. marcescens* pigmentation at 37°C.

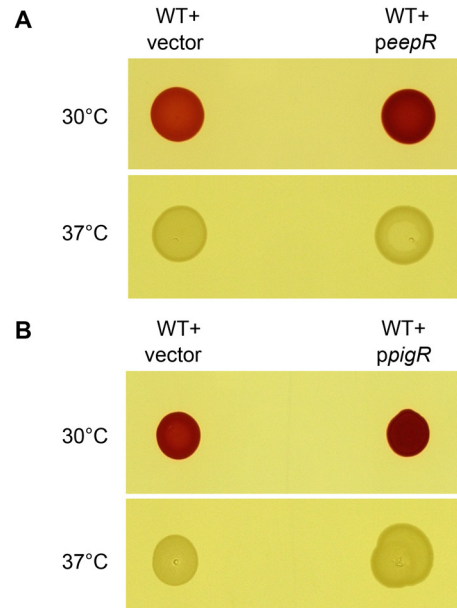


Fig. 5. Multicopy expression of *eepR* and *pigP* does not restore pigmentation at 37°C. Bacteria were plated on LB medium, incubated at 30 and 37°C for 18 hours and photographed. Multicopy expression of *eepR* (A) and *pigP* (B), increased pigmentation at 30°C, but not 37°C. Vector – pMQ132; *ppepR* – pMQ364; *ppigP* – pMQ221. Images show macrocolonies resulting from spotting broth from liquid culture onto LB agar plates.

and PigP were positive regulators of *pig* transcription in *S. marcescens* and another *Serratia* species (Fineran et al. 2005; Shanks et al. 2013; Stella et al. 2015; Shanks et al. 2017a). A model depicting the interaction between these transcription factors and the *pig* operon is shown in Fig. 4. Based on these data, we predicted that the increased expression of *eepR* and *pigP* in the *crp* and *hexS* mutants could be responsible for the increased pigmentation at 37°C. The wild-type strain with either a vector or wild-type *eepR* and *pigP* on a plasmid was grown at 30°C and 37°C, and while more pigmentation was observed at 30°C with the *eepR* and *pigP* plasmids, no pigmentation was observed at 37°C (Fig. 5). These plasmids were previously shown to complement *eepR* and *pigP* mutant phenotypes and are under control of the *E. coli lac* promoter (Shanks et al. 2013). We confirmed that the *lac* promoter is highly expressed in *S. marcescens* at both 30°C and 37°C using a transcriptional *hcred* fluorescent reporter-fusion. Although fluorescence was 2.7-fold higher at 30°C than 37°C (10745 ± 1019 RFU at 30°C versus 3997 ± 947 RFU at 37°C), at both temperatures fluorescence was much higher than background levels of ~ 10 RFU at both temperatures. Together these control experiments suggest that the plasmids are functional and expressing the genes at both temperatures. Moreover, data presented here suggest that thermoregulation of pigmentation is largely independent of EepR and PigP and is partially due to direct repression of *pig* by HexS at 37°C.

Discussion

The results of our study indicate that thermoregulation predominantly occurs at the transcriptional level. Our study: 1) correlated the nonpermissive temperature with a lack of *pig* transcription, and 2) demonstrated that artificial induction of *pig* operon transcription was sufficient for pigmentation at 37°C. This latter result indicated that the prodigiosin biosynthetic genes were translated and function at the nonpermissive temperature and that the chemical substrates needed to generate prodigiosin were present in the cell at the non-permissive temperature. Whereas post-transcriptional thermoregulation may be occurring, it was below the level of detection of the assays used in this study. Therefore, the findings in this study support the conclusion that thermoregulation of prodigiosin biosynthesis by *S. marcescens* occurs predominantly at the transcriptional level.

There are a large number of other stimuli that influence prodigiosin production at the transcriptional level, such as sugars, phosphate, ATP, cyclic nucleotides, indole, and quorum sensing molecules in *S. marcescens* and other *Serratia* species, presumably through the action of transcription factors that respond to the stimuli (Williamson et al. 2006; Haddix et al. 2008; Fender et al. 2012; Hidalgo-Romano et al. 2014; Haddix and Shanks 2018). It is possible that altered concentrations of one or more of these factors at 37°C is responsible for the pigment inhibition effect. Negative regulators of *S. marcescens* prodigiosin production include CRP (Kalivoda et al. 2010; Stella and Shanks 2014), HexS (Tanikawa et al. 2006; Stella et al. 2012), and RssAB (Horng et al. 2010). Previously, Horng and colleagues (2010) tested whether mutation of the *rssBA* genes would restore pigmentation at 37°C, and found that the CH-1 strain of *S. marcescens* with mutation of *rssA* or both *rssA* and *rssB* did not produce prodigiosin at 37°C. The authors concluded that prodigiosin production is inhibited by an unknown mechanism independent of the RssB/A two-component system (Horng et al. 2010). Here, we found that mutation of *crp* allowed production of faintly red colonies at 37°C, but liquid cultures were not red at 37°C. This may be due to a number of different variables between growth in liquid and on plates such as oxygen levels, as oxygen is necessary for pigment production (Heinemann et al. 1970). A similar pattern was observed at 30°C with a *pigP* mutant of strain PIC3611 and *gumB* and *eepR* mutants of the strain K904 background, all of which produced pink colonies on plates, but no detectable pigmentation in aerated liquid cultures (Shanks et al. 2013; Stella et al. 2015; Stella et al. 2018). Another example is evident with the wild-type strain grown at 30°C on LB

agar plates becomes bright red (Fig. 1A) whereas in LB broth, the bacteria are clearly less pigmented (Fig. 2A). Evidence suggests that CRP does not directly bind to the pigment biosynthetic operon promoter (Kalivoda et al. 2010), implying that one or more of the many genes regulated by CRP, in turn, alters *pig* operon expression at 37°C. The CRP protein is implicated in heat shock responses in *E. coli* and other bacteria, indicating that a *crp* mutation can impact bacterial temperature responses (Nagai et al. 1990; Choudhary et al. 2014). Here, we found a relatively minor role for CRP, with some pigment being observed on agar plates in the *crp* mutant at 37°C.

The *hexS* gene of *S. marcescens* was originally isolated by Tanikawa and colleagues (2006) in a screen for mutations, in strain 274, that allowed prodigiosin and serrawettin W1 (also known as serratamolide) production at 37°C. The *hexS* mutant produced a faintly red colony at 37°C and overproduced prodigiosin at 30°C. This result was different from our study where the *hexS* mutant produced a robustly red colony at 37°C on the same medium over a similar time frame suggesting that there may be some differences between pigment regulation between strains, as has been shown for cyclic-AMP regulation of prodigiosin (Stella and Shanks 2014). Nevertheless, these studies confirm that HexS is a key transcription factor in the inhibition of pigment biosynthesis at 37°C.

Given the potential of prodigiosin and similar compounds as antimicrobial, antitumor, and anti-inflammatory therapeutics (Perez-Tomas et al. 2003; Williamson et al. 2006; Perez-Tomas and Vinas 2010), understanding regulation of the natural biosynthesis of these compounds can inform their industrial production. This study provides evidence that barriers to prodigiosin production at 37°C can be overcome at the transcriptional level, and that mutations such as in *hexS* can be used to increase prodigiosin production, and provides insight into the basic biological question of secondary metabolite thermoregulation by *S. marcescens*.

ORCID

Robert M.Q. Shanks 0000-0002-7699-5396

Acknowledgments

The authors would like to thank Mohammed AlHigaylan and Kimberly Brothers for critical reading of the manuscript. This work was supported by NIH Core Vision Research grant EY08098, NIH grant AI085570, unrestricted funds from the Research to Prevent Blindness, and the Eye and Ear Foundation of Pittsburgh.

Conflict of interest

The authors do not report any financial or personal connections with other persons or organizations, which might negatively affect the contents of this publication and/or claim authorship rights to this publication.

Literature

- Barriuso J, Hogan DA, Keshavarz T, Martínez MJ.** Role of quorum sensing and chemical communication in fungal biotechnology and pathogenesis. *FEMS Microbiol Rev.* 2018;42(5):627–638. doi:10.1093/femsre/fuy022 [Medline](#)
- Benedetti IM, de Lorenzo V, Silva-Rocha R.** Quantitative, non-disruptive monitoring of transcription in single cells with a broad-host range GFP-*luxCDABE* dual reporter system. *PLoS One.* 2012;7(12):e52000. doi:10.1371/journal.pone.0052000 [Medline](#)
- Bertani G.** Studies on lysogenesis. I. The mode of phage liberation by lysogenic *Escherichia coli*. *J Bacteriol.* 1951;62(3):293–300. [Medline](#)
- Blizzard JL, Peterson GE.** Selective inhibition of proline-induced pigmentation in washed cells of *Serratia marcescens*. *J Bacteriol.* 1963;85:1136–1140. [Medline](#)
- Cheng MF, Lin CS, Chen YH, Sung PJ, Lin SR, Tong YW, Weng CF.** Inhibitory growth of oral squamous cell carcinoma cancer via bacterial prodigiosin. *Mar Drugs.* 2017;15(7):224. doi:10.3390/md15070224 [Medline](#)
- Chiang SL, Rubin EJ.** Construction of a mariner-based transposon for epitope-tagging and genomic targeting. *Gene.* 2002;296(1–2):179–185. doi:10.1016/S0378-1119(02)00856-9 [Medline](#)
- Choi SY, Im H, Mitchell RJ.** Violacein and bacterial predation: promising alternatives for priority multidrug resistant human pathogens. *Future Microbiol.* 2017;12(10):835–838. doi:10.2217/fmb-2017-0090 [Medline](#)
- Choudhary E, Bishai W, Agarwal N.** Expression of a subset of heat stress induced genes of *Mycobacterium tuberculosis* is regulated by 3',5'-cyclic AMP. *PLoS One.* 2014;9(2):e89759. doi:10.1371/journal.pone.0089759 [Medline](#)
- Danevčič T, Borić Vežjak M, Tabor M, Zorec M, Stopar D.** Prodigiosin induces autolysins in actively grown *Bacillus subtilis* cells. *Front Microbiol.* 2016a;7:27. doi:10.3389/fmicb.2016.00027 [Medline](#)
- Danevčič T, Borić Vežjak M, Zorec M, Stopar D.** Prodigiosin – A multifaceted *Escherichia coli* antimicrobial agent. *PLoS One.* 2016b;11(9):e0162412. doi:10.1371/journal.pone.0162412 [Medline](#)
- Daniels R, Vanderleyden J, Michiels J.** Quorum sensing and swarming migration in bacteria. *FEMS Microbiol Rev.* 2004;28(3):261–289. doi:10.1016/j.femsre.2003.09.004 [Medline](#)
- Demain AL, Fang A.** The natural functions of secondary metabolites. *Adv Biochem Eng Biotechnol.* 2000;69:1–39. doi:10.1007/3-540-44964-7_1 [Medline](#)
- Fender JE, Bender CM, Stella NA, Lahr RM, Kalivoda EJ, Shanks RMQ.** *Serratia marcescens* quinoprotein glucose dehydrogenase activity mediates medium acidification and inhibition of prodigiosin production by glucose. *Appl Environ Microbiol.* 2012;78(17):6225–6235. doi:10.1128/AEM.01778-12 [Medline](#)
- Fineran PC, Slater H, Everson L, Hughes K, Salmond GPC.** Biosynthesis of tripyrrole and β -lactam secondary metabolites in *Serratia*: integration of quorum sensing with multiple new regulatory components in the control of prodigiosin and carbapenem antibiotic production. *Mol Microbiol.* 2005;56(6):1495–1517. doi:10.1111/j.1365-2958.2005.04660.x [Medline](#)
- Haddix PL, Jones S, Patel P, Burnham S, Knights K, Powell JN, LaForm A.** Kinetic analysis of growth rate, ATP, and pigmentation suggests an energy-spilling function for the pigment prodigiosin of *Serratia marcescens*. *J Bacteriol.* 2008;190(22):7453–7463. doi:10.1128/JB.00909-08 [Medline](#)
- Haddix PL, Shanks RMQ.** Prodigiosin pigment of *Serratia marcescens* is associated with increased biomass production. *Arch Microbiol.* 2018;200(7):989–999. doi:10.1007/s00203-018-1508-0 [Medline](#)
- Hage-Hülsmann J, Grünberger A, Thies S, Santiago-Schübel B, Klein AS, Pietruszka J, Binder D, Hilgers F, Domröse A, Drepper T, et al.** Natural biocide cocktails: combinatorial antibiotic effects of prodigiosin and biosurfactants. *PLoS One.* 2018;13(7):e0200940. doi:10.1371/journal.pone.0200940 [Medline](#)
- Heinemann B, Howard AJ, Palocz HJ.** Influence of dissolved oxygen levels on production of L-asparaginase and prodigiosin by *Serratia marcescens*. *Appl Microbiol.* 1970;19(5):800–804. [Medline](#)
- Hidalgo-Romano B, Gollihar J, Brown SA, Whiteley M, Valenzuela E Jr, Kaplan HB, Wood TK, McLean RJC.** Indole inhibition of N-acylated homoserine lactone-mediated quorum signalling is widespread in Gram-negative bacteria. *Microbiology.* 2014;160(Pt_11):2464–2473. doi:10.1099/mic.0.081729-0 [Medline](#)
- Hoefler BC, Stubbendieck RM, Josyula NK, Moisan SM, Schulze EM, Straight PD.** A Link between linear mycin biosynthesis and extracellular vesicle genesis connects specialized metabolism and bacterial membrane physiology. *Cell Chem Biol.* 2017;24:1238–1249.e7. doi:10.1016/j.chembiol.2017.08.008 [Medline](#)
- Hornig YT, Chang KC, Liu YN, Lai HC, Soo PC.** The RssB/RssA two-component system regulates biosynthesis of the tripyrrole antibiotic, prodigiosin, in *Serratia marcescens*. *Int J Med Microbiol.* 2010;300(5):304–312. doi:10.1016/j.ijmm.2010.01.003 [Medline](#)
- Im H, Choi SY, Son S, Mitchell RJ.** Combined application of bacterial predation and violacein to kill polymicrobial pathogenic communities. *Sci Rep.* 2017;7(1):14415. doi:10.1038/s41598-017-14567-7 [Medline](#)
- Kadouri DE, Shanks RMQ.** Identification of a methicillin-resistant *Staphylococcus aureus* inhibitory compound isolated from *Serratia marcescens*. *Res Microbiol.* 2013;164(8):821–826. doi:10.1016/j.resmic.2013.06.002 [Medline](#)
- Kalivoda EJ, Stella NA, Aston MA, Fender JE, Thompson PP, Kowalski RP, Shanks RMQ.** Cyclic AMP negatively regulates prodigiosin production by *Serratia marcescens*. *Res Microbiol.* 2010;161(2):158–167. doi:10.1016/j.resmic.2009.12.004 [Medline](#)
- Khan A, Singh P, Srivastava A.** Synthesis, nature and utility of universal iron chelator – Siderophore: A review. *Microbiol Res.* 2018;212–213:103–111. doi:10.1016/j.micres.2017.10.012 [Medline](#)
- Klein AS, Brass HUC, Klebl DP, Classen T, Loeschcke A, Drepper T, Sievers S, Jaeger KE, Pietruszka J.** Preparation of cyclic prodiginines by mutasynthesis in *Pseudomonas putida* KT2440. *Chembiochem.* 2018;19:1445–1552. [Medline](#)
- Klein AS, Domröse A, Bongen P, Brass HUC, Classen T, Loeschcke A, Drepper T, Laraia L, Sievers S, Jaeger KE, et al.** New prodigiosin derivatives obtained by mutasynthesis in *Pseudomonas putida*. *ACS Synth Biol.* 2017;6(9):1757–1765. doi:10.1021/acssynbio.7b00099 [Medline](#)
- Lin SR, Fu YS, Tsai MJ, Cheng H, Weng CF.** Natural compounds from herbs that can potentially execute as autophagy inducers for cancer therapy. *Int J Mol Sci.* 2017;18(7):1412. doi:10.3390/ijms18071412 [Medline](#)
- Nagai H, Yano R, Erickson JW, Yura T.** Transcriptional regulation of the heat shock regulatory gene *rpoH* in *Escherichia coli*: involvement of a novel catabolite-sensitive promoter. *J Bacteriol.* 1990;172(5):2710–2715. doi:10.1128/jb.172.5.2710-2715.1990 [Medline](#)
- Pérez-Tomás R, Montaner B, Llagostera E, Soto-Cerrato V.** The prodigiosins, proapoptotic drugs with anticancer properties. *Biochem Pharmacol.* 2003;66(8):1447–1452. doi:10.1016/S0006-2952(03)00496-9 [Medline](#)
- Pérez-Tomás R, Viñas M.** New insights on the antitumoral properties of prodiginines. *Curr Med Chem.* 2010;17(21):2222–2231. doi:10.2174/092986710791331103 [Medline](#)
- Shanks RMQ, Caiazza NC, Hinsä SM, Toutain CM, O'Toole GA.** *Saccharomyces cerevisiae*-based molecular tool kit for manipulation of genes from gram-negative bacteria. *Appl Environ Microbiol.* 2006;72(7):5027–5036. doi:10.1128/AEM.00682-06 [Medline](#)
- Shanks RMQ, Kadouri DE, MacEachran DP, O'Toole GA.** New yeast recombineering tools for bacteria. *Plasmid.* 2009;62(2):88–97. doi:10.1016/j.plasmid.2009.05.002 [Medline](#)

- Shanks RMQ, Lahr RM, Stella NA, Arena KE, Brothers KM, Kwak DH, Liu X, Kalivoda EJ.** A *Serratia marcescens* PigP homolog controls prodigiosin biosynthesis, swarming motility and hemolysis and is regulated by cAMP-CRP and HexS. *PLoS One*. 2013;8(3):e57634. doi:10.1371/journal.pone.0057634 [Medline](#)
- Shanks RMQ, Stella NA, Lahr RM, Aston MA, Brothers KM, Callaghan JD, Sigindere C, Liu X.** Suppressor analysis of *eepR* mutant defects reveals coordinate regulation of secondary metabolites and serralyisin biosynthesis by EepR and HexS. *Microbiology*. 2017;163(2):280–288. doi:10.1099/mic.0.000422 [Medline](#)
- Slater H, Crow M, Everson L, Salmond GPC.** Phosphate availability regulates biosynthesis of two antibiotics, prodigiosin and carbapenem, in *Serratia* via both quorum-sensing-dependent and -independent pathways. *Mol Microbiol*. 2003;47(2):303–320. doi:10.1046/j.1365-2958.2003.03295.x [Medline](#)
- Stella NA, Brothers KM, Callaghan JD, Passerini AM, Sigindere C, Hill PJ, Liu X, Wozniak DJ, Shanks RMQ.** An IgaA/UmoB-family protein from *Serratia marcescens* regulates motility, capsular polysaccharide, and secondary metabolite production. *Appl Environ Microbiol*. 2018;84(6):e02575-17. doi:10.1128/AEM.02575-17 [Medline](#)
- Stella NA, Fender JE, Lahr RM, Kalivoda EJ, Shanks RM.** The LysR transcription factor, HexS, is required for glucose inhibition of prodigiosin production by *Serratia marcescens*. *Adv Microbiol*. 2012;2(4):511–517. doi:10.4236/aim.2012.24065 [Medline](#)
- Stella NA, Lahr RM, Brothers KM, Kalivoda EJ, Hunt KM, Kwak DH, Liu X, Shanks RMQ.** *Serratia marcescens* cyclic AMP-receptor protein controls transcription of EepR, a novel regulator of antimicrobial secondary metabolites. *J Bacteriol*. 2015;197(15):2468–2478. doi:10.1128/JB.00136-15 [Medline](#)
- Stella NA, Shanks RMQ.** Cyclic-AMP inhibition of fimbriae and prodigiosin production by *Serratia marcescens* is strain-dependent. *Arch Microbiol*. 2014;196(5):323–330. doi:10.1007/s00203-014-0970-6 [Medline](#)
- Tanaka Y, Yuasa J, Baba M, Tanikawa T, Nakagawa Y, Matsuyama T.** Temperature-dependent bacteriostatic activity of *Serratia marcescens*. *Microbes Environ*. 2004;19(3):236–240. doi:10.1264/jsme2.19.236
- Tanikawa T, Nakagawa Y, Matsuyama T.** Transcriptional down-regulator hexS controlling prodigiosin and serrawettin W1 biosynthesis in *Serratia marcescens*. *Microbiol Immunol*. 2006;50(8):587–596. doi:10.1111/j.1348-0421.2006.tb03833.x [Medline](#)
- Vining LC.** Functions of secondary metabolites. *Annu Rev Microbiol*. 1990;44(1):395–427. doi:10.1146/annurev.mi.44.100190.002143 [Medline](#)
- Waters CM, Bassler BL.** Quorum sensing: cell-to-cell communication in bacteria. *Annu Rev Cell Dev Biol*. 2005;21(1):319–346. doi:10.1146/annurev.cellbio.21.012704.131001 [Medline](#)
- Williams RP, Goldschmidt ME, Gott CL.** Inhibition by temperature of the terminal step in biosynthesis of prodigiosin. *Biochem Biophys Res Commun*. 1965;19(2):177–181. doi:10.1016/0006-291X(65)90500-0 [Medline](#)
- Williamson NR, Fineran PC, Leeper FJ, Salmond GPC.** The biosynthesis and regulation of bacterial prodiginines. *Nat Rev Microbiol*. 2006;4(12):887–899. doi:10.1038/nrmicro1531 [Medline](#)

Clinical Interpretation of Detection of IgM Anti-*Brucella* Antibody in the Absence of IgG and *Vice Versa*; a Diagnostic Challenge for Clinicians

REEM AL JINDAN¹, NIDA SALEEM^{1*}, AAMIR SHAFI² and SHEIKH MUHAMMAD AMJAD³

¹Department of Microbiology, College of Medicine, Imam Abdulrahman Bin Faisal University, Dammam, Saudi Arabia

²Department of Computer Science, College of Computer Science and Information Technology, Imam Abdulrahman Bin Faisal University, Dammam, Saudi Arabia

³Department of Nephrology, King Salman Center of Kidney Diseases, Riyadh, Saudi Arabia

Submitted 7 September 2018, revised 1 November 2018, accepted 7 November 2018

Abstract

Non-specific and often misleading clinical presentation of active brucellosis has made it a diagnostic puzzle for treating physicians. Clinicians rely greatly on the detection of IgG and IgM anti-*Brucella* antibodies by ELISA. Different patterns of positivity have been observed for IgG and IgM anti-*Brucella* antibodies in different cases, which further increases the risk of an erroneous diagnosis. Detailed herein is our two-years data with varied *Brucella* serology patterns and their clinical interpretation. Between January 2015 to December 2017, 1102 samples were processed in the Immunology Laboratory of KFHU for *Brucella* serology. 68 samples were positive for both IgG and IgM, 28 samples were positive for IgG and negative for IgM while 15 samples were positive for IgM and negative for IgG antibodies against *Brucella*. Electronic medical records, history of exposure, signs, symptoms, laboratory data, and the final diagnosis were recorded for all these patients. None of the patients with only positive IgM antibodies was finally diagnosed with brucellosis, while a diagnosis of brucellosis was established for only one patient with IgG antibodies positive in his serum. All the double-positive (IgG- and IgM-positive) serology patterns were diagnosed as having brucellosis. We concluded that determination of single IgM or IgG anti-*Brucella*-antibodies by ELISA could both be considered as definite and should ideally be interpreted in the context of appropriate clinical scenario and confirmation by other laboratory assays.

Key words: *Brucella*-specific IgG, *Brucella*-specific IgM, Brucellosis, ELISA for *Brucella*

Introduction

Human brucellosis is a common zoonotic infection and is still prevalent in many countries of Africa, Middle East, the Mediterranean area, Indian subcontinent, Central America and Central Asia (Papas et al. 2006). In the Middle East, the incidence of human Brucellosis was the highest during the 1990s, although a gradual decline in incidence has been witnessed afterward; still, Saudi Arabia is considered an endemic zone for Brucellosis. The clinical manifestation of the disease constitutes a broad range of signs and symptoms. Patients commonly present with fever, chills, fatigue, joint, muscle and back pain. The fact that symptoms are non-specific and can be shared by other infectious diseases makes it even more difficult for clinicians to diagnose it clinically.

Although the diagnosis is confirmed by isolation of the *Brucella* spp. from tissues or body fluids, the

occupational risk of infection transmission to laboratory staff and the time-consuming and less sensitive culture examination has led to consider other diagnostic techniques more useful in the diagnostic workup of brucellosis.

Serologically, ELISA is the most popular and widely used diagnostic assay. *Brucella*-specific IgM antibodies are produced in the first week after the disease onset, reaching a maximum after two months. On the other hand, IgG antibodies are detected after the second week of infection, attaining a peak level of six to eight weeks later. While IgG response coincides more closely with the clinical course, the detection of specific IgM antibody in the absence of specific IgG antibody might be confusing for treating physician and therefore risks misdiagnosis of active brucellosis. Likewise, clinical interpretation of *Brucella*-specific IgG antibodies in the absence of IgM also creates confusion for clinicians.

* Corresponding author: N. Saleem, Department of Microbiology, College of Medicine, Imam Abdulrahman Bin Faisal University, Dammam, Saudi Arabia; e-mail: nida.saleem84@gmail.com

© 2019 Reem Al Jindan et al.

This work is licensed under the Creative Commons Attribution-NonCommercial-NoDerivatives 4.0 License (<https://creativecommons.org/licenses/by-nc-nd/4.0/>)

While some studies conducted on the diagnostic accuracy of ELISA mentioned a combined specificity of 100% for *Brucella*-specific IgM and IgG (Özdemir et al. 2011; Asaad et al. 2012), some other studies also highlighted the possible detection of *Brucella*-specific antibodies in cases without active brucellosis. Literature review reveals a great variation between studies performed on the sensitivity and specificity of *Brucella*-specific IgM and IgG antibodies detected by ELISA. Gomez et al. (2008) assigned a combined specificity of 100% for IgG and IgM and individual sensitivity of 60% and 84% for IgM and IgG, respectively. Mantur et al. (2010), on the other hand, reported a combined IgM and IgG ELISA specificity of 71.3% and a combined sensitivity of 100%. Welch et al. (2010) found a combined specificity and a combined sensitivity of 55% and 92.3%, respectively. While anti-*Brucella* antibody detection does not always indicate brucellosis, a negative antibody profile does not exclude the infection, so results of *Brucella* serology should be interpreted with great caution (Welch et al. 2010).

Experimental

Materials and Methods

A retrospective search was performed on the serum samples that were analyzed by ELISA for the presence of IgG and IgM anti-*Brucella* antibodies at the Immunology Laboratory of King Fahad Hospital of the University (KFHU) from January 2015 to December 2017. Our hospital mainly serves eastern region population of Saudi Arabia and just like other provinces, overall incidence of brucellosis has decreased significantly in the eastern province. The ethical review board of KFHU approved the study protocol.

A total number of 1051 patients were evaluated for the presence of *Brucella*-specific antibodies. Out of these patients 512 (46%) were females and 590 (53%) were males. Mean age of the patient was 37 ± 12 years. Electronic files of these patients were reviewed for their detailed medical records including age, gender, previous history of exposure, signs, symptoms, the results of other laboratory tests to support the diagnosis of brucellosis (culture, rapid slide agglutination assay), and the number of times the serology was repeated for each patient. Final diagnosis, antibiotic treatment, and all other relevant clinical information were also recorded for the patients from progress and discharge notes of the treating physician.

IgG and IgM ELISA were performed using Abcam kits (Cambridge, UK; Cat #ab100547 and Cat #ab214568, respectively). All the steps were performed following instructions from the manufacturer. Sera and

controls (50 μ l) were dispensed to the antigen-coated wells of micro-test plates followed by first incubation for 60 min at 37°C. The wells were then washed followed by addition of anti-human IgG or IgM antibodies conjugated with an alkaline phosphatase enzyme. Later ELISA plates were incubated for another 30 min at 37°C and well were washed again. Enzyme substrate (50 μ l) was then added to all wells followed by another incubation for 30 min and finally the stopping solution was added to all wells to inhibit the reaction. The color intensity was measured by ELISA reader.

IgG and IgM values above 11 standard units were considered positive. Values between 9 and 11 were considered uncertain while antibody levels below 9 standard units were considered negative for both IgM and IgG *Brucella* antibodies.

Blood culture was performed using a minimum of two culture set (one aerobic and one anaerobic) from two different venipuncture sites using a volume of 7–10 ml blood per vial for adult and 1–5 ml blood per vial for pediatric. All the vials were loaded to the Baltic system, which detected any CO₂ level change in blood culture vial as an indicator of the growth of the organisms. On identifying specific vial with CO₂ level change, subculture was performed for the sample using four plates (5% blood agar plate, Chocolate blood agar, MacConkey agar plate, and *Brucella* selective media).

RSAT (Rapid Slide Agglutination Assay Test) was performed using Atlas Medical Kits (Cambridge, UK; Cat #8.01.15.0.0010). All the steps were performed following instructions from the manufacturer. One drop (50 μ l) each of serum and control was dispensed into separate circles on the slide test followed by one drop (50 μ l) of the antigen into each well. Slides were placed on a mechanical rotator for one minute and agglutination was noted in bright indirect light.

Results

A total of 1102 samples were processed in the Immunology Laboratory of KFHU over a period of two years from January 2015 to December 2017 and ELISA serology was performed on them for IgM and IgG anti-*Brucella* antibodies.

Out of these samples, 991 were negative for both IgG and IgM antibodies, 68 samples were positive for both IgG and IgM, 28 samples were positive for IgG and negative for IgM while 15 samples were positive for IgM and negative for IgG antibodies against *Brucella*.

68 double-positive (IgG- and IgM-positive) samples belonged to 38 patients. The number of times serology was repeated for these patients and the number of times the result was the same (IgG and IgM positive) ranged between 2 and 5. The *Brucella* culture was

Table I
The serology patterns for *Brucella*-specific antibodies (ELISA).

Serology Pattern	Number of Samples	Number of Patients	Number of times serology was repeated with the same results
1 IgG ⁺ IgM ⁻	991	976	1
2 IgG ⁺ IgM ⁺	68	38	2–5
3 IgG ⁻ IgM ⁻	28	22	1–5
4 IgG ⁻ IgM ⁺	15	15	0

advised for all of these patients and turned out positive for 36 of them. RSAT was requested for only 13 patients and turned out positive for all of these double positive patients (Table I).

We have further divided single-positive patients into two groups. The first group included patients with serology positive for IgG and negative for IgM and the second group included patients who were positive for IgM and negative for IgG against *Brucella*.

Patients who had positive IgG and negative IgM anti-*Brucella* antibodies. The 28 samples positive for IgG and negative for IgM anti-*Brucella* antibodies belonged to 22 patients. The number of times per patient when the serology was IgG-*Brucella* positive and IgM-*Brucella* negative ranged between 1 and 5 (Table I). Of these patients, 81% (n=18) were males while 19% (n=4) were females. The age range of these patients varied from 7 to 64 years.

Of the 22 patients, two had additional risk factors of possible exposure to *Brucella* spp. other than residing in a *Brucella*-endemic country. One was a worker in a local slaughterhouse while other was a medical laboratory technologist. Both were residents of Dammam city, which lies in the Eastern province of Saudi Arabia.

Most common presenting complaint was fever followed by musculoskeletal pain. 12 patients presented with fever while five patients had joint-related symptoms that led the physician to request serology. Other symptoms leading to a serological assessment of *Brucella* antibodies included abdominal pain, pancytopenia, and dizziness.

RSAT test was requested for only two patients and the serology was negative for both. Blood culture for *Brucella* was performed for 21 out of 22 patients and turned out negative for all of them but one patient for whom the diagnosis of brucellosis was confirmed. Serology was requested for antinuclear antibodies (ANA) for all five patients with musculoskeletal symptoms. Four out of five patients demonstrated the presence of ANA in their sera. Anti-VCA-IgM and Monospot tests were positive in one patient and therefore a diagnosis of EBV-mononucleosis was established. Another patient was diagnosed as having HIV based on positive HIV serology on one occasion followed by a positive HIV-

PCR. Hepatitis B surface antigen was detected in the serum of one patient that led to the final diagnosis of hepatitis B. In another patient, the diagnosis of syphilis was established after the demonstration of antibodies against *Treponema pallidum* in his serum.

The definite clinical diagnosis of these patients is presented in Table II. Out of 12 patients that presented with fever, the infectious cause was identified in seven with only one patient diagnosed with active brucellosis. Out of five patients with musculoskeletal pains, three were diagnosed as having connective tissue disease, while polyarthralgia and mechanical neck pain was a diagnosis in remaining two. Out of three patients with the symptoms of abdominal pain, one patient with accompanying fever was diagnosed as having syphilis, while the other two were diagnosed with self-limited abdominal pain and prostate malignancy. The diagnosis of lymphoproliferative disorder was established in one patient with pancytopenia. Stroke was the diagnosis in one patient with the weakness of limbs. No final diagnosis could be established in the remaining two patients who presented with dizziness and were treated symptomatically by the local physician.

Patients who had positive IgM and negative IgG anti-*Brucella* antibodies. All the 15 samples positive for IgM and negative for IgG belonged to 15 patients and serology was not repeated for these patients. The age of these patients at which serology was requested ranged from 14 to 40 years. 53% (n=8) of these IgM-positive and IgG-negative patients were male, while 47% (n=7) were females.

Other than the risk of living in a high prevalence country, one patient had an additional risk of working as a nurse in the infectious diseases clinic for two years.

Fever was the most common presenting symptom and the reason behind requesting Brucellosis workup in eight out of 15 patients. Joint pains became the second most common cause leading to request ELISA for anti-*Brucella* antibodies. Other causes leading to request *Brucella* serology included a cough associated with chest pain in two patients and hematuria in one patient. Only one patient presented with splenomegaly and abdominal pain.

RSAT was performed for 13 patients and turned out positive for four patients and culture was performed for 13 patients and turned out negative for all of them. The final diagnosis for each patient with IgM positive and IgG negative anti-*Brucella* antibodies is presented in Table III.

Not a single patient was diagnosed as having brucellosis. Of all the patients that presented with fever, one had influenza while another had syphilis as definite diagnosis after demonstration of positive the Influenza PCR and the Syphilis-Ig, respectively. Pyrexia of unknown origin (PUO) was diagnosed in two patients

Table II
Patients with positive IgG and negative IgM anti-*Brucella* antibodies.

	Age	Sex	Risk factors	Symptoms	Other diagnostic tests	Final diagnosis
1	48 yr	M	No	Arthralgia	Culture negative, ANA positive	Connective tissue disease
2	45 yr	F	No	Fever, knee joint pain	Culture negative, Rubella IgG positive, ANA positive	Connective tissue disease
3	59 yr	M	No	Paralysis (TIA)	Culture negative	Stroke
4	36 yr	M	No	Fever, cough,	Culture negative	Tuberculosis
5	31 yr	M	No	Fever and fatigue	Culture negative, Monospot positive, VCA-IgM positive	EBV – infectious mononucleosis
6	35 yr	F	No	Joint pain	Culture negative, ANA positive	Polyarthralgia
7	7 yr	M	No	Fever	Culture negative, RSAT negative	Meningitis
8	34 yr	M	Worker at slaughter-house	Fever	Culture positive, VCA-IgM negative	Brucellosis
9	35 yr	M	No	Fever, fatigue, malaise	Culture negative	PUO
10	45 yr	M	No	High-grade fever	Culture negative	Self-limited febrile syndrome
11	64 yr	M	No	Fever and weight loss	Culture negative, HIV-Ab positive	HIV
12	27 yr	M	No	Fever and low BP	Culture and RSAT negative	Septic shock of unknown origin
13	17 yr	M	No	Fatigue and dizziness	Culture negative	–
14	26 yr	M	No	dizziness	–	–
15	46 yr	M	No	Pancytopenia	Culture negative	Lymphoproliferative disease
16	17 yr	F	No	Joint pain	Culture negative, ANA positive	Connective Tissue Disease
17	31 yr	F	No	Fever	Culture negative	PUO
18	17 yr	M	No	Fever and abdominal pain	Culture negative, Syphilis-Ig positive	Syphilis
19	28 yr	M	No	Abdominal pain	Culture negative	Self-limited unspecified abdominal pain
20	44 yr	M	Medical laboratory Technologist	Generalized abdominal pain	Culture negative	Prostate malignancy
21	22 yr	M	No	Neck and right shoulder pain	Culture negative, ANA negative	Mechanical neck pain
22	32 yr	M	No	Low-grade fever	Culture negative, HBsAg positive	Hepatitis-B

with fever. In another two patients, the diagnosis of acute cystitis and spondylarthrosis was established. Tuberculosis and community-acquired pneumonia remained the final diagnosis in two patients that presented with a cough and chest pain. In four patients, the demonstration of antinuclear antibodies (ANA) led to the diagnosis of systemic lupus erythematosus (SLE). Cervicalgia was diagnosed in one patient who presented with shoulder pain while another patient with arthralgia was diagnosed with multiple sclerosis. One patient with hematuria as the chief presenting complaint was diagnosed as having renal stones.

Discussion

Saudi Arabia is considered a high prevalence zone for brucellosis and the prevalence is higher in a rural community as compared to urban areas. Non-specific presentation and a high index of suspicion on part of

local physicians enabled us to describe a large series of patients who presented to the KFUH ID clinic with the clinical picture suggestive of brucellosis and variable patterns of serology results. Most common symptoms were fever and musculoskeletal pains.

Serology was performed by ELISA for all patients. Different patterns of positivity were observed for IgG and IgM anti-*Brucella* antibodies in these patients. Other laboratory assays that were performed to confirm the diagnosis included blood culture for *Brucella* and RSAT.

ELISA has a diagnostic advantage over other serological assays in an endemic setting where there is a need to process a huge number of samples. However, sensitivity and specificity of IgG and IgM anti-*Brucella* antibodies have been a topic of debate in many studies (Gomez et al. 2008). Presence of IgM antibodies is indicative of acute infection but at the same time, IgM antibodies are well known for their cross-reactions with other bacterial species, like *Yersinia*, *Escherichia coli* O157, *Salmo-*

Table III
Patients with positive IgM and negative IgG anti-*Brucella* antibodies.

	Age	Sex	Risk factors	Symptoms	Other diagnostic tests	Final diagnosis
1	14 yr	F	No	Chest pain, cough and fever	Negative blood culture and RSAT	URTI
2	30 yr	M	No	Shoulder pain	Negative blood culture and RSAT	Cervicalgia
3	40 yr	F	No	Fever and arthralgia	Negative blood culture and positive RSAT	Acute cystitis
4	32 yr	F	No	Abdominal pain and splenomegaly	Negative blood culture and RSAT, ANA positive	SLE
5	22 yr	F	No	Arthralgia	–	Multiple sclerosis
6	37 yr	F	No	Fever and back ache	–	Spondylarthrosis
7	25 yr	M	No	Fever and body aches	Positive Syphilis-Ig, Negative blood culture and RSAT	Syphilis, HTN
8	17 yr	M	No	Myalgia and arthralgia	Positive ANA, Negative blood culture and RSAT	Connective tissue disease/SLE
9	31 yr	F	No	Arthralgia	Positive ANA and dsDNA, Negative blood culture and positive RSAT	SLE
10	24 yr	M	Nurse in a Medical Unit	Fever and fatigue	Negative blood culture and positive RSAT	PUO
11	30 yr	M	No	Fever and Myalgia	Influenza PCR positive, Negative blood culture and positive RSAT	Influenza
12	30 yr	F	No	Backache	Negative blood culture and negative RSAT, ANA positive	CTD/SLE
13	39 yr	M	No	Fever cough chest pain hemoptysis	Negative RSAT	Community acquired pneumonia
14	22 yr	M	No	Hematuria	Negative blood culture and negative RSAT	Renal stones
15	24 yr	M	No	Fever	Negative blood culture and negative RSAT	PUO

nella spp. and *Francisella tularensis* (Aranis et al. 2008). Since infections have been identified as the cause of fever in most of our patients, cross-reactions are probably responsible for the detection of IgM anti-*Brucella* antibodies in these patients.

Out of 53 patients who had IgM-antibodies in their sera, 38 were also positive for IgG and all of these double-positive patients were diagnosed for brucellosis based on suggestive clinical picture and isolation of the organism from the blood culture. None of the 15 patients who had only IgM antibodies against *Brucella* in their sera were actually diagnosed as having active brucellosis.

Furthermore, the other possible reason for false positive IgM antibodies could be the presence of rheumatoid factor (ISCI 2018). Therefore, it is recommended to remove rheumatoid factor by pre-absorption before the determination of IgM anti-*Brucella* antibodies in sera to avoid possible interference with the result. One study has described a positivity of 8.8% for rheumatoid factor in patients with osteoarticular brucellosis (Corbel et al. 1985). Since most of the patients with IgM only antibodies in their sera presented with fever and joint-related symptoms and none of the sample was pre-treated to absorb rheumatoid factor, the false positivity of IgM antibodies can be attributed to interference due to rheumatoid factor.

Mantecón et al. (2006) have described IgG anti-*Brucella* antibodies more sensitive as compared to IgM in the diagnosis of brucellosis. Just like IgM antibodies, cross-reactivity leading to a false positivity has been described for IgG anti-*Brucella* antibodies. Binnicker et al. (2012) reported cross-reactivity of IgG with syphilis, while Varshoch et al. (2011) documented that tuberculosis might result in false-positive IgG antibodies. Similarly, in our series of patients, we found out a number of different infections leading to false-positive determination of IgG antibodies, including tuberculosis, syphilis, infectious mononucleosis, HIV and hepatitis B infections.

Only one patient with IgG only antibodies detected in his serum was diagnosed with brucellosis on confirmation by isolation of *Brucella* spp. from his blood culture. A possible explanation for the absence of IgM antibodies in this patient could be the fact that excess of IgG can lead to false-negative IgM in some immunoassays (Sharma et al. 2008). Al Dahouk et al. (2011) reported 11% of the patients with acute brucellosis to be negative for IgM antibodies.

The RSAT is considered a suitable screening test for the diagnosis of brucellosis; however, considering a great proportion of false-positive and false-negative results reported by RSAT, it is recommended to use a supplementary laboratory technique like ELISA or

MAT to further confirm the results of RSAT (Geresu et al. 2016). Four out of 13 patients with IgM only antibodies against *Brucella* in their sera were reported a positive by RSAT. Since none of these patients were diagnosed with brucellosis, the cross-reactions responsible for false-positive IgM were possibly leading to false-positive RAST results in these patients.

Different studies carried out on the sensitivity and specificity of IgG and IgM anti-*Brucella* antibodies reveal a great degree of variation. Furthermore, variability between the ability of different commercial IgM and IgG ELISA kits to diagnose brucellosis should be taken into account. A study conducted by Fadeel et al. (2011) evaluated the performance of four commercial kits for diagnosing brucellosis. Most of the investigation concluded the sensitivity of more than 90% for all kits with variable specificity. None of the kits obtained 100% diagnostic accuracy for diagnosing brucellosis. Authors further concluded that sensitivity of ELISA is increased when the levels of IgG and IgM against *Brucella* are considered in combination and that serology results should be interpreted in tandem with clinical history, symptoms of patients and other diagnostic tests. We found a sensitivity and specificity of 99% and 36%, respectively for *Brucella*-specific IgG ELISA. The individual sensitivity and specificity of *Brucella*-specific IgM were calculated to be 97% and 58%, respectively, when compared to bacterial culture. We further reported combined IgM and IgG ELISA specificity of 94% and a combined sensitivity of 98%, which is in accordance with above-mentioned studies (Welch et al. 2010) and therefore can help improve clinicians confidence in cases with double-positive (IgG⁺/IgM⁺) serology.

Being retrospective research, our study is subjected to some limitations. It was not possible to compare ELISA results with the MAT, the gold standard for serological diagnosis, to rule out false-positive and false-negative results for the determination of IgG and IgM anti-*Brucella* antibodies. Nevertheless, in our study, the false-positive results of IgM and IgG anti-*Brucella* antibodies may be supported by other diagnostic assays like blood culture and by taking into account the history and clinical course. Therefore, we believe that our results are in the clinical interest of the physicians who find it challenging to interpret different patterns of serology results by ELISA.

To conclude, the combined sensitivity of IgG and IgM against *Brucella* is higher when compared to individual sensitivity of IgG or IgM antibodies in the diagnosis of brucellosis. In case of positive IgM-only antibodies, the test should be repeated after preabsorption of the sample to remove rheumatoid factor. Our study highlighted the significance of cross-reactions leading to false-positive level of antibodies and there-

fore overdiagnosis of brucellosis in a region where medical conditions like tuberculosis, syphilis and connective tissue disorder can possibly simulate brucellosis. We further concluded that determination of IgG only or IgM only anti-*Brucella*-antibodies by ELISA should not be regarded as definite and should be interpreted in the context of appropriate clinical scenario and confirmation by other laboratory assays like MAT (Poester et al. 2010).

Conflict of interest

The authors do not report any financial or personal connections with other persons or organizations, which might negatively affect the contents of this publication and/or claim authorship rights to this publication.

Literature

- Al Dahouk S, Nöckler K.** Implications of laboratory diagnosis on brucellosis therapy. *Expert Rev Anti Infect Ther.* 2011;9(7):833–845. doi:10.1586/eri.11.55
- Aranís JC, Oporto CJ, Espinoza M, Riedel KI, Pérez CC, García CP.** [Usefulness of the determination of IgG and IgM antibodies by ELISA and immunocapture in a clinical series of human brucellosis] (in Spanish). *Rev Chilena Infectol.* 2008;25(2):116–121. doi:10.4067/S0716-10182008000200006
- Asaad AM, Alqahtani JM.** Serological and molecular diagnosis of human brucellosis in Najran, Southwestern Saudi Arabia. *J Infect Public Health.* 2012;5(2):189–194. doi:10.1016/j.jiph.2012.02.001 Medline
- Binnicker MJ, Theel ES, Larsen SM, Patel R.** A high percentage of serum samples that test reactive by enzyme immunoassay for anti-*Brucella* antibodies are not confirmed by the standard tube agglutination test. *Clin Vaccine Immunol.* 2012;19(8):1332–1334. doi:10.1128/CVI.00197-12 Medline
- Corbel MJ.** Recent advances in the study of *Brucella* antigens and their serological cross-reactions. *Vet Bull.* 1985;55:927–942.
- Fadeel MA, Hoffmaster AR, Shi J, Pimentel G, Stoddard RA.** Comparison of four commercial IgM and IgG ELISA kits for diagnosing brucellosis. *J Med Microbiol.* 2011;60(12):1767–1773. doi:10.1099/jmm.0.033381-0 Medline
- Geresu MA, Kassa GM.** A Review on diagnostic methods of brucellosis. *J. Veterinar. Sci. Techno.* 2016;7(1):323.
- Gómez MC, Nieto JA, Rosa C, Geijo P, Escrubano MA, Muñoz A, López C.** Evaluation of seven tests for diagnosis of human brucellosis in an area where the disease is endemic. *Clin Vaccine Immunol.* 2008;15(6):1031–1033. doi:10.1128/CVI.00424-07 Medline
- ISCII.** Spanish national records of notifiable diseases [Internet]. (in Spanish). 2018. Madrid (Spain): Carlos III Health Institute; [cited 2018 Aug 27]. Available from <http://www.isciii.es/ISCIII/es/contenidos/fd-servicios-cientifico-tecnicos/fd-vigilancias-alertas/fd-enfermedades/enfermedades-declaracion-obligatoria-series-temporales.shtml>
- Mantecón MÁ, Gutiérrez P, Zarzosa MP, Dueñas AI, Solera J, Fernández-Lago L, Vizcaino N, Almaraz A, Bratos MA, Torres AR, et al.** Utility of an immunocapture-agglutination test and an enzyme-linked immunosorbent assay test against cytosolic proteins from *Brucella melitensis* B115 in the diagnosis and followup of human acute brucellosis. *Diagn Microbiol Infect Dis.* 2006;55(1):27–35. doi:10.1016/j.diagmicrobio.2005.11.003 Medline

- Mantur B, Parande A, Amarnath S, Patil G, Walvekar R, Desai A, Parande M, Shinde R, Chandrashekar M, Patil S.** ELISA versus conventional methods of diagnosing endemic brucellosis. *Am J Trop Med Hyg.* 2010;83(2):314–318. doi:10.4269/ajtmh.2010.09-0790 [Medline](#)
- Özdemir M, Feyzioğlu B, Kurtoğlu MG, Doğan M, Dağı HT, Yüksekaya Ş, Keşli R, Baysal B.** A comparison of immunocapture agglutination and ELISA methods in serological diagnosis of brucellosis. *Int J Med Sci.* 2011;8(5):428–432. doi:10.7150/ijms.8.428 [Medline](#)
- Pappas G, Papadimitriou P, Akritidis N, Christou L, Tsianos EV.** The new global map of human brucellosis. *Lancet Infect Dis.* 2006;6(2):91–99. doi:10.1016/S1473-3099(06)70382-6 [Medline](#)
- Poester FP, Nielsen K, Ernesto Samartino L, Ling Yu W.** Diagnosis of Brucellosis. *The Open Vet Sci J.* 2010;4(1):46–60. doi:10.2174/1874318801004010046
- Sharma R, Chisnall C, Cooke RPD.** Evaluation of in-house and commercial immunoassays for the sero-diagnosis of brucellosis in a non-endemic low prevalence population. *J Infect.* 2008;56(2):108–113. doi:10.1016/j.jinf.2007.10.010 [Medline](#)
- Varshochi M, Majidi J, Amini M, Ghabili K, Shoja MM.** False positive seroreactivity to brucellosis in tuberculosis patients: a prevalence study. *Int J Gen Med.* 2011;4:207–210. [Medline](#)
- Welch RJ, Litwin CM.** A comparison of Brucella IgG and IgM ELISA assays with agglutination methodology. *J Clin Lab Anal.* 2010;24(3):160–162. doi:10.1002/jcla.20382 [Medline](#)

***In Vitro* and *In Vivo* Activity of Zabofloxacin and Other Fluoroquinolones Against MRSA Isolates from A University Hospital in Egypt**

NELLY M. MOHAMED^{1*}, AZZA S. ZAKARIA¹, EVA A. EDWARD¹ and AMANY ABDEL-BARY²

¹Department of Microbiology and Immunology, Faculty of Pharmacy, Alexandria University, Alexandria, Egypt

²Department of Pathology, Faculty of Medicine, Alexandria University, Alexandria, Egypt

Submitted 6 September 2018, revised 31 October 2018, accepted 9 November 2018

Abstract

The widespread of infections caused by methicillin-resistant *Staphylococcus aureus* (MRSA), has necessitated the search for alternative therapies; introduction of new agents being a suggestion. This study compares the *in vitro* and *in vivo* activities of zabofloxacin, a novel fluoroquinolone, with moxifloxacin, levofloxacin and ciprofloxacin against clinical isolates of MRSA from patients hospitalized in the Alexandria Main University hospital; a tertiary hospital in Alexandria, Egypt, where zabofloxacin has not been yet introduced. The strains tested showed the highest percentage of susceptibility to zabofloxacin (61.2%) among the tested fluoroquinolones with the most effective MIC₅₀ and MIC₉₀ (0.25 and 2 µg/ml, respectively). Time-kill curve analysis revealed a rapid bactericidal activity of zabofloxacin after 6 h of incubation with a quinolone-resistant isolate and complete killing when tested against a quinolone-sensitive isolate with inhibition of regrowth in both cases. PCR amplification and sequencing of QRDRs in selected strains revealed the following amino acid substitutions: Ser-84→Leu in GyrA, Ser-80→Phe in GrlA and Pro-451→Ser in GrlB. The *in vivo* studies demonstrated that zabofloxacin possessed the most potent protective effect against systemic infection in mice (ED50: 29.05 mg/kg) with lowest count in the dissected lungs (3.66 log₁₀ CFU/ml). The histopathological examination of lung specimens of mice treated with zabofloxacin displayed least congestion, inflammation, oedema and necrosis with clear alveolar spaces and normal vessels. In conclusion, zabofloxacin was proved to possess high *in vitro* and *in vivo* efficacy encompassing its comparators and could be considered as a possible candidate for the treatment of infections caused by MRSA. To our knowledge, this is the first study evaluating the *in vitro* and *in vivo* activity of zabofloxacin against Egyptian MRSA clinical isolates.

Key words: MRSA; ED50; fluoroquinolones; quinolone resistance-determining regions; zabofloxacin

Introduction

Staphylococcus aureus has been considered as one of the pathogenic bacteria responsible for a wide variety of diseases. Such diseases range from slight skin infections to critical infections including septicemia (Tokajian 2014). After the introduction of methicillin in 1959, methicillin-resistant *S. aureus* (MRSA) has transpired as a significant hospital-associated pathogen (Tokajian 2014). The widespread of MRSA and its capability for escalating in hospitals and community settings represent a real threat that stands against infection control practices (Tokajian 2014). The epidemiology of MRSA differs noticeably worldwide even at regional levels (Borg et al. 2007). In comparison with other African, southern and eastern Mediterranean countries, Egypt

showed the highest rates of MRSA occurrence among *S. aureus* clinical isolates (Abdel-Maksoud et al. 2016). According to the Antibiotic Resistance Surveillance and Control in the Mediterranean Region, more than 50% of the *S. aureus* isolates, obtained from blood cultures in Egypt, during a three-year study period (2003–2005), were recognized to be methicillin-resistant (Borg et al. 2007). Poor and problematic healthcare system in the majority of African countries, not excluding Egypt, inadequate financing, poor provision of properly trained healthcare professionals, poverty in infrastructure and occasional lack of adequate medications aggravate the problem, making the fight of these countries against this pathogen a real challenge (Falagas et al. 2013).

Fluoroquinolones have been recognized as promising and potent antibiotics which inhibit DNA gyrase

* Corresponding author: N.M. Mohamed, Department of Microbiology and Immunology, Faculty of Pharmacy, El-Khartoom Square, Azarita, Alexandria, Egypt; e-mail: nellymostafa@hotmail.com

© 2019 Nelly M. Mohamed et al.

This work is licensed under the Creative Commons Attribution-NonCommercial-NoDerivatives 4.0 License (<https://creativecommons.org/licenses/by-nc-nd/4.0/>)

and topoisomerase IV resulting in impeding the super-coiling of the DNA and causing bacterial death (Kocsis et al. 2016). The classic fluoroquinolones possess a considerable antimicrobial activity against Gram-negative bacteria, but their potency against Gram-positive bacteria has been controverted (Park et al. 2006). Therefore, research in the field of fluoroquinolones was oriented towards potentiating the antimicrobial efficacy against Gram-positive cocci, anaerobes and fluoroquinolone-resistant strains by finding substituents with better binding affinity to target enzymes (Kwon et al. 2006). Consequently, a number of new agents have been developed, among which was zabofloxacin (Kocsis et al. 2016). Zabofloxacin is a novel member in the family of fluoroquinolones (Park et al. 2006) with reported activity against methicillin-resistant coagulase-negative staphylococci, *Streptococcus pyogenes*, *Streptococcus pneumoniae* and *Enterococcus faecalis*. Its activity against these organisms is regarded to be superior to other fluoroquinolones as ciprofloxacin, moxifloxacin, and gemifloxacin (Park et al. 2006; Karpiuk and Tyski 2013). Zabofloxacin is slightly inferior in comparison with other fluoroquinolones against *Enterobacteriaceae* family. However, it is effective against the Gram-negative respiratory bacteria, such as *Haemophilus influenzae* and *Moraxella catarrhalis* (Karpiuk and Tyski 2013). Owing to the double mechanism of binding of zabofloxacin to the complex enzyme-DNA, the likelihood of the development of bacterial resistance is markedly diminished (Karpiuk and Tyski 2013).

The present study compared the *in vitro* activity of zabofloxacin with moxifloxacin, levofloxacin and ciprofloxacin against MRSA clinical isolates collected from hospitalized patients admitted to the Alexandria Main University hospital (AMUH); a tertiary hospital based in Alexandria, Egypt, where zabofloxacin has not been yet introduced. In addition, the *in vivo* protective activity of zabofloxacin and comparator fluoroquinolones against systemic infection caused by MRSA clinical isolate was evaluated using a mice model.

Experimental

Materials and Methods

Test organisms and bacterial identification. One hundred-sixteen clinical isolates of MRSA were collected from the routine laboratory of Alexandria Main University Hospital (AMUH) over a six-month period between January 2017 to July 2017. The clinical origins of these isolates were as follow: bronchoalveolar lavages (n = 66), blood (n = 19), urine (n = 16), pus (n = 11), and wound swabs (n = 4). As a quality control, a reference strain of methicillin-sensitive *S. aureus* (MSSA; ATCC 25923)

and a strains of methicillin-resistant *S. aureus* (MRSA; ATCC 43300) strains were included in this study.

The specimens were cultured on Mannitol Salt Agar and identified by colony morphology, Gram stain, as well as, by biochemical characteristics, which were estimated by the commercial test system Dry Spot Staphytest Plus (Oxoid, UK). Methicillin resistance was confirmed by cefoxitin and oxacillin disc diffusion methods according to the Clinical and Laboratory Standards Institute guidelines (CLSI 2013).

Antibiotics. Ciprofloxacin, CIP, (Amryia Pharm. Ind., Egypt), levofloxacin, LEV, (Sanofi-Aventis, Germany) and moxifloxacin, MOX, (Alcon, Belgium) were purchased from pharmaceutical markets. Zabofloxacin powder, ZAB, was provided by the courtesy of Dongwha Pharm. Co., Ltd. (Seoul, Korea).

Laboratory animals. Five-week-old male Swiss albino mice (body weight, 17–21 g) were purchased from Theodor Bilharz Research Institute, Giza, Egypt. All mouse experiments were performed in accordance with the ethical guidelines of the Institutional Animal Care and Use Committee, Faculty of Pharmacy, Alexandria University (ACUC Project # ACUC18/28). Mice were housed in animal rooms maintained at $23 \pm 2^\circ\text{C}$ with $50 \pm 20\%$ relative humidity.

Antimicrobial susceptibility testing. Minimum inhibitory concentrations (MICs) were determined by the microtiter broth dilution method according to the guidelines of CLSI (2012). Microtiter plates containing 5.0×10^5 CFU/ml were incubated with serial dilutions of each antibiotic in Mueller-Hinton broth (Oxoid, UK) at 35°C for 18 h, and the lowest concentration of the antibiotic that prevented visible growth was considered as the MIC.

Time-kill analysis. The time-kill studies were performed following CLSI M26-A guidelines (1999). Two isolates, one resistant and one susceptible to the four tested fluoroquinolones, named S13 and S15 respectively, were selected for this analysis. The bacterial cultures in Muller-Hinton broth (Oxoid, UK) were diluted to reach an approximate count of 10^5 to 10^6 CFU/ml and preincubated for 2 h. Then, ZAB, MOX, LEV and CIP were added to the cultures at concentrations of 0.5, 1, 2, and 4 MIC. The bacterial count was determined after 0, 3, 6 and 24 h of incubation with the antibiotics tested by culturing the bacteria on Muller-Hinton agar (Oxoid) at 37°C for 18 h following serial dilution. The antibiotic was considered as bactericidal at a concentration, which decreased the control count by 3 log CFU/ml (99.9%) at specified time intervals. The procedure was performed in triplicates and a graph of the log CFU/ml was then plotted against time with calculation of standard deviation.

Quinolone resistance-determining region (QRDR) sequence analysis. PCR was used to amplify the QRDRs of the *gyrA*, *parC* and *parE* genes using extracted

genomic DNA of the strains tested as a template and the previously described primer pairs and cycling conditions (Pan et al. 1996). To determine alterations in the DNA gyrase or topoisomerase IV, selected PCR products were purified using Zymo Research™ DNA Purification Kit and then sequenced using a system from LGC Co. Ltd. (Germany).

Determination of ED50. To determine and to compare the *in vivo* efficacy of ZAB to other fluoroquinolones in systemic infection murine model, four groups of four mice were challenged intraperitoneally with 0.2 ml of bacterial suspension adjusted with 5% gastric mucin (Oxoid, UK) in 0.9% NaCl solution at a dose 100 times higher than the minimal lethal dose. The challenge inoculum was sufficient to kill 100% of the untreated control mice, which died within 48 h after infection. An aliquot of 0.2 ml of each of ZAB, MOX, LEV and CIP was administered twice orally to mice at 1 h and 4 h post infection. Four dose levels were used: 0.63, 2.5, 10 and 40 mg/kg of body weight for each fluoroquinolone. Mortality was recorded for seven days and the effective dose needed to protect 50% of the mice (ED50) was calculated by the method of Miller and Tainter with modifications (Randhawa 2009) from the survival rates on day 7 post infection.

Bacteriological and histopathological examinations. Twenty-five mice were allocated into five treatment groups: ZAB, MOX, LEV, CIP and normal saline (control). The doses of the antibiotics were adjusted

to 10 mg/kg of body weight and injected intraperitoneally into mice twice daily beginning 24 h after infection. Mice were sacrificed by cervical dislocation on day 3 (12 h after the fourth administration). For bacteriological count, the lungs (n=4 for each group) were dissected under aseptic conditions, suspended in 0.9% NaCl solution and homogenized. Serial dilutions were performed and bacterial count in homogenized lung was determined. Lung tissue for histological examination (n=2 for each group) was fixed in 10% buffered formalin then stained with hematoxylin-eosin. Histopathological evaluation was done by an investigator who was blinded to the sample origin.

Results

***In vitro* activity.** The microtiter broth dilution MICs were determined for 116 MRSA clinical isolates (Table I). The strains showed the highest percentage of susceptibility to zabofloxacin (61.2%) among the fluoroquinolones tested. Comparing the MIC₅₀ and MIC₉₀, ZAB showed the highest potency with values of 0.25 and 2 µg/ml, respectively. Moxifloxacin followed ZAB in activity (MIC₅₀ 0.5 µg/ml, MIC₉₀ 8 µg/ml), then LEV (MIC₅₀ 4 µg/ml, MIC₉₀ 16 µg/ml) and the least effective was CIP (MIC₅₀ 8 µg/ml, MIC₉₀ 64 µg/ml). The distribution of MICs values for the four fluoroquinolones are shown in Table II. The lowest MIC range among

Table I
In vitro activity of zabofloxacin, moxifloxacin, levofloxacin and ciprofloxacin against 116 MRSA clinical isolates.

Antimicrobial agent	MIC (µg/ml)			% Susceptible	% Intermediate	% Resistant
	MIC range	MIC ₅₀ [*]	MIC ₉₀ [*]			
Zabofloxacin	0.03 – 4	0.25	2	61.2	0.9	37.9
Moxifloxacin	0.06 – 16	0.5	8	50.9	8.6	40.5
Levofloxacin	0.125 – 64	4	16	46.5	0.9	52.6
Ciprofloxacin	0.125 – > 64	8	64	42.3	1.7	56

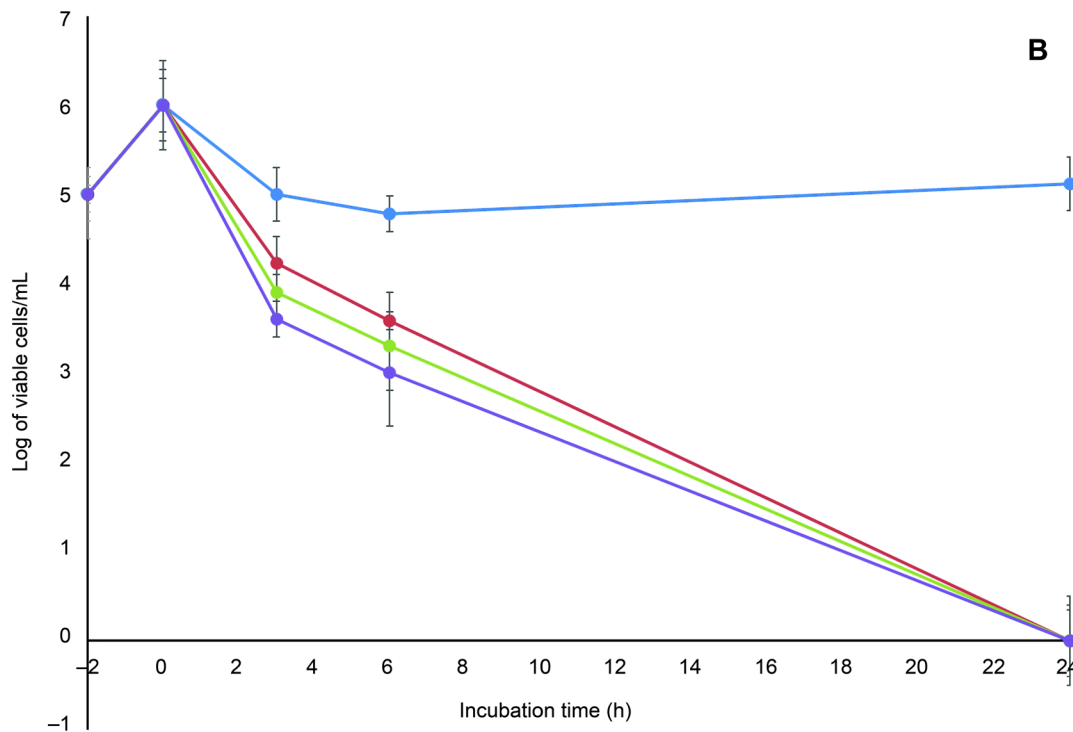
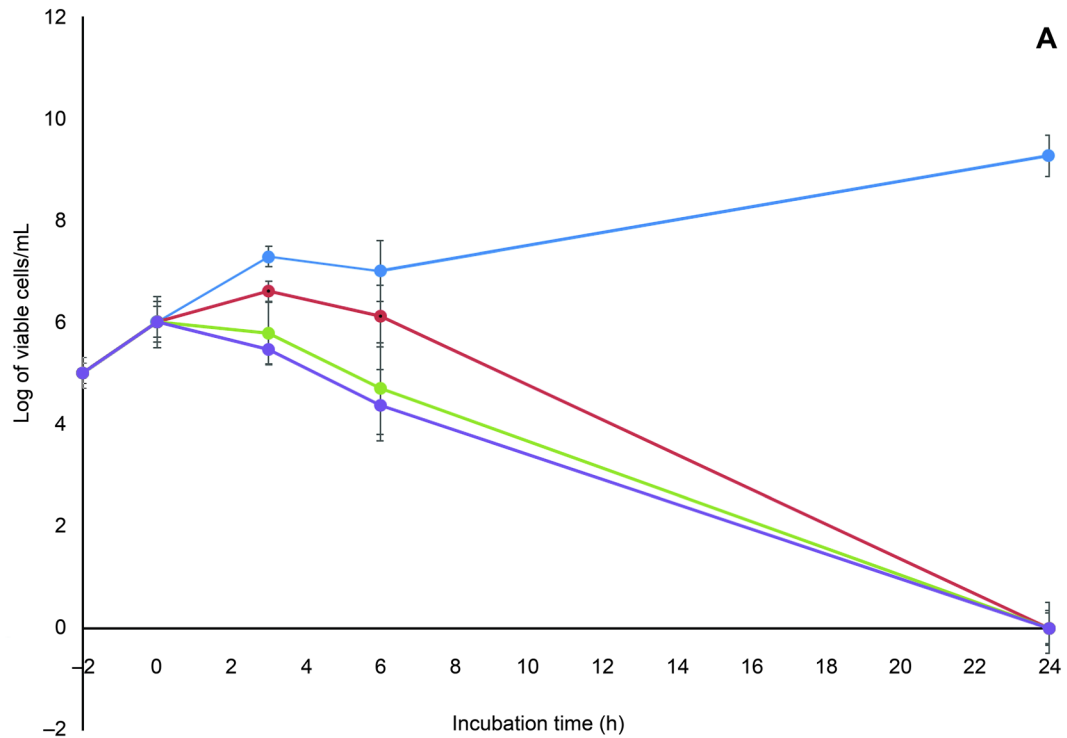
* MIC₅₀ and MIC₉₀, MICs (µg/ml) for 50% and 90% of isolates tested, respectively.

Table II
MIC distribution of zabofloxacin, moxifloxacin, levofloxacin and ciprofloxacin determined by broth microdilution method for 116 MRSA isolates.

Antimicrobial agent	MIC (µg/ml)												
	0.03	0.06	0.125	0.25	0.5	1	2	4	8	16	32	64	> 64
Zabofloxacin	10	17	25	12	7	1	32	12	0	0	0	0	0
Moxifloxacin	0	2	7	35	15	10	11	21	13	2	0	0	0
Levofloxacin	0	0	10	33	11	0	1	8	22	29	0	2	0
Ciprofloxacin	0	0	4	18	19	8	2	4	11	19	14	14	3 ^a

Bold figures indicate CLSI breakpoints applied for resistant isolates; zabofloxacin and moxifloxacin: 2 µg/ml, levofloxacin and ciprofloxacin: 4 µg/ml.

^a MIC for these isolates was greater than or equal to the indicated value.



the tested fluoroquinolones was displayed by ZAB (0.03–4 µg/ml). A comparable range (0.06–16 µg/ml) was obtained by MOX while old generation fluoroquinolones, LEV and CIP, had a much higher range (0.125–>64 µg/ml). In the presence of omeprazole, an efflux pump inhibitor (Vidaillac et al. 2007), the ZAB MIC values of all tested isolates remained unaffected (data not shown).

The bactericidal activity of the fluoroquinolones tested against MRSA was compared by time-kill analysis. As illustrated in figure 1A–D, ZAB and MOX showed a comparable rapid bactericidal activity with a decrease in the viable count by $\geq 3 \log_{10}$ CFU/ml after 6 h of contact when tested at the concentrations of 2 and 4 MIC against the fluoroquinolone-resistant clinical strain S13 (Fig. 1A and 1B). Against the fluoroquinolone-sensitive strain, S15,

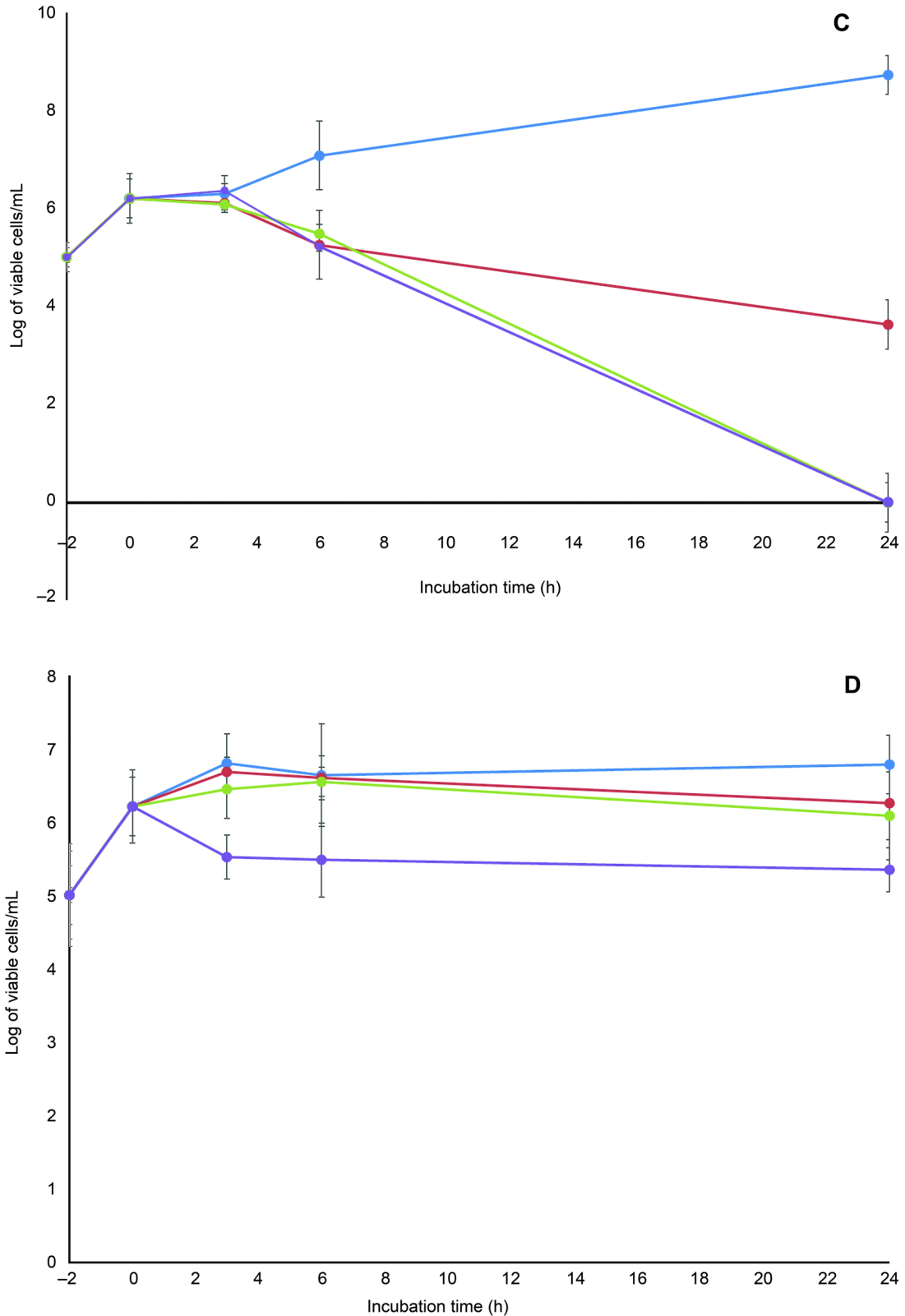
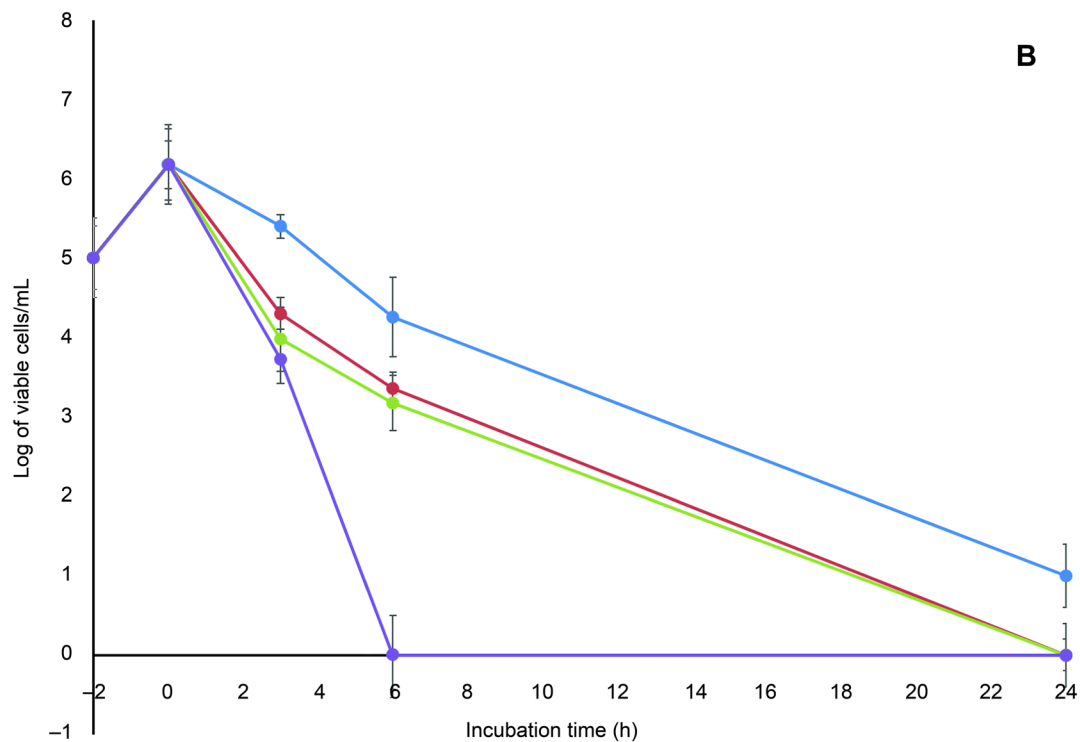
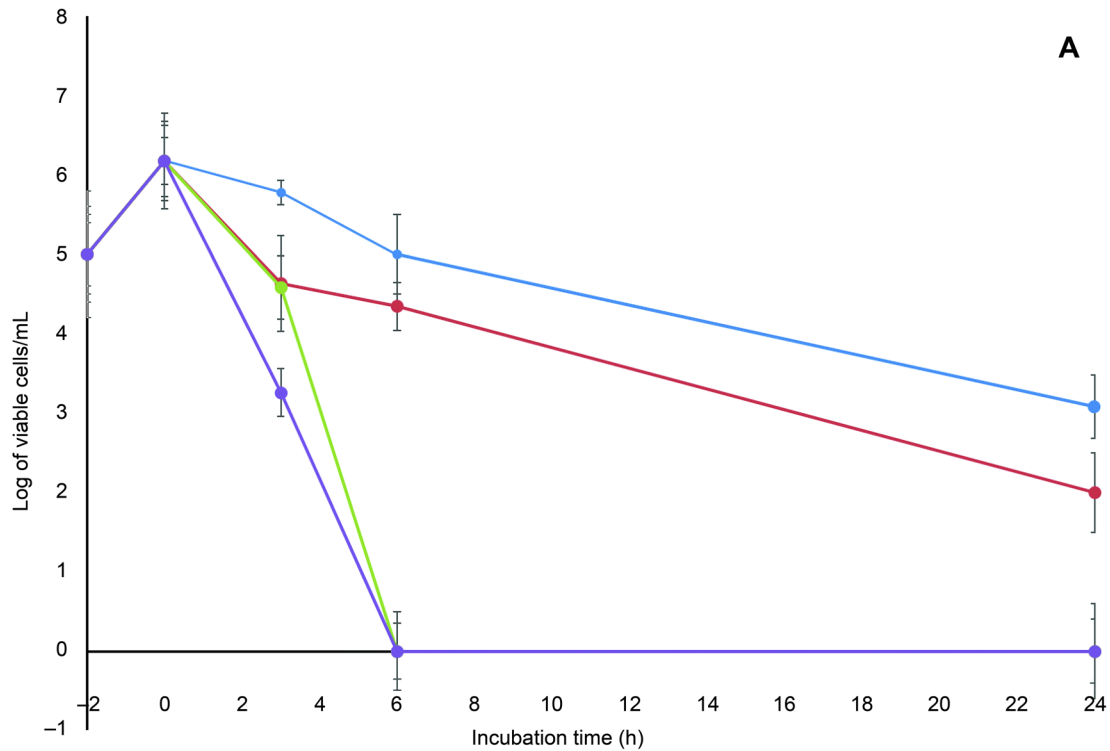


Fig. 1. Bactericidal activities of (A) zabofloxacin, (B) moxifloxacin, (C) levofloxacin and (D) ciprofloxacin against fluoroquinolone-resistant MRSA clinical isolate S13. Blue line, 0.5 MIC; red line, 1 MIC; green line, 2 MIC; purple line, 4 MIC. Data points are geometric means with error bars being one standard deviation of replicate experiments (n=3).

complete killing was achieved at 6 h when ZAB was used at a concentration of 2 MIC and at a concentration of 4 MIC when MOX was used (Fig. 2A and 2B). Regrowth

of both isolates was completely inhibited by ZAB. Older classes fluoroquinolones, LEV and CIP, exhibited an inferior pattern of bactericidal activity (Fig. 2A–D).



Analysis of QRDRs in selected MRSA strains. PCR amplification of QRDR sequences of the *gyrA*, *parC* and *parE* genes were performed for fluoroquinolone-resistant isolates. Seven isolates showing different resistance patterns were selected for sequencing analysis to detect mutations in DNA gyrase and topoisomerase IV as shown in Table III. The detected mutations revealed the following amino acid substitutions: Ser-84→Leu in

GyrA, Ser-80→Phe in *GrlA* and Pro-451→Ser in *GrlB*. Clinical isolates displaying resistance to ZAB had three mutations in the QRDRs of the *gyrA*, *parC* and *parE* genes, while isolates resistant to other fluoroquinolones, but not to ZAB, displayed a single or double point mutations.

In vivo activity. The protective efficacy of ZAB against systemic infection in mice was compared with

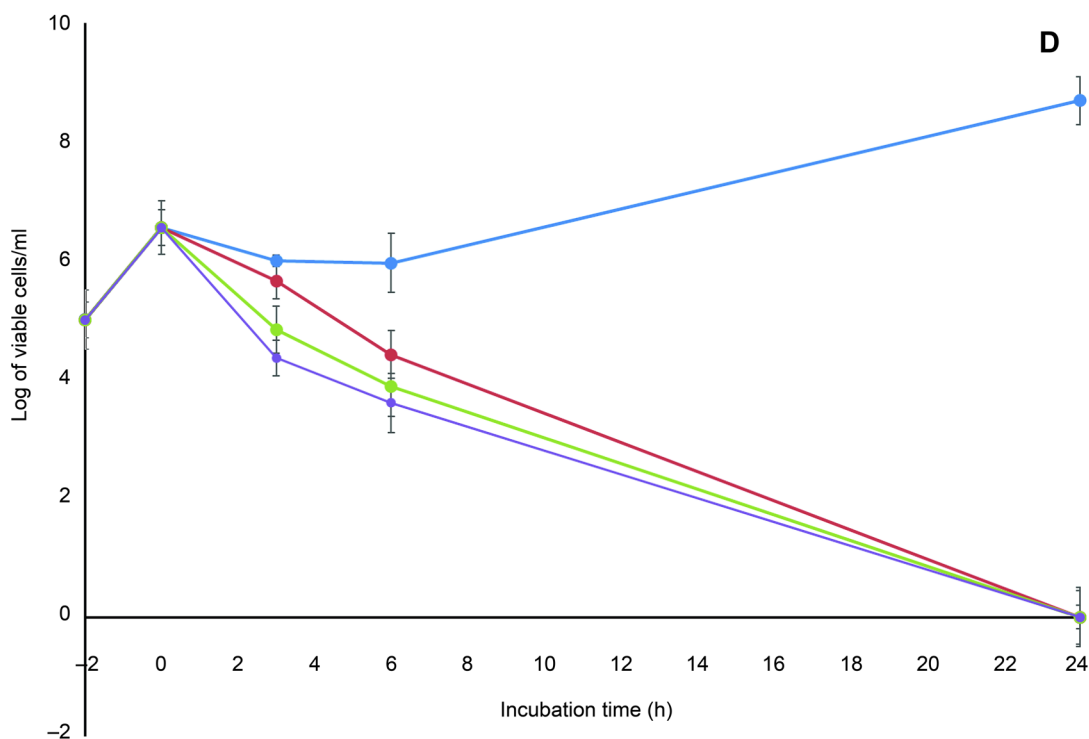
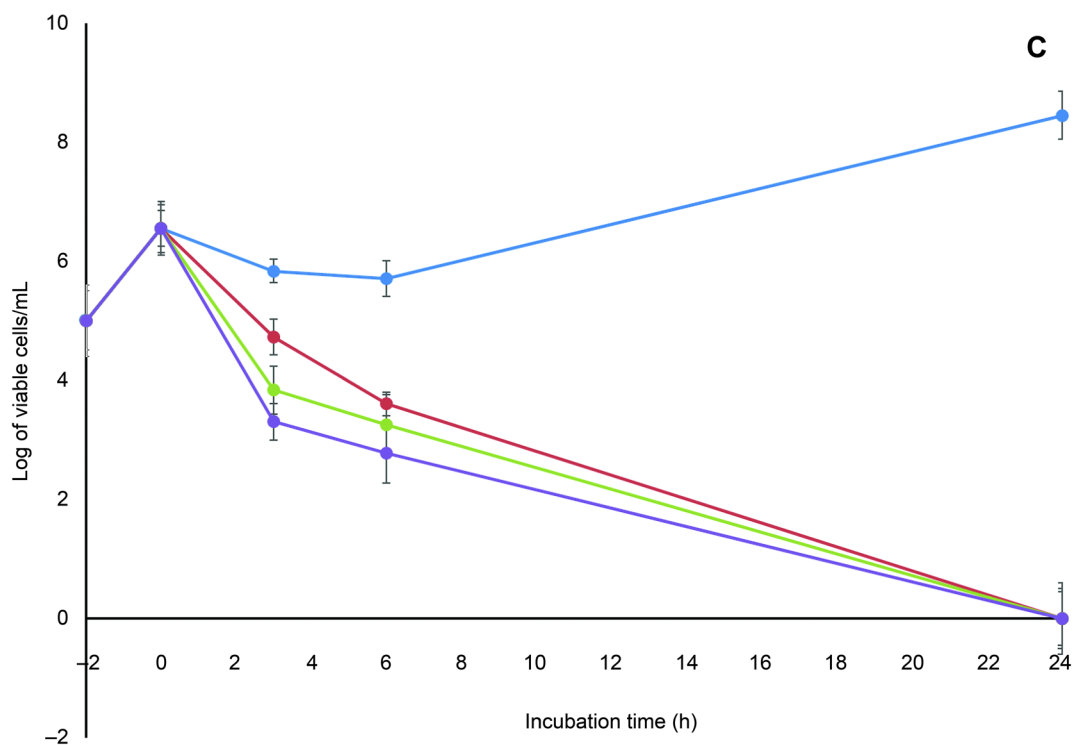


Fig. 2. Bactericidal activities of (A) zabofloxacin, (B) moxifloxacin, (C) levofloxacin and (D) ciprofloxacin against fluoroquinolone-sensitive MRSA clinical isolate S15. Blue line, 0.5 MIC; red line, 1 MIC; green line, 2 MIC; purple line, 4 MIC. Data points are geometric means with error bars being one standard deviation of replicate experiments ($n=3$).

those of MOX, LEV and CIP (Table IV). Zabofloxacin exerted the most potent protective activity (MIC: 0.06 $\mu\text{g/ml}$; ED50: 29.05 mg/kg) followed by MOX (MIC: 0.06 $\mu\text{g/ml}$; ED50: 38.69 mg/kg), while LEV and CIP required a dose of more than 40 mg/kg to elicit

a protective activity against the systemic infection (Table IV). These *in vivo* results were in accordance with the *in vitro* MICs values.

The mice group treated with ZAB showed the lowest count in the dissected lungs (3.66 \log_{10} CFU/ml),

Table III
MICs of zabofloxacin, moxifloxacin, levofloxacin and ciprofloxacin for selected 7 clinical MRSA isolates with detected mutations in QRDRs.

Strain No.	MIC ($\mu\text{g/ml}$)				Detected Mutation in QRDRs		
	ZAB ^a	MOX	LEV	CIP	<i>gyrA</i>	<i>parC</i>	<i>parE</i>
S37	4	8	32	64	S84L ^b	S80F ^c	P451S ^d
S30	2	8	16	64	S84L	S80F	P451S
S5	2	4	16	64	S84L	S80F	P451S
S3	2	8	32	64	S84L	S80F	P451S
S11	0.125	0.25	8	32	S84L	None	P451S
S38	0.25	0.25	8	16	None	S80F	None
S22	0.03	0.25	4	8	None	S80F	None

^a ZAB: zabofloxacin, MOX: moxifloxacin, LEV: levofloxacin and CIP: ciprofloxacin.

^b Serine \rightarrow Leucine, ^c Serine \rightarrow Phenylalanine, ^d Proline \rightarrow Serine.

Table IV
In vivo activities of zabofloxacin, moxifloxacin, levofloxacin and ciprofloxacin against mice infected with MRSA S19 clinical isolate.

Microorganism inoculum (CFU/mouse)	Antimicrobial agent ^a	MIC ($\mu\text{g/ml}$)	Count in dissected lungs \log_{10} (CFU/ml) ^b	ED50 ^c (mg/kg)
Methicillin-resistant <i>S. aureus</i> clinical isolate S19	Zabofloxacin	0.06	3.66	29.05
	Moxifloxacin	0.06	4.31	38.69
	Levofloxacin	8	4.01	> 40.00
	Ciprofloxacin	16	4.24	> 40.00

^a Each antimicrobial agent was administrated twice orally at 1 and 4 h post infection.

^b Count in control group receiving saline was \log_{10} 5.5 CFU/ml.

^c ED50: median effective dose needed to protect 50% of the mice.

when compared to other tested fluoroquinolones or to the control receiving saline (Table IV). These results again agreed with the *in vitro* time-kill curve findings in which ZAB showed the highest bactericidal activity as compared to the fluoroquinolones under investigation (Fig. 1A–D and Fig. 2A–D).

The histopathological examination of lung tissue sections obtained from CIP-treated mice group showed obvious features of acute bronchopneumonia almost the same as those in the untreated control with marked congestion, oedema, inflammatory infiltration, necrosis with accumulation of necro-inflammatory exudate within the lumen of bronchioles (Fig. 3). The lungs of ZAB-treated mice group revealed very mild congestion and inflammation with scarce inflammatory cells in the interstitial spaces. The mice group treated with MOX and LEV displayed moderate interstitial inflammation, moderate congestion and oedema (Fig. 3). Figure 4 demonstrates a patent alveolus dissected from ZAB-treated mice group, showing clear alveolar spaces and normal vessels and bronchioles lined by a layer of pneumocytes. The degree of congestion, inflammation, oedema and necrosis was scored using a scoring system adapted from Dubin and Kolls (2007) and summarized in Table V. Mice groups infected with MRSA clinical

Table V
Scoring of detected congestion, inflammation, oedema and necrosis in lung tissues of mice groups infected with MRSA clinical isolate S19 and treated with zabofloxacin, moxifloxacin, levofloxacin and ciprofloxacin at a dose of 20 mg/kg of body weight/day.

Histological observation ^a	(Score 0–3)			
	ZAB ^b	MOX	LEV	CIP
Congestion	0 (40%)			
	+1 (20%)	+1 (60%)	+2 (80%)	+3 (60%)
	+2 (40%)	+2 (40%)	+1 (20%)	+1 (40%)
Inflammation	0 (40%)			
	+1 (20%)	+1 (60%)	+2 (80%)	+3 (60%)
	+2 (40%)	+2 (40%)	+1 (20%)	+1 (40%)
Edema	0 (40%)			
	+1 (20%)	+1 (60%)	+2 (80%)	+3 (60%)
	+2 (40%)	+2 (40%)	+1 (20%)	+1 (40%)
Necrosis	0 (40%)			
	+1 (20%)	+1 (60%)	+2 (80%)	+3 (60%)
	+2 (40%)	+2 (40%)	+1 (20%)	+1 (40%)

^a Randomly selected sections blindly scored with a score applied to review of a whole lung section, scored at X10 magnification.

^b ZAB: Zabofloxacin, MOX: moxifloxacin, LEV: levofloxacin and CIP: ciprofloxacin.

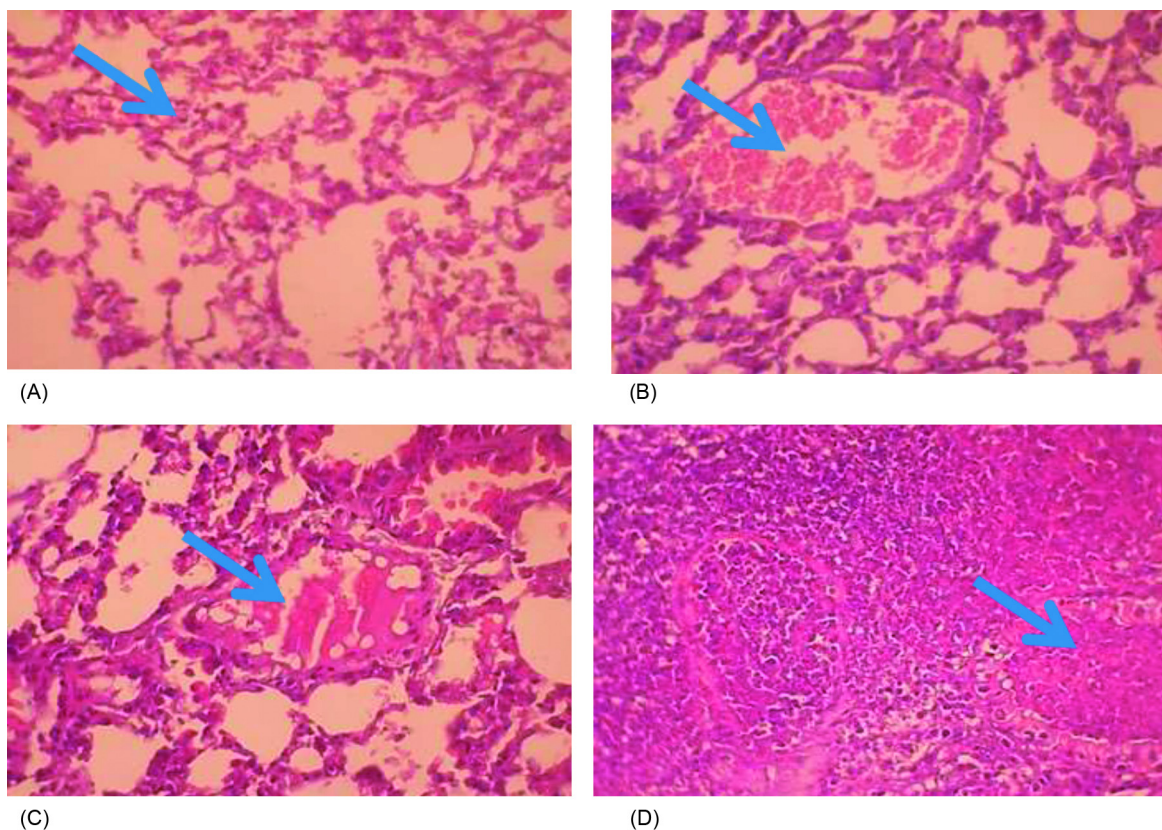


Fig. 3. Lung tissue sections dissected from mice infected with MRSA clinical isolate and treated with (A) zabofloxacin showing very mild congestion (arrow) and inflammation with scarce inflammatory cells in the interstitial spaces; (B) moxifloxacin showing moderate congestion with ectatic vessels (arrow) and moderate interstitial inflammation; (C) levofloxacin showing moderate inflammation, congestion and oedema, with a dilated lymphatic vessel (arrow); and (D) ciprofloxacin showing bronchopneumonic changes with marked congestion, oedema, inflammatory infiltration and necrosis, with accumulation of necro-inflammatory exudate within the lumen of bronchioles (arrow) (H&E x400).

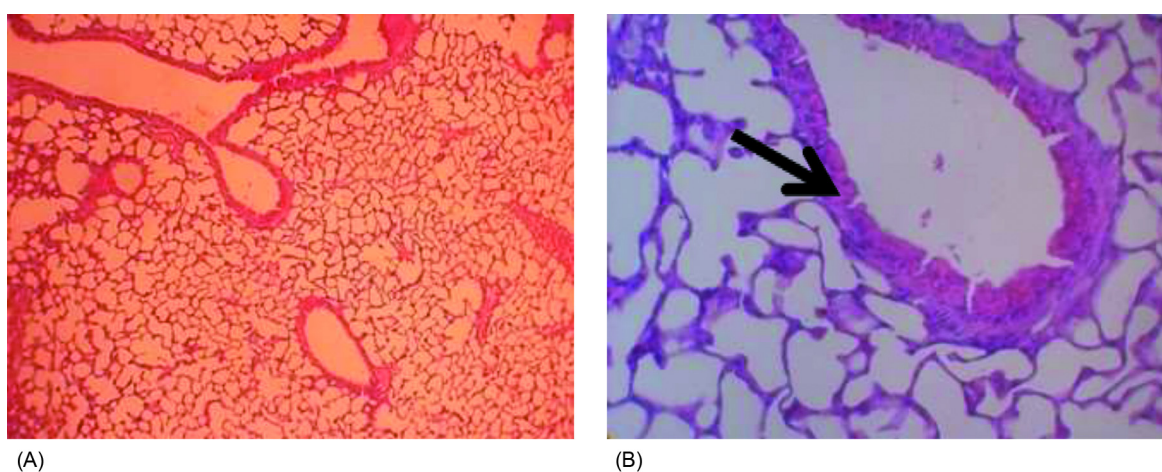


Fig. 4. (A, $\times 100$) cross section of lung tissue dissected from mice treated with zabofloxacin showing patent alveoli, (B, $\times 400$) clear alveolar spaces and normal vessels, the bronchioles are lined by a layer of pneumocytes (arrow).

isolate S19 and treated with ZAB at an adjusted dose of 20 mg/kg of body weight/day, displayed best scores with least detected congestion, inflammation, oedema and necrosis followed by MOX, then LEV and finally CIP, all administrated at same dose regimen.

Discussion

Zabofloxacin is a novel fluoroquinolone recently approved and launched in South Korea (Kocsis and Szabo 2016) with reported potent *in vitro* and *in vivo* activities

against pathogens responsible for respiratory tract and uncomplicated skin infections such as *S. pneumoniae*, *H. influenzae*, *M. catarrhalis* and *S. aureus* (Kwon et al. 2006; Park et al. 2006). This fluoroquinolone targets DNA gyrase and topoisomerase IV, and due to its double mechanism of binding to the DNA-enzyme complex, mutations in both proteins are required for the development of high-level of resistance (Park et al. 2010). This agent has not been yet introduced to Egyptian health-care facilities, including AMUH, a tertiary hospital with a heavy patient turnover and a significantly high prevalence rate (71%) of MRSA emerging as a nosocomial pathogen in its different departments (Sadaka et al. 2009). Therefore, the present study was designed to evaluate and to compare the *in vitro* and *in vivo* activity of ZAB against MRSA clinical isolates to older fluoroquinolones available on the Egyptian market.

The MIC results showed that ZAB was 4, 8 and 32-fold more active than MOX, LEV and CIP, respectively (Tables I and II). Among the 116 tested MRSA isolates, 61.2% showed susceptibility to ZAB, the highest rate obtained among comparators. The MIC₅₀ and MIC₉₀ of ZAB were 0.25 and 2 µg/ml, respectively. These values were lower than that reported by Kwon et al. (2006) and Park et al. (2006) for MRSA isolates; probably due to lack of exposure of Egyptian isolates to this new antibiotic. In addition, ZAB exhibited a rapid bactericidal activity with a decrease in the viable count by $\geq 3 \log_{10}$ CFU/ml after 6 h of contact when tested against a fluoroquinolone-resistant isolate and complete killing when tested against a fluoroquinolone-sensitive strain with inhibition of regrowth in both cases (Fig. 1A–D and 2A–D). Similar rapid bactericidal activity was reported by Park et al. (2016), when ZAB was tested against clinical isolates of *S. pneumoniae*.

In *S. aureus*, topoisomerase IV and the A subunit of the DNA gyrase are the primary targets for quinolones (Sierra et al. 2002; Karpiuk and Tyski 2013; Fernandes and Martens 2017); consequently, the *gyrA*, *parC* and *parE* genes were screened for mutations in seven isolates showing different patterns of quinolone resistance. Isolates displaying resistance to ZAB (MIC: 2–4 µg/ml) were found to have their amino acids altered in positions: Ser84 in GyrA, Ser80 in ParC and Pro451 in ParE. Mutations at Ser84 in GyrA, Ser80 in ParC (Yun et al. 2005) and Pro451 in ParE (Hannachi-M'Zali et al. 2002) were reported to be associated with a high-level of quinolone resistance in *S. aureus*. A single point mutation or double point mutation were not able to elicit a considerable increase in MIC values of ZAB (Table III). Park et al. (2016) reported previously that multiple mutations are required to produce significant elevations in MIC values of ZAB against *S. pneumoniae* isolates. Dual targeting and high susceptibility are desirable features in ZAB underlying its importance as a pos-

sible candidate for the treatment of infections caused by MRSA. The association of efflux mechanism with elevated MICs values has been reported for CIP and MOX (Kaatz et al. 2002) while ZAB was shown to be a poor efflux substrate (Park et al. 2016), similar finding was obtained in the present study suggesting that ZAB is a poor substrate for NorA efflux pump.

The *in vivo* studies demonstrated that ZAB possessed the most potent protective effect against systemic infection caused by a MRSA strain isolated from bronchoalveolar lavage (Table IV), similar findings being reported by Kwon et al. (2006) and Park et al. (2006). The histopathological examination of lung specimens of mice infected with MRSA isolate and treated with ZAB displayed least congestion, inflammation, oedema and necrosis (Table V; Fig. 3); the examined alveoli displayed clear alveolar spaces and normal vessels (Fig. 4).

In conclusion, ZAB, a new fluoroquinolone not yet introduced to the Egyptian market, was proved to possess high *in vitro* and *in vivo* potency encompassing its comparators and might be regarded as an effective treatment option for infections caused by MRSA. The clinical usefulness of ZAB needs further establishment and confirmation in studies with larger number of isolates. To our knowledge, this is the first study evaluating the *in vitro* and *in vivo* activities of ZAB against Egyptian MRSA clinical isolates.

ORCID

Nelly M. Mohamed 0000-0001-9073-5032
Azza S. Zakaria 0000-0003-3772-1381
Eva A. Edward 0000-0001-9426-5074

Acknowledgments

The authors acknowledge Dongwha Pharm. Co., Ltd. for kindly supplying zafloxacin powder used in this study. No funding was provided.

Conflict of interest

The authors do not report any financial or personal connections with other persons or organizations, which might negatively affect the contents of this publication and/or claim authorship rights to this publication.

Literature

- Abdel-Maksoud M, El-Shokry M, Ismail G, Hafez S, El-Kholy A, Attia E, Talaat M. Methicillin-Resistant *Staphylococcus aureus* recovered from healthcare- and community-associated infections in Egypt. Int J Bacteriol. 2016;2016:1–5. doi:10.1155/2016/5751785 Medline
- Borg MA, de Kraker M, Scicluna E, van de Sande-Bruinsma N, Tiemersma E, Monen J, Grundmann H; ARMed Project Members and Collaborators. Prevalence of methicillin-resistant *Staphylococcus aureus* (MRSA) in invasive isolates from southern and eastern Mediterranean countries. J Antimicrob Chemother. 2007; 60(6):1310–1315. doi:10.1093/jac/dkm365 Medline

- CLSI.** Methods for determining Bactericidal Activity of Antimicrobial Agents: approved guideline M26-A, 1999. Wayne (USA): Clinical and Laboratory Standards Institute.
- CLSI.** Methods for dilution antimicrobial susceptibility tests for bacteria that grow aerobically: approved standard-Ninth Edition M07-A9. 2012. Wayne (USA): Clinical and Laboratory Standards Institute.
- CLSI.** Performance standards for antimicrobial susceptibility testing. CLSI approved standard M100-S23. 2013. Wayne (USA): Clinical and Laboratory Standards Institute.
- Dubin PJ, Kolls JK.** IL-23 mediates inflammatory responses to mucoid *Pseudomonas aeruginosa* lung infection in mice. *Am J Physiol Lung Cell Mol Physiol.* 2007;292(2):L519–L528. doi:10.1152/ajplung.00312.2006 [Medline](#)
- Falagas ME, Karageorgopoulos DE, Leptidis J, Korbila IP.** MRSA in Africa: filling the global map of antimicrobial resistance. *PLoS One.* 2013;8(7):e68024. doi:10.1371/journal.pone.0068024 [Medline](#)
- Fernandes P, Martens E.** Antibiotics in late clinical development. *Biochem Pharmacol.* 2017;133:152–163. doi:10.1016/j.bcp.2016.09.025 [Medline](#)
- Hannachi-M'Zali F, Ambler JE, Taylor CF, Hawkey PM.** Examination of single and multiple mutations involved in resistance to quinolones in *Staphylococcus aureus* by a combination of PCR and denaturing high-performance liquid chromatography (DHPLC). *J Antimicrob Chemother.* 2002;50(5):649–655. doi:10.1093/jac/dkf243 [Medline](#)
- Kaatz GW, Moudgal VV, Seo SM.** Identification and characterization of a novel efflux-related multidrug resistance phenotype in *Staphylococcus aureus*. *J Antimicrob Chemother.* 2002;50(6):833–838. doi:10.1093/jac/dkf224 [Medline](#)
- Karpiuk I, Tyski S.** Looking for the new preparations for antibacterial therapy III. New antimicrobial agents from the quinolones group in clinical trials. *Przegl Epidemiol.* 2013;67(3):455–460. [Medline](#)
- Kocsis B, Domokos J, Szabo D.** Chemical structure and pharmacokinetics of novel quinolone agents represented by avarofloxacin, delafloxacin, finafloxacin, zabofloxacin and nemonoxacin. *Ann Clin Microbiol Antimicrob.* 2016;15(1):34. doi:10.1186/s12941-016-0150-4 [Medline](#)
- Kocsis B, Szabo D.** Zabofloxacin for chronic bronchitis. *Drugs Today (Barc).* 2016;52(9):495–500. doi:10.1358/dot.2016.52.9.2530595 [Medline](#)
- Kwon AR, Min YH, Ryu JM, Choi DR, Shim MJ, Choi EC.** *In vitro* and *in vivo* activities of DW-224a, a novel fluoroquinolone antibiotic agent. *J Antimicrob Chemother.* 2006;58(3):684–688. doi:10.1093/jac/dkl304 [Medline](#)
- Pan XS, Ambler J, Mehtar S, Fisher LM.** Involvement of topoisomerase IV and DNA gyrase as ciprofloxacin targets in *Streptococcus pneumoniae*. *Antimicrob Agents Chemother.* 1996;40(10):2321–2326. doi:10.1128/AAC.40.10.2321 [Medline](#)
- Park HS, Jung SJ, Kwak JH, Choi DR, Choi EC.** DNA gyrase and topoisomerase IV are dual targets of zabofloxacin in *Streptococcus pneumoniae*. *Int J Antimicrob Agents.* 2010;36(1):97–98. doi:10.1016/j.ijantimicag.2010.02.022 [Medline](#)
- Park HS, Kim HJ, Seol MJ, Choi DR, Choi EC, Kwak JH.** *In vitro* and *in vivo* antibacterial activities of DW-224a, a new fluoronaphthyridone. *Antimicrob Agents Chemother.* 2006;50(6):2261–2264. doi:10.1128/AAC.01407-05 [Medline](#)
- Park HS, Oh SH, Kim HS, Choi DR, Kwak JH.** Antimicrobial activity of zabofloxacin against clinically isolated *Streptococcus pneumoniae*. *Molecules.* 2016;21(11):1562. doi:10.3390/molecules21111562 [Medline](#)
- Randhawa MA.** Calculation of LD50 values from the method of Miller and Tainter, 1944. *J Ayub Med Coll Abbottabad.* 2009;21(3):184–185. [Medline](#)
- Sadaka SM, El-Ghazzawy EF, Harfoush RA, Meheissen M.** Evaluation of different methods for the rapid diagnosis of methicillin-resistance in *Staphylococcus aureus*. *Afr J Microbiol Res.* 2009; 3:49–55.
- Sierra JM, Marco F, Ruiz J, Jiménez de Anta MT, Vila J.** Correlation between the activity of different fluoroquinolones and the presence of mechanisms of quinolone resistance in epidemiologically related and unrelated strains of methicillin-susceptible and -resistant *Staphylococcus aureus*. *Clin Microbiol Infect.* 2002;8(12):781–790. doi:10.1046/j.1469-0691.2002.00400.x [Medline](#)
- Tokajian S.** New epidemiology of *Staphylococcus aureus* infections in the Middle East. *Clin Microbiol Infect.* 2014;20(7):624–628. doi:10.1111/1469-0691.12691 [Medline](#)
- Vidaillac C, Guillon J, Arpin C, Forfar-Bares I, Ba BB, Grellet J, Moreau S, Caignard DH, Jarry C, Quentin C.** Synthesis of omeprazole analogues and evaluation of these as potential inhibitors of the multidrug efflux pump NorA of *Staphylococcus aureus*. *Antimicrob Agents Chemother.* 2007;51(3):831–838. doi:10.1128/AAC.01306-05 [Medline](#)
- Yun HJ, Min YH, Jo YW, Shim MJ, Choi EC.** Increased antibacterial activity of DW286, a novel fluoronaphthyridone antibiotic, against *Staphylococcus aureus* strains with defined mutations in DNA gyrase and topoisomerase IV. *Int J Antimicrob Agents.* 2005; 25(4):334–337. doi:10.1016/j.ijantimicag.2004.11.013 [Medline](#)

Biodiversity of Bacteria Associated with Eight *Pleurotus ostreatus* (Fr.) P. Kumm. Strains from Poland, Japan and the USA

MARIUSZ ADAMSKI* and STANISŁAW J. PIETR

Agricultural Microbiology Lab, Department of Plant Protection, The Faculty of Life Sciences and Technology,
Wrocław University of Environmental and Life Sciences, Wrocław, Poland

Submitted 26 June 2018, revised 29 October 2018, accepted 14 November 2018

Abstract

Few publications report the occurrence of bacteria associated with fungal cells. The presence of bacteria associated with one strain of *Pleurotus ostreatus* (Fr.) P. Kumm. was described in the literature. We describe the biodiversity of bacteria associated with eight oyster mushroom strains from Japan, Poland, and the USA. The presence of microorganisms associated with all tested *P. ostreatus* strains was confirmed using fluorescent microscopy. Among 307 sequences, 233 of clones representing 34 genera and 74 sequences were identified as *Bacteria*. Most of the bacteria associated with the strain PUSAS were related to *E. coli* and two clones were related to *Cupriavidus* genus. The biodiversity of clones isolated from fungal strains originating from Japan and Poland ranged from 15 to 32 different bacterial clones. The most often the bacteria related to genus *Curvibacter*, *Pseudomonas*, *Bacillus*, *Cupriavidus*, *Pelomonas*, and *Propionibacterium* were associated with the strains of fungi mentioned above. Laccase-like (LMCO) genes were identified in whole bacterial DNA isolated from the associated bacteria but β -glucosidase and β -xylanase genes were not detected.

Key words: *Pleurotus ostreatus*, biodiversity, associated bacteria, fluorescent microscopy, 16S rRNA PCR

Introduction

Various types of relationship between two or more organisms are well known among plants and in the animal kingdom. However, little is known about the relationship and interactions between fungi and bacteria. There are three most common types of these relationships. Bacteria can live in the same environment as fungi where both organisms live close to each other but not in direct contact. This kind of relationship is common in various environments like forests, fermented food or animal tissues affected by diseases (Frey-Klett et al. 2011). More complicated type of bacterial-fungal association is mixed biofilms, where bacteria may live on fungal hyphae and are held by the extracellular matrix formed from molecules secreted by both organisms (Donlan and Costerton 2002). This kind of coexistence can be found in medical equipment (Pierce 2005) as well as in some infections (Hogan et al. 2007) or mycorrhizal systems (Sarand et al. 1998). The third type of interactions between these two groups of organisms is endosymbiosis when bacteria live inside fungal cells and

do not produce any specific structures. It is the most complex type of relationship and often, in contrast to free-living fungi-associated bacteria it is impossible to cultivate such bacteria outside a fungal host. The presence of unculturable endosymbiotic bacteria was described mostly in cells of arbuscular mycorrhizal fungi belonging to *Gigasporaceae* family (Bianciotto et al. 1996, 2000, 2003; Bonfante 2003; Cruz et al. 2008). The endosymbiotic bacteria were also observed in the cells of pathogenic fungus *Rhizopus microsporus* although in this case, authors were able to grow isolated bacteria on microbiological media (Partida-Martinez et al. 2007a; 2007b). Among *Basidiomycota* such relationship was found in *Laccaria bicolor*. Similarly to *Gigasporaceae* endosymbionts, these bacteria were also unculturable (Bertaux et al. 2003). Only one report described bacteria of *Burkholderia cepacia* complex related with oyster mushroom *P. ostreatus*. Authors, however, did not establish if these bacteria are endosymbionts or just fungi-related organisms (Yara et al. 2006).

The aim of this work was to identify bacteria associated with eight *P. ostreatus* strains, and also the

* Corresponding author: M. Adamski, Agricultural Microbiology Lab, Department of Plant Protection, The Faculty of Life Sciences and Technology, Wrocław University of Environmental and Life Sciences, Wrocław, Poland; e-mail: ma.mariusz.adamski@gmail.com
© 2019 Mariusz Adamski and Stanisław J. Pietr

This work is licensed under the Creative Commons Attribution-NonCommercial-NoDerivatives 4.0 License (<https://creativecommons.org/licenses/by-nc-nd/4.0/>)

description of their biodiversity and assessment of their ability for N₂ fixation, cellulose, xylanase, and laccase-like multicopper oxidase activity.

Experimental

Materials and Methods

Fungal strains. Eight strains from different geographical zones (PB63S, PBo6S, PxS, P234, P112 – Poland; PB7'96, PB8 – Japan, PUSAS – the USA) of *P. ostreatus* were analyzed. All strains were shared by the Department of Fruit, Vegetable and Mushroom Technology at the University of Life Sciences in Lublin. According to our knowledge, the strains analyzed were never cultivated on media containing antibiotics. Before experiments the fungal strains were cultivated for seven days in 28°C on Petri dishes with onion medium (onion extract 1000 ml (150 g of chopped onion boiled in 500 ml distilled H₂O, filtered on cotton filter and filled with distilled H₂O to 1000 ml, glucose 20 g, peptone 3 g, KH₂PO₄ 1 g, MgSO₄ 0.5 g, agarose 20 g).

Observation of bacteria-like organisms associated with *P. ostreatus*. Observation of living bacteria-like organisms associated with fungal cells was carried out using a fluorescent microscope and a set of fluorescent dyes (Bianciotto et al. 2000). Total fungal mycelium from one Petri dish of every oyster mushroom strain cultivated for seven days was collected and grounded in a sterile glass mortar in 1 ml of sterile 0.1 M MgSO₄. The obtained suspension was stained in a 50-μl volume with the fluorescent dye (Viability/Cytotoxicity Assay Kit for Bacteria, Biotium, USA) according to the manufacturer's protocol. Observations were made using Nikon Eclipse 90i fluorescent microscope with the Omega XF25 filter. Pictures and videos were taken in the same conditions. The fluorescent kit used in the experiments is composed of two dyes. DMAO migrates through a cell membrane and stains double-stranded DNA of both living and dead bacteria on green or yellow-green color. The second dye, EthD-III migrates through damaged membranes of dead cells only and stains bacterial DNA on red color. This dye is stronger than DMAO and covers its color, thus dead bacteria are visible as red and live bacteria are visible as green or yellow-green organisms.

Isolation of organisms associated with *P. ostreatus*. Isolation of organisms associated with fungal strains was done from seven-days old fungal culture. The 16 mm diameter roundel was picked and placed mycelium towards to the medium on base and modified solid TSB medium (Sigma-Aldrich, USA), called later in this article as TSA_t. The modification consisted of the addition of 1% of Tween 20 to the medium (ApliChem GmbH, Germany) as described by Yara et al. (2006).

After 14 days of cultivation in 28°C, 25-mm² square area of the solid medium with visible microcolonies was picked and placed in 50 ml of liquid TSA_t medium (TSB with 1% of Tween 20) in Erlenmeyer flasks. Samples were cultivated for 14 days in 28°C stationary. After cultivation TSA_t fragment was removed from samples and samples were centrifuged in 10 000 × g for 10 minutes. The supernatant was poured out and the precipitate was used for further experiments.

DNA isolation. Genomic DNA was extracted from precipitates using Genomic Mini AX Bacteria (A&A Biotechnology, Poland) according to the instructions of the manufacturer. The obtained DNA was purified with PowerClean DNA Clean-Up Kit (MO BIO Laboratories, Inc., USA) in accordance with the manufacturer's protocol. Purified DNA was stored at -20°C for further experiments.

The identification of the associated organisms was performed using whole DNA isolated from fungal strains. Fresh fungal mycelia were harvested from 25 mm² square area of the solid medium of 7 days old fungal colonies, then suspended and rubbed in 1 ml of 0.1 M MgSO₄ in sterile glass mortars. Suspension in a volume of 100 μl of each fungal strain was used for DNA isolation using PowerSoil DNA Isolation Kit (MO-BIO Laboratories, Inc., USA) according to the manufacturer's protocol. DNA was purified as described above.

16S rRNA amplification and identification. The confirmation of the bacterial nature of isolated microcolonies was carried out by determining the size of the 16S rRNA gene fragment by PCR. The reaction mixture contained isolated DNA, 2 × PCR RED Master Mix (DNA-GDANSK, Poland) kit, 799f, and 1492r primers, according to a procedure designed to distinguish bacteria and plant mitochondrial the 16S rRNA gene fragment as described by Chelius and Triplett (2001). DNA from *Pseudomonas fluorescens* PE16 strain was used as bacterial control. DNA isolated from maize cv. Cyrkon (*Zea mays* L.) was used as plant control. The controls were shared by the Agriculture Microbiology Lab at the Wrocław University of Environmental and Life Sciences. The electrophoresis of the products obtained was performed (70 min, 100 V) on the agarose gel (0.8%) with 5% ethidium bromide. Bands were visualized in Dark Hood DH 40/50 and analyzed with Gelix-One 1D Software (Biostep GmbH, Germany).

The identification of bacteria was performed using a molecular cloning technique. Products of 16S rRNA PCR were purified with PCR SureClean Plus (Bioline LTD., UK) kit. Cloning was carried out with Zero Blunt PCR Cloning Kit (Life Technologies, USA) according to manufacturer's protocol. The ligation mixture was prepared in 50:1 insert:vector ratio (250 ng of purified product), the ligation step was 30 minutes long. Competent *E. coli* TOP10 cells (Life Technologies,

Table I
Accessing numbers of *P. ostreatus* clones sequences deposited in NCBI database with most similar strains from NCBI database.

NCBI accessing number	Parent strain	Number of clones	The most similar strains in NCBI database	
			Strain name	Accessing number and similarity (%)
KR779716	PxS; PBo6S	2	<i>Methylobacterium</i> sp. 63	JF905617 (99)
KR779718	PBo6S	1	<i>Corynebacterium ureicelerivorans</i> IMMIB RIV-2301	CP009215 (99)
KR779719	PBo6S	1	<i>Corynebacterium</i> sp. clone YHSS1	EF658675 (100)
KR779720	PB8	1	<i>Corynebacterium</i> sp. clone OD-12	KX379256 (100)
KR779721	PxS; PBo6S; PB7'96	4	<i>Weissella cibaria</i> BM2	CP027427 (99)
MH424523	P112	2	<i>Weissella confusa</i> SM10	KU060300 (100)
KR779722	PBo6S; PB63S; P234; PxS	5	<i>Paracoccus</i> sp. clone SL36	HQ264096 (100)
MH424529	PB7'96	1	<i>Paracoccus yeei</i> TWCC 57946	LC371258 (100)
KR779723	P234	1	<i>Bacillus</i> sp. 1NLA3E	CP005586 (99)
KR779725	PB7'96	1	<i>Bacillus</i> sp. R-66632	KT185191 (99)
KR779726	P234; PB8; P112; PBo6S	8	<i>Bacillus</i> sp. CHORDb1	MG995009 (100)
MH424530	P112	2	<i>Bacillus</i> sp. clone D	JX505089 (99)
MH424531	PB8	1	<i>Bacillus megaterium</i> Y103	MH368091 (99)
KR779727	PxS	1	<i>Nocardioides</i> sp. clone EHFS1_S02a	EU071473 (100)
KR779728	PBo6S; PB7'96	4	<i>Nocardioides terrigena</i> DS-17	NR_044185 (99)
KR779729	PxS	1	<i>Citricoccus</i> sp. PL13f_S6	JF274870 (99)
KR779730	PxS	1	<i>Micrococcus</i> sp. EF1B-B144	KC545358 (99)
MH424533	P234	1	<i>Micrococcus luteus</i> JGTA-S5	KT805418 (99)
MH424534	PB8	1	<i>Micrococcus</i> sp. cpRA422	KJ510213 (100)
MH424535	P112	1	<i>Micrococcus</i> sp. strain CAU1456	MG214549 (99)
MH424536	P234; PxS	2	<i>Micrococcus terreus</i> IHBB 9339	KU921566 (99)
KR779731	PxS; P112; PB7'96; P234; PB8	9	<i>Pelomonas saccharophila</i> ATCC 15946	NR_115049 (99)
KR779732	P112; P234; PB8	5	<i>Staphylococcus epidermidis</i> FDAARGOS_161	CP014132 (99)
MH424568	PxS	1	<i>Staphylococcus epidermidis</i> TWSL_19	KT184899 (100)
MH424569	PxS	1	<i>Staphylococcus caprae</i> OZK14	KT591476 (99)
MH424570	P112	1	<i>Staphylococcus</i> sp. JCE 11	LT899997 (100)
MH424571	PB8	1	<i>Staphylococcus</i> sp. clone 12L_53	KP183056 (99)
KR779733	PB8; PBo6S	2	<i>Ralstonia solanacearum</i> RSCM	CP025986 (99)
MH426745	PBo6S	1	<i>Ralstonia</i> sp. clone DVBSW_M180	KF755496 (100)
KR779734	PUSAS; PBo6S; P234; PB7'96; P112	11	<i>Cupriavidus metallidurans</i> Ni-2	CP026544 (100)
MH424572	PBo6S	1	<i>Cupriavidus</i> sp. EF11(2012)	JX912460 (99)
KR779735	PxS; P112	2	<i>Propionibacterium granulosum</i> JCM 6498	NR_113367 (99)
MH424575	P112	1	<i>Propionibacterium</i> sp. clone JPL-2_O14	FJ957593 (99)
KR779736	PB7'96; P112; PxS; P234; PB63S; Pbo6S	11	<i>Propionibacterium</i> sp. clone 12L_77	KP183061 (99)
KR779737	PxS; PB8; P234; P112	5	<i>Pseudomonas</i> sp. 09C 129	CP025261 (100)
KR779738	PB7'96	1	<i>Pseudomonas fluorescens</i> 2F9	KT695813 (100)
MH424593	PB7'96	2	<i>Pseudomonas fluorescens</i> PF85	MF838663 (100)
MH424580	PB8; PB63S	2	<i>Pseudomonas simiae</i> strain 4G1010	KY939757 (100)
MH424594	P112	1	<i>Pseudomonas fluorescens</i> L228	CP015639 (100)
MH424599	PB7'96	1	<i>Pseudomonas lurida</i> MYb11	CP023272 (100)
KR779740	P112; PB63S; PB7'96	4	<i>Acidovorax</i> sp. clone M_KL_81_14	KP967499 (100)
MH427201	PB63S; PBo6S	3	<i>Acidovorax</i> sp. clone CSC28	JN541150 (100)
KR779742	PUSAS	11	<i>Escherichia coli</i> DA33137	CP029579 (100)
MH427368	PUSAS	21	<i>Escherichia coli</i> 2012C-4502	CP027440 (100)
KR779743	PUSAS	31	<i>Escherichia coli</i> 2015C-3125	CP027763 (100)

Table I. Continued.

NCBI accessing number	Parent strain	Number of clones	The most similar strains in NCBI database	
			Strain name	Accessing number and similarity (%)
MH427381	PUSAS	1	<i>Escherichia coli</i> 2013C-3342	CP027766 (100)
KR779745	PxS	1	<i>Lactobacillus sakei</i> PR11	KX139193 (99)
MH427585	PxS	1	<i>Lactobacillus sakei</i> DS4	CP025839 (99)
MH427654	PB8	1	<i>Lactobacillus sakei</i> FAM18311	CP020459 (99)
KR779746	PxS	1	<i>Legionella</i> sp. L-29	AB856218 (98)
KR779747	PxS	1	<i>Finegoldia magna</i> JCM 1766	NR_113383 (99)
KR779748	PxS	1	<i>Sporosarcina psychrophila</i> DSM 6497	CP014616 (100)
KR779749	PBo6S	1	<i>Streptococcus pneumoniae</i> 11A	CP018838 (99)
KR779750	PB8	1	<i>Kocuria rhizophila</i> 3330	KP345929 (100)
KR779751	PB8	1	<i>Lactococcus garvieae</i> MJF010	MH057260 (100)
KR779752	P234	1	<i>Delftia lacustris</i> SH2	MH014970 (100)
KR779753	P234	1	<i>Pectobacterium carotovorum</i> subsp. <i>brasiliense</i> BC1	CP009769 (100)
KR779754	P234	1	<i>Oryzihumus leptocrescens</i> S32011-b	AB649006 (100)
KR779755	P234	1	<i>Tumebacillus</i> sp. 7B-408	KF441681 (99)
KR779756	P112	1	<i>Achromobacter mucicolens</i> OZK37	KT716268 (100)
KR779757	PB7'96	1	<i>Herbaspirillum</i> sp. WW2	KU495919 (100)
MH427999	P234; PBo6S; PB8; PB63S; PxS; PB7'96; P112	35	<i>Curvibacter</i> sp. clone Z2_KL_466-12	KP967473 (100)
MH428000	PB63S, PB7'96; P112	3	<i>Curvibacter</i> sp. clone CX 18.4	KX260804 (99)
MH428038	P234	1	<i>Acidobacteria</i> clone SEW_08_293	HQ598999 (99)
MH428102	PB7'96	1	<i>Acidobacteria</i> clone SEW_08_084	HQ598816 (99)
MH428220	P112	1	<i>Paenibacillus typhae</i> xj7	NR_109462 (99)
MH428377	P112	1	<i>Paenibacillus marchantiophytorum</i> R55	NR_148618 (99)
MH428379	P234	1	<i>Acinetobacter</i> sp. SWBY1	CP026616 (99)
MH428572	P234	1	<i>Acinetobacter townneri</i> MTCC11368T	KM070563 (99)
MH428659	PBo6S	1	<i>Streptomyces rishiriensis</i> JCM 4686	LC002811 (99)
MH428674	PBo6S	1	<i>Streptomyces</i> sp. 111013air4	KP262513 (99)
MH428833	PB7'96	1	<i>Sphingomonas</i> sp. CAU-S5	MF113252 (99)

USA) were transformed with the ligand, spread on LB medium with 50 ppm of kanamycin and inoculated for 24 h in 37°C. Randomly 48 colonies, grown on plates, representing every analyzed fungal strain were picked up and inoculated on LB medium with 50 ppm of kanamycin in 96-well plates. Clones were incubated for 24 h in 37°C and sent to LGC Genomics (Berlin) for plasmids sequencing using the Sanger method with primer M13-29R (5'-CAGGAAACAGCTATGACC-3'). Because of unusual results of PUSAS strain, the clones' identification procedure was repeated and 96 associated bacteria clones were sent for identification again. Sequences with the length of approximately 700 bp were analyzed using BLAST program in NCBI (USA) database. Sequences of clones identified to species or genus were deposited in NCBI database (Table I). Phylogenetic tree of the identified species or genus was build using the neighbor-joining method with maximum sequence difference set to 0.75. The tree was built in

BLAST program and visualized in FigTree 1.4.3 (<http://tree.bio.ed.ac.uk>).

NifH gene identification. The identification of *NifH* gene was performed by PCR with PolF and PolR primers according to the procedure described by Poly et al. (2001). The reaction mixture contained the tested DNA, 5 × Hot FIREPol Blend Master Mix buffer, and the primers mentioned above. Agarose gel electrophoresis of products was performed (agarose 2%, ethidium bromide 5%, electrophoresis time of 60 min, voltage 100 V). Products were visualized as described above. As a control, *Azospirillum barseliense* 35Bb strain was used (Król and Perzynski 2005).

β-glucosidase gene identification. The identification of β-glucosidase gene was performed by PCR with bgluF and bgluR2 primers according to the procedure described by Canizares et al. (2011). The reaction mixture contained the isolated DNA, 5 × Hot FIRE-Pol Blend Master Mix buffer, and the primers men-

tioned above. Products visualization was performed as described above.

β -xylanase gene identification. For the identification of the β -xylanase gene, PCR was performed with XynF and XynR primers according to the procedure described by Khandeparker et al. (2011). The reaction mixture contained the isolated DNA, 5 \times Hot FIRE-Pol Blend Master Mix buffer and the primers mentioned above. Products visualization was performed as described above.

LMCO genes identification. The identification of LMCO (laccase-like multicopper oxidase) genes was performed by PCR with Cu1AF and Cu2R primers according to the procedure described by Kellner et al. (2008). The reaction mixture contained the isolated DNA, 5 \times Hot FIRE-Pol Blend Master Mix buffer and the primers mentioned above. Products visualization was performed as described above.

Results

A number of small bacteria-like organisms were observed inside and outside of cells of all analyzed oyster mushroom strains. They were visible as small green or yellow-green rods. The microscopic image is shown in Fig. 1. The bacteria-like organisms were marked with white arrows. Several of the cells observed were motile inside of fungal hyphae what is presented in materials published online (PxS – <https://youtu.be/G93Rm0tHIgg>; P234 – <https://youtu.be/pxApJvCshQ0>;

PB7'96 – <https://youtu.be/JZdGXSyDdG4>; PB63S – <https://youtu.be/A4U4MtUeliU>). After 10 days of cultivation, a lot of small objects were observed growing deeply in the medium around and outside fungal mycelia of all inoculates (Fig. 2). Such growth was not observed on TSA medium without addition of Tween 20. Tween 20 is used usually as a surfactant to disperse cells in solutions. Some of the bacteria also use Tween 20 as a source of fatty acids. No objects were observed in control samples that were not inoculated with fungi. Similar results were described previously by Yara et al. (2006). Blocks of media containing objects were used for cells isolation. After 14 days of stationary cultivation in the liquid TSBt medium, a white precipitate was observed on flask bottom for all oyster mushrooms strains analyzed. After centrifugation, this precipitate was used for DNA amplification protocol.

As a result of PCR performed with DNA obtained from precipitant and 799f and 1492r primers, a 700 bp product was obtained (Fig. 3). Product that size is characteristic only for bacterial DNA as it is a part of the bacterial 16S rRNA gene. For comparison, the reaction with maize DNA provided two bands: one of 1100 bp which is characteristic for plant mitochondrial DNA and second of size about 700 bp, characteristic for bacteria. The reason for this phenomenon is that maize cultivar used in experiment carry endophytic bacteria in its tissues (Pisarska and Pietr 2015).

The total number of 307 sequences was obtained as a result of the sequencing of plasmid clones. The detailed number of identified clones with the most

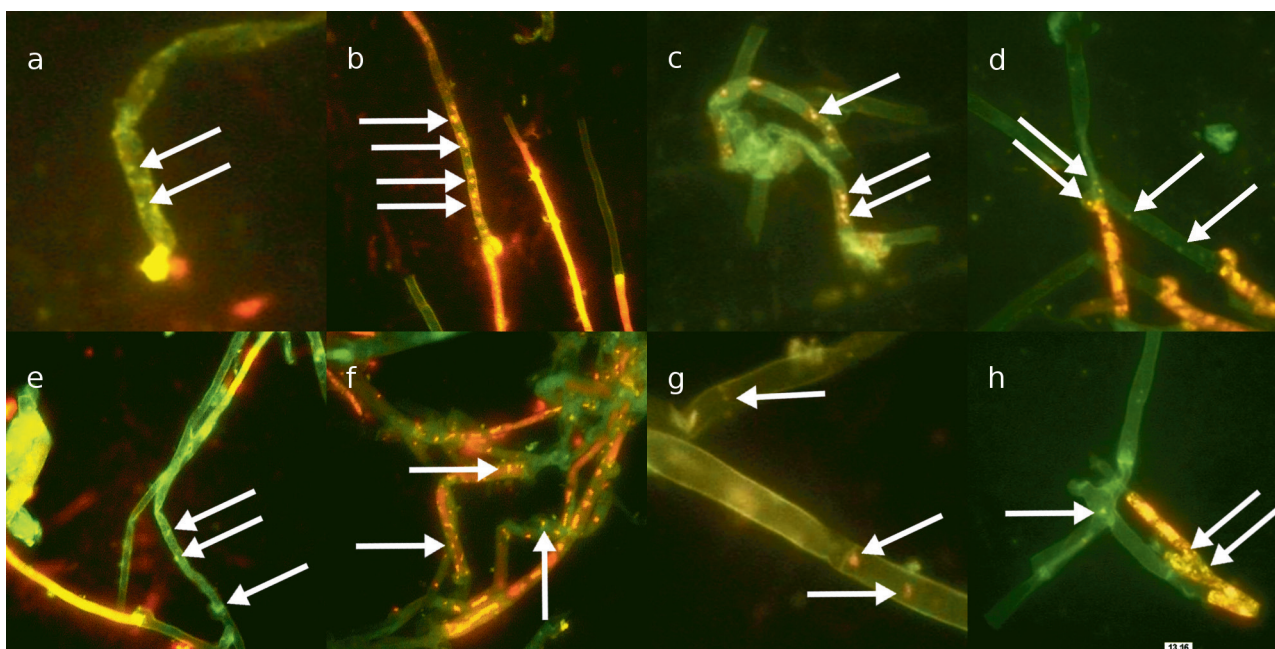


Fig. 1. Microscopic picture of analyzed oyster mushroom cells treated with fluorescent dyes under the fluorescent microscope. Strains: a) P234, b) PB63S, c) PB8, d) P112, e) PB63S, f) PUSAS, g) PB7'96, h) PxS. Bacteria-like organisms, marked with white arrows, are visible as small green or yellow-green rods against fungal cells.

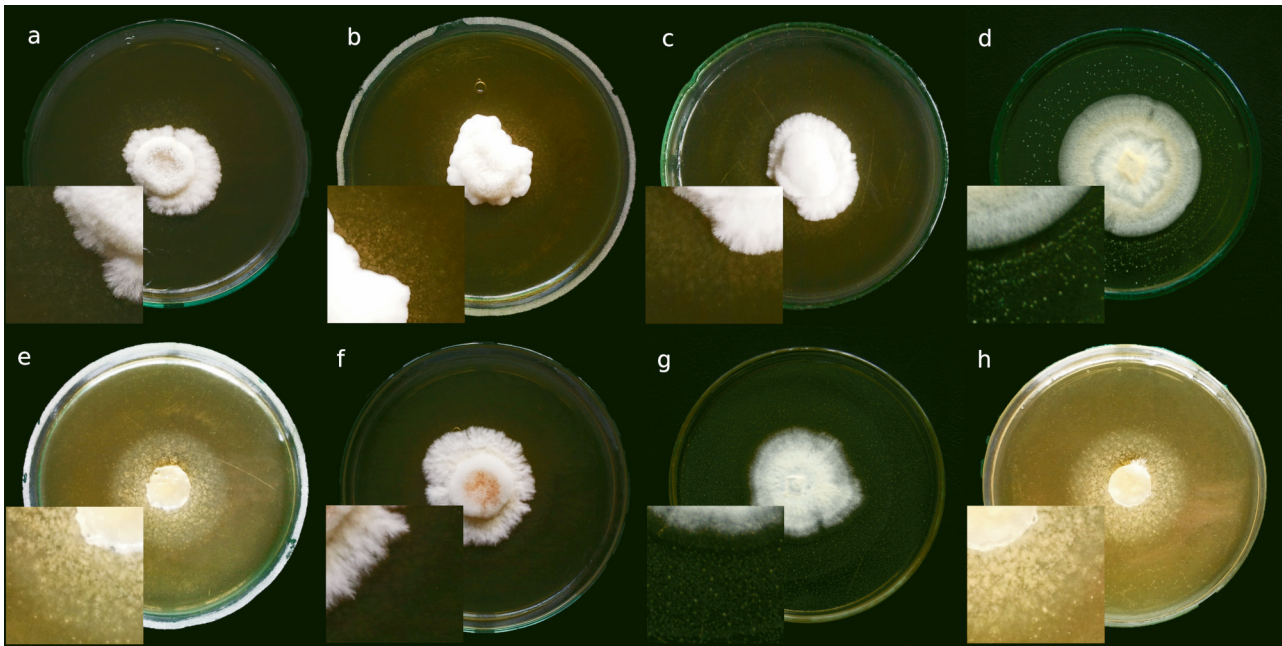


Fig. 2. Bacteria-like organisms microcolonies growing deeply in TSA medium after 10 days long cultivation. Strains: a) P234, b) PBo6S, c) PB8, d) P112, e) PB63S, f) PUSAS, g) PB7'96, h) PxS.

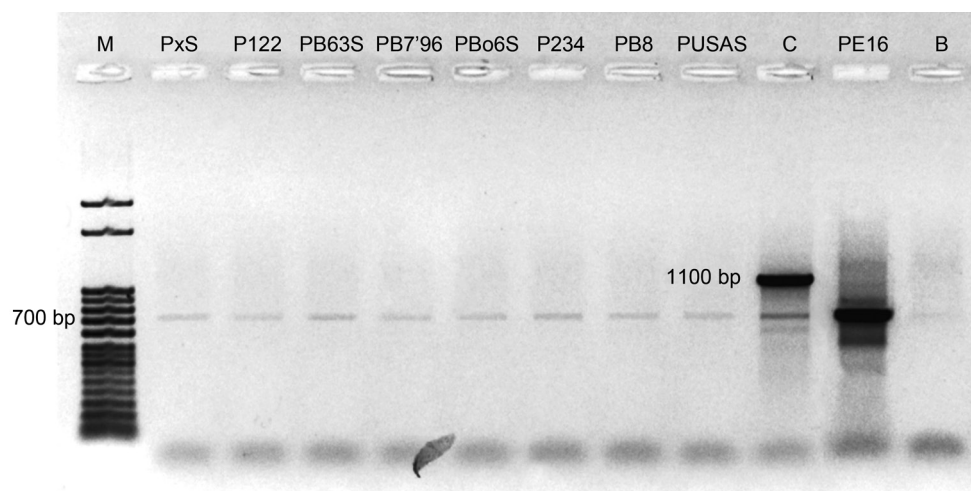


Fig. 3. Agarose gel electrophoresis showing products of PCR with 799f and 1942r primers of analyzed oyster mushroom, maize cv. Cyrkon (*Zea mays* L.) (line C) and bacterial strain *Pseudomonas fluorescens* PE16 (line PE16) DNA. The product of 700 bp is characteristic for bacterial 16S rRNA, the product of 1100 bp is characteristic for plant mitochondrial DNA. M – marker; B – blind control.

similar strains from NCBI database is presented in Table II. The species or genus was determined for 233 of them and for the remaining 74 sequences we were not able to identify higher taxonomic level than domain of *Bacteria*. All clones were identified only for PUSAS strain originated from the USA. Among other seven fungal strains, the unidentified clones occurred in the range from 7 to 15. Among tested strains of fungi, the lower biodiversity of bacteria was found for the strain PUSAS, which contained 64 clones closely related to *E. coli* and only two clones related to *Cupriavidus* genus. The only one genus, which occurred in all fungal strains analyzed but PUSAS, was *Curvibacter* and it was repre-

sented by 38 clones. *Propionibacterium* genus was found in six of eight fungal strains analyzed. It was not present only in PUSAS and PB8 strains. The total number of identified *Propionibacterium* strains was 14. Another genus found in six of *P. ostreatus* strains was *Cupriavidus*. It occurred in a total number of 13 clones in all fungal strains except PxS and PB63S. Bacteria belonging to genus *Pseudomonas* were also identified in a number of 12 clones from six fungal strains (except PUSAS and PBo6S). Genus *Pelomonas* was identified as nine clones from five fungal strains: P234, PB7'96, PB8, PxS, and P112. Bacteria from genus *Paracoccus* in a number of six were found in almost all of *P. ostreatus* strains from

Table II
Number and identification of clones obtained from analyzed *P. ostreatus* strains.

Genus	Similarity based on 700 bp sequence of the 16S rRNA gene		Number of clones	Origin <i>P. ostreatus</i> strains							
	The most closely related strain in NCBI	NCBI accession number (% of similarity)		USA		Japan		Poland			
				PUSAS	PB8	PB7'96	PBo6S	P234	PxS	PB63S	P112
<i>Escherichia</i>	<i>E. coli</i> DA33137	CP029579 (100)	64	11	0	0	0	0	0	0	0
	<i>E. coli</i> 2012C-4502	CP027440 (100)		21	0	0	0	0	0	0	0
	<i>E. coli</i> 2015C-3125	CP027763 (100)		31	0	0	0	0	0	0	0
	<i>E. coli</i> 2013C-3342	CP027766 (100)		1	0	0	0	0	0	0	0
<i>Curvibacter</i>	<i>Curvibacter</i> sp. clone Z2_KL_466-12	KP967473 (100)	38	0	6	8	4	6	4	2	5
	<i>Curvibacter</i> sp. clone CX 18.4	KX260804 (99)		0	0	1	0	0	0	1	1
<i>Propionibacterium</i>	<i>Propionibacterium</i> sp. clone 12L_77	KP183061 (100)	14	0	0	1	1	2	2	2	3
	<i>P. granulosum</i> JCM 6498	113367 (99)		0	0	0	0	0	1	0	1
	<i>Propionibacterium</i> sp. clone JPL-2_O14	FJ957593 (99)		0	0	0	0	0	0	0	1
<i>Bacillus</i>	<i>Bacillus</i> sp. CHORDb1	MG995009 (100)	13	0	2	0	1	2	0	0	3
	<i>Bacillus</i> sp. clone D	JX505089 (99)		0	0	0	0	0	0	0	2
	<i>Bacillus</i> sp. 1NLA3E	CP005586 (99)		0	0	0	0	1	0	0	0
	<i>Bacillus</i> sp. R-66632	KT185191 (99)		0	0	1	0	0	0	0	0
	<i>Bacillus megaterium</i> Y103	MH368091 (99)		0	1	0	0	0	0	0	0
<i>Cupriavidus</i>	<i>C. metallidurans</i> Ni-2	CP026544 (100)	12	2	2	1	3	2	0	0	2
	<i>Cupriavidus</i> sp. EF11(2012)	JX912460 (99)		0	0	0	1	0	0	0	0
<i>Pseudomonas</i>	<i>Pseudomonas</i> sp. 09C 129	CP025261 (100)	12	0	2	0	0	1	1	0	1
	<i>P. fluorescens</i> PF85	MF838663 (100)		0	0	2	0	0	0	0	0
	<i>P. simiae</i> 4G1010	KY939757 (100)		0	1	0	0	0	0	1	0
	<i>P. fluorescens</i> L228	CP015639 (100)		0	0	0	0	0	0	0	1
	<i>P. fluorescens</i> 2F9	KT695813 (100)		0	0	1	0	0	0	0	0
	<i>P. lurida</i> MYb11	CP023272 (100)		0	0	1	0	0	0	0	0
<i>Staphylococcus</i>	<i>S. epidermidis</i> FDAARGOS_161	CP014132 (99)	9	0	1	0	0	2	0	0	2
	<i>S. epidermidis</i> TWSL_19	KT184899 (100)		0	0	0	0	0	1	0	0
	<i>S. caprae</i> OZK14	KT591476 (99)		0	0	0	0	0	1	0	0
	<i>Staphylococcus</i> sp. JCE 11	LT899997 (100)		0	0	0	0	0	0	0	1
	<i>Staphylococcus</i> sp. clone 12L_53	KP183056 (100)		0	1	0	0	0	0	0	0
<i>Pelomonas</i>	<i>P. saccharophila</i> ATCC 15946	NR_115049 (99)	9	0	2	1	0	2	3	0	1
<i>Acidovorax</i>	<i>Acidovorax</i> sp. clone M_KL_81_14	KP967499 (100)	4	0	0	1	0	0	0	1	2
	<i>Acidovorax</i> sp. clone CSC28	JN541150 (100)	3	0	0	0	1	0	0	2	0
<i>Weissella</i>	<i>W. cibaria</i> BM2	CP027427 (99)	6	0	0	1	2	0	1	0	0
	<i>W. confusa</i> SM10	KU060300 (100)		0	0	0	0	0	0	0	2
<i>Micrococcus</i>	<i>M. luteus</i> JGTA-S5	KT805418 (100)	6	0	0	0	0	1	0	0	0
	<i>Micrococcus</i> sp. cpRA422	KJ510213 (100)		0	1	0	0	0	0	0	0
	<i>Micrococcus</i> sp. EF1B-B144	KC545358 (99)		0	0	0	0	0	1	0	0
	<i>Micrococcus</i> sp. strain CAU1456	MG214549 (99)		0	0	0	0	0	0	0	1
	<i>M. terreus</i> IHBB 9339	KU921566 (99)		0	0	0	0	1	1	0	0
<i>Paracoccus</i>	<i>Paracoccus</i> sp. clone SL36	HQ264096 (100)	6	0	0	0	1	1	2	1	0
	<i>P. yeii</i> TWCC 57946	LC371258 (100)		0	0	1	0	0	0	0	0
<i>Nocardioideis</i>	<i>N. terrigena</i> DS-17	NR_044185 (99)	5	0	0	2	2	0	0	0	0
	<i>Nocardioideis</i> sp. clone EHFS1_S02a	EU071473 (99)		0	0	0	0	0	1	0	0
<i>Ralstonia</i>	<i>R. solanacearum</i> RSCM	CP02598 (99)	3	0	1	0	1	0	0	0	0
	<i>Ralstonia</i> sp. clone DVBSW_M180	KF755496 (100)		0	0	0	1	0	0	0	0

Table II. Continued.

Genus	Similarity based on 700 bp sequence of the 16S rRNA gene		Number of clones	Origin <i>P. ostreatus</i> strains							
	The most closely related strain in NCBI	NCBI accession number (% of similarity)		USA		Japan		Poland			
				PUSAS	PB8	PB7'96	PBo6S	P234	PxS	PB63S	P112
<i>Corynebacterium</i>	<i>C. ureicelerivorans</i> IMMIB RIV-2301	CP009215 (99)	3	0	0	0	1	0	0	0	0
	<i>Corynebacterium</i> sp. clone YHSS1	EF658675 (100)		0	0	0	1	0	0	0	0
	<i>Corynebacterium</i> sp. clone OD-12	KX379256 (100)		0	1	0	0	0	0	0	0
<i>Lactobacillus</i>	<i>L. sakei</i> FAM18311	CP020459 (99)	3	0	0	0	1	0	0	0	0
	<i>L. sakei</i> PR11	KX139193 (99)		0	0	0	0	0	1	0	0
	<i>L. sakei</i> DS4	CP025839 (99)		0	0	0	0	0	1	0	0
<i>Acidobacteria</i>	<i>Acidobacteria</i> clone SEW_08_293	HQ598999 (99)	2	0	0	0	0	1	0	0	0
	<i>Acidobacteria</i> clone SEW_08_084	HQ598816 (99)		0	0	1	0	0	0	0	0
<i>Paenibacillus</i>	<i>P. typhae</i> xj7	NR_109462 (99)	2	0	0	0	0	0	0	0	1
	<i>P. marchantiophytorum</i> R55	NR_148618 (99)		0	0	0	0	0	0	0	1
<i>Acinetobacter</i>	<i>Acinetobacter</i> sp. SWBY1	CP026616 (99)	2	0	0	0	0	1	0	0	0
	<i>A. towneri</i> MTCC11368T	KM070563 (99)		0	0	0	0	1	0	0	0
<i>Streptomyces</i>	<i>S. rishiriensis</i> JCM 4686	LC002811 (99)	2	0	0	0	1	0	0	0	0
	<i>Streptomyces</i> sp. 111013air4	KP262513 (99)		0	0	0	1	0	0	0	0
<i>Legionella</i>	<i>Legionella</i> sp. L-29	AB856218 (98)	1	0	0	0	0	0	1	0	0
<i>Finegoldia</i>	<i>F. magna</i> JCM 1766	NR_113383 (99)	1	0	0	0	0	0	1	0	0
<i>Sporosarcina</i>	<i>S. psychrophila</i> DSM 6497	CP014616 (100)	1	0	0	0	0	0	1	0	0
<i>Streptococcus</i>	<i>S. pneumoniae</i> 11A	CP018838 (99)	1	0	0	0	1	0	0	0	0
<i>Kocuria</i>	<i>K. rhizophila</i> 3330	KP345929 (100)	1	0	1	0	0	0	0	0	0
<i>Lactococcus</i>	<i>L. garvieae</i> MJF010	MH057260 (100)	1	0	1	0	0	0	0	0	0
<i>Delftia</i>	<i>D. lacustris</i> SH2	MH014970 (100)	1	0	0	0	0	1	0	0	0
<i>Pectobacterium</i>	<i>P. carotovorum</i> subsp. <i>brasiliense</i> BC1	CP009769 (100)	1	0	0	0	0	1	0	0	0
<i>Oryzihumus</i>	<i>O. leptocrescens</i> S32011-b	AB649006 (100)	1	0	0	0	0	1	0	0	0
<i>Tumebacillus</i>	<i>Tumebacillus</i> sp. 7B-408	KF441681 (99)	1	0	0	0	0	1	0	0	0
<i>Achromobacter</i>	<i>A. mucicolens</i> OZK37	KT716268 (100)	1	0	0	0	0	0	0	0	1
<i>Herbaspirillum</i>	<i>Herbaspirillum</i> sp. WW2	KU495919 (100)	1	0	0	1	0	0	0	0	0
<i>Citricoccus</i>	<i>Citricoccus</i> sp. PL13f_S6	JF274870 (99)	1	0	0	0	0	0	1	0	0
<i>Sphingomonas</i>	<i>Sphingomonas</i> sp. CAU-S5	MF113252 (99)	1	0	0	1	0	0	0	0	0
Number of different clones	X	X	X	5	15	16	17	18	17	8	17
Number of genus	X	X	32	2	9	13	13	15	13	5	12
Number of unidentified clones of <i>Bacteria</i>	X	X	74	0	6	10	14	10	15	7	12

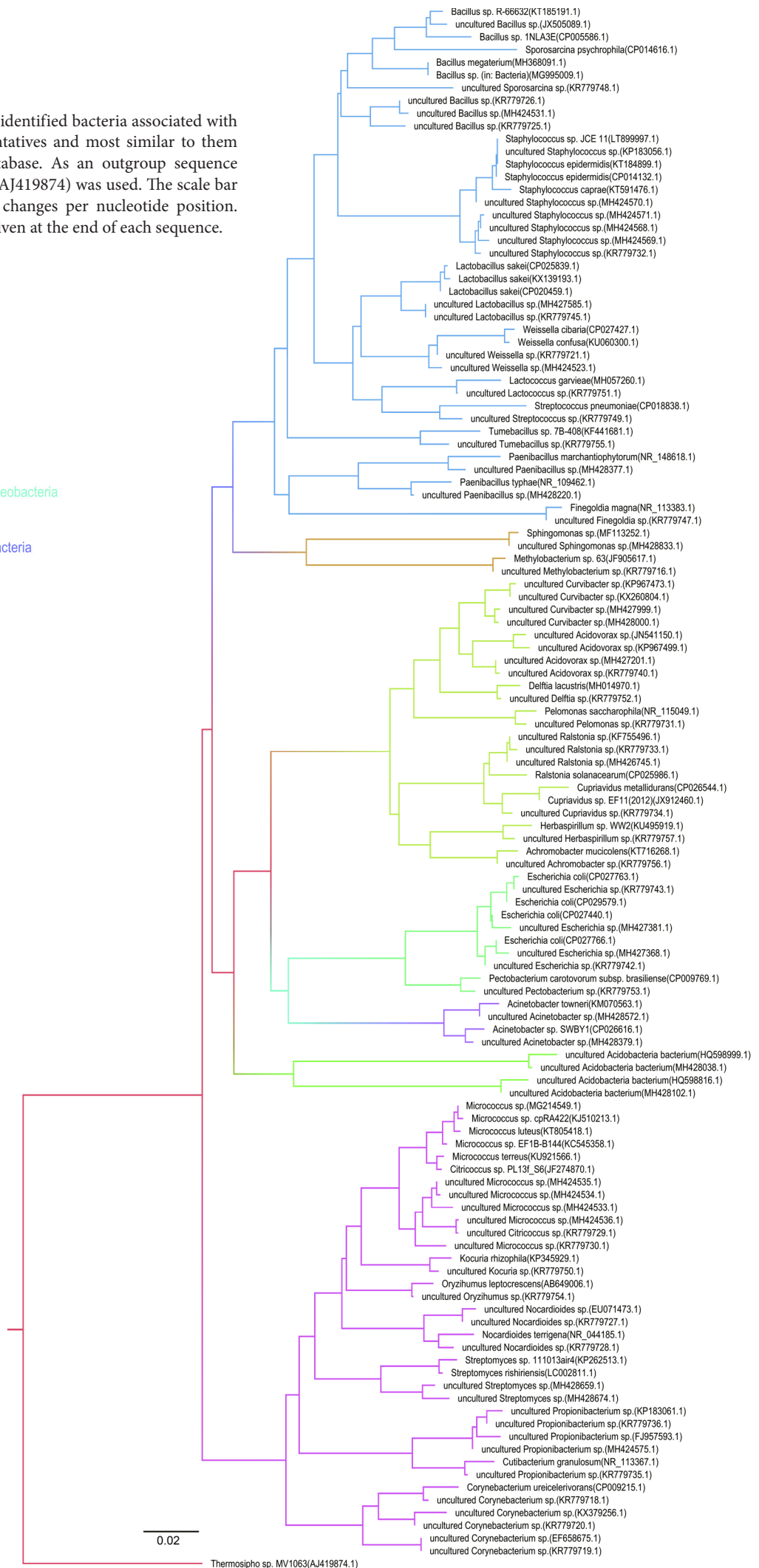
Poland (except P112). The remaining clones identified were as follows: *Bacillus* – 13 clones (in P234, PBo6S, PB8, P112), *Staphylococcus* – nine clones (in P234, PB8, PxS, P112), *Acidovorax* – seven clones (in PB7'96, PBo6S, PB63S, P112), *Weisella* – six clones (in PB7'96, PBo6S, PxS, P112), *Micrococcus* – six clones (in P234, PB8, PxS, P112), *Nocardioideis* – five clones (in PB7'96, PBo6S, PxS), *Ralstonia* – three clones (in PBo6S, PB8), *Corynebacterium* – three clones (in PBo6S, PxS), *Lactobacillus* – three clones (in PBo6S, PxS), *Acidobacteria*

– two clones (in P234, PB7'96), *Paenibacillus* – two clones (in P112), *Acinetobacter* – two clones (in P234), *Streptomyces* – two clones (in PBo6S), *Legionella* – one clone (PxS), *Finegoldia* – one clone (PxS), *Sporosarcina* – one clone (PxS), *Streptococcus* – one clone (PBo6S), *Kocuria* – one clone (PB8), *Lactococcus* – one clone (PB8), *Delftia* – one clone (P234), *Pectobacterium* – one clone (P234), *Oryzihumus* – one clone (P234), *Tumebacillus* – one clone (P234), *Achromobacter* – one clone (P112), *Herbaspirillum* – one clone (PB7'96),

Fig. 4. Phylogenetic tree of identified bacteria associated with *P. ostreatus* strains representatives and most similar to them sequences from NCBI database. As an outgroup sequence *Thermosiphonia* sp. MV1063 (AJ419874) was used. The scale bar represents the number of changes per nucleotide position. Accession numbers are given at the end of each sequence.

label

- Multiple_organisms
- a-proteobacteria
- b-proteobacteria
- bacteria
- enterobacteria
- enterobacteria_and_g-proteobacteria
- firmicutes
- firmicutes_and_a-proteobacteria
- g-proteobacteria
- high_GC_Gram+



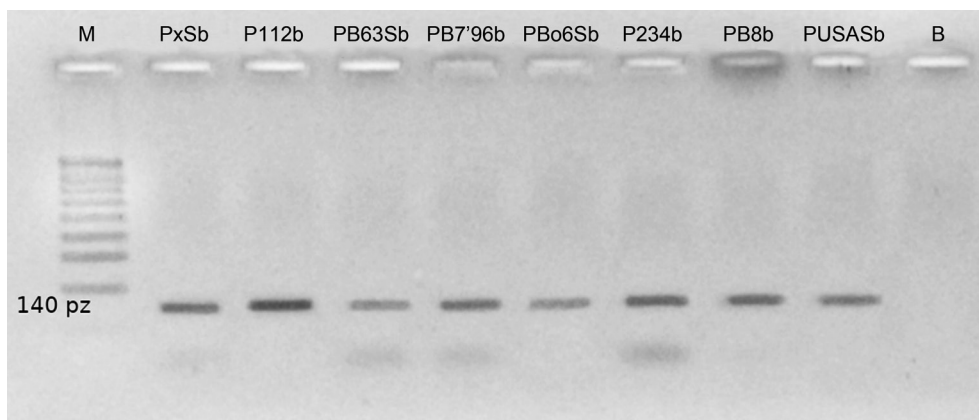


Fig. 5. Agarose gel electrophoresis showing products of PCR with Cu1AF and Cu2R primers and analyzed oyster mushroom DNA. Visible 140 bp band represents amplified LMCO genes. M – marker; B – blind control.

Citrococcus – one clone (PxS), *Sphingomonas* – one clone (PB7'96). The detailed number of identified clones with the most similar strains from NCBI database is presented in Table II. Phylogenetic tree of representatives of all identified genotypes with most similar sequences from NCBI database is presented in Fig. 4. As an out-group sequence, the *Thermosiphon* sp. MV1063 (AJ419874) was used. The detailed number of identified clones with the most similar strains from NCBI database is presented in Table II.

The PCR reactions designed for detection of *NifH*, β -glucosidase and β -xylosidase genes gave no product for all analyzed fungal strains. However, LMCO genes were detected (Fig. 5). LMCO is a complex of enzymes, which include laccases (EC 1.10.3.2) among others.

Discussion

Yara et al. (1999, 2006) reported that bacteria or bacteria-like organisms could interact with only one strain of *P. ostreatus*. However, authors did not confirm the endocellular character of these bacteria, they described them only as bacteria associated with *P. ostreatus* G2 hyphae. Using fluorescent microscopy technique, which was described by Bianciotto et al. (2000), we found bacteria associated with all eight tested strains of *P. ostreatus* originating from different geographic zones (Japan, Poland, and the USA). Every specimen was prepared from living cells and their movement was possible to observe under a microscope. These observations and lack of growth of isolated organisms without the presence of host on microbiological media strongly suggested the endosymbiotic character of the observed bacteria. This hypothesis was also strongly supported by the fact that cultivation of the fungal strains on media with wide range of antibacterial antibiotics (ampicillin, neomycin, gentamicin, penicillin G, streptomycin,

polymyxin B, kanamycin, ciprofloxacin, detreromycin, tobramycin (200 ppm), meropenem, and ceftadizine (30 ppm), data unpublished) did not eradicate bacteria from fungal mycelia. Similar techniques used for the isolation of bacteria from five strains of *Lentinula edodes* not revealed the presence of associated bacteria (data unpublished). Due to the fact that it was not possible to fully distinguish between endosymbiotic and associated bacteria among the isolates tested we decided to use in this study the term “bacteria associated with”. Literature of subject shows the presence of one or two species of bacteria associated with *P. ostreatus*. Yara et al. (2006) described bacteria associated with one strain of *P. ostreatus* belonging to *B. cepacia* complex, which is complex of at least 20 different species from *Burkholderia* genus (LiPuma 2005). In this work, we report the presence of bacteria related to at least 34 different genera living in association with eight *P. ostreatus* strains originating from different geographical regions. It was noticeable that bacteria from genus *Curvibacter* were isolated from almost all analyzed fungal strains. The only one strain that did not contain these bacteria was a PUSAS strain. This strain also was the only one associated with *E. coli* bacteria what is difficult to explain due to lack of knowledge of history of this strain, The bacteria from the *Curvibacter* genus were reported endosymbionts of *Oryza sativa* roots (Singh et al. 2006), similarly as an uncultured bacterium from *Chlorella* cultures (Otsuka et al. 2008) and tomato rhizosphere (Lioussanne et al. 2010) and the bacteria associated with *Hydra*, which serve as a protective factor against pathogen infections (Fraune et al. 2015). Bacteria of genera *Bacillus* and *Pseudomonas* are well-known plant growth-promoting bacteria due to competitive and antagonistic activity versus several pathogens (Compant et al. 2010). The occurrence of *Curvibacter*, *Bacillus* and *Pseudomonas* bacteria associated with *P. ostreatus* could be related to the known lower susceptibility of this edible mushroom

when compare to *Agaricus bisporus* (J.E. Lange) Imbach. *Gigasporaceae* sp. endosymbionts were described as N₂ fixing bacteria (Bianciotto et al. 2003). However, our study did not show the presence of nitrogenase reductase genes using *PolF* and *PolR* primers; however, the occurrence of clones similar to *Cupriavidus* suggest that these bacteria could be N₂-fixers associated with oyster mushroom. Strains of *Cupriavidus taiwanensis*, previously were isolated from nodules of *Mimosa*, can nodulate also legumes and fix N₂. However, the *nifH* gene is only distantly related to other alphaproteobacterial rhizobial strains (Gyaneshwar et al. 2011), what was probably a reason that used primers were not specific in this case. The bacteria associated with *P. ostreatus* could also influence their hosts' capability for lignocellulolytic substrates utilization. PCR reactions with specific primers for β -glucosidase, β -xylanase genes did not reveal their presence, which suggests that these bacteria did not play important role in degradation of polysaccharides. However, the presence of LMCO genes was identified in this study. Laccases are a group of enzymes able to use a variety of substrates, including lignin (Rekuc et al. 2006). This suggests that although oyster mushroom-associated bacteria were able to produce neither β -glycosidase nor β -xylanase, they still could be able to support the lignocellulolytic activity of the strains tested due to laccase activity.

The origin of identified *P. ostreatus*-associated bacteria, their phylogenesis, and relationship with hosts were difficult to determine. In the natural environment, the oyster mushroom is a saprophyte, which develops on dead trunks and deciduous trees. Occasionally, it can develop in places of cuts on living trees. Such a variety of hosts may be the reason for the biodiversity of bacterial associations. Different non-pathogenic species probably inhabited mycelium of *P. ostreatus* during colonization of various hosts.

Acknowledgments

We would like to thank Janusz Kalbarczyk, retired full professor of Department of Fruits, Vegetables and Mushrooms Technology, Faculty of Food Science and Biotechnology, University of Life Sciences in Lublin, for sharing fungal strains used in this study.

The work was created as a result of the research project No. 2012/07/N/NZ9/00943 financed from the funds of the National Science Center, Poland.

Conflict of interest

The authors do not report any financial or personal connections with other persons or organizations, which might negatively affect the contents of this publication and/or claim authorship rights to this publication.

Literature

Bertaux J, Schmid M, Prevost-Boure NC, Churin JL, Hartmann A, Garbaye J, Frey-Klett P. *In situ* identification of intracellular bacteria related to *Paenibacillus* spp. in the mycelium of the

ectomycorrhizal fungus *Laccaria bicolor* S238N. *Appl Environ Microbiol.* 2003;69(7):4243–4248.

doi:10.1128/AEM.69.7.4243-4248.2003 Medline

Bianciotto V, Bandi C, Minerdi D, Sironi M, Tichy HV, Bonfante P. An obligately endosymbiotic mycorrhizal fungus itself harbors obligately intracellular bacteria. *Appl Environ Microbiol.* 1996;62(8):3005–3010. Medline

Bianciotto V, Lumini E, Lanfranco L, Minerdi D, Bonfante P, Perotto S. Detection and identification of bacterial endosymbionts in arbuscular mycorrhizal fungi belonging to the family *Gigasporaceae*. *Appl Environ Microbiol.* 2000;66(10):4503–4509. doi:10.1128/AEM.66.10.4503-4509.2000 Medline

Bianciotto V, Lumini E, Bonfante P, Vandamme P. 'Candidatus *Glomeribacter gigasporarum*' gen. nov., sp. nov., an endosymbiont of arbuscular mycorrhizal fungi. *Int J Syst Evol Microbiol.* 2003; 53(1): 121–124. doi:10.1099/ijs.0.02382-0 Medline

Bonfante P. Plants, mycorrhizal fungi and endobacteria: a dialog among cells and genomes. *Biol Bull.* 2003;204(2):215–220. doi:10.2307/1543562 Medline

Cañizares R, Benitez E, Ogunseitán OA. Molecular analyses of β -glucosidase diversity and function in soil. *Eur J Soil Biol.* 2011; 47(1):1–8. doi:10.1016/j.ejsobi.2010.11.002

Chelius MK, Triplett EW. The diversity of archaea and bacteria in association with the roots of *Zea mays* L. *Microb Ecol.* 2001;41(3): 252–263. doi:10.1007/s002480000087 Medline

Compant S, Clément C, Sessitsch A. Plant growth-promoting bacteria in the rhizo- and endosphere of plants: their role, colonization, mechanisms involved and prospects for utilization. *Soil Biol Biochem.* 2010;42(5): 669–678. doi:10.1016/j.soilbio.2009.11.024

Cruz AF, Horii S, Ochiai S, Yasuda A, Ishii T. Isolation and analysis of bacteria associated with spores of *Gigaspora margarita*. *J Appl Microbiol.* 2008;104(6):1711–1717. doi:10.1111/j.1365-2672.2007.03695.x Medline

Donlan RM, Costerton JW. Biofilms: survival mechanisms of clinically relevant microorganisms. *Clin Microbiol Rev.* 2002;15(2): 167–193. doi:10.1128/CMR.15.2.167-193.2002 Medline

Fraune S, Anton-Erxleben F, Augustin R, Franzenburg S, Knop M, Schröder K, Willoweit-Ohl D, Bosch TCG. Bacteria-bacteria interactions within the microbiota of the ancestral metazoan Hydra contribute to fungal resistance. *ISME J.* 2015;9(7): 1543–1556. doi:10.1038/ismej.2014.239 Medline

Frey-Klett P, Burlinson P, Deveau A, Barret M, Tarkka M, Sarniguet A. Bacterial-fungal interactions: hyphens between agricultural, clinical, environmental, and food microbiologists. *Microbiol Mol Biol Rev.* 2011;75(4):583–609. doi:10.1128/MMBR.00020-11 Medline

Gyaneshwar P, Hirsch AM, Moulin L, Chen WM, Elliott GN, Bontemps C, Estrada-de los Santos P, Gross E, dos Reis FB Jr, Sprent JL, et al. Legume-nodulating betaproteobacteria: diversity, host range, and future prospects. *Mol Plant Microbe Interact.* 2011;24(11):1276–1288. doi:10.1094/MPMI-06-11-0172 Medline

Hogan DA, Wargo MJ, Beck N. Bacterial biofilms on fungal surfaces, In: Kjelleberg S, Givskov M, editors. *The biofilm mode of life: mechanisms and adaptations.* Norfolk (United Kingdom): Horizon Scientific Press. 2007; p. 235–245.

Kellner H, Luis P, Buscot F. Diversity of laccase-like multicopper oxidase genes in *Morchellaceae*: identification of genes potentially involved in extracellular activities related to plant litter decay. *FEMS Microbiol Ecol.* 2007;61(1):153–163. doi:10.1111/j.1574-6941.2007.00322.x Medline

Khandeparker R, Verma P, Deobagkar D. A novel halotolerant xylanase from marine isolate *Bacillus subtilis* cho40: gene cloning and sequencing. *N Biotechnol.* 2011;28(6):814–821. doi:10.1016/j.nbt.2011.08.001 Medline

- Król MJ, Perzynski A.** [Utilization of benzene as the sole carbon source in fixation of free nitrogen by *Azospirillum* spp. and *Pseudomonas stutzeri* strains of bacteria]. (in Polish). Pam Puław (Poland). 2005;140:103–115.
- LiPuma JJ.** Update on the *Burkholderia cepacia* complex. Curr Opin Pulm Med. 2005;11(6):528–533.
[doi:10.1097/01.mcp.0000181475.85187.ed](https://doi.org/10.1097/01.mcp.0000181475.85187.ed) [Medline](#)
- Lioussanne L, Perreault F, Jolicoeur M, St-Arnaud M.** The bacterial community of tomato rhizosphere is modified by inoculation with arbuscular mycorrhizal fungi but unaffected by soil enrichment with mycorrhizal root exudates or inoculation with *Phytophthora nicotianae*. Soil Biol Biochem. 2010;42(3):473–483.
[doi:10.1016/j.soilbio.2009.11.034](https://doi.org/10.1016/j.soilbio.2009.11.034)
- Otsuka S, Abe Y, Fukui R, Nishiyama M, Sendoo K.** Presence of previously undescribed bacterial taxa in non-axenic *Chlorella* cultures. J Gen Appl Microbiol. 2008;54(4):187–193.
[doi:10.2323/jgam.54.187](https://doi.org/10.2323/jgam.54.187) [Medline](#)
- Partida-Martinez LP, Groth I, Schmitt I, Richter W, Roth M, Hertweck C.** *Burkholderia rhizoxinica* sp. nov. and *Burkholderia endofungorum* sp. nov., bacterial endosymbionts of the plant-pathogenic fungus *Rhizopus microsporus*. Int J Syst Evol Microbiol. 2007a;57(11):2583–2590.
[doi:10.1099/ijs.0.64660-0](https://doi.org/10.1099/ijs.0.64660-0) [Medline](#)
- Partida-Martinez LP, Monajembashi S, Greulich KO, Hertweck C.** Endosymbiont-dependent host reproduction maintains bacterial-fungal mutualism. Curr Biol. 2007b;17(9):773–777.
[doi:10.1016/j.cub.2007.03.039](https://doi.org/10.1016/j.cub.2007.03.039) [Medline](#)
- Pisarska K, Pietr SJ.** Biodiversity of dominant cultivable endophytic bacteria inhabiting tissues of six different cultivars of maize (*Zea mays* L. ssp. *mays*) cropped under field conditions. Pol J Microbiol. 2015;64(2):163–170. [Medline](#)
- Pierce GE.** *Pseudomonas aeruginosa*, *Candida albicans*, and device-related nosocomial infections: implications, trends, and potential approaches for control. J Ind Microbiol Biotechnol. 2005;32(7):309–318. [doi:10.1007/s10295-005-0225-2](https://doi.org/10.1007/s10295-005-0225-2) [Medline](#)
- Rekuc A, Kruczkiewicz P, Kielczynski R, Jastrzebska B, Bryjak J.** [Laccase production and its immobilization on selected media]. (in Polish). Acta Sci Pol Biotechnol. 2006;1(05):3–15.
- Sarand I, Timonen S, Nurmiäho-Lassila EL, Koivula T, Haahtela K, Romantschuk M, Sen R.** Microbial biofilms and catabolic plasmid harbouring degradative fluorescent pseudomonads in Scots pine mycorrhizospheres developed on petroleum contaminated soil. FEMS Microbiol Ecol. 1998 Oct;27(2):115–126.
[doi:10.1111/j.1574-6941.1998.tb00529.x](https://doi.org/10.1111/j.1574-6941.1998.tb00529.x)
- Singh RK, Mishra RPN, Jaiswal HK, Kumar V, Pandey SP, Rao SB, Annapurna K.** Isolation and identification of natural endophytic rhizobia from rice (*Oryza sativa* L.) through rDNA PCR-RFLP and sequence analysis. Curr Microbiol. 2006;52(2):117–122.
[doi:10.1007/s00284-005-0136-5](https://doi.org/10.1007/s00284-005-0136-5) [Medline](#)
- Yara R, Azevedo JL, Maccheroni W, Kitajima EW, Leite B.** Mycoplasma associated with cultures of the ligno-cellulolytic fungus *Pleurotus* sp. Acta Microsc. 1999;8:851–852.
- Yara R, Maccheroni W Jr, Horii J, Azevedo JL.** A bacterium belonging to the *Burkholderia cepacia* complex associated with *Pleurotus ostreatus*. J Microbiol. 2006;44(3):263–268. [Medlin](#)

Microbiota and Chemical Compounds in Fermented *Pinelliae Rhizoma* (Banxiaqu) from Different Areas in the Sichuan Province, China

BO SHU², JING YING¹, TAO WANG¹, MENGQIAN XIA¹, WENYU ZHAO¹ and LING YOU^{1*}

¹Solid-state Fermentation Resource Utilization Key Laboratory of Sichuan Province, Yibin University, Yibin, China

²Affiliated Hospital of Northern Sichuan Medical College, Nanchong, Sichuan, China

Submitted 30 September 2018, revised 26 November 2018, accepted 29 November 2018

Abstract

This study focused on the microbiota and chemical compounds of the fermented *Pinelliae Rhizoma* produced in Longchang (LC), Zizhong (ZZ) and Xindu (XD), in Sichuan Province (China). High-throughput sequencing was used to analyze the microbiota. GC-MS and LC-MS were used to detect the compounds produced during the three different *Pinelliae Rhizoma* fermentation processes. The bacteria and fungi of the three fermented *Pinelliae Rhizoma* differed substantially, with the bacterial content mainly composed of the *Bacillus* genus, while the common fungi were only included in four OTUs, which belong to three species of *Eurotiomycetes* and *Aspergillus cibarius*. 51 volatile compounds were detected; they varied between LC, XD, and ZZ fermented *Pinelliae Rhizoma*. C10 and C15 terpenes were most frequently detected, and only curcumen and β -bisabolene were detected in the three fermented *Pinelliae Rhizoma*. 65 non-volatile compounds were detected by LC-MS, most were of C16, C18, C20, C21 and C22 structures. Cluster analysis showed more similarity between LC and XD fermented *Pinelliae Rhizoma* with regards to volatile compound content, but more similarity between the XD and ZZ fermented *Pinelliae Rhizoma* for non-volatiles. Moreover, no correlation between geographical distance and microflora or compounds of fermented *Pinelliae Rhizoma* was observed. These results showed that hundreds of compounds are produced by the natural mixed fermentation of *Pinelliae Rhizoma*, and may mostly relate to the microorganisms of five species.

Key words: Fermented *Pinelliae Rhizoma*, components, microbiota, regions

Introduction

Mixed solid fermentation is advantageous in the formation of many active compounds (Boratynski et al. 2018; Try et al. 2018) and is a widely used process in food production and traditional Chinese medicine for thousands of years (Chen 2013; Zhao et al. 2016; Wu et al. 2018). Fermented *Pinelliae Rhizoma* (Banxiaqu) is a traditional Chinese Medicine made from the *Pinellia ternata* (Thunb) Breit by mixed solid fermentation (Hu et al. 2018). It has been shown to remove phlegm, strengthen the stomach and improve digestion (Wagner et al. 2011; Gong, et al. 2015; Qu et al. 2016; Zhao et al. 2018). The fermentation process follows key sequential steps: 16 kg of licorice is boiled and filtered. The filtrate is then mixed with 20 kg of quick lime, and the supernatant is used to soak 100 kg of *Pinelliae Rhizoma* for 4–5 days. The soaked *Pinelliae Rhizoma* is then removed, washed and ground into fine powder,

which is then mixed with 10–20 kg of flour and enough water to form the dough. The dough is subsequently fermented at 30°C–35°C with a humidity of 70–80% for 3–5 days, then dried at 70°C–80°C until the dough becomes loose and porous (Chinese Pharmacopoeia Commission, 2015). As a result of this fermentation process, *Pinelliae Rhizoma* attains better clinical efficacy relative to mouth and throat numbness. A mixture of fungi and bacteria from the surrounding environment carries out complex biochemical reactions during the fermentation. Because the mixed solid fermentation is carried out by different microorganisms in different regions or seasons, the quality of fermented *Pinelliae Rhizoma* may drastically fluctuate, thus explaining the difference in the quality of fermented *Pinelliae Rhizoma* during different seasons, or produced in different districts (Hu et al. 2018). Due to the lack of standardization, the clinical application of fermented *Pinelliae Rhizoma* is severely hindered. As such, only the fermented

* Corresponding author: L. You, Solid-state Fermentation Resource Utilization Key Laboratory of Sichuan Province, Yibin University, Yibin, China; e-mail: 23686037@qq.com

© 2019 Bo Shu et al.

This work is licensed under the Creative Commons Attribution-NonCommercial-NoDerivatives 4.0 License (<https://creativecommons.org/licenses/by-nc-nd/4.0/>)

Pinelliae Rhizoma made from certain large traditional factories are still used in hospitals.

Sichuan is an important region of *Pinelliae Rhizoma* production, although this herb grows all over the region. The dried tuber is mainly fermented in the three counties of Longchang (LC), Zizhong (ZZ) and Xindu (XD). The active components of *Pinellia ternate* have not been yet conclusively identified, but clinical applications showed similar efficacies between these three different regionally fermented *Pinelliae Rhizoma*, despite their disparate geographical localizations (Shen et al. 2009). Importantly, as these three preparations of fermented *Pinelliae Rhizoma* are fermented by microorganisms in different locations, and the varied microorganisms produce a range of distinct compounds. It is likely that among these compounds, some contribute more to the clinical efficacy of fermented *Pinelliae Rhizoma* than others, particularly those components that exist across multiple different preparations of fermented *Pinelliae Rhizoma*. It, therefore, stands to reason that studying these common components may reveal the key active compounds in fermented *Pinelliae Rhizoma* and support a model to research the role of microbiota in the fermentation of *Pinelliae Rhizoma*. The purpose of this research is also to help identify the key species of microorganisms involved in *Pinelliae Rhizoma* fermentation, with the objective to thereby improve the controllability of its solid mixed fermentation processes.

Experimental

Materials and Methods

Sample collection. Three fermented *Pinelliae Rhizoma* were produced in three factories located respectively in Longchang (Lianghui company, Shengdeng town, Longchang County, Neijiang city, Sichuan Province), Xindu (Qianfang company, Satellite City Industrial Development Zone, Xindu District, Chengdu, Sichuan Province) and Zizhong (Hongsheng company, Qiuxi town, Zizhong County, Neijiang city, Sichuan Province) using the same raw materials and technology. When the fermentation was complete, three samples were collected and identified respectively as LC, XD, and ZZ.

Physical and chemical testing. The content of all water-soluble saccharides, mannose-oligosaccharides, and polysaccharides in the fermented *Pinelliae Rhizoma* was determined by sulfuric acid-anthrone colorimetry (Cianchetta et al. 2017).

The content of non-protein nitrogen of 0.5 g fermented *Pinelliae Rhizoma* was determined directly by the Kjeldahl method using a Kjeltac-8400 automatic Kjeldahl nitrogen analyzer (FOSS company) (Rédei

2008). Briefly, 0.5 g fermented *Pinelliae Rhizoma* was dissolved for 0.5 h in 20 ml of 98% H_2SO_4 , and the content of total nitrogen was determined by the method stated earlier, where the protein nitrogen content corresponded to the difference between total nitrogen and non-protein nitrogen. Protein content was measured as protein nitrogen content multiplied by 6.25, for the average content of nitrogen in proteins is 16%, and therefore use the value to convert nitrogen to protein.

Enzyme activity detection. 5.0 g of fermented *Pinelliae Rhizoma* powder was mixed with 50 ml of ddH₂O, shaken at 40°C for 1 h to fully solubilize the digestive enzymes (amylase, protease, and lipase). The mixture was then centrifuged at 3000 rpm for 5 min, and 5 vml of supernatant was collected for enzymatic activity determination.

The amylase activity was measured as follows: 20 ml of soluble starch blended with 5 ml PBS (pH 6.0) was preheated to 60°C for 8 min. Then 1 ml of the *Pinelliae Rhizoma* supernatant from earlier was added and incubated for 5 min. 1 ml of this solution was then collected and mixed with 0.5 ml of 0.1 M HCl and 5 ml of iodine solution (0.1 g/l iodine and 40 g/l potassium iodide), and its absorbance was measured at 660 nm. One amylase activity unit was defined as: 1 g soluble starch degraded in 1 h at 60°C, pH 6.0 (China National Standard, GB/T 24401-2009).

The protease activity was measured as follows: 1 ml supernatant was preheated to 40°C and added to 10 ml of 1% casein, preheated to 40°C. The mixture was then incubated at 40°C for 10 min, the reaction was quenched by adding 200 ml of 0.4 M $C_2HCl_3O_2$ at the same temperature for 10 minutes. This mixture was left at 40°C for an additional 20 minutes and then centrifuged at 10 000 rpm for 10 minutes. 100 ml of the supernatant was mixed with 0.5 ml of 0.4 M Na_2CO_3 and blended with 1 ml of Folin reagent. After blending, the mixture was kept at 40°C for 20 minutes and the absorbance was measured at 660 nm. One unit of protease activity was defined as 1 μ g tyrosine produced per minute at 40°C using casein as a substrate (China Commercial Standard, SB/T 10317-1999).

Lipase activity was determined as follows: 150 ml of polyvinyl alcohol was added to 50 ml of virgin olive oil and the mixture was homogenized for 5 min, and after 2 min again for 3 min. 4 ml of this solution was then added to 5 ml of PBS (pH 7.5) and preheated at 40°C for 5 min, mixed with 1 ml of the *Pinelliae Rhizoma* supernatant from the earlier preparation and left to react for 15 min. 15 ml of 95% CH_3CH_2OH was added to quench the reaction, and the solution was titrated to neutral pH using 0.05 M NaOH. One unit of lipase activity was defined as 1 μ mol of titratable fatty acids produced per minute at 40°C using olive oil as a substrate (China National Standard, GB/T 23535-2009).

Microbial community analysis. The fermented *Pinelliae Rhizoma* were crushed under sterile conditions. The total DNA of the samples was extracted using the Omega Kit according to the operating instructions. Bacterial amplification primers were 338F (ACTCCTACGG-GAGGCAGCAG) and 806R (GGACTACHVGGGT-WTCTAAT) (“H” means A, T or C; “V” means G, A or C; “W” means A or T) (Fan et al. 2014). Fungi primers were ITS1F (CTTGGTCATTTAGAGGAGTAA) and 2043R (GCTGCGTTCTTCATCGATGC) (Pranab et al. 2014). The PCR reaction was performed in a total volume of 25 μ l, where the reaction conditions were 95°C 3 min; 95°C 30 sec, 55°C 30 sec, 72°C 45 sec, 27 cycles; 72°C 10 min. The amplification fragments were detected by loading 3 μ l of the total product on a 2% agarose gel for electrophoresis and sequencing on the Illumina platform by Pisino Company.

For the sequencing data, the Silva database was used to identify bacterial species (Quast et al. 2013), and the Unite database was used to identify fungal species (Köljalg et al. 2013). The Mothur software was used to analyze the Alpha diversity which is expressed as the index of Shannon, Chao 1, Simpson, and ACE.

By comparing the existing community composition data with the known reference genome database and correcting the microbial abundance data against the original data, the metabolic function of the community samples was predicted using the software PICRUSt (Phylogenetic Investigation of Communities by Reconstruction of Unobserved States) (Langille et al. 2013).

Detection of volatiles. 5.0 g of fermented *Pinelliae Rhizoma* powder was added to a 20 ml headspace vial, with 65 μ m PDMS/DVB solid-phase microextraction (Supelco) used to absorb the powder for 40 min at 65°C. This microextraction was then dissolved at 250°C for 5 min for injection on gas chromatography-mass (7890A-5975C, Agilent). Volatile compounds were detected as follows: Helium was used as the carrier gas, which flowed at a rate of 1.0 ml/min. The HP-5MS column (300 mm \times 0.25 mm \times 0.25 μ m) was kept at 50°C for 3 min, then, the temperature was raised to 150°C at 5°C/min and kept for 3 min, then raised to 220°C at 10°C/min and kept for 2 min. The ionization energy was 70 eV; the ionization temperature was 230°C, and the scanning range was 45–550 amu.

Detection of non-volatiles. 20.0 g of fermented *Pinelliae Rhizoma* powder was extracted using 100 ml of 95% CH₃CH₂OH for 15 min, then centrifuged at 3000 rpm for 5 min. The supernatant was collected as an ethanol extraction, and the precipitate was mixed with 50 ml of ddH₂O and extracted by adding 50 ml CH₃(CH₂)₃OH and 50 ml CH₃COOCH₂CH₃ sequentially. The extraction was collected sequentially as a butanol extraction, and then an ethyl acetate extraction. All extractions were filtered through 0.22 μ m

filters and chemical content was detected by liquid chromatography-mass spectrometry (6530 Accurate-Mass Q-TOF, Agilent) using the following conditions: 5 μ l samples were injected into the Hermo-C18 column (2.1 mm \times 50 mm \times 1.8 μ m). The mobile phase was a mixture of 0.1% formic acid solution (A) and methanol (B) which flowed at 0.2 ml/min. The entire column elution was introduced into the Q-Tof mass spectrometer. Ion detection was achieved in ESI cation mode using a source capillary voltage of 3.5 kV, and a scanning range of 50 to 1000 m/z. The source temperature was 110°C, drying temperature was 350°C, and the drying gas flowed at 8.0 l/min, with the spray pressure set to 40 psi.

Results

Comparison of physiochemical indexes and enzyme activities. From Table I it is noted that nitrogen in the fermented *Pinelliae Rhizoma* mainly exists in the form of non-protein nitrogen. This indicated successful degradation of the proteins in *Pinellia ternate*. The protease activity and soluble nitrogen content of ZZ fermented *Pinelliae Rhizoma* were significantly higher than those in the other two samples, indicating that the fermentation of the *Pinelliae Rhizoma* carried out in the regions of LC, ZZ and XD may differ in nitrogen metabolism. The starch content in *Pinellia ternate* was about 75% of the total mass of the material (Gong et al. 2015), while the total sugar was roughly 0.1% in fermented *Pinelliae Rhizoma*, which indicates poor degradation of the starch because of low amylase activity. The amylase activity of LC was significantly lower than the other two samples, and in all three fermented *Pinelliae Rhizoma*, the lipase activity was only 0.3 U/g. Protease activity was very elevated, suggesting that increased protein degradation may be more important in the fermentation than the degradation of other macromolecular components. Furthermore, since the digestive enzymes generated during the fermentation of *Pinelliae Rhizoma* are mainly produced by microorganisms, the difference of microbial flora in the three counties may influence the activity of enzymes, and thus influence the efficacy in promoting digestion of fermented *Pinelliae Rhizoma*.

Bacterial community in the three fermented *Pinelliae Rhizoma*. The total number of OTUs of bacteria in the three fermentation samples of *Pinelliae Rhizoma* was 3978, while only 228 common OTUs existed in all three samples (Fig. 1). The differences in unique bacterial identifiers between regions was clear. 629 unique OTUs were found in XD, 300 unique OTUs were found in LC, and 248 unique OTUs were found in ZZ. The 285 OTUs found in common between LC and ZZ, were more numerous than the common OTUs between LC and XD (187) or ZZ and XD (131). Thirteen genera

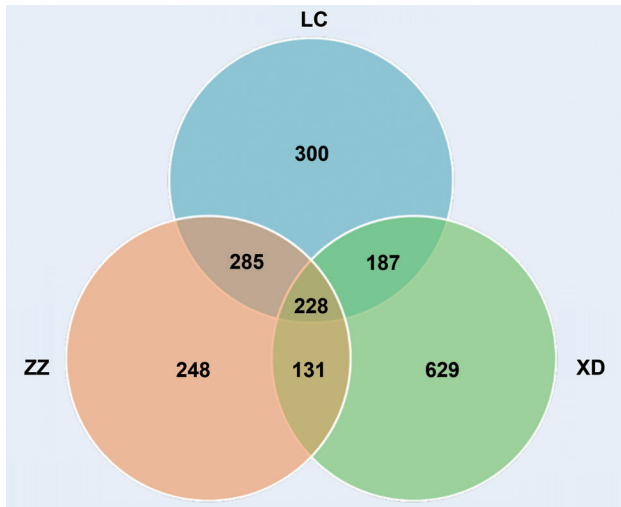


Fig. 1. The similarity of the bacterial communities in three fermented *Pinelliae Rhizoma*.

(*Bacillus*, *Sediminibacterium*, *Ralstonia*, *Lactococcus*, *Ochrobactrum*, *Carnobacterium*, *Planomicrobium*, *Sphingomonas*, *Deinococcus*, *Oscillospira*, *Adlercreutzia*, *Bradyrhizobium*, and *Virgibacillus*) were found both in LC and ZZ. Thus, among the three fermented *Pinelliae Rhizoma*, the bacterial similarity between LC and ZZ was the highest, correlating with the distance between

Longchang and Zizhong being the shortest at only 76 kilometers. The distance between Longchang and Xindu is 235 kilometers and the distance between Zizhong and Xindu is 144 kilometers). Furthermore, the environment of Longchang and Zizhong are more similar.

The OTUs and alpha diversity of bacteria in XD is significantly higher than that in LC and ZZ (Table II), with 16 genera (*Klebsiella*, *Enterococcus*, *Facklamia*, *Gemmata*, *Gluconobacter*, *Proteus*, *Aerococcus*, *Aristolochia*, *Zea*, *Rhodospirillum*, *Staphylococcus*, *Anaerobacillus*, *Bacteroides*, *Stenotrophomonas*, *Comamonas*, and *Planococcus*) only detected in XD-fermented *Pinelliae Rhizoma*. This revealed a more complex and unique bacterial community in fermented *Pinelliae Rhizoma* produced in Xindu county.

The abundance of bacterial species in three fermented *Pinelliae Rhizoma* differed from each other (Fig. 2). As the dominant genus in all three fermented *Pinelliae Rhizoma*, the relative abundance of *Bacillus* in LC and ZZ fermented *Pinelliae Rhizoma* was much higher than that in XD.

Differences in biodegradation, nucleic acid metabolism, vitamin metabolism, energy metabolism, lipid metabolism, and amino acid metabolism in the three fermented *Pinelliae Rhizoma* were predicted by KEGG analysis (Fig. 3). The level of carbohydrate metabolism

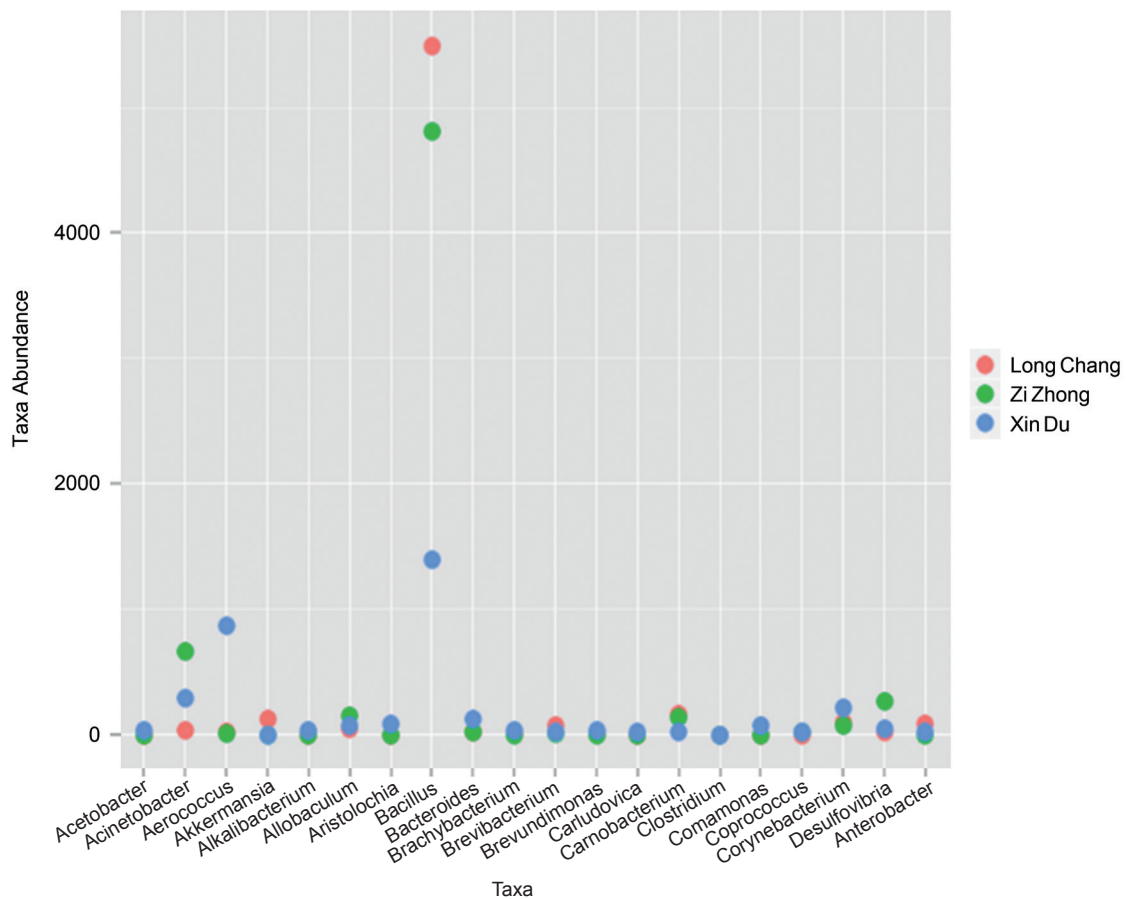


Fig. 2. Taxa abundances of bacterial species in three fermented *Pinelliae Rhizoma*.

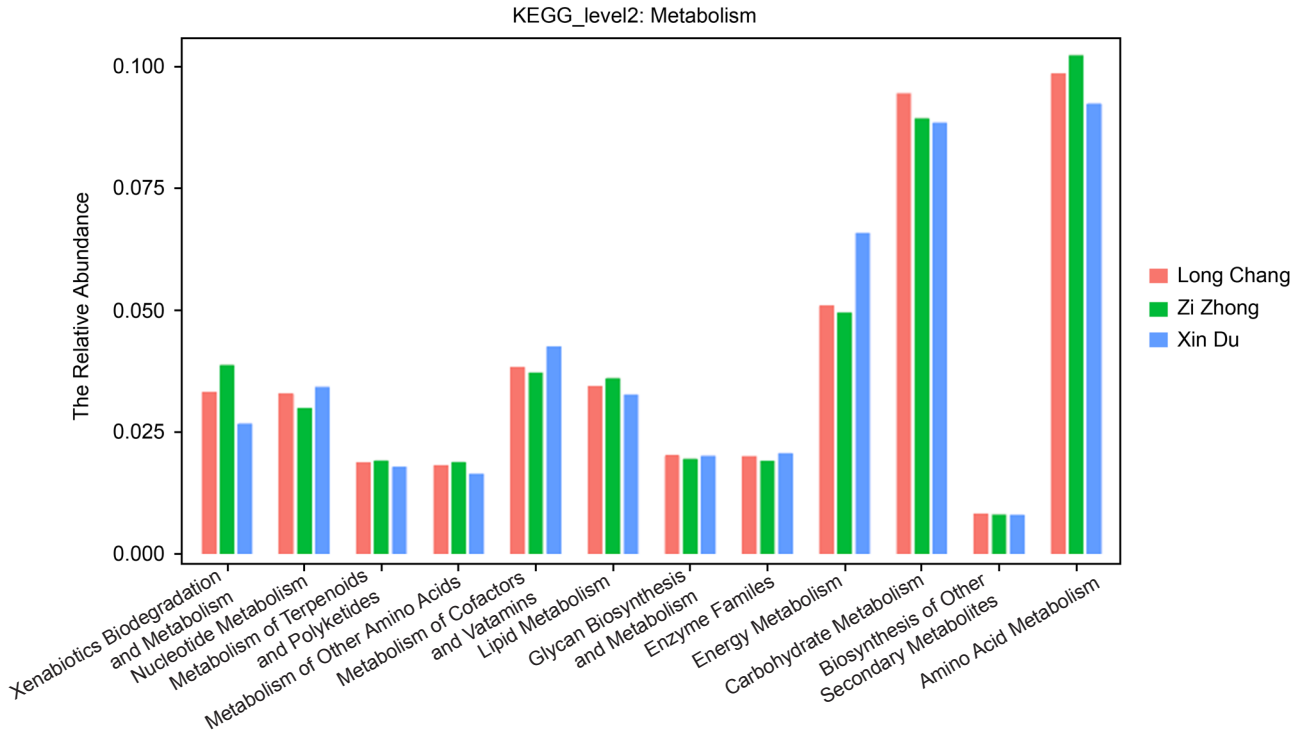


Fig. 3. Comparison of bacterial metabolic differences in the three fermented *Pinelliae Rhizoma*.

by bacteria in LC was significantly higher than ZZ and XD, while the amylase activity of LC was lowest. These results suggest that bacteria were not the main functional microorganisms in the process of carbohydrate metabolism; the level of amino acid metabolism in LC and ZZ fermented *Pinelliae Rhizoma* is higher than that in XD, and the protease activity was also the lowest, which indicated more decomposition of protein by bacteria in the LC and ZZ fermented *Pinelliae Rhizoma*; the level of xenobiotic biodegradation metabolism in XD was weaker than that in LC and ZZ fermented *Pinelliae Rhizoma*, suggesting that the bacterial-degraded xenobiotics occurred less frequently in the Xindu fermentation process of *Pinelliae Rhizoma*. Energy metabolism, cofactors, vitamin metabolism and nucleic acid metabolism related to bacteria in XD fermented *Pinelliae Rhizoma* were higher than LC and ZZ, which may be related to a stronger metabolism by more aerobic bacteria such as *Aerobacoccus* sp. (Fig. 2) in XD fermented *Pinelliae Rhizoma*; since, aerobic bacteria tend to grow faster and produce more energy.

Fungi communities in three fermented *Pinelliae Rhizoma* samples. The alpha diversities of fungi were lower than that of bacteria in all three fermented *Pinelliae Rhizoma*, the alpha diversities of fungi in XD is much lower than that in LC or ZZ (Table III). Over 30 000 total fungal sequences were identified in the three fermented *Pinelliae Rhizoma*, while the number of OTUs was only 100–208, and only 37 OTUs are detected in all three samples (Fig. 4). The number of

common OTUs was far less than the number of unique OTUs belonging to each sample.

More than 200 OTUs of fungi detected in three fermented *Pinelliae Rhizoma* were identified and found to belong to four large groups (Fig. 5). The fungi community in XD fermented *Pinelliae Rhizoma* clustered in a single branch, while the fungi community in LC and ZZ clustered in another branch. The genus of *Auricularia delicata* was found in both LC and ZZ at a relative abundance of 47% in LC and 14% in ZZ but was not detected in XD. Four OTUs existed in all three

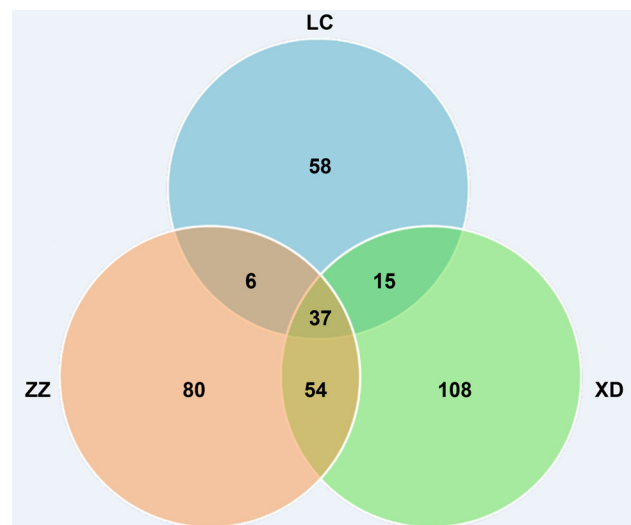


Fig. 4. The similarity of the fungi communities in three fermented *Pinelliae Rhizoma*.

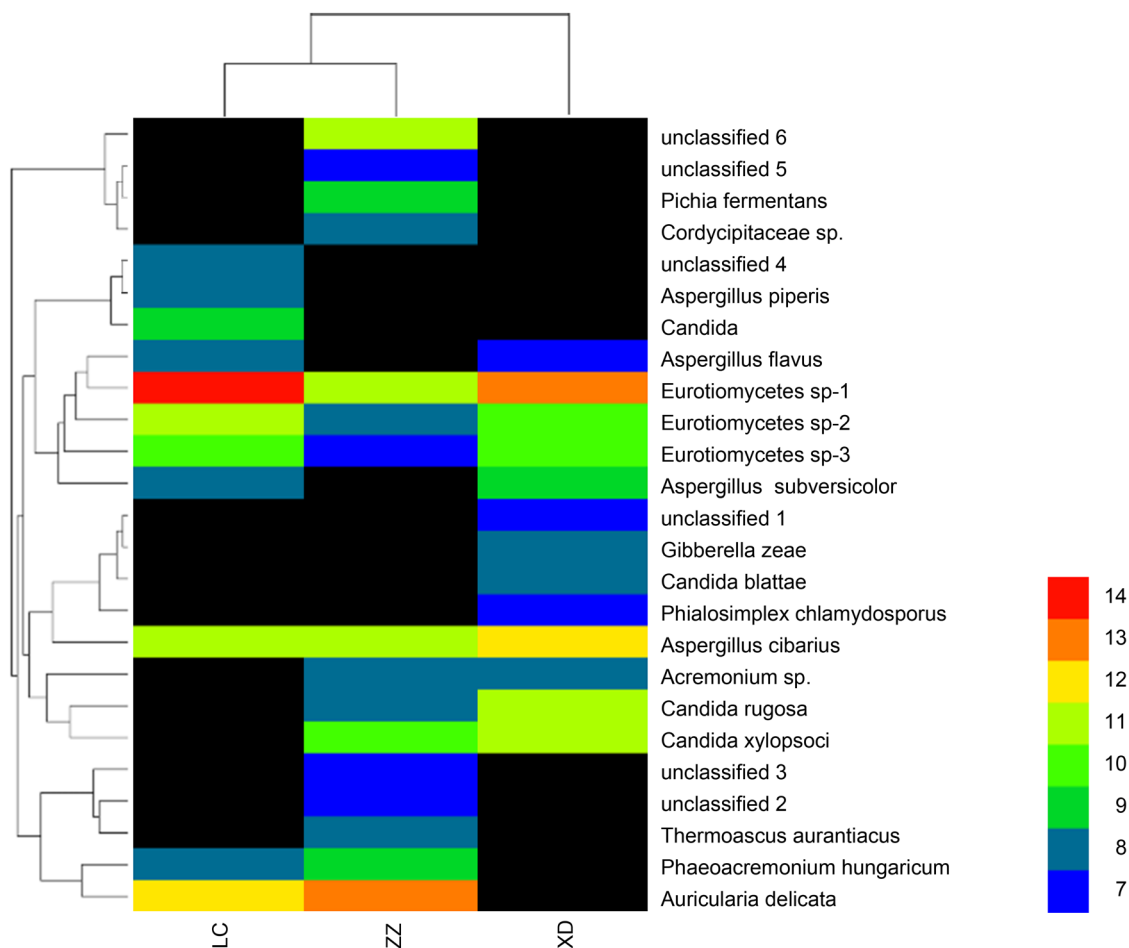


Fig. 5. Heat maps of fungi community in three fermented *Pinelliae Rhizoma*.

fermented *Pinelliae Rhizoma*, which were identified as three species of *Eurotiomyces* and *Aspergillus cibarius*, and the relative abundance of three *Eurotiomyces* sp. in XD, ZZ, LC were 46%, 11%, and 67% respectively, with the relative abundance of *Aspergillus cibarius* in XD, ZZ, LC measured at 22%, 9%, and 10%, respectively.

Volatile components in three fermented *Pinelliae Rhizoma*. A total of 51 volatile compounds were detected in the three samples of fermented *Pinelliae Rhizoma*, but each contained roughly 20 different compounds in different abundances (Table IV). Only curcumen and β -bisabolene were found in all three fermented *Pinelliae Rhizoma*. The relative contents of volatile components of C15 structures of bisabolene were 18.8%, 64.09%, and 27.26% in LC, XD, and ZZ, respectively. The relative contents of volatile components of C10 structure were 30.45%, 22.41%, and 7.04% respectively. It seems that steroids or terpenes of C10 and C15 account for most of the total volatile substances and may contribute to the activity of fermented *Pinelliae Rhizoma*.

In LC fermented *Pinelliae Rhizoma*, geraniol, curcumen (ginger), and α -terpineol were three volatile components with the highest relative content of

7.96%, 7.51%, 7.05% respectively. In XD fermented *Pinelliae Rhizoma*, [S-(R*,S*)]-2-methyl-5-(1,5-dimethyl-4-hexenyl)-1,3-cyclohexadiene, curcumen, and [S-(R*,S*)]-3-(1,5-dimethyl-4-hexenyl)-6-methylene-cyclohexene were three volatile components with the highest relative content of 23.07%, 14.21%, 10.62%, respectively. In ZZ fermented *Pinelliae Rhizoma*, curcumen, patchouli alcohol, and (E)-2-nonenal were three volatile components with the highest relative content of 10.98%, 8.55%, and 4.12%, respectively. These results show clear differences between the three fermented *Pinelliae Rhizoma*.

Non-volatile components in three fermented *Pinelliae Rhizoma* samples. More than 400 non-volatile components were detected in the three fermented *Pinelliae Rhizomas*, with 65 of the main non-volatile components (with a peak area over 100 000) shown in Table V. Because these non-volatile components were detected in the ethanol, butanol or ethyl acetate extractions, the relative content is calculated based on the total peak area of all components detected in three extractions.

In the LC, XD and ZZ fermentations, 26, 26 and 29 components were found respectively. In LC fermented *Pinelliae Rhizoma*, glyceride-1,3-dipalmito-

2-sorbate and 7-hydroxycadalenal were the main components detected in the butanol extraction, while 1-methyl-2-[(4Z,7Z)-4,7-tridecadienyl]-4-(1H)-quinolone, pyroglutamic acid, versicolactone D,L(-)-alpha-monopalmitin, dendroside D, 5-O-methylembelin, ethylpentadecanoate, ditertbutyl phthalate in the ethanol extraction were detected. In XD fermented *Pinelliae Rhizoma* benzyl formate, albopetasin, glyceride-1,3-dipalmito-2-sorbate, phthalic anhydride, gentiatibetine, capsorubin, muscone, docosandioic acid, ginsenoyn K, and allosioleucine were detected in the butanol extraction, while styrene, 10-gingediol, villosolside, 10-methoxyheptadeca-1-ene-4,6-diyne-3,9-diol, L-arginine, ethylpentadecanoate were detected in the ethanol extraction. Amarasterone A and linolenic acid were detected in the ethyl acetate extraction. In ZZ fermented *Pinelliae Rhizoma*, non-volatile components mainly extracted in butanol included glyceride-1,3-dipalmito-2-sorbate, pyrrole-2-aldehyde, 8-gingediol, muscone, phthalic anhydride, ambonic acid, 4-methyl heptadecanoic acid, 11-eicosenoic acid, 7-hydroxycadalenal and alpha-monoolein. Although only glyceride-1,3-dipalmito-2-sorbate, linolenic acid and (Z,Z)-9,12-octadecadienoic acid were detected in all three fermented *Pinelliae Rhizoma*, a series of components with C16, C18, C20, C21 and C22 framework were also found in the three fermented *Pinelliae Rhizoma*. Some new active non-volatile components that did not exist in *Pinelliae Rhizoma* were also detected in the three fermented *Pinelliae Rhizoma*, such as 16-carboxytotarol, 21-O-methyl-5,14-pregndiene-3beta,14beta,17beta,21-tetrol-20-one, canavanine, anacardic acid C, kurchiphyllamine, fumotoshidin A, muscone, coronaric acid, 13beta,17beta-epoxyalisol A, lemmasterone, ardisinol II, houpu lignan A, albopetasin, capsorubin, ginsenoyn K, phthalic anhydride, ambonic acid, and 7-hydroxycadalenal. These new components were produced through the fermentation of *Pinelliae Rhizoma*.

Discussion

In our study, *Bacillus* sp. was found to be the dominant bacteria and *Eurotiomycetes* sp. (including 3 OTUs), *Aspergillus cibarius* were found to be the dominant fungi in the three fermented *Pinelliae Rhizoma* produced in Longchang, Xindu, and Zizhong. While Guo et al. (2016) found that the dominant bacteria in the fermentation process of fermented *Pinelliae Rhizoma* were *Streptomyces* sp., *Bacillus pumilus*, *B. subtilis*, *B. aryabhatai*, *Bacillus* sp., and the dominant fungi were *Meyerozyma guilliermondii*, *Paecilomyces variotii*, *Byssochlamy spectabilis* and *Aspergillus niger* by culture methods. This observation difference may be due to

the following three reasons: firstly, our samples were dry fermented *Pinelliae Rhizoma*, and some bacteria that grow at higher humidity or occurred occasionally in the fermentation process of *Pinellia ternate* could not be reliably detected, especially those which do not produce spores. Secondly, high-throughput sequencing can supply more comprehensive information about the microbiota compared to the culture method. Finally, the results of our study were summarized from three fermented *Pinellia ternate*, that ensured most common species could be found and less accidental microorganisms caused by different environmental factors.

Five genera may play important roles in the fermentation process of *Pinelliae Rhizoma* according to our study. From the aspect of bacteria, the abundance of *Bacillus* was higher in LC and ZZ, and the fermented *Pinelliae Rhizoma* produced in Longchang and Zizhong have been found to be generally more clinically effective than the one from Xindu, so *Bacillus* may closely correlate with the quality of fermented *Pinelliae Rhizoma*. For the fungi, three fermented *Pinelliae Rhizoma* have very different fungi community, four fungal species may play more important roles in the fermentation process of *Pinelliae Rhizoma* and could be isolated on selected medium for further study. Some detected OTUs could not be successfully identified using the UNITE or Genbank databases, strongly suggesting that some new fungal species may exist in these fermentations. As such, the traditionally fermented Chinese medicines could supply fungal resources as novel and important materials.

These dominant microorganisms species are mainly derived from raw materials as the endophyte of *Pinelliae Rhizoma*, while some other genera of microorganisms from local environmental sources may also influence the fermentation. For the bacteria, the OTUs and alpha diversity of bacteria in XD is significantly higher than that in LC and ZZ, and the microbiota was more similar between LC and ZZ; it may be attributed to the fact that Xindu county is only 25 kilometers from Chendu, the capital of Sichuan. The average PM 2.5 value in the air of Xindu in May 2016 is 53 $\mu\text{g}/\text{m}^3$, while it is 40 $\mu\text{g}/\text{m}^3$ in Zizhong and 35 $\mu\text{g}/\text{m}^3$ in Longchang. These data suggest that the fermentation of *Pinelliae Rhizoma* could have been influenced by more complex environmental factors stemming from a modern metropolis. So do the fungi, the genus of *Auricularia delicata* was found in both LC and ZZ, but was not detected in XD, so it may be associated with the local environment of Longchang and Zizhong.

Although above five genera are thought to be effective in the fermentation of *Pinelliae Rhizoma*, the composition of volatile or non-volatile components obviously differed among three fermented *Pinelliae Rhizoma* produced from the same material in Longchang,

Zizhong and Xindu counties. For example, non-volatile components in LC and ZZ fermented *Pinelliae Rhizoma* were similar in total peak area, while these same components yielded only half the peak area in XD, which indicated that the composition of the three fermented *Pinelliae Rhizoma* was greatly different. Therefore, it is not that the closer the two areas are, the more similar the components are, and the differences among samples seem to change geographically in an unregular way. The unique identities of fermented *Pinelliae Rhizoma* were also related to the region where the fermentation was carried out, in addition to the variety and cultivation management of *Pinellia ternate* (Lu 2012), for the results of fermentation also reflects the complexity of local microbiota.

For the most common volatile components, the activity of [S-(R*,S*)]-2-methyl-5-(1,5-dimethyl-4-hexenyl)-1,3-cyclohexadiene and [S-(R*,S*)]-3-(1,5-dimethyl-4-hexenyl)-6-methylene-cyclohexene have not been discovered. However, curcumene (Grzanna et al. 2005; Shirvani et al. 2015), geraniol (Carneseccchi et al. 2004), α -terpineol (de Sousa et al. 2007), geraniol (Chen et al. 1980) in fermented *Pinelliae Rhizoma* have been reported to have at least one kind of function. Other components containing β -bisabolene, endo-borneol, citronellol, patchouli alcohol, camphor, alloaromadendrene, citral have been shown to have antioxidant and anti-inflammatory activities (Miguel 2010), but these components were only detected in one or two fermented *Pinelliae Rhizoma*. Furthermore, fungi is more closely related to the formation of terpenoids or terpenoid volatiles (Lemfack et al. 2018), [S-(R,S)]-2-methyl-5-(1,5-dimethyl-4-hexenyl)-1,3-cyclohexadiene and [S-(R,S)]-3-(1,5-dimethyl-4-hexenyl)-6-methylene-cyclohexene were detected as main volatile components in the XD fermented *Pinelliae Rhizoma*, while not found in LC or ZZ fermented *Pinelliae Rhizoma*. This indicated that these compounds may be derived from its different fungal flora from the other two fermentations.

Non-volatile components have been shown to have many activities, for example, alkaloids contained in *Pinelliae Rhizoma* or fermented *Pinelliae Rhizoma* have the effects of sedation, hypotension and saliva secretion (Zhou et al. 2006; Xiao et al. 2016). Gentiati-betine has certain anticonvulsant and brain protective effects (Peng 2016), gingediol (curcumin) could be used to treat cold and vomiting (Hatcher et al. 2008), amarasterone A can reduce blood sugar (Catalan et al. 1982), linolenic acid has been suggested to have anti-tumor properties (Huan et al. 2012). Houpu lignan A has therapeutic effects on dyspepsia, abdominal distention, constipation and also has certain anti-cancer properties (Si et al. 2002), albopetasin can relieve swelling and pain (Zhang 2009), ginsenoynone K could invig-

orate the spleen and benefit the lung (He et al. 1993), ambonic acid has antibacterial effect (Omar et al. 2017), 7-hydroxycadalenal can relieve pain (State Administration of Traditional Chinese Medicine 2005), etc. These activities may attribute to the function of fermented *Pinelliae Rhizoma*.

Fermented *Pinelliae Rhizoma* produced in different counties showed equivalent or similar clinical efficacy, while in this study, on the whole, the composition of volatile and non-volatile components in LC, ZZ and XD fermented *Pinelliae Rhizoma* seem to differ substantially and be affected by their location, only a few of the same volatile or non-volatile components were found in all three fermented *Pinelliae Rhizoma*. Of note, the clinical holistic effect of fermented *Pinelliae Rhizoma* cannot be achieved by these several components alone, instead, a variety of bioactive volatile components with C10 and C15 structures as well as non-volatile components with C16, C18, C20, C21, and C22 structures were also detected in the three fermented *Pinelliae Rhizoma*. This indicates that the efficacy of fermented *Pinelliae Rhizoma* may originate from a series of structurally similar components. In the fermentation of *Pinelliae Rhizoma* by a mix of environmental microorganism, the same component in the raw material is transformed into a variety of substances with similar structures and possibilities of mutual transformation through secondary metabolism. The metabolic pathways of secondary metabolism are very complex, so despite different mixtures of microorganisms, these groups may act on similar secondary metabolite pathways creating a plethora of different compounds. The components of fermented *Pinellia ternata* neither reflect the composition of its microbiota microscopically nor geographical features macroscopically. The results also help to explain why no unique active components have been identified in those traditional Chinese medicines which demonstrate wide and definite curative effects.

With such a wide range of microbes and active compounds present in the fermentation process, we were unable to achieve a one-to-one correspondence between certain species and active compounds. Therefore, we do not yet know which species produce certain active compounds in the context of controlled mixed fermentation. These results do however provide clear evidence that many complex active compounds are produced through the solid-state mixed fermentation of *Pinelliae Rhizoma*, and as such, similar solid-state mixed fermentation processes may be also used in the preparation of other traditional Chinese medicines or natural products. Further study may be focused on the identification of the main microorganisms and their metabolic products, that may initiate controlled mixed fermentation by functional pure microbial strains with the variety of traditional Chinese herbs.

Acknowledgements

This work was financially supported by supported Solid-state Fermentation Resource Utilization Key Laboratory of Sichuan Province of China (Grant No. 2015GTJ005) and the innovation research team of Yibin University (Grant No.2017TD01).

Conflict of interest

The authors do not report any financial or personal connections with other persons or organizations, which might negatively affect the contents of this publication and/or claim authorship rights to this publication.

Literature

- Boratyński F, Szczepańska E, Grudniewska A, Olejniczak T.** Microbial kinetic resolution of aroma compounds using solid-state fermentation. *Catalysts*. 2018;8(1):28. doi:10.3390/catal8010028
- Carnesecchi S, Bras-Gonçalves R, Bradaia A, Zeisel M, Gossé F, Poupon MF, Raul F.** Geraniol, a component of plant essential oils, modulates DNA synthesis and potentiates 5-fluorouracil efficacy on human colon tumor xenografts. *Cancer Lett*. 2004;215(1):53–59. doi:10.1016/j.canlet.2004.06.019 [Medline](#)
- Catalan RE, Martinez AM, Aragones MD.** *In vitro* effect of ecdysterone on protein kinase activity. *Comp Biochem Physiol B Comp Biochem*. 1982;71(2):301–303. doi:10.1016/0305-0491(82)90259-0
- Chen H.** Anaerobic Solid-State Fermentation. In: *Modern Solid State Fermentation*. Dordrecht (Netherlands): Springer Netherlands. 2013; p. 199–242.
- Chen Y, Zhang YQ, Qian BC, Gong WG, Xu HJ, Zhang LX.** [Pharmacological study of geraniol] (in Chinese). *Chinese Traditional Patent Medicine*. 1980;01:26–30.
- China National Standard.** GB/T 23535-2009 [Lipase preparation] (in Chinese).
- China National Standard.** GB/T 24401-2009 [α -Amylase preparation] (in Chinese).
- China Commercial Standard.** SB/T 10317-1999 [Measurement of proteinase activity] (in Chinese).
- Chinese Pharmacopoeia Commission.** Chinese pharmacopoeia 2015 part 1. (in Chinese). Beijing (China): China Medical Science & Technology Press. 2015; p. 135.
- Cianchetta S, Bregoli L, Galletti S.** Microplate-based evaluation of the sugar yield from giant reed, giant miscanthus and switchgrass after mild chemical pre-treatments and hydrolysis with tailored trichoderma enzymatic blends. *Appl Biochem Biotechnol*. 2017; 183(3):876–892. doi:10.1007/s12010-017-2470-z
- de Sousa DP, Quintans Jr. L, de Almeida RN.** Evolution of the anticonvulsant activity of a terpeneol. *Pharm Biol*. 2007;45(1):69–70.
- Editorial Committee of Chinese Materia Medica.** State Administration of Traditional Chinese Medicine. *Chinese Materia Medica* (in Chinese). Shanghai (China): Shanghai Science and Technology Publishing House. 2005.
- Fan W, Tang Y, Qu Y, Cao F, Huo G.** Infant formula supplemented with low protein and high carbohydrate alters the intestinal microbiota in neonatal SD rats. *BMC Microbiol*. 2014;14:279.
- Gong DF, Wang FC, Ji DH, Zhang L.** [Advances in studies on chemical constituents, pharmacological and toxicological activities of *Pinellia ternate*]. (in Chinese). *J Yangtze Univ (Nat Sci Ed)*. 2015; 12(18):77–79.
- Grzanna R, Lindmark L, Frondoza CG.** Ginger – an herbal medicinal product with broad anti-inflammatory actions. *J Med Food*. 2005;8(2):125–132.
- Guo JJ, Su MS, Wang LY, Ren JX, Yang M, Xie XM.** [Identification of dominant microorganisms in the processing of *Pinellia Quailata*]. (in Chinese). *China Journal of Chinese Materia Medica*. 2016. 41(16): 3027–3031.
- Hatcher H, Planalp R, Cho J, Torti FM, Torti SV.** Curcumin: from ancient medicine to current clinical trials. *Cell Mol Life Sci*. 2008;65(11):1631–1652.
- He GZ, Zhang J, Xue XM, Wang J.** [The effect of ginsenosides on immune function enhancement and regulation in patients with chronic cor pulmonale]. (in Chinese). *J Jilin Univ (Med Ed)*. 1993;1:50–53.
- Hu C, Nögel R, Hummelsberger J, Engelhardt U.** Monographie 40: *Pinelliae Rhizoma* (Banxia). In: Hu C, Nögel R, Hummelsberger J, Engelhardt U, editors. *Paozhi: Die Aufbereitung chinesischer Arzneimittel*. Berlin, Heidelberg (Germany): Springer. 2018.
- Huan M, Cui H, Teng Z, Zhang B, Wang J, Liu X.** *In vivo* anti-tumor activity of a new doxorubicin conjugate via α -linolenic acid. *J Agric Chem Soc Japan*. 2012;76(8):1577–1579.
- Köljalg U, Nilsson RH, Abarenkov K, Tedersoo L, Taylor AF, Bahram M, Bates ST, Bruns TD, Bengtsson-Palme J, Callaghan TM, et al.** Towards a unified paradigm for sequence-based identification of fungi. *Mol Ecol*. 2013;22(21):5271–5277. doi:10.1111/mec.12481
- Langille MG, Zaneveld J, Caporaso JG, McDonald D, Knights D, Reyes JA, Clemente JC, Burkpile DE, Vega Thurber RL, Knight R, et al.** Predictive functional profiling of microbial communities using 16S rRNA marker gene sequences. *Nat Biotechnol*. 2013;31(9):814–821. doi:10.1038/nbt.2676
- Lemfack MC, Gohlke BO, Toguem SMT, Preissner S, Piechulla B, Preissner R.** mVOC 2.0: a database of microbial volatiles. *Nucleic Acids Res*. 2018;46(D1):D1261–D1265. doi:10.1093/nar/gkx1016
- Lu DH.** [Quality evaluation of *Pinellia ternata* in different regions and identification of counterfeit and related varieties]. (in Chinese). Chengdu (China): Chengdu University of Traditional Chinese Medicine. 2012.
- Miguel MG.** Antioxidant and anti-inflammatory activities of essential oils: a short review. *Molecules*. 2010;15(12):9252–9287.
- Mukherjee PK, Chandra J, Retuerto M, Sikaroodi M, Brown RE, Jurevic R, Salata RA, Lederman MM, Gillevet PM, Ghanoum MA.** Oral microbiome analysis of HIV-infected patients: identification of *Pichia* as an antagonist of opportunistic fungi. *PLoS Pathog*. 2014;10(3):e1003996. doi:10.1371/journal.ppat.1003996
- Omar R, Igoli JO, Zhang T, Gray AI, Ebiloma GU, Clements CJ, Fearnley J, Ebel RE, Paget T, Koning HP, et al.** The chemical characterization of Nigerian propolis samples and their activity against *Trypanosoma brucei*. *Sci Re*. 2017;7(1):923. doi:10.1038/s41598-017-01038-2
- Peng DU.** [Artificial alkaloids and chemical constituents of *Gentiana crassicaulis* Duthie ex Burk]. (in Chinese). *J Anhui Agric Sci*. 2016;44(26):91–94.
- Qu HH, Qu BP, Liu SC, Qin GF, Kong H, Zhao Y.** Mechanism of baicalin compatibility in Chinese medicine formula banxia xiexin decoction by pharmacokinetics and indirect competitive enzyme-linked immunosorbent assays in mice. *Chin J Integr Med*. 2016;2:1–5.
- Quast C, Pruesse E, Yilmaz P, Gerken J, Schweer T, Yarza P, Peplies J, Glöckner FO.** The SILVA ribosomal RNA gene database project: improved data processing and web-based tools. *Nucleic Acids Res*. 2013;41(Database issue):D590–D596. doi:10.1093/nar/gks1219
- Rédei GP.** Kjeldahl Method. In: Rédei GP. *Encyclopedia of Genetics, Genomics, Proteomics and Informatics*. Dordrecht (Netherlands): Springer Netherlands. 2008.
- Shen DR, Zhang LR, Ye LL.** [Analysis of the efficacy of fermented *Pinellia ternate*]. (in Chinese). *China Pharm*. 2009;18(16):73–74.
- Shirvani MA, Motahari-Tabari N, Alipour A.** The effect of mefenamic acid and ginger on pain relief in primary dysmenorrhea: a randomized clinical trial. *Arch Gynecol Obstet*. 2015;291(6): 1277–1281.

- Si J, Tong Z, Zeng Y, Jiang X, Liu R.** Quality evaluation and utilization of germplasm resources of *Magnolia officinalis*. Journal of Chinese Medicinal Materials. 2002;25(2):79.
- Try S, Voilley A, Chunhieng T, De-Coninck J, Waché Y.** Aroma compounds production by solid state fermentation, importance of *in situ* gas-phase recovery systems. Appl Microbiol Biotechnol. 2018;102(17):7239–7255.
- Wagner H, Bauer R, Melchart D, Xiao PG, Staudinger A.** *Rhizoma pinelliae* – Banxia. In: Wagner H, Bauer R, Melchart D, Xiao PG, Staudinger A, editors. Chromatographic Fingerprint Analysis of Herbal Medicines. Vienna (Austria): Springer. 2011.
- Wu X, Wang S, Lu J, Jing Y, Li M, Cao J, Bian B, Hu C.** Seeing the unseen of Chinese herbal medicine processing (*Paozhi*): advances in new perspectives. Chin Med. 2018;13:4.
[doi:10.1186/s13020-018-0163-3](https://doi.org/10.1186/s13020-018-0163-3)
- Xiao Q, Yang WW, Zhang DW, Yi XX.** [Advances in the study of influencing factors and pharmacological effects of total alkaloids in *Pinellia ternata*]. (in Chinese). Chinese Pharmaceuticals. 2016; 25(3):123–126.
- Zhang FJ.** [Preparation and bioactivity of total lactones from *Betula pilosa*]. (in Chinese). Doctoral dissertation. Shanghai (China): Second Military Medical University. 2009.
- Zhao H, Yun J.** Isolation, identification and fermentation conditions of highly acetoin-producing acetic acid bacterium from Liangzhou fumigated vinegar in China. Ann Microbiol. 2016;66(1): 279–288. [doi:10.1007/s13213-015-1106-1](https://doi.org/10.1007/s13213-015-1106-1)
- Zhao JL, Li Q, Ding YY, Gu XY, Feng WW, Wang W, Zhang M, Zhao T, Yang LQ, Wu XY.** Sedative activity of the chemical constituents of *Rhizoma pinelliae*, praeparatum. Chem Nat Compd. 2018;54(1): 215–217.
[doi:10.1007/s10600-018-2304-4](https://doi.org/10.1007/s10600-018-2304-4)
- Zhou Q, Wu H, Wang QR, Lu AJ.** Anti-inflammatory effects of total alkaloids in *Pinellia ternata*. (in Chinese). J Nanjing Univ Trad Chinese Med. 2006;22(2):86–88.

New Insight into Genotypic and Phenotypic Relatedness of *Staphylococcus aureus* Strains from Human Infections or Animal Reservoirs

KLAUDIA LISOWSKA-ŁYSIAK^{1#}, MAJA KOSECKA-STROJEK^{1#}, JOANNA BIAŁECKA²,
ANDRZEJ KASPROWICZ², KATARZYNA GARBACZ³, LIDIA PIECHOWICZ⁴, VLADIMIR KMET⁵,
VINCENZO SAVINI⁶ AND JACEK MIĘDZOBRODZKI^{1*}

¹Department of Microbiology, Faculty of Biochemistry, Biophysics and Biotechnology, Jagiellonian University, Krakow, Poland

²Centre of Microbiological Research and Autovaccines, Krakow, Poland

³Department of Oral Microbiology, Medical Faculty, Medical University of Gdansk, Gdansk, Poland

⁴Department of Medical Microbiology, Medical Faculty, Medical University of Gdansk, Gdansk, Poland

⁵Centre of Biosciences, Institute of Animal Physiology, Slovak Academy of Sciences, Slovakia

⁶Clinical Microbiology and Virology, Spirito Santo Hospital, Pescara (PE), Italy

Submitted 28 September 2018, revised 22 November 2018, accepted 7 December 2018

Abstract

Staphylococcus aureus is a common human and livestock opportunistic pathogen, and there is evidence of animal to human transmission. This paper aimed to recognize properties of the isolates from collections of human and livestock *S. aureus* strains and to estimate compatibility of results based on phenotypic tests, microarrays and the *spa* typing methods. The second goal was to study differences between human and animal isolates in terms of specificity of their hosts and the strain transmission among various hosts. Most strains showed multi-susceptible profiles and produced enzymes on a high level, and they were phenotypically and genetically similar. However, in contrast to the Polish bovine mastitis strains, the Slovakian strains were multi-resistant. In this research, the strains showed significant differences in terms of their phenotypic manifestations and the presence of hemolysins genes; however, other enzyme-encoding genes correlated to a higher extent with the microarrays results. Interestingly, there was a lack of enterotoxin genes in human Poultry-like protein A+ strains in comparison to other human strains. Our study showed that differences between virulence profiles of the human and animal strains correlated with their origin rather than their hosts, and any trait allowed clearly distinguishing between them based on the microarray results.

Key words: genetic profile, infection, microarrays, phenotype, *Staphylococcus aureus*

Introduction

A common human and animal opportunistic pathogen *Staphylococcus aureus* occurs mostly in the skin and/or nose vestibule mucous membrane as consistent of natural microflora in healthy individuals. Colonization can lead to an invasive mode of infection under particular conditions of a host organism, mostly immunodeficiency, surgical interventions or longitudinal hospitalization of patients (Malachowa et al. 2011; O’Gara 2017). The European Centre for Disease Prevention and Control alarms that the most antimicrobial-resistant healthcare-associated infections are caused by the methicillin-resistant *S. aureus* (MRSA). Estimating

the level of distribution, the MRSA isolates are responsible for 10% to 25% of all staphylococcal infections in Poland; in Slovakia, these rates are even higher (25% to 50%). Moreover, an increasing problem is the expansion of community-acquired MRSA (ECDC 2015).

Staphylococcal strains carrying antimicrobial-resistance genes colonize a vast range of animal species, especially household or livestock animals, with clear evidence of the intra-species transmission of staphylococci (Angen et al. 2017; Kmet et al. 2018).

Under particular conditions, *S. aureus* causes infections, and become high-risk pathogens due to several virulence determinants such as toxins and enzymes combined with other survival strategies of bacteria

Equal shares in the paper composition.

* Corresponding author: J. Międzobrodzki, Department of Microbiology, Faculty of Biochemistry, Biophysics and Biotechnology, Jagiellonian University, Krakow, Poland; e-mail: jacek.miedzobrodzki@uj.edu.pl

© 2019 Klaudia Lisowska-Łysiak et al.

This work is licensed under the Creative Commons Attribution-NonCommercial-NoDerivatives 4.0 License (<https://creativecommons.org/licenses/by-nc-nd/4.0/>)

like antibiotic resistance and biofilm production (Goldmann and Medina 2017). An important staphylococcal strategy is to damage host cell membranes, caused by hemolysins, bi-component leukocidins, and phenol soluble modulins. For example, α -hemolysin and bi-component leukocidins act as pore-forming toxins, while β -haemolysin is sphingomyelinase, which hydrolyzes lipids of plasma membrane into ceramide and phosphorylcholine (Herrera et al. 2016). Additionally, α -hemolysin and Panton-Valentine leucocidin (PVL) promote apoptosis of phagocytes (Seilie and Bubeck-Wardenburg 2017). Another group of virulence factors is an enterotoxin superfamily. These toxins are responsible for staphylococcal food poisoning, but they also affect some immune system cells, with further consequences (Zhang et al. 2017).

S. aureus strains also secrete a variety of enzymes. Proteases include a vast group of secreted enzymes, such as aureolysin, serine proteases, and staphopains, which are engaged in the evasion of complement-mediated bacterial killing (Miedzobrodzki et al. 2002; Sabat et al. 2008; Otto 2014). Nuclease, another extracellular enzyme, degrades neutrophil extracellular traps (NETs), providing the strain resistant to NET-mediated killing (Zawrotniak and Rapala-Kozik 2013; Paharik and Horswill 2016). *S. aureus* also produces lipase, which lyses triglycerides to free fatty acids – but the biological function of this process is still unknown (Cadieux et al. 2014). Finally, extracellular urease is involved in biofilm regulation and protection against low pH. Urease catalyzes the hydrolysis of urea and neutralizes acids using ammonia (Vandecandelaere et al. 2017). Triggering calculus formation, an increased pH level plays a significant role in urinary tract diseases (Paharik and Horswill 2016).

The progress of *S. aureus* infections depends on the secretion of surface proteins, numerous extracellular toxins, and enzymes that destruct host cells and tissues (Kong et al. 2016). Due to this fact, this work aimed to recognize the characteristic properties of *S. aureus* strains based on phenotypic and genetic features such as the production of enzymes and toxins, their resistance profiles and MRSA detection. Firstly, the strains were genetically characterized by microarrays' profiling and *spa* typing. Secondly, the human and animal strains were compared based on microarray testing and phenotypic manifestations, together with the analysis of their relatedness or differences between them.

Experimental

Materials and Methods

Strains collection. Fifty-three not duplicate *S. aureus* strains were isolated from deep tissue infections of ambulatory patients and from animals (Table I). The

number of strains was sufficient to group the strains based on their similarities, to define dominant properties of the strains and groups, and to compare them. The 26 human strains were obtained from four medical institutions and universities: (i) 11 isolates from the Centre of Microbiological Research and Autovaccines and different hospital wards in Kraków (Poland), (ii) 11 Poultry-like protein A positive (P-like pA+) isolates from the Medical University of Gdańsk, (Poland), and (iii) four isolates from the Spirito Santo Hospital, Pescara (Italy). Among these strains, 21 isolates originated from the following infections: wound infections (n=9), boils (n=3), deep skin lesions (n=2), ulcers (n=2), conjunctivitis (n=2), blood (n=1), cyst (n=1), and pus (n=1); the other five were isolated from throats (n=3) and nose swabs (n=2). Moreover, the collection was enriched with 11 P-like pA+ strains isolated from patients in Gdańsk, an atypical origin of P-like pA+ biotype, although there is no information about the link between these strains occurrence and patient's employment. Interestingly, these strains are usually detected in meat products, in people having direct contact with meat, and in the places where fresh meat occurs in abundance (Piechowicz and Garbacz 2016).

The 27 animal strains were isolated from animals, which had daily physical contact with people. The strains were obtained from four veterinary institutions and universities: (i) 15 bovine isolates from the Faculty of Biology and Animal Breeding, University of Life Sciences, Lublin (Poland); (ii) seven bovine isolates from the Institute of Animal Physiology, Centre of Biosciences, Slovak Academy of Sciences, Košice (Slovakia); (iii) four canine isolates from the Medical University of Gdańsk (Poland); and (iv) one canine isolate from the Faculty of Veterinary Medicine, University of Environmental and Life Sciences, Wrocław (Poland). Only one animal strain was isolated from throat infection of a dog while the others were isolated from eczema, eye, or skin infections. All the strains were isolated from animals inhabiting human environments with frequent contact with people what facilitates the inter-genus transmission of bacteria.

Taking into consideration a widespread and active transmission of staphylococci, the bacteria from various sources and different geographic regions were used in this research.

Antibiotic susceptibility testing. Before molecular analysis the antibiotic susceptibility testing was performed using the disc diffusion according to the European Committee on Antimicrobial Susceptibility Testing (EUCAST 2017). The bacteria were cultivated for 24 hours at 37°C on MH agar plates with antibiotic discs. The 24 h incubation is required for ceftiofur susceptibility testing according to according to EUCAST (Żabicka and Hryniewicz 2009). The strains were tested using a

Table I
A list of the strains collected, their origin and place of isolation.

Strain no.	Host	Lesions/Material	Place of origin
1	human	wound infection	Kraków (Poland)
2	human	cyst	Kraków (Poland)
3	human	wound infection	Kraków (Poland)
4	human	wound infection	Kraków (Poland)
5	human	wound infection	Kraków (Poland)
6	human	wound infection	Gdańsk (Poland)
7	human	wound infection	Gdańsk (Poland)
8	human	boil	Gdańsk (Poland)
9	human	boil	Gdańsk (Poland)
10	human	boil	Gdańsk (Poland)
11	human	throat	Gdańsk (Poland)
12	human	pus	Gdańsk (Poland)
13	human	throat	Gdańsk (Poland)
14	human	throat	Pescara (Italy)
15	human	skin infection	Pescara (Italy)
16	human	blood	Pescara (Italy)
17	human	skin infection	Pescara (Italy)
18	human	nose swab	Gdańsk (Poland)
19	human	ulcer	Gdańsk (Poland)
20	human	ulcer	Gdańsk (Poland)
21	human	wound infection	Kraków (Poland)
22	human	wound infection	Kraków (Poland)
23	human	conjunctivitis	Kraków (Poland)
24	human	conjunctivitis	Kraków (Poland)
25	human	wound infection	Kraków (Poland)
26	human	nose swab	Kraków (Poland)
27	animal	eczema	Gdańsk (Poland)
28	animal	eye	Gdańsk (Poland)

Strain no.	Host	Lesions/Material	Place of origin
29	animal	eye	Gdańsk (Poland)
30	animal	throat	Gdańsk (Poland)
31	animal	skin infection	Wrocław (Poland)
32	animal	mastitis	Košice (Slovakia)
33	animal	mastitis	Košice (Slovakia)
34	animal	mastitis	Košice (Slovakia)
35	animal	mastitis	Košice (Slovakia)
36	animal	mastitis	Košice (Slovakia)
37	animal	mastitis	Košice (Slovakia)
38	animal	mastitis	Košice (Slovakia)
39	animal	mastitis	Łęczna (Poland)
40	animal	mastitis	Łęczna (Poland)
41	animal	mastitis	Lubartów (Poland)
42	animal	mastitis	Łęczna (Poland)
43	animal	mastitis	Łęczna (Poland)
44	animal	mastitis	Łuków (Poland)
45	animal	mastitis	Łuków (Poland)
46	animal	mastitis	Gawrolin (Poland)
47	animal	mastitis	Świdnik (Poland)
48	animal	mastitis	Świdnik (Poland)
49	animal	mastitis	Świdnik (Poland)
50	animal	mastitis	Tomaszów Lubelski (Poland)
51	animal	mastitis	Tomaszów Lubelski (Poland)
52	animal	mastitis	Tomaszów Lubelski (Poland)
53	animal	mastitis	Tomaszów Lubelski (Poland)

set of 12 antibacterial agents, including the following: i) aminoglycosides: amikacin and gentamicin; ii) beta-lactams: amoxicillin with clavulanic acid, cefoxitin, and penicillin; iii) fluoroquinolones: ciprofloxacin and norfloxacin; iv) lincosamides: trimethoprim/sulfamethoxazole; v) macrolides: clindamycin and erythromycin; and others: chloramphenicol and doxycycline. The diameter of the transparent zones of growth inhibition was measured, and clinical breakpoints were evaluated.

Evaluation of enzymatic activity. A single colony of each bacterial strain was transferred from a TSA agar plate (Sigma Aldrich, Merck KGaA, Darmstadt, Germany) to specific media, including substrates dedicated to particular enzymes: a TSA agar plate supplemented with 10% of skim milk proteins; a blood agar plate with 5% sheep blood (Graso Biotech, Starogard Gdański, Poland); a TSA agar plate enriched with 2% Tween 80; 10% of 1M CaCl₂; DNase test agar (Becton Dickinson, New Jersey, USA); and Christensen's Urea

Agar Base (REFE112L), containing 40% of Urea Solution (EBO48), (Becton Dickinson, New Jersey, USA) for proteolysis testing, hemolysis testing, lipases activity testing, nucleases activity testing, and ureases activity testing, respectively. Bacterial strains on appropriate plates were then cultured for 24 hours at 37°C. To evaluate proteolysis activity, the diameters of transparent zones around the colonies were measured (Puacz et al. 2015). To rate types of hemolysis the transparent zones for β -hemolysis (including the second zone observed in double β -hemolysis) and dark-green opalization for α -hemolysis were evaluated (Puacz et al. 2015). Lipase activity was measured by the size of a turbidity zone around colonies, nuclease activity – by the size of a transparent zone after HCl addition to the culture test, while urease activity – by the color change of the medium from yellow to purple (Black et al. 1971; dos Santos Rodrigues et al. 2014; Posteraro et al. 2015). To evaluate enzymatic activity, a sample was assessed

as either negative (no activity) or positive (with low, moderate, high or very high activity).

Molecular techniques. The *spa* typing. The *spa* typing technique was used following Aires-de-Souza et al. (2006). The method is based on the sequence analysis of amplified fragments of the X region of the protein A gene, resulting in *spa* types, assigned by the Ridom StaphType software version 2.1.1 (Ridom GmbH, Würzburg, Germany) and the Ridom SpaServer (<http://www.spaserver.ridom.de>). Based on *spa* types, *spa* clonal complexes (*spa*-CCs) are then calculated using the Based Upon Repeat Pattern (BURP) algorithm with the following parameters: (i) no exclusion criteria related to the number of repeats were used; (ii) cost equal to 4; (iii) a cluster composed of 2 or more related *spa* types was regarded as a clonal complex (CC); and (iv) a *spa* type that was not grouped into a CC was considered a singleton.

Microarray analysis. Microarray assays were done using the StaphyType system (StaphyType, Alere Technologies, Jena, Germany). The StaphyType kit allows the simultaneous detection of 334 *S. aureus* target sequences, including approximately 170 distinct genes and their allelic variants. The DNA microarray procedures were carried out according to the manufacturer's instructions. According to Monecke's et al. (2008) methodology, the strains were automatically assigned to CCs or sequence types (STs) by the StaphyType software. The results for individual genes were converted into the following scale: A = positive, T = negative, and C = ambiguous.

Results

Antibiotic susceptibility testing. All the *S. aureus* strains tested were susceptible to trimethoprim/sulfamethoxazole (Table II). Five human (19%) and ten animal (37%) strains were susceptible to all the antibiotics tested. Eight strains (15%), the Slovakian bovine strains together with one human strain originated from Kraków were multi-resistant (resistant to more than three antibiotics). The highest resistance rate was observed for penicillin ($n = 33$; 62%), with 17 human (65%) and 16 animal (59%) resistant strains. The detection of resistance to cefoxitin helped to identify nine strains (two from humans and seven from animals) as methicillin-resistant (MRSA), and one of them did not exhibit resistance to benzylpenicillin/ amoxicillin. Among the MRSA strains, bovine strains from Slovakia ($n = 7$) were resistant to other antibiotics. All of these strains demonstrated resistance to erythromycin and clindamycin, and they were classified to have an inducible MLS_B (macrolides-lincosamides-streptogramin B resistance) phenotype. Bovine strains of non-Slova-

Table II
Antibiotic susceptibility of *S. aureus* strains. MRSA strains are bolded in text.

Antibiotic	Number of strains		
	Human (%) n = 26	Animal (%) n = 27	All (%) n = 53
Resistant to all antibiotics tested	0 (0)	0 (0)	0 (0)
Multi-resistant	1 (4)	7 (26)	8 (15)
BEN	17 (65)	16 (59)	33 (62)
AMC	2 (8)	7 (26)	9 (17)
FOX	2 (8)	7 (26)	9 (17)
SXT	0 (0)	0 (0)	0 (0)
CHL	1 (4)	1 (4)	2 (4)
DOX	3 (12)	1 (4)	4 (8)
ERY	6 (23)	8 (30)	14 (26)
CLI	0 (0)	7 (26)	7 (13)
AMI	2 (8)	2 (7)	4 (8)
GEN	2 (8)	0 (0)	2 (4)
CIP	0 (0)	4 (15)	4 (8)
NOR	0 (0)	4 (15)	4 (8)
Susceptible to all antibiotics tested	5 (19)	10 (37)	15 (28)

BEN: benzylpenicillin, AMC: amoxicillin with clavulanic acid, FOX: cefoxitin, SXT: trimethoprim/sulfamethoxazole, CHL: chloramphenicol, DOX: doxycycline, ERY: erythromycin, CLI: clindamycin, AMI: amikacin, GEN: gentamicin, CIP: ciprofloxacin, NOR: norfloxacin. Multi-resistant – resistant to more than three antibiotics.

kian origins were susceptible to the majority of antibiotics tested. Among methicillin-susceptible *S. aureus* (MSSA) strains, 18 (54%) demonstrated resistance only to penicillin/amoxicillin, two (6%) to penicillin and doxycycline, four (12%) to penicillin and erythromycin, and one to chloramphenicol and aminoglycosides. The susceptibility rate was high for both human and animal isolates. In both collections, however, the proportions of strains resistant to antimicrobials other than β -lactams were equal.

Enzymatic activity. In the *S. aureus* collection, 42 strains (79%) demonstrated β -hemolytic activity: 18 strains showed a double zone of hemolysis (Savini et al. 2013), and 24 strains presented a single zone of hemolysis; 11 strains (21%) did not demonstrate hemolysis (Fig. 1.1). Double-zone hemolysis occurred mostly in human strains ($n = 12$, 23%), and 17 animal strains showed regular β -hemolysis zone. Both human and animal populations showed similar number of β -hemolytic strains.

Fifty-two (98%) strains demonstrated proteolytic activity. Most of the strains showed low ($n = 21$, 40%) or moderate ($n = 23$, 43%) proteolysis. Seven (13%) strains, of which five were the human origin, showed high proteolytic activity. Most human ($n = 12$) and ani-

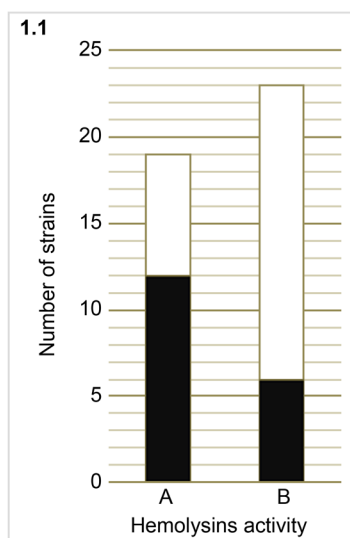
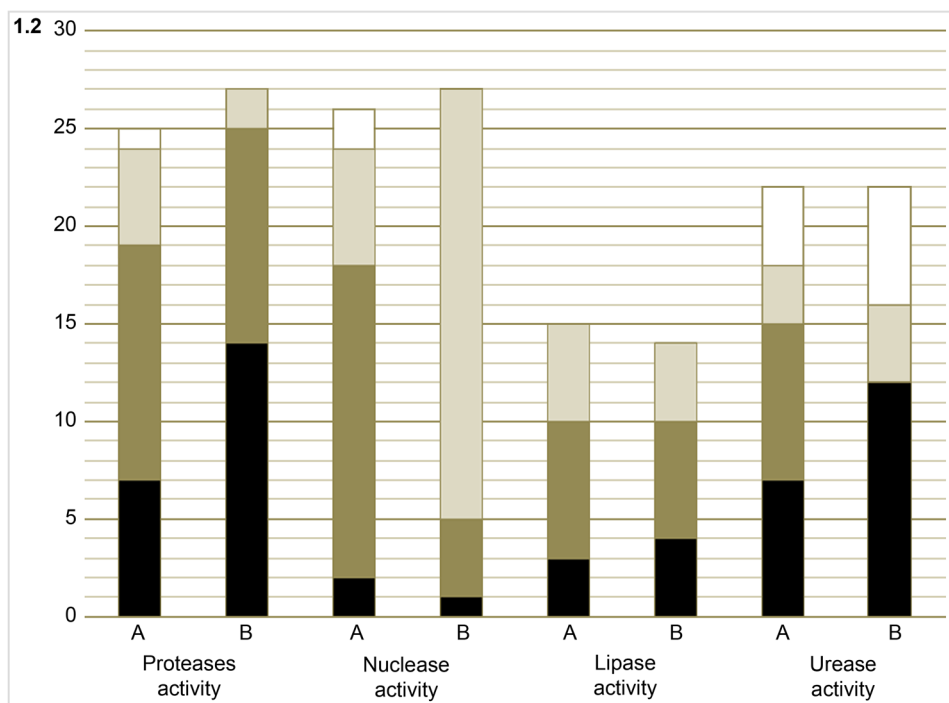


Fig. 1. Positive results of phenotypic tests.

Columns A: human strains, B: animal strains. 1.1. Total number of positive results for hemolysins activity. Black: double-zone β-hemolysis; white: single-zone β-hemolysis. 1.2. Total number of positive results for proteases, nuclease, lipase and urease activity. Black, low activity. Dark grey, moderate activity. Grey, high activity. White, very high activity.



mal ($n = 11$) strains showed moderate while 14 animal strains ($n = 14$) showed low proteolytic activity (Fig. 1.2).

All the strains showed nuclease activity, usually high ($n = 28$, 53%) or moderate ($n = 20$, 38%). The animal strains ($n = 22$; 81%) showed higher nuclease activity than human strains, which mostly exhibited moderate activity ($n = 16$; 62%).

Twenty-nine (55%) strains showed lipase activity, high activity was presented by nine strains (16%; five were human and four animal), moderate activity exhibited 13 strains (25%; seven were human and six animal), and low activity – seven strains (13%; three were human and four animal). Twenty-four (45%) strains did not exhibit any lipase activity. The human and animal bacteria collections showed an almost identical rate of lipase activity.

Forty-four (83%) strains demonstrated urease activity, but in most cases ($n = 19$, 36%) it was low. Six animal and four human strains showed very high urease activity ($n = 10$, 19%), three human and seven animal strains showed high activity ($n = 10$, 19%), and eight human strains showed moderate activity (15%). Nine strains (five from animals and four from humans; $n = 9$; 17%) did not exhibit urease activity. Human and animal strains did not differ in terms of urease activity. Figure 1 shows the results of phenotypic testing.

The *spa* typing. Based on the *spa* typing, 35 *S. aureus* strains were assigned into 20 *spa* types (Table III). Eighteen singletons were found, including the following *spa* types: t053, t091, t127, t150, t335, t723, t793, t3165, t4087, t5447, t14393, t14394, t14403, and t14404. Table III shows bacterial isolates assigned to *spa* types

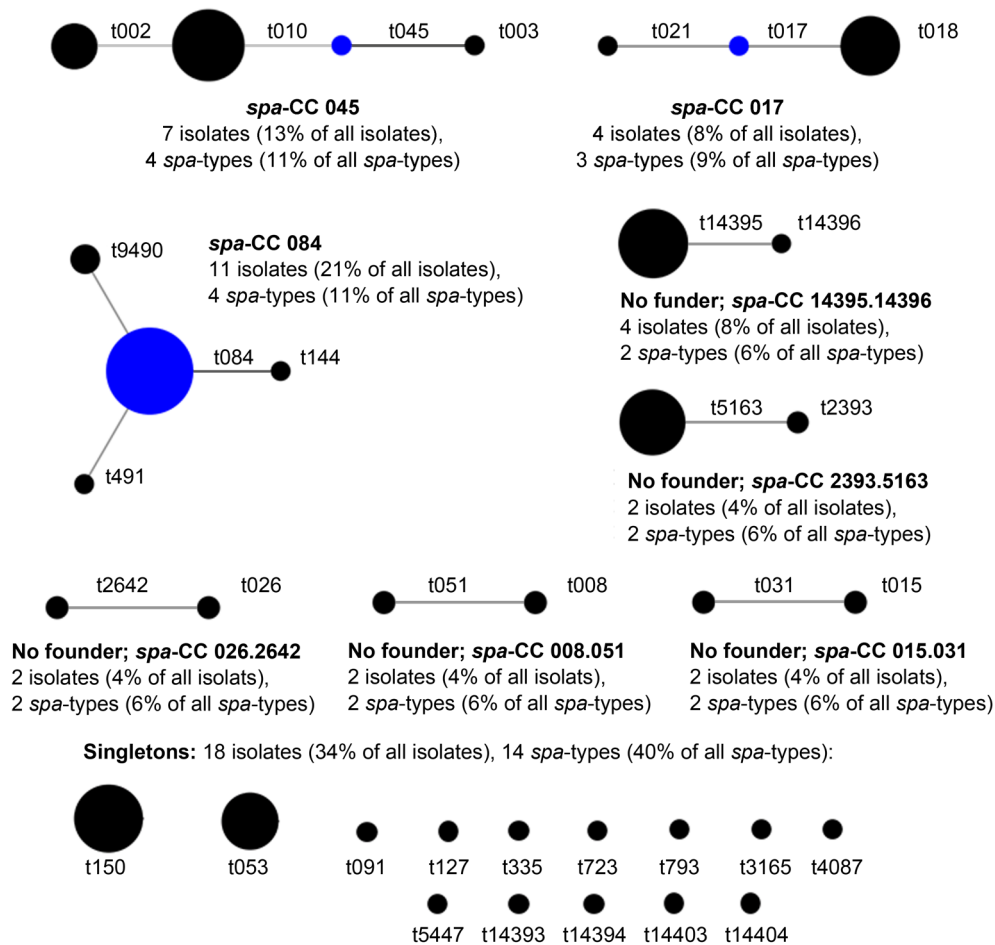


Fig. 2. The results of BURP analysis. The 20 *spa* types were assigned to proper clonal complexes. Eighteen singletons were found among the 53 strains analyzed. Black circles represent the *spa* types assigned to the proper clonal complexes, and the blue circles represent the ancestor within the clonal complex.

and clonal complexes together with their resistance and virulence genes. Figure 2 presents the results of BURP analysis, which demonstrates the clonal complexes based on the *spa* gene sequence similarities. Interestingly, *spa*-CC 045 was previously described as *spa*-CC 002 using Ridom StaphType software version 1.4 (Ridom GmbH, Würzburg, Germany), but a further update to version 2.1.1 resulted in changing the founder strain within the clonal complex.

The human strains belonged into more different *spa*-CCs than animal strains did. Most human strains ($n=10$) and only one animal strain were assigned to *spa*-CC 084. Interestingly, these ten human strains and one canine strain originated from the same city Gdańsk. Other *spa*-CCs of human strains were as follows: *spa*-CC 008.051 ($n=2$), *spa*-CC 017 ($n=3$), *spa*-CC 015.031 ($n=2$), and *spa*-CC 026.2642 ($n=2$). Among the animal strains, *spa*-CCs were also distinct, but there was a strong correlation between *spa*-CC and a place of strain isolation. The most numerous clonal complex was *spa*-CC 084 ($n=11$). The geographic *spa* type division was distinctly observed among the strains originat-

ing from bovine mastitis infections. Four bovine strains originating from Tomaszów Lubelski were assigned to one *spa*-CC 14395.14396, four strains originating from Łęczna to *spa*-type t150, and two strains originating from Łuków to *spa*-type t053. Among the bovine strains received from Košice (Slovakia), two *spa*-CCs were reported: *spa*-CC 045 ($n=4$) and *spa*-CC 2393.5163 ($n=3$). The former *spa*-CC was also identified in Świdnik ($n=3$).

Microarray testing. All the strains demonstrated positive results for the species markers: *gapA* (glyceraldehyde 3-phosphate dehydrogenase), *kata* (catalase), *coa* (coagulase), *spa* (*Staphylococcus* protein A), *sbi* (IgG-binding protein), *nuc* (thermostable nuclease), *fnbA* (fibronectin-binding protein A), *vraS* (sensor protein), *sarA* (staphylococcal accessory regulator A), *eno* (enolase), and *saeS* (histidine protein kinase). The presence of *nuc* gene was also confirmed phenotypically (Fig. 1). Five strains presented negative results, and two strains – ambiguous results for the 23S-rRNA gene, and they were probably caused by RNA contamination. The results for these strains were reliable because the

Table III
The results of the *spa* typing. Bacterial isolates were assigned to *spa* types and clonal complexes (CCs).

Strain number	<i>spa</i> types	Sequence type (ST)*	Clonal complex	Resistance and virulence genes
26	t008	ST-8, ST-427, ST-250, ST-254	<i>spa</i> -CC 008.051	Human strains: 26/23 Resistance: blaZ/I/R (+/-), <i>tetEfflux</i> , <i>fosB</i> Enterotoxins: sea (-/+), sed (+/-), seg (+/-), sej (+/-), ser (+/-) Enzymes within hemolysins: <i>sak</i> , <i>hla</i> , <i>hly</i> , lukM/luk F (+/-), <i>hlgA</i> , <i>lukD</i> , <i>lukE</i> , <i>lukX</i> , Proteases: <i>aur</i> , <i>splA</i> , <i>splB</i> , <i>splE</i> Adhesion and biofilm formation: <i>bbp</i> , <i>fnbB</i> , <i>map</i> , <i>sdrC</i> , <i>sdrD</i> , <i>sasG</i>
23	t051	ST-250, ST-254		
4	t015	ST-45	<i>spa</i> -CC 015.031	Human strains: 4/21 Resistance: mecA (+/-), blaZ/I/R , erm(A) (-/+), <i>tetEfflux</i> Enterotoxins: seb (-/+), <i>sec</i> , <i>seg</i> , sej (+/-), sel (-/+), <i>sei</i> , <i>sem</i> , <i>sen</i> , <i>seo</i> , <i>seu</i> , <i>egc-cluster</i> Enzymes within hemolysins: <i>sak</i> , <i>hla</i> , <i>hlgA</i> , <i>lukX</i> , Proteases: <i>aur</i> Adhesion and biofilm formation: <i>bbp</i> , <i>cna</i> , <i>fnbB</i> , map (+/-), <i>sdrC</i> , <i>sdrD</i>
21	t031	ST-45		
25	t017	nd	<i>spa</i> -CC 017	Human strains: 25/5/ animal strain: 31 Resistance: blaZ/I/R (-/+/+), erm(A) (-/+/-), tet(K) (-/+/-), <i>tetEfflux</i> , <i>fosB</i> Enterotoxins: <i>seg</i> , <i>sei</i> , <i>sem</i> , <i>sen</i> , <i>seo</i> , <i>seu</i> , <i>egc-cluster</i> Enzymes within hemolysins: sak (+/+/-), <i>hla</i> , <i>hly</i> , <i>hlgA</i> , lukX (+/-/-), lukX (-/-/+) Proteases: <i>aur</i> , <i>splE</i> Adhesion and biofilm formation: <i>bbp</i> , <i>cna</i> , fnbB (+/+/-), map (-/+/+), <i>sdrC</i> , <i>sdrD</i>
5	t021	ST-30, ST33, ST-55		
16, 31	t018	ST-30, ST36, ST-38		
15	t026	ST-45, ST-47	<i>spa</i> -CC 026.2642	Human strains: 15/2 Resistance: mecA (-/+), erm(C) (-/+), addD (-/+), mupR (-/+), <i>tetEfflux</i> , fosB (+/-), cat (-/+) Enterotoxins: <i>sec</i> , <i>seg</i> , <i>sei</i> , sel (+/-), <i>sem</i> , <i>sen</i> , <i>seo</i> , <i>seu</i> , <i>egc-cluster</i> Enzymes within hemolysins: <i>sak</i> , <i>hla</i> , <i>hlgA</i> , lukX (-/+) Proteases: <i>aur</i> Adhesion and biofilm formation: bbp (-/+), cna (+/-), <i>fnbB</i> , <i>map</i> , <i>sdrC</i> , sdrD (-/+)
2	t2642	nd		
50, 51, 52, 53	t14395	nd	<i>spa</i> -CC 14395.14396	Animal strains: 50/51/52/53 Resistance: <i>tetEfflux</i> , <i>fosB</i> Enterotoxins: <i>seg</i> , <i>sei</i> , <i>sem</i> , <i>sen</i> , <i>seo</i> , <i>seu</i> , <i>egc-cluster</i> Enzymes within hemolysins: <i>hla</i> , <i>hly</i> , <i>hlgA</i> , <i>lukX</i> Proteases: <i>aur</i> Adhesion and biofilm formation: <i>bbp</i> , <i>fnbB</i> , <i>map</i> , <i>sdrC</i> , sdrD (51, 53: +, 50, 52: -)
32, 34	t002	ST-5, ST-231	<i>spa</i> -CC 045	Animal strains: 32/34/33/35 Resistance: mecA , blaZ/I/R (strain no. 34: -), erm(A) (strains no. 34, 35: +), <i>addD</i> , <i>tetEfflux</i> , cat (strain no. 35: +), <i>fosB</i> Enterotoxins: sea (strains no. 33, 35: +), sed (strain no. 34: -), <i>seg</i> , <i>sei</i> , sej (strain no. 34: -), <i>sem</i> , <i>sen</i> , <i>seo</i> , ser (strain no. 34: -), <i>seu</i> , <i>egc-cluster</i> Enzymes within hemolysins: <i>sak</i> , <i>hla</i> , <i>hly</i> , <i>hlgA</i> , <i>lukD</i> , <i>lukE</i> , <i>lukX</i> Proteases: <i>aur</i> , <i>splA</i> , <i>splB</i> Adhesion and biofilm formation: <i>bbp</i> , fnbB (strains no. 33, 35: +), <i>map</i> , <i>sdrC</i> , <i>sdrD</i> , <i>sasG</i>
33	t003	ST-5, ST-225		
35	t045	ST-5, ST-225		
47, 48, 49	t010	ST-5		Animal strains: 47/48/49 Resistance: blaZ/I/R , <i>tetEfflux</i> , <i>fosB</i> Enterotoxins: <i>seg</i> , <i>sei</i> , <i>sem</i> , <i>sen</i> , <i>seo</i> , <i>seu</i> , <i>egc-cluster</i> Enzymes within hemolysins: <i>hla</i> , <i>hly</i> , <i>hlgA</i> , <i>lukD</i> , <i>lukE</i> , <i>lukX</i> Proteases: <i>aur</i> , <i>splA</i> , <i>splB</i> Adhesion and biofilm formation: <i>bbp</i> , <i>map</i> , <i>sdrC</i> , <i>sdrD</i> , <i>sasG</i>

Table III. Continued

Strain number	<i>spa</i> types	Sequence type (ST)*	Clonal complex	Resistance and virulence genes
1, 7, 10, 11, 12, 18, 19	t084	ST-15, ST-18	<i>spa</i> -CC084	Human strains: 1/7/10/11/12/18/19/8/20 Animal strain: 28 Resistance: <i>blaZ/I/R</i> (strains no. 12, 18: -), <i>tet(K)</i> (strains no. 7, 12, 19, 20: +), <i>tetEfflux</i> , <i>fosB</i> (strain no. 7: -) Enterotoxins: - Enzymes within hemolysins: <i>sak</i> (strain no. 28: +), <i>hla</i> (strains no. 10, 28: -), <i>lukM/lukF</i> (strains no. 19, 20: +), <i>hlgA</i> (strains no. 10, 28: -), <i>lukD</i> (strain no. 10: -), <i>lukE</i> (strains no. 18, 19: +), <i>lukF</i> (strain no. 20: +), <i>lukX</i> (strains no. 18, 19, 20: +) Proteases: <i>aur</i> (strains no. 10, 11, 28: -), <i>splA</i> , <i>splB</i> , <i>splE</i> (strains no. 10, 28: -) Adhesion and biofilm formation: <i>bbp</i> (strains no. 10, 8: -), <i>fnbB</i> (strain no. 11: -), <i>map</i> , <i>sdrC</i> , <i>sdrD</i> , <i>sasG</i>
8,9	t9490	nd		
28	t144	nd		
20	t491	nd		
38	t2393	nd	<i>spa</i> -CC 2393.5163	Animal strains: 38/36/37 Resistance: <i>mecA</i> , <i>blaZ/I/R</i> , <i>erm(C)</i> , <i>tet(K)</i> , <i>tetEfflux</i> Enterotoxins: <i>sea</i> Enzymes within Hemolysins: <i>sak</i> , <i>hla</i> , <i>hnb</i> , <i>hlgA</i> , <i>lukD</i> , <i>lukE</i> , <i>lukX</i> Proteases: <i>aur</i> , <i>splA</i> , <i>splB</i> Adhesion and biofilm formation: <i>bbp</i> , <i>fnbB</i> , <i>map</i> , <i>sdrC</i> , <i>sdrD</i> , <i>sasG</i>
36, 37	t5163	nd		

* The proposed sequence type retrieved from Ridom SpaServer. Genes exhibited by all the analyzed strains: hemolysins: *hld*, *luk F*, *lukS*, *lukY*; proteases: *sspA*, *sspB*, *sspP*; adhesion and biofilm formation: *icaA*, *icaC*, *icaD*, *clfA*, *clfB*, *ebh*, *eno*, *fib*, *ebpS*, *fnbA*, *vwb*.

number of ambiguous results did not exceed 3%. All isolates but one (n = 52; 98%) carried the *tetEfflux* gene, which encodes tetracycline efflux protein, and the *fosB* gene (n = 43; 81%), which confers resistance to fosfomicin and bleomycin. In 32 strains (17 from humans and 15 from animals), the genes involved in penicillin resistance by the production of β -lactamase (*blaZ*, *blaI*, and *blaR*) were detected; among these strains, eight were MRSA strains. Strains carrying the other resistance genes did not exceed 17%. The most prevalent resistance patterns were: *tetEfflux*, *fosB*, and *blaZ/I/R*, *tetEfflux*, *fosB* (Table III). The first one was carried by strains belonged to *spa*-CC 084 (n = 6; t084, t144, t9490), *spa*-CC 045 (n = 3; t010), and *spa*-CC 008.015 (n = 1, t008). Strains with *spa* type t010 were the only MSSA strains from the *spa*-CC 045. The other strain from *spa*-CC 008.015 (no. 23; t051), and two strains from *spa*-CC 084 (no. 9, 18), harbored the second most frequent pattern. The same resistance genes were present also in *spa*-CC 017 (n = 1; t021), and all of the strains from *spa*-CC 14395.14396. The animal strains of *spa*-CC 2393.5163 carried a unique resistance pattern among other strains from the collections (Table III).

These MRSA strains carried *mecA* or *mecR*, and associated with the SCC*mec* element genes for glicerophosphoryl-diester-phosphodiesterase (*upgQ*), and cassette chromosome recombinases (*ccrA-2*, *ccrB-2*). Four of these strains carried also potassium-transporting ATPases (*kdp* operon); a DNA-binding response regu-

lator; the *mecI* gene; and *xyIR*, encoding a pseudogene of xylose repressor. The most MRSA strains belonged to *spa*-CC 045 (n = 4), and *spa*-CC 2393.5163 (n = 3). Two strains carried the *mecA* gene and they were *blaZ/I/R* negative. One of them exhibited *spa* type t002 (*spa*-CC 045), and the other belonged to *spa* type t2642 (*spa*-CC 026.2642) (Table III).

All the 53 isolates harbored the δ -hemolysin gene, components of other hemolysins, and the leucocidin D component (*lukF/S*, *lukY*, *hl*, *hld*, *hldIII*). All but three strains carried also the gene for α -hemolysin (*hlgA*, n = 50; 94%); the β -hemolysin gene (*hnb*, n = 35, 66%); and the staphylokinase gene (*sak*, n = 24; 45%). The absence of both - *hnb* and *sak* genes was a characteristic feature of P-like pA+ genotype of the strains in comparison to other human strains which carried *hnb* (n = 11) and *sak* (n = 12) gene in more than 70%. Lack of the *sak* genes were observed also in animal stains from t010, and t14395. On the other hand, the *hnb* gene was absent in human *spa*-CCs 026.2642 and 015.031. Human P-like pA+ strains were in majority grouped in *spa*-CC 084 (t084, t9490, t491), and two of them were classified as singletons (t335, t793). The characteristic property of these stains was also lack of enterotoxins genes.

Fifteen enterotoxin genes frequently occurred in human and animal strains from most regions, including *sea* (n = 11; 21%), *seb* (n = 2; 4%), *sec* (n = 3; 6%) *sed* (n = 5; 9%), *seg* (n = 25; 47%), *seh* (n = 1; 2%), *sei* (n = 24; 45%), *sej* (n = 5; 9%), *sel* (n = 3; 6%), *selm* (n = 24; 45%),

seln (n = 24; 45%), *selo* (n = 24; 45%), *ser* (n = 5; 9%), *selu* (n = 24; 45%), and *ego*-cluster (n = 24, 45%), which encodes enterotoxins *seg*, *sei*, *selm*, *seln*, *selo*, and *selu*. Although, strains from *spa* types t008, t2393, and t5163 carried only enterotoxin A gene (*sea*).

All the 53 isolates harbored the V8-protease gene (*sspA*) and staphopain A and B (*sspP*, *sspB*), and 47 strains (89%) carried the aureolysin gene (*aur*). Genes for serine proteases also were detected frequently: 20 human and 21 animal strains (n = 41; 77%) carried the *splA* and *splB* genes. Additionally, 10 animal and 20 human strains (n = 30; 57%) carried the *splE* gene, encoding serine protease E.

Adhesin and biofilm formation genes frequently occurred in the strains analyzed. All of them exhibited following genes: *icaA/C* (intercellular adhesion protein A/C), *icaD* (biofilm PIA synthesis protein D), *clfA/B* (clumping factor A/B), *ebh/ebpS* (cell wall-associated fibronectin-binding proteins), *eno* (enolase), *fib/fnbA* (fibrinogen binding proteins), and *vwb* (Willebrand factor). Strains from *spa*-CC 015.031, and *spa*-CC 017 carried *cna* (collagen-binding adhesin) genes, which differentiated them from other strains from the collections.

All the 53 isolates harbored the clumping factor genes (*clfA*, *clfB*), cell wall-associated fibronectin-binding protein gene (*ebh*, *ebpS*), enolase gene (*eno*), fibrinogen-binding protein (*fib*), fibronectin-binding protein (*fnb*), immunodominant antigen B (*isaB*), heme/transferrin-binding protein (*isdA*), putative transporter protein (*ImrP*), and hyaluronate lyase A1 (*hysA1*). The capsule-5 encoding gene (*capsule 5*) occurred mostly in animal strains while the capsule-8 encoding gene's (*capsule 8*) rate was higher in human strains.

Discussion

The research presented here aimed to characterize the properties of isolates of two particular collections of human and livestock *S. aureus* strains, using phenotypic and genetic methods, and to assess the compatibility of results between microarray and phenotypic manifestations. The investigation focused on the comparison of human and animal strains because studies have shown that animals are a reservoir of pathogens for people (Petinaki and Spiliopoulou 2012). Therefore, dogs have been reported as hosts for MRSA strains, genetically closely related to human strains (Strommenger et al. 2006; Nienhoff et al. 2009).

The next group of animal strains originated from cows. Transmission of bovine strains from cows and cow milk to people and the other way round has been reported as a result of close contact in the dairy environment (Schmidt et al. 2017). Other authors reported a high share of nasal MRSA colonization among vol-

unteers working in farms. However, only 6% MRSA contaminations survive more than 48 hours (Angen et al. 2017). It has been shown that high persistence of multi-resistant isolates increases the importance of monitoring of intra-species strains transmission (Petinaki and Spiliopoulou 2012).

Another way of bovine strains transmission is the contamination of dairy products (Kummel et al. 2016; Nunes and Caldas 2017), and as a result, foodborne infections in human. There was also shown that laboratory investigation detected *S. aureus* in stool samples of 15 patients who had gastrointestinal symptoms, and the strains isolated harbored the *seg*, *sei*, *selm*, *seln*, *selo*, and *selu* genes (Umeda et al. 2017). These results provided the convincing evidence of potential foodborne outbreaks caused by *S. aureus* strains, underlining the significance of bovine strain monitoring to human health prevention.

It was epidemiologically crucial to estimate the resistance to antibiotics for both human and animal pathogens, although the collected strains exhibited low rates of resistance. The low number of MRSA likely resulted from the origin of strains, because all the human strains were received from outdoor patients, and from canine or bovine strains usually presented methicillin-susceptible profiles (Kronenberg et al. 2011; Jagielski et al. 2014). The human and animal collections did not differ in resistance profiles, despite methicillin resistance, which was higher in animal strains.

Detection of the appropriate genes with microarrays also tested all the strains' antibiotic resistance. MRSA strains (n = 9, 17%) were correctly identified by phenotypic antibiotic tests because all of these strains showed the presence of the *mecA* gene. Other genetic traits of antibiotic resistance differed from these phenotypically observed. For the *blaZ/II/R* genes, such differences occurred for three strains (two from humans and one from an animal). Two of them did not carry *blaZ/II/R* genes, but phenotyping showed their resistance to penicillin, and one of them presented an opposite correlation (there was no phenotypic resistance and the appropriate genes were present). The second situation probably resulted from the phenotypic method drawback, so the presence of *blaZ/II/R* genes confirmed by microarrays was recognized as a correct result. For some strains the antibiotic resistance genes presence did not correlate with the phenotypic manifestation: for chloramphenicol (n = 2), doxycycline (n = 6), erythromycin (n = 7), amikacin (n = 3), and gentamicin (n = 7). These data partially agree with results by others in which the occurrence rate of resistance genes was higher than the corresponding phenotypic manifestation of resistance (Li et al. 2015). In the present research, the resistance to antibiotics detected by phenotypic methods only, without any confirmation of the presence of resistance

genes, was possibly a result of mutations or a novel or not tested resistance gene presence.

The next approach was to compare the phenotypic profiles to genetic ones, and for 23 isolates they differed. The *hla* gene was detected in 51 (96%) and *hly* gene in 35 (66%) strains. These results suggest that hemolysin genes are widespread in staphylococcal populations, even if they do not show any phenotypic manifestation. Thus, there is a strong need to introduce molecular analyses into the hospital and veterinary laboratories, without which many strains may go unnoticed during standard laboratory examinations of patients and ill animals (Moraveji et al. 2014). However, nuclease and protease phenotypic testing gave similar results to molecular analysis.

Furthermore, the human and animal strains were compared based on the microarray patterns, and as it was shown in other investigation, this was the most discriminatory method for strain characterization (Kosecka-Strojek et al. 2016). No specific feature clearly differentiated them when based on the microarray results that concerned resistance genes, virulence genes, adhesion and biofilm formation genes, and immune evasion assay. However, bovine mastitis strains from Poland harbored less resistance and virulence genes than human strains did; this result was in agreement with the recent studies by Schmidt et al. (2017). Interestingly, the bovine strains from Slovakia showed multi-resistant profile. Microarray patterns also demonstrated the close similarity between strains originated from the same geographical places of isolation. However, the human P-like pA+ strains originated from Gdańsk showed slightly different microarray patterns than other strains. The reports have shown that the characteristic property of the P-like pA+ strains was lack of *hly* and *sak* genes, and the present study confirmed this thesis (Piechowicz and Garbacz 2016). Therefore, these strains did not contain any enterotoxin genes in opposite to other human strains of the collections among which most the strains (67%) included genes of *egc*-cluster. Other investigation confirmed a high number of enterotoxin genes ($n=90$, 56%) of the strains from Kraków (Ilczyszyn et al. 2016). Interestingly, animal strains from Gdańsk showed a low level of those genes ($n=1$). This suggests that the P-like pA+ strains are less virulent than other human strains and that virulence is more comparable to animal strains. As widely known, colonization of various hosts by staphylococci requires adaptive changes, which in turn can be reflected by the acquisition of new genetic characteristics. Against the above data, it cannot be excluded that the P-like pA+ isolates described hereby are animal strains that are at a certain stage of the evolutionary process aimed at transforming them into human strains.

The human and animal strains were also compared

based on the *spa* typing, and both collections had different *spa* types and *spa*-CCs. The only exception was *spa*-CC 084, containing ten human strains and an animal strain but all ten strains originated from Gdańsk. Among both human and animal strains, *spa*-CC strongly correlated with the place of strain isolation. Only one *spa*-CC 045 was identified in Świdnik (Poland) and Košice (Slovakia), but according to Ridom SpaServer (www.ridom.de), it is one of the most common *spa*-CCs, with a global frequency of 6.03%. Our study showed that similarities between strains were more due to their geographic origin than due to the host species from which they originated. According to Ridom SpaServer (www.ridom.de) the most frequent *spa*-types in the world are t032, t003, t002, and t008. Asadollahi et al. (2018) have analyzed the most prevalent *spa*-types occurred human strains in particular continents and countries. Authors presented that the most prevalent *spa*-types in Europe are t008, t002, and t003, while in Poland the most frequent are *spa*-types are t003, t037, t053, t127, and t021. In contrast, in our study, the majority of human strains belonged to t084, and t9490 of *spa*-CC084.

The animal strains mostly belonged to t14395, and t010, and bovine strains were grouped. According to Ridom SpaServer (www.ridom.de) the *spa* type t010 belongs to ST5, whereas in Europe the most frequent are ST97, ST126, ST133, ST151, ST497, and ST771 (Holmes and Zadoks 2011).

Conclusions

The human and animal *S. aureus* collections were characterized by the phenotypic and molecular methods. The results obtained showed that phenotypically demonstrated resistance profiles and virulence factors were comparable to microarray's profiling.

Analysis of human and animal strains did not demonstrate any specific marker clearly differentiating them in the microarray results. However, human P-like pA+ strains were characterized by lack of *hly*, *sak*, and enterotoxin genes in comparison to other human strains. Moreover, the bovine mastitis strains from Poland showed sensitivity to almost all antibiotics used in the project in opposite to the Slovakian ones that demonstrated a broad range of antibiotic resistance.

Our study showed that similarities between strains were more due to their geographic origin than due to the host species from which they were isolated.

ORCID

Jacek Międzobrodzki 0000-0003-4252-880X
Maja Kosecka-Strojek 0000-0001-8337-6975

Acknowledgements

The authors thank to Dr. Jarosław Król from Veterinary Department of the University of Wrocław, and Dr. Elżbieta Puacz from National Chamber of Medical Laboratory Specialists (Warszawa, Poland) for providing bacterial isolates to the presented project.

Founding

This project was partly financed by funds granted by the National Science Centre (NCN, Poland) on the basis of the decision No. UMO-2016/21/N/NZ6/00981 (to M.K.S.)

This study was partly founded by Slovak grant No. APVV-16-0171 (to V.K.).

Faculty of Biochemistry, Biophysics, and Biotechnology of the Jagiellonian University is a part of a Leading National Research Centre (KNOW), which is supported by the Ministry of Science and Higher Education in Poland.

Author contributions

M.K.S. and J.M. designed the project. J.B., A.K., K.G., L.P., V.K., V.S. and J.M. provided the strains and their data. K.L.L., M.K.S., J.B. performed the experiments. All authors interpreted the data. K.L.L., M.K.S. and J.M. composed the manuscript. All authors reviewed the manuscript.

Ethical approval

This article does not contain any studies with human participants or animals performed by any of the authors.

Conflict of interest

The authors do not report any financial or personal connections with other persons or organizations, which might negatively affect the contents of this publication and/or claim authorship rights to this publication.

Literature

- Aires-de-Sousa M, Boye K, de Lencastre H, Deplano A, Enright MC, Etienne J, Friedrich A, Harmsen D, Holmes A, Huijsdens XW, et al. High interlaboratory reproducibility of DNA sequence-based typing of bacteria in a multicenter study. *J Clin Microbiol.* 2006; 44(2):619–621. doi:10.1128/JCM.44.2.619-621.2006 Medline
- Angen Ø, Feld L, Larsen J, Rostgaard K, Skov R, Madsen AM, Larsen AR. Transmission of methicillin-resistant *Staphylococcus aureus* to human volunteers visiting a swine farm. *Appl Environ Microbiol.* 2017;83(23):e01489–17. doi:10.1128/AEM.01489-17 Medline
- Asadollahi P, Farahani NN, Mirzaii M, Khoramrooz SS, van Belkum A, Asadollahi K, Dadashi M, Darban-Sarokhalil D. Distribution of the most prevalent *Spa* types among clinical isolates of methicillin-resistant and -susceptible *Staphylococcus aureus* around the World: A review. *Front Microbiol.* 2018;9:163. doi:10.3389/fmicb.2018.00163 Medline
- Black WA, Hodgson R, McKechnie A. Evaluation of three methods using deoxyribonuclease production as a screening test for *Serratia marcescens*. *J Clin Pathol.* 1971;24(4):313–316. doi:10.1136/jcp.24.4.313 Medline
- Cadieux B, Vijayakumaran V, Bernardis MA, McGavin MJ, Heinrichs DE. Role of lipase from community-associated methicillin-resistant *Staphylococcus aureus* strain USA300 in hydrolyzing triglycerides into growth-inhibitory free fatty acids. *J Bacteriol.* 2014; 196(23):4044–4056. doi:10.1128/JB.02044-14 Medline
- dos Santos Rodrigues JB, Pinto TS, De Oliveira CP, De Sousa Freitas FI, Vieira Pereira MDS, De Souza EL, De Siqueira-Júnior JP. Lipolytic activity of *Staphylococcus aureus* from human wounds, animals, foods, and food-contact surfaces in Brazil. *J Infect Dev Ctries.* 2014;8(08):1055–1058. doi:10.3855/jidc.3697 Medline
- ECDC. Antimicrobial resistance surveillance in Europe. Annual report of the European Antimicrobial Resistance Surveillance Network [Internet]. Solna (Sweden): European Centre for Disease Prevention and Control; [cited 2017 Jan 30]. 2017. Available from: <https://ecdc.europa.eu/sites/portal/files/media/en/publications/Publications/antimicrobial-resistance-europe-2015.pdf>
- EUCAST. Disk diffusion method for antimicrobial susceptibility testing [Internet]. Basel (Switzerland): European Committee on Antimicrobial Susceptibility Testing; [cited 2017 Jan 30]. 2017. Available from: http://www.eucast.org/fileadmin/src/media/PDFs/EUCAST_files/Disk_test_documents/2017_manuals/Manual_v_6.0_EUCAST_Disk_Test_final.pdf
- Holmes MA, Zadoks RN. Methicillin resistant *S. aureus* in human and bovine mastitis. *J Mammary Gland Biol Neoplasia.* 2011;16(4): 373–382. doi:10.1007/s10911-011-9237-x Medline
- Kmeť V, Čuvalová A, Stanko M. Small mammals as sentinels of antimicrobial-resistant staphylococci. *Folia Microbiol (Praha).* 2018;63(5):665–668. doi:10.1007/s12223-018-0594-3 Medline
- Kosecka-Strojek M, Ilcyszyn WM, Buda A, Polakowska K, Murzyn K, Panz T, Bialecka A, Kasproicz A, Jakubczak A, Krol J, et al. Multiple-locus variable-number tandem repeat fingerprinting as a method for rapid and cost-effective typing of animal-associated *Staphylococcus aureus* strains from lineages other than sequence type 398. *J Med Microbiol.* 2016;65(12):1494–1504. doi:10.1099/jmm.0.000378 Medline
- Kronenberg A, Koenig S, Droz S, Mühlemann K. Active surveillance of antibiotic resistance prevalence in urinary tract and skin infections in the outpatient setting. *Clin Microbiol Infect.* 2011; 17(12):1845–1851. doi:10.1111/j.1469-0691.2011.03519.x Medline
- Kümmel J, Stessl B, Gonano M, Walcher G, Bereuter O, Fricker M, Grunert T, Wagner M, Ehling-Schulz M. *Staphylococcus aureus* entrance into the dairy chain: tracking *S. aureus* from dairy cow to cheese. *Front Microbiol.* 2016;7:1603. doi:10.3389/fmicb.2016.01603 Medline
- Li L, Feng W, Zhang Z, Xue H, Zhao X. Macrolide-lincosamide-streptogramin resistance phenotypes and genotypes of coagulase-positive *Staphylococcus aureus* and coagulase-negative staphylococcal isolates from bovine mastitis. *BMC Vet Res.* 2015;11(1):168. doi:10.1186/s12917-015-0492-8 Medline
- Malachowa N, Kohler PL, Schlievert PM, Chuang ON, Dunny GM, Kobayashi SD, Miedzobrodzki J, Bohach GA, Seo KS. Characterization of a *Staphylococcus aureus* surface virulence factor that promotes resistance to oxidative killing and infectious endocarditis. *Infect Immun.* 2011;79(1):342–352. doi:10.1128/IAI.00736-10 Medline
- Miedzobrodzki J, Kaszycki P, Bialecka A, Kasproicz A. Proteolytic activity of *Staphylococcus aureus* strains isolated from the colonized skin of patients with acute-phase atopic dermatitis. *Eur J Clin Microbiol Infect Dis.* 2002;21(4):269–276. doi:10.1007/s10096-002-0706-4 Medline
- Monecke S, Slickers P, Ehrlich R. Assignment of *Staphylococcus aureus* isolates to clonal complexes based on microarray analysis and pattern recognition. *FEMS Immunol Med Microbiol.* 2008; 53(2):237–251. doi:10.1111/j.1574-695X.2008.00426.x Medline
- Moraveji Z, Tabatabaei M, Shirzad Aski H, Khoshbakht R. Characterization of hemolysins of *Staphylococcus* strains isolated from human and bovine, southern Iran. *Iran J Vet Res.* 2014;15(4): 326–330. Medline
- Nienhoff U, Kadlec K, Chaberny IF, Verspohl J, Gerlach GF, Schwarz S, Simon D, Nolte I. Transmission of methicillin-resistant *Staphylococcus aureus* strains between humans and dogs: two case reports. *J Antimicrob Chemother.* 2009;64(3):660–662. doi:10.1093/jac/dkp243 Medline

- Nunes MM, Caldas ED. preliminary quantitative microbial risk assessment for *Staphylococcus* enterotoxins in fresh Minas cheese, a popular food in Brazil. *Food Control*. 2017;73:524–531. doi:10.1016/j.foodcont.2016.08.046
- O’Gara JP. Into the storm: chasing the opportunistic pathogen *Staphylococcus aureus* from skin colonisation to life-threatening infections. *Environ Microbiol*. 2017;19(10):3823–3833. doi:10.1111/1462-2920.13833 Medline
- Otto M. *Staphylococcus aureus* toxins. *Curr Opin Microbiol*. 2014;17:32–37. doi:10.1016/j.mib.2013.11.004 Medline
- Paharik AE, Horswill AR. The staphylococcal biofilm: adhesins, regulation, and host response. *Microbiol Spectr*. 2016;4(2). doi:10.1128/microbiolspec.VMBF-0022-2015 Medline
- Petinaki E, Spiliopoulou I. Methicillin-resistant *Staphylococcus aureus* among companion and food-chain animals: impact of human contacts. *Clin Microbiol Infect*. 2012;18(7):626–634. doi:10.1111/j.1469-0691.2012.03881.x Medline
- Piechowicz L, Garbacz K. Poultry-like pA+ biotype of *Staphylococcus aureus* CC346/084 clone in human population. *Curr Microbiol*. 2016;73(1):124–131. doi:10.1007/s00284-016-1033-9 Medline
- Posteraro B, Posteraro P, Sanguinetti M. *Helicobacter pylori*. In: Tang YW, Sussman M, Liu D, Poxton I, Schwartzman J, editors. *Molecular Medical Microbiology*, 2nd Edition. Amsterdam (Netherlands): Elsevier Science. 2015; p. 1237–1258.
- Puacz E, Ilczyszyn WM, Kosecka M, Buda A, Dudziak W, Polakowska K, Panz T, Białecka A, Kasproicz A, Lisowski A, et al. Clustering of *Staphylococcus aureus* bovine mastitis strains from regions of Central-Eastern Poland based on their biochemical and genetic characteristics. *Pol J Vet Sci*. 2015;18(2):333–342. doi:10.1515/pjvs-2015-0043 Medline
- Sabat AJ, Wladyka B, Kosowska-Shick K, Grundmann H, van Dijl J, Kowal J, Appelbaum PC, Dubin A, Hryniewicz W. Polymorphism, genetic exchange and intragenic recombination of the aureolysin gene among *Staphylococcus aureus* strains. *BMC Microbiol*. 2008;8(1):129. doi:10.1186/1471-2180-8-129 Medline
- Savini V, Barbarini D, Polakowska K, Gherardi G, Białecka A, Kasproicz A, Polilli E, Marrollo R, Di Bonaventura G, Fazii P, et al. Methicillin-resistant *Staphylococcus pseudintermedius* infection in a bone marrow transplant recipient. *J Clin Microbiol*. 2013;51(5):1636–1638. doi:10.1128/JCM.03310-12 Medline
- Schmidt T, Kock MM, Ehlers MM. Molecular characterization of *Staphylococcus aureus* isolated from bovine mastitis and close human contacts in South African dairy herds: genetic diversity and inter-species host transmission. *Front Microbiol*. 2017;8:511. doi:10.3389/fmicb.2017.00511 Medline
- Seilie ES, Bubeck Wardenburg J. *Staphylococcus aureus* pore-forming toxins: the interface of pathogen and host complexity. *Semin Cell Dev Biol*. 2017;72:101–116. doi:10.1016/j.semcdb.2017.04.003 Medline
- Strommenger B, Kehrenberg C, Kettlitz C, Cuny C, Verspohl J, Witte W, Schwarz S. Molecular characterization of methicillin-resistant *Staphylococcus aureus* strains from pet animals and their relationship to human isolates. *J Antimicrob Chemother*. 2006;57(3):461–465. doi:10.1093/jac/dki471 Medline
- Umeda K, Nakamura H, Yamamoto K, Nishina N, Yasufuku K, Hirai Y, Hirayama T, Goto K, Hase A, Ogasawara J. Molecular and epidemiological characterization of staphylococcal foodborne outbreak of *Staphylococcus aureus* harboring *seg*, *sei*, *sem*, *sen*, *seo*, and *selu* genes without production of classical enterotoxins. *Int J Food Microbiol*. 2017;256:30–35. doi:10.1016/j.ijfoodmicro.2017.05.023 Medline
- Vandecastelaere I, Van Nieuwerburgh F, Deforce D, Coenye T. Metabolic activity, urease production, antibiotic resistance and virulence in dual species biofilms of *Staphylococcus epidermidis* and *Staphylococcus aureus*. *PLoS One*. 2017;12(3):e0172700. doi:10.1371/journal.pone.0172700 Medline
- Zawrotniak M, Rapala-Kozik M. Neutrophil extracellular traps (NETs) – formation and implications. *Acta Biochim Pol*. 2013;60(3):277–284. Medline
- Zhang X, Hu X, Rao X. Apoptosis induced by *Staphylococcus aureus* toxins. *Microbiol Res*. 2017;205:19–24. doi:10.1016/j.micres.2017.08.006 Medline
- Żabicka D, Hryniewicz W. Rekomendacje doboru testów do oznaczania wrażliwości bakterii na antybiotyki i chemioterapeutyki. Oznaczanie wrażliwości ziarniaków Gram-dodatnich z rodzaju *Staphylococcus* spp. [Internet]. Warsaw (Poland): Krajowy Ośrodek Referencyjny ds. Lekowrażliwości Drobnoustrojów; [cited 2018 Sep 24]. 2009. Available from: http://www.korld.edu.pl/pdf/Rekomendacje_2010_gronkowce.pdf

The Influence of Temperature and Nitrogen Source on Cellulolytic Potential of Microbiota Isolated from Natural Environment

AGNIESZKA WITA¹, WOJCIECH BIAŁAS¹, RADOSŁAW WILK², KATARZYNA SZYCHOWSKA²
and KATARZYNA CZACZYK^{1*}

¹Department of Biotechnology and Food Microbiology, Poznań University of Life Sciences, Poland

²INTERMAG Sp. z o.o., Olkusz, Poland

Submitted 2 October 2018, revised 19 November 2018, accepted 7 December 2018

Abstract

Bacteria from the genus *Bacillus* are a rich source of commercial enzymes, including amylases, proteases, cellulases, glucose isomerase, and pullulanase. Cellulases account for 15% of the global market of industrial enzymes; thus, new microorganisms producing cellulases in a higher concentration and new ingredients, which can enhance the level of enzyme synthesis, are still needed. Many of cellulose-degrading microorganisms have been isolated so far and characterized in various regions of the world. In this study, we were looking for the bacteria isolated from the natural environment with the high cellulolytic potential, which could be used as components of a biopreparation to accelerate decomposition of postharvest leftovers in agriculture. The 214 bacterial strains were isolated from environmental samples rich in cellulose and their ability to synthesize cellulases were examined using the diffusion method. Six strains, which have the highest diameter of clearing zone both for biomass and supernatant, were selected for identification. Optimization of biosynthesis of the cellulose-degrading enzymes indicated that optimal temperature of this process fluctuated in the range of 21–42°C (depending on the strain and carbon source). The highest cellulolytic activity was observed for the isolates designed as 4/7 (identified as *Bacillus subtilis*) and 4/18 (identified as *Bacillus licheniformis*) in a temperature of 32°C. With the use of a desirability function methodology, the optimal medium composition to achieve a simple, cost-efficient process of cellulases production was developed for both strains. These experiments show that microorganisms isolated from natural environmental samples have unique properties and potential for commercial applications (e.g. for biopreparations production).

Key words: *Bacillus* spp., cellulose-degrading microorganisms, nitrogen source

Introduction

Cellulose is the most abundant organic material in the biosphere and dominating waste in agriculture (Shrestha et al. 2017). One of the agriculture by-products with a large cellulose content is cereal straws. Wheat, rye, barley, oats, and oilseed rape are the most popular straws in Poland. Some of them can be collected and used for various applications as bedding or compost production or a food supplement. However, much simpler for farmers and much better for soil is to leave the straw residues to increase the content of available nutrients and humus in the soil. Microorganisms play the important role in cellulose degrading in the natural environment. They evolved different mechanisms to degrade cellulose, lignocellulose, and hemicelluloses,

mostly based on producing and secreting a combination of synergistically active enzymes (hydrolytic glycoside hydrolases, carbohydrate esterases, polysaccharide lyases and cellodextrin phosphorylases) (Bomble et al. 2017). Microorganisms with such activity often occur in niches rich in cellulose. Generally, that microorganisms isolated from the natural environment have better activity than these from laboratory collections and may be used as a component of biopreparations (Pietraszek and Walczak 2014).

Nowadays agriculture is based on the economy, process efficiency, and ecology. The balance between those factors is possible only in the case of simultaneously increasing of the crops productivity and decrease of costs. One of the most important issues in ecological agriculture is the use of microbial biopreparations for

* Corresponding author: K. Czaczyk, Department of Biotechnology and Food Microbiology, Poznań University of Life Sciences, Poznań, Poland; e-mail: katarzyna.czaczyk@up.poznan.pl

© 2019 Agnieszka Wita et al.

This work is licensed under the Creative Commons Attribution-NonCommercial-NoDerivatives 4.0 License (<https://creativecommons.org/licenses/by-nc-nd/4.0/>)

the crop production instead of chemicals. These biopreparations may contain microorganisms (bacteria or fungi) with valuable properties, such as the ability to synthesize enzymes (e.g. cellulases), fix molecular nitrogen, and also to be active against plant pathogens, etc. (Kyrychenko 2015). Their roles consist of restoration of soil fertility, ensuring of plants in biologically active substances (e.g. hormones or vitamins), improvement of nitrogen and phosphorus nutrition of plants, and biological protection against pathogenic organisms.

The aim of this study was to isolate from the environmental samples the microorganisms with high cellulolytic activity, which are able to grow and synthesize of the enzyme in a wide spectrum of temperature from cheap nitrogen source and may be used as a component of biopreparations.

Experimental

Materials and Methods

Strains isolation. The strains were obtained from the sources rich in cellulose like wheat straw, compost, soil, etc. Overall, 72 strains were isolated from straw (one sample), 22 from compost (one sample) and 120 strains from soil reach in postharvest leftovers (six samples). Samples were collected in sterile plastic jars and stored in the refrigerator until experimentations. The strains were isolated using serial dilutions and pour plate technique. The sample suspensions were cultured on medium I (according to Gupta et al. 2012) containing (in g/l) casein peptone 10.0; carboxy-methyl cellulose-Na (CMC-Na) 10.0; $(\text{NH}_4)_2\text{SO}_4$ 2.5; K_2HPO_4 2.0; gelatin 2.0; $\text{MgSO}_4 \cdot 7\text{H}_2\text{O}$ 0.3; agar 15.0; pH 6.9–7.1, and incubated at 32°C for 72 h. Subsequently, single colonies were picked and spread onto modified

medium II (according to Liang et al. 2014) consisted of (g/l): K_2HPO_4 1.5; $(\text{NH}_4)_2\text{SO}_4$ 1.5; $\text{MgSO}_4 \cdot 7\text{H}_2\text{O}$ 0.3; $\text{Na}_2\text{HPO}_4 \cdot 7\text{H}_2\text{O}$ 2.5; MnSO_4 0.0016; agar 15; pH 7.0. The plates were incubated for 48 h, at 32°C. After incubation, the pure cultures were transferred to nutrient broth (in g/l: peptone 15.0; glucose 10.0) and preserved at 4°C for further screening. Two strains of *Bacillus* spp. (26b – *Bacillus circulans*, 29b – *Bacillus coagulans*) from the collection of the Department of Biotechnology and Food Microbiology were also used as reference samples.

Screening of cellulose-degrading bacteria. The strains isolated were pre-cultured overnight in nutrient broth at 32°C. Subsequently, 0.2 ml of the culture was inoculated into 20 ml test-tube containing 10 ml of the medium I (without agar and gelatin – liquid medium), incubated at 32°C for 48 h with shaking (160 rpm). After incubation, the cultures were centrifuged at 4500 rpm for 10 min. The supernatant and biomass were collected for further experiments. The ability of isolated strains to degrade cellulose was investigated using a diffusion method (Mayrhofer et al. 2008; Pastuszewska and Gryń 2013). Biomass was inoculated directly on the medium I (as a spot). Additionally, for the cell-free supernatant control, a sterile cork borer (12 mm of diameter) was used to cut uniform wells. Each well was filled with 250 µl of the supernatant obtained from the selected isolates. After incubation, the plates were stained with 1% Congo red solution for 15 min, discolored with 1 M NaCl for 15 min, and the clearance zones were observed (Kasana et al. 2008) – Fig. 1.

Cell morphology of isolated microorganisms was determined using a Gram-staining method and observation under a light microscope (Zeiss Primo Star, magnitude 1000×). The Schaeffer-Fulton staining method was used for evaluation of the spore formation ability by the bacteria examined.

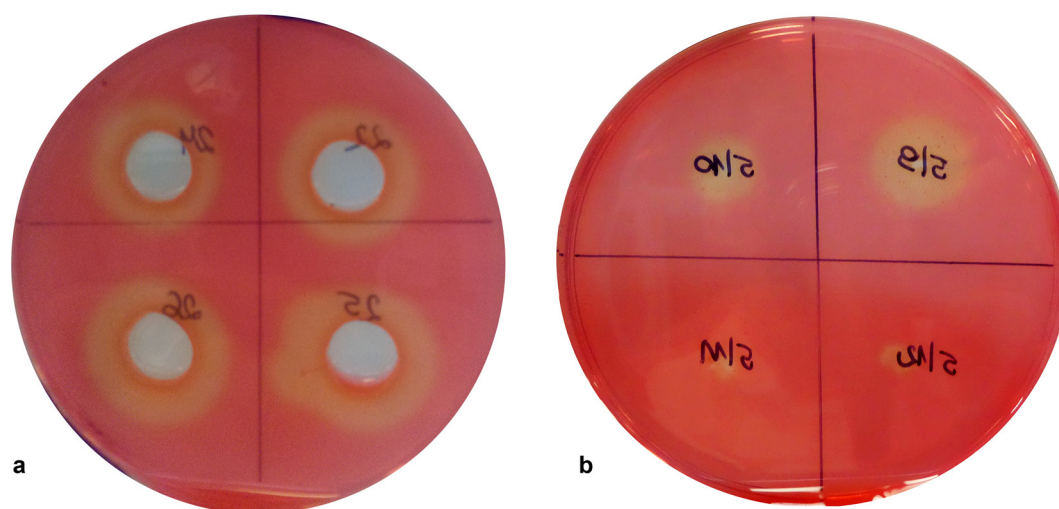


Fig. 1. CMC agar plate after staining with Congo red and NaCl. (a) determination of the supernatant activity; (b) determination of the biomass activity.

Identification of bacterial species. Total DNA from the bacteria was extracted using Genome Mini AX Bacteria Kit (A&A Biotechnology, Gdańsk, Poland) after initial incubation in 50 mg/ml lysozyme (Sigma) for 1 h at 37°C. Sequences encoding a small subunit of rRNA were amplified in PCR reaction using primers SDBact0008aS20 and SUniv1492bA21 (Suau et al. 1999). PCR products were purified using Clean-up Kit (A&A Biotechnology, Gdańsk, Poland) and sequenced at the Genomed, Warsaw, Poland with primers used for PCR and additionally for the inner sequence with the primer of the following sequence: GTGCCAGC-MGCCGCCCTAA. The sequences obtained were then arranged into contigs and identified in BLAST services of the GenBank database (Altschul et al. 1990).

Enzyme assay. The cellulose-degrading enzyme's activity was measured by the amount of reducing sugar using the 3,5-dinitrosalicylic acid (DNS) (Miller 1959). The selected isolates were grown in the medium I at 32°C. Enzyme production during fermentation was tested at 24 h intervals for four days. The culture broth was subjected to centrifugation at 4500 rpm for 10 min at 4°C. The supernatant was collected and used as a crude enzyme for further study. In this study, three types of cellulose substrates were used: CMC-Na (Sigma), filter paper (Whatman no 1) and wheat straw (milled straw, Retsh SM 100). The supernatant (1.0 ml) was added to: 0.5 ml of 1% CMC-Na in 0.05 M phosphate buffer (Irfan et al. 2012), 0.5 ml of 0.05 M sodium citrate buffer containing Whatman no. 1 filter paper strip (1 cm × 1 cm) (Gupta et al. 2012) and 0.5 ml of 0.05 M sodium citrate buffer containing chopped straw (0.05 g). The mixtures were incubated for 1 h at 30°C. The reaction was stopped by adding 1.5 ml of DNS reagent and the samples were heated for 5 min in boiling water. The amount of reducing sugar was determined by measuring absorbance at 540 nm. In these tests, the enzyme production was estimated using glucose standard and was defined in units (U). One unit (U) of enzyme activity was expressed as the amount of enzyme, which released 1 μmol of reducing sugars equivalent to glucose per ml per minute (Adney and Baker 1996).

Optimization of biosynthesis of cellulose-degrading enzymes. Temperature. The selected isolates colonies were inoculated in 300 ml Erlenmeyer flask containing 150 ml medium I and incubated under the shaking (100 rpm) for 48 h at different temperatures: 4, 15, 21, 27, 32, 37, and 42°C. After incubation, 10 ml of culture was centrifuged (10 min, 4500 rpm) and 1 ml of supernatant was used for the measurement of reducing sugars (Enzyme Assay).

Nitrogen source. All experiments were carried out in 300 ml flasks containing 150 ml of the basic medium, inoculated with 2% inoculum and then incubated at

32°C for 120 h. The basic culture medium was composed of 10 g/l of various carbon source (CMC-Na, filter paper, and milled wheat straw), 2.0 g/l K_2HPO_4 , 2.5 g/l $MgSO_4 \cdot 7H_2O$, and the initial pH was 7.0. The preparation of basic culture medium containing various nitrogen sources was carried out considering the fractions of substitution determined by the mixture design. D-optimal mixture design was adopted to study the relationship between the proportion of the four different nitrogen sources (casein peptone, ammonium sulfate, yeast extract, and ammonium chloride) and activity of cellulose-degrading enzymes. A characteristic feature of the experimental design of the mixtures is the condition of factor summability and linear restrictions on the values of these factors. In practice, it means that in an assumed experimental variant, the individual factor levels were fractions, which sum was always equal to 1 (Białas et al. 2016). The following vertexes were adopted in the experimental design: permutations of blends containing only one compound, permutations of blends containing two compounds at equal quantities, permutations of blends containing three compounds, and permutations of blends containing four compounds at equal as well as different quantities (Table I). The design was implemented using Design Expert 11.0 software (Stat-Ease Inc., USA) and the proportion of

Table I
Composition of the nitrogen sources blends according to the mixture design.

Run	A: Casein peptone (g/l)	B: $(NH_4)_2SO_4$ (g/l)	C: Yeast extract (g/l)	D: NH_4Cl (g/l)
1	5.00	0.000	0.000	0.000
2	0.00	5.000	0.000	0.000
3	0.00	0.000	5.000	0.000
4	0.00	0.000	0.000	5.000
5	1.25	1.250	1.250	1.250
6	3.13	0.625	0.625	0.625
7	0.63	3.125	0.625	0.625
8	0.63	0.625	3.125	0.625
9	0.63	0.625	0.625	3.125
10	2.50	0.000	0.000	2.500
11	2.50	0.000	2.500	0.000
12	2.50	2.500	0.000	0.000
13	0.00	2.500	0.000	2.500
14	0.00	2.500	2.500	0.000
15	0.00	0.000	2.500	2.500
16	2.50	0.000	2.500	0.000
17	5.00	0.000	0.000	0.000
18	0.00	5.000	0.000	0.000
19	0.00	0.000	5.000	0.000
20	0.00	0.000	0.000	5.000

each nitrogen source varied from 0 to 1 (0 to 5 g/l). The center point and check blends were added to the design. The order in which the experiments were performed was randomized, which fulfills the requirement for independent and random distribution of observations. Such practice helps avoid the influence of unknown nuisance variables.

The statistical analysis of the experimental mixture design was performed by backward stepwise regression. The model was simplified to exclude terms that were not considered statistically significant ($p > 0.05$) by analysis of variance (ANOVA). The accuracy and general ability of the mathematical model were evaluated using the adjusted coefficient of determination Adj-R^2 and model p -value. The final goal of this part of the study was to find an optimal mixture composition, which maximizes enzyme activity. To solve the optimization problem, the desirability function approach developed by Deringer and Suich (1980) was applied. Before optimization, the predicted values of dependent variables in different combinations of levels of the predictor variables were transformed into individual desirability scores and then the overall desirability of the outcomes at different combinations of levels of the predictor variables was computed. To determine the optimal mixture composition, maximization of the overall desirability function was performed. If the response variable was at its goal or target, then $D = 1$, and if the response variable was outside of an acceptable region, then $D = 0$.

Results and Discussion

Isolation, screening, and identification of cellulose-degrading microorganisms. The potential cellulose-degrading microorganisms were isolated from soil habitats. All of the 214 bacterial strains were isolated from habitats rich in cellulose. The ability of isolates to degrade cellulose was verified using the agar diffusion method, the medium I containing CNC-Na and Congo red staining (Fig. 1). The results obtained indicated that only 84 strains showed cellulolytic activity. Among these 84 strains, 34 isolates indicated strong activity (clearance zone over 20 mm). It was certainly found that there were no significant differences between supernatant and biomass isolates activity. The next step of screening of cellulose-degrading microorganisms was to observe the morphology of 34 strains by Gram staining method. Before staining, the strains were spread onto the poor medium with the addition of manganese salt (medium II) to determine the ability of strains to spore formation (Ryu et al. 2005). Our main goal was to find the spore-forming bacteria because they are useful for producing the bioprepara-

Table II
The results of identification of cellulose-degrading bacteria, based on the 16 rRNA gene sequencing.

Number of strain	Identity (%)	Strain of the closest match
4/3	86.09	<i>Bacillus pseudomycolides</i>
	85.84	<i>Bacillus cereus</i>
4/7	99.86	<i>Bacillus subtilis</i>
4/11	99.93	<i>Bacillus cereus</i>
	99.86	<i>Bacillus thuringiensis</i>
4/18	99.86	<i>Bacillus licheniformis</i>
6/5	100.00	<i>Achromobacter piechaudi</i>
	100.00	<i>Alcaligenes faecalis</i>
	99.93	<i>Achromobacter xylosoxidans</i>
6/6	99.97	<i>Lactococcus lactis</i>

tion. The results showed that 17 from the isolates studied belong to bacilli and form spores. The six isolates, which had the highest diameter of clearing zone both for biomass and supernatant, were selected for 16 rRNA gene sequencing and identification (strain assigned as 6/5, 6/6, 4/3, 4/7, 4/11, 4/18).

The results of the identification of these strains were given in Table II. Not all isolates were clearly identified using this method. The strains 6/5 and 6/6 belong to other genera than *Bacillus* and for this reason they were excluded. The other strains (4/3, 4/7, 4/11, 4/18) were selected for further studies.

The microorganisms with high cellulolytic potential have previously been isolated from various natural environments, like soil (Irfan et al. 2012; Liang et al. 2014; Hussain et al. 2017), mangrove soil (Behera et al. 2014), gut of termites (Upadhyaya et al. 2012) or grass carp (Li et al. 2016), woody organisms (caterpillar, bookworm, snail) (Gupta et al. 2012), and kitchen wastes (Kaur and Arora 2012). Cellulolytic enzymes are synthesized by aerobic and anaerobic bacteria, actinomycetes, fungi, and certain protozoa. The bacteria with such activity, belong to *Clostridium*, *Aeromonas*, *Enterobacter*, *Actinomyces*, *Bacillus*, *Bacteroides*, *Butyrivibrio*, *Ruminococcus*, *Methanobrevibacter*, *Sedimentibacter*, *Comamonas*, and other genera (Gupta et al. 2012; Li et al. 2016; Kanokratana et al. 2018). The strains with high cellulolytic activity isolated in our work were identified as *Bacillus* spp. Bacilli are a group of rod-shaped, gram-positive, aerobic or relatively anaerobic bacteria, which are able to form dormant spores (endospores) under adverse environmental conditions (Maughan and Auwera 2011). Spores may remain viable for a long time and are resistant to high and low temperatures, chemicals, sunlight and drought (Nicholson et al. 2000). These features make the bacilli nearly ideal bacteria for biopreparation.

The effect of temperature on the synthesis of cellulolytic enzymes. The ability to growth and synthesis

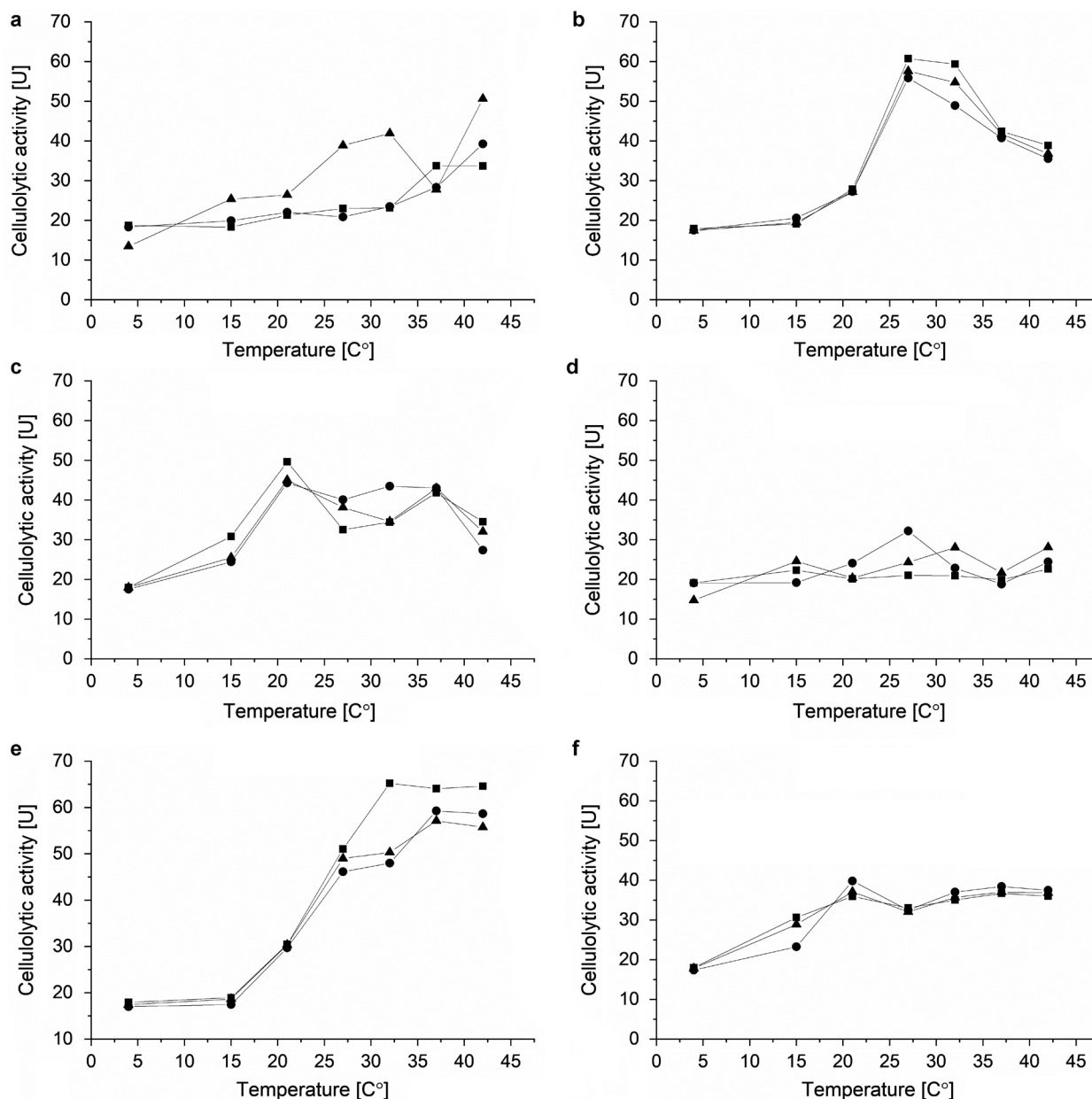


Fig. 2. The influence of temperature on cellulolytic activity of the strains examined.

(a) 4/3; (b) 4/7; (c) 29.b; (d) 4/11; (e) 4/18; (f) 26.b. (■) CMC-Na; (●) Tissue paper; (▲) Straw.

of cellulose-degrading enzymes by the selected bacterial strains was investigated in liquid cultures (medium I, according to Gupta et al. 2012) containing CMC-Na, filter paper or milled straw as the sole source of carbon. The range of cellulose substrates was extended to tissue paper (a frequently used substrate) and straw (a target substrate), because CMC is very convenient in isolation media (soluble derivatives of cellulose), but can be degraded by microorganisms able to endoglucanase synthesis in the absence of significant activity against native cellulose (McDonald et al. 2012). *Bacillus circulans* 26b and *Bacillus coagulans* 29b from the collection of the Department of Biotechnology and Food Microbiology, with confirmed cellulolytic activity, were used for comparative purposes. The results of these investiga-

tions were shown in Fig. 2. All strains examined showed cellulolytic enzymes activity in the temperature range studied (4–42°C). All cellulose substrates as a carbon source could be utilized by these strains. The lowest cellulolytic activity was noticed at 4 and 15°C (Fig. 2). The optimal temperature of cellulolytic enzymes synthesis was in the range of 21–42°C (depending on the strain and carbon source). The highest activity was observed for isolates 4/7 (identified as *Bacillus subtilis*) and 4/18 (identified as *Bacillus licheniformis*) in temperature 32°C and these isolates were selected for further studies.

Most complexes of cellulolytic enzymes indicate the highest activity between 50–60°C (Irfan et al. 2012; Liang et al. 2014; Wesołowska-Trojanowska and Targoński 2014). In our study, the range of temperature

Table III

The response data for the cellulose-degrading enzymes activity [U] of each experimental point after the cultivation of the selected strains on the media containing various substrates for 120 h.

Run	4/7 – <i>Bacillus subtilis</i>			4/18 – <i>Bacillus licheniformis</i>		
	CMC-Na	Tissue paper	Straw	CMC-Na	Tissue paper	Straw
1	73.341	69.931	76.155	84.545	45.651	54.975
2	51.870	46.036	57.331	47.838	48.956	18.901
3	78.858	81.562	70.540	86.859	43.448	33.492
4	44.842	37.608	38.008	49.592	16.792	20.351
5	86.250	69.578	90.502	67.032	47.400	25.125
6	67.130	59.652	22.006	70.089	42.723	51.931
7	63.610	61.600	55.361	59.664	45.89	21.751
8	75.801	61.600	31.052	72.537	46.864	31.312
9	65.790	70.978	64.362	52.856	35.44	30.849
10	64.633	45.841	18.583	47.315	40.568	21.191
11	67.991	46.718	48.692	40.523	69.297	25.819
12	81.805	74.096	67.183	41.298	50.323	21.398
13	58.227	64.584	67.386	17.805	33.017	41.822
14	91.841	46.815	55.102	22.799	38.85	20.497
15	66.825	71.173	41.523	32.724	42.395	23.676
16	67.451	30.849	48.943	40.674	58.946	20.022
17	66.886	66.850	74.287	80.405	45.374	56.023
18	48.983	41.919	54.057	43.417	48.097	19.754
19	72.537	76.958	68.496	78.736	43.021	34.637
20	42.529	32.785	35.983	43.71	16.822	20.972

examined was between 4 and 42°C. It was due to the fact that we were looking for the bacteria, which could be a component of biopreparation, able to grow and cellulases synthesis during autumn in Poland when the temperatures are not so high. The results obtained indicated that some environmental strains (4/7 and 4/18) were able to effective production of cellulose-degrading enzymes in temperatures lower than 50°C (in comparison with strains 26b and 29b). Similar findings were also reported by Liang et al (2014), who indicated the good cellulases activity and thermostability at 30°C (enzymes from *Paenibacillus terrae* that were isolated from natural reserves in China). The optimum pH for such enzymes is 5.5–6.5 for cellulases of fungal origin (Wesołowska-Trojanowska and Targoński 2014; Duta et al. 2018) and pH value up to 8 for cellulases of bacterial origin (Irfan et al. 2012). The most efficient bacterial growth of the species examined (*Bacillus subtilis* and *Bacillus licheniformis*) was found at pH 7 (data not present) and further experiments were carried out at the temperature 32°C and pH 7.

The effect of nitrogen sources on the synthesis of cellulolytic enzymes. The data collected in Table III indicated that the activity of cellulose-degrading enzymes differed significantly depending on the composition of the cultivation media. The highest enzyme

activity of 91.8 U was obtained for strain 4/7 with the mixture comprising a 1:1 ratio of yeast extract and $(\text{NH}_4)_2\text{SO}_4$ (run 14). When NH_4Cl was used as the sole nitrogen source, the enzyme activity reached the lowest values – 16.7 U for strain 4/18 (run 4).

To estimate the true influence of the cultivation medium composition on the enzyme activity, the collected data was analyzed with the use of backward stepwise regression. Reduced special cubic \times main effects model was adequately fitted to the response of enzyme activity for both strains. Regression models for strain 4/7 and 4/18 accounted for about 89 and 94% of variations, respectively (Table IV).

According to the results obtained, the concentration of casein peptone and yeast extract has the most significant impact on enzyme activity. For instance, yeast extract had the lowest *p*-value (< 0.0001) and the highest positive beta value (16.565), indicating that an increase in the concentration of this compound will increase enzyme production (Table IV). The same pattern was found with a casein peptone, which is confirmed by the literature data, e.g. Ray et al. (2007). On the other hand, in the concentration range tested in this experimental design, NH_4Cl was found to have a weak influence on enzyme production. As demonstrated in this study, with a growth-limiting concentration of

Table IV
Regression coefficients and the selected fit statistics for two strains investigated.

Component in model	4/7 – <i>Bacillus subtilis</i>			4/18 – <i>Bacillus licheniformis</i>		
	CMC-Na	Tissue paper	Straw	CMC-Na	Tissue paper	Straw
A	14.010	13.758	15.113	16.453	9.146	11.111
B	9.885	8.696	11.233	9.128	9.797	3.789
C	15.096	15.718	13.633	16.565	8.661	6.956
D	8.724	7.120	7.468	9.490	3.248	4.099
A×B	3.277	3.000	0.597	-3.483	0.494	-2.712
A×C	-0.808	-5.549	-3.786	-6.638	3.085	-3.472
A×D	1.294	-0.602	-5.714	-2.414	1.225	-2.800
B×C	4.399	-2.491	-1.287	-6.412	-1.193	-0.983
B×D	1.619	4.134	3.687	-4.134	-0.166	3.289
C×D	1.161	2.324	-1.994	-4.717	1.665	-0.530
A×B×C	-5.876	-4.340	-31.119	18.744	-8.735	-6.175
B×C×D	5.785	9.842	24.012	8.648	8.648	8.648
Adj-R ²	0.886			0.941		
Model <i>p</i> -value	<0.0001			<0.0001		

A: Casein peptone; B: (NH₄)₂SO₄; C: Yeast extract; D: NH₄Cl

organic nitrogen source, the *Bacillus* strains produced lower levels of cellulose-degrading enzymes when compared to a medium with a sufficient nitrogen source concentration. Probably, some organic and inorganic compounds present in the yeast extract and casein peptone could induce the extracellular enzyme production. Glutamine is one of the most important compounds because it provides the link between carbon and nitrogen metabolism in living cells. It has been reported by Manabe et al. (2011) that glutamate metabolism influences the synthesis of secreted proteins. Toya et al. (2014) added it to the medium and found that the cellulase production by *Bacillus subtilis* increased approximately 10 times. Furthermore, 80–88% of the

nitrogen that is incorporated into biomass is delivered by glutamate (Gunka and Commichau 2012). As glutamate is part of any naturally occurring protein, it is also present in yeast extract, a complex hydrolysate of yeasts, rich in nitrogenous compounds, carbon, trace nutrients and vitamin B. Glutamate content accounts for approximately 8% or more of a total mass of yeast extract (Podpora et al. 2016). This might be an explanation for the predominant role of yeast extract in the synthesis of bacterial cellulases by both *Bacillus* strains investigated.

On the other hand, for both strains, the CMC-Na brought the highest cellulases production compared to other carbon sources at 120 h incubation (Fig. 3).

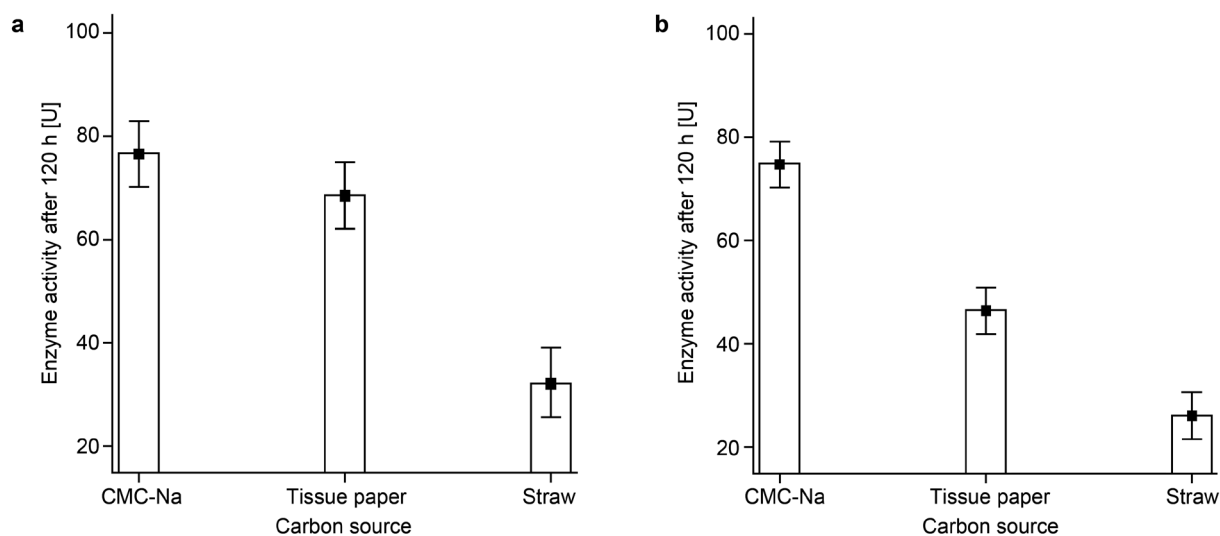


Fig. 3. Comparison of the activity of cellulose-degrading enzymes from *B. subtilis* (2a) and *B. licheniformis* (2b). An initial casein peptone, (NH₄)₂SO₄, yeast extract and NH₄Cl concentrations were 1.25 g/l.

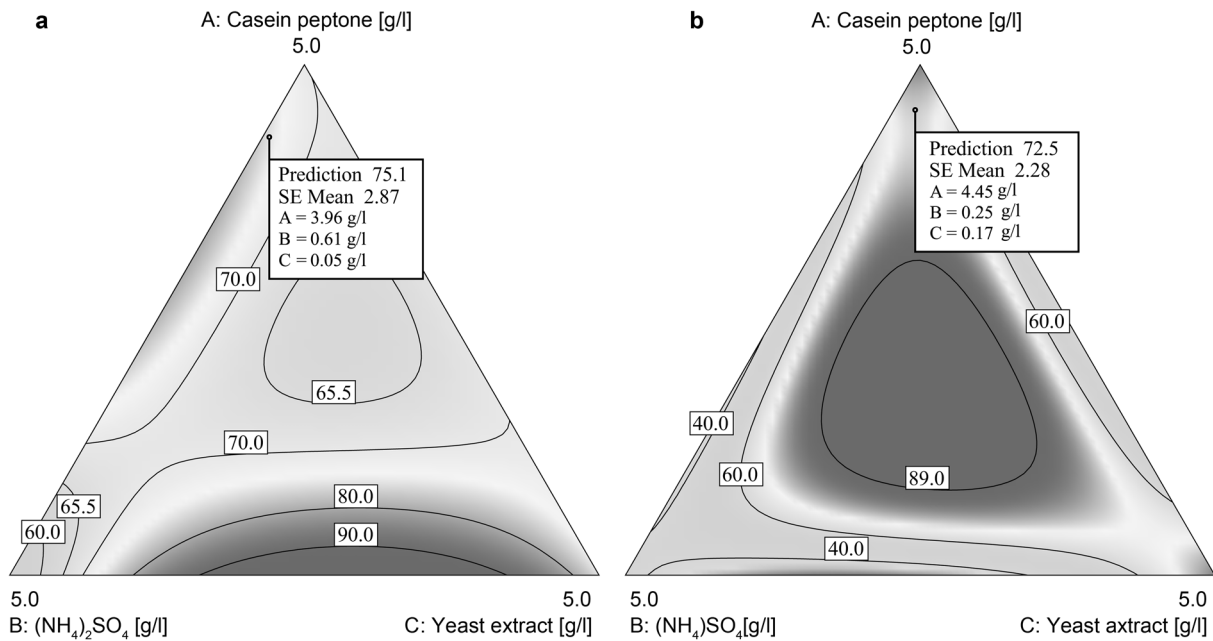


Fig. 4. Contour plot depicting the relation between casein peptone, $(\text{NH}_4)_2\text{SO}_4$ and yeast extract and the cellulolytic activity of both strains, *Bacillus subtilis* (a) and *Bacillus licheniformis* (b).

A soluble CMC-Na molecule provides a distinct advantage over the other materials used. Fibrous material such as mentioned above tissue paper and straw have a tendency to absorb some quantities of water and thus lead to highly viscous media. The limitations of using tissue paper and straw for cellulases production are related also to the nutrient availability. According to Wood and Bhat (1988), CMC-Na is less complex structure and therefore, the bacteria can more easily assimilate it. Due to these considerations, CMC-Na seems desirable carbon source for the strains investigated. The effect of various carbon sources (glucose, xylose, carboxymethyl cellulose) on the production of cellulases by the fungus *Phlebia gigantean* has been conducted, with CMC proving the best results (Niranjane et al. 2007).

To estimate the optimum composition of the cultivation media regarding nitrogen source, the optimization calculations were conducted using the simplex method, which provides excellent results in the search for the local maximums of functions of several variables (Białaś et al. 2016). It is worth to point out that a common problem in the industrial microbial processes is to find a set of conditions for the input variables (e.g. concentration of raw materials) that ensures the highest enzyme activity and low manufacturing cost as well. The standard growth media employed to cultivate *Bacillus* strains, containing yeast and beef extract, are expensive for industrial applications. The yeast extract cost is about 5.95 euro/kg, which is two times higher than the current price of the casein peptone. Thus, with regard to cost economics, casein peptone should be more efficient than yeast extract. Therefore, the follow-

ing conditions were imposed during optimization: the casein peptone, $(\text{NH}_4)_2\text{SO}_4$ and NH_4Cl had the goal limits in the range tested in design space. At the same time, the yeast extract was maintained at the lowest possible level, as it was the most expensive component of the medium. Since the standard error of dependent variable plays an important role in the assessment of prediction quality, optimization of the overall desirability function involved also minimization of this statistical parameter.

Applying desirability function methodology, the optimal medium compositions to achieve a simple, cost-efficient cellulases production process were developed for both strains. According to these calculations, the medium should contain only casein peptone, $(\text{NH}_4)_2\text{SO}_4$ and yeast extract in its composition (Fig. 4). There is no need to use the fourth of the studied compound, NH_4Cl . The predicted cellulolytic enzyme activity should be equal to 75.1 ± 2.87 U and 75.1 ± 2.28 U, for a strain 4/7 and 4/18, respectively.

Conclusions

New microbial species producing higher concentrations of cellulases should be searched to develop economically competitive biostrategies, like biopreparation. Natural environment may be a rich source of microorganisms with unique properties. We isolated from habitats rich in cellulose bacteria belonging to *Bacillus* spp., which were further identified as *Bacillus subtilis* (4/7) and *Bacillus licheniformis* (4/18). These bacteria strains, living in niches rich in cellulose,

developed the ability to effectively synthesize cellulose-degrading enzymes in environmental conditions. Organic nitrogen sources were found to be more suitable for optimizing cellulase production by *Bacillus subtilis* and *Bacillus licheniformis* than inorganic sources.

Acknowledgements

This study was supported by research grant No UDA-POIG. 01.04.00-12-386/13-00 from The National Centre for Research and Development.

Conflict of interest

The authors do not report any financial or personal connections with other persons or organizations, which might negatively affect the contents of this publication and/or claim authorship rights to this publication.

Literature

- Adney B, Baker J.** Measurement of cellulase activities, Technical Report NREL/TP-510-42628 [Internet]. Golden, Colorado (USA): National Renewable Energy Laboratory; [cited 2018 Sep 02]. 2008. Available from: <https://www.nrel.gov/docs/gen/fy08/42628.pdf>
- Altschul SE, Gish W, Miller W, Myers EW, Lipman DJ.** Basic local alignment search tool. *J Mol Biol.* 1990;215(3):403–410. doi:10.1016/S0022-2836(05)80360-2 Medline
- Behera BC, Parida S, Dutta SK, Thantoi HN.** Isolation and identification of cellulose degrading bacteria from mangrove soil of Mahandi river delta and their cellulase production ability. *Am J Microb Res.* 2014;2(1):41–46.
- Białas W, Czerniak A, Dobrowolska A, Wojciechowska J, Grajek W.** Controlling microbial growth in innovative dietary supplement based on the biomass of yeast *Yarrowia lipolytica*. *J Microbiol Biotechnol Food Sci.* 2016;05(05):389–395. doi:10.15414/jmbfs.2016.5.5.389-395
- Bomble YJ, Lin CY, Amore A, Wei H, Holwerda EK, Ciesielski PN, Donohoe BS, Decker SR, Lynd LR, Himmel ME.** Lignocellulose deconstruction in the biosphere. *Curr Opin Chem Biol.* 2017;41:61–70. doi:10.1016/j.cbpa.2017.10.013 Medline
- Derringer G, Suich R.** Simultaneous optimization of several response variables. *J Qual Technol.* 1980;12(4):214–219. doi:10.1080/00224065.1980.11980968
- Dutta S, Tarafder M, Islam R, Datta B.** Characterization of cellulolytic enzymes of *Fusarium* soil Isolates. *Biocatal Agric Biotechnol.* 2018;14:279–285. doi:10.1016/j.cbab.2018.03.011
- Gunka K, Commichau FM.** Control of glutamate homeostasis in *Bacillus subtilis*: a complex interplay between ammonium assimilation, glutamate biosynthesis and degradation. *Mol Microbiol.* 2012; 85(2):213–224. doi:10.1111/j.1365-2958.2012.08105.x Medline
- Gupta P, Samant K, Sahu A.** Isolation of cellulose-degrading bacteria and determination of their cellulolytic potential. *Int J Microbiol.* 2012;2012:1–5. doi:10.1155/2012/578925 Medline
- Hussain AA, Abdel-Salam MS, Abo-Ghalia HH, Hegazy WK, Hafez SS.** Optimization and molecular identification of novel cellulose degrading bacteria isolated from Egyptian environment. *J Genet Eng Biotech.* 2017;15(1):77–85. doi:10.1016/j.jgeb.2017.02.007
- Irfan M, Safdar A, Syed Q, Nadeem M.** Isolation and screening of cellulolytic bacteria from soil and optimization of cellulase production and activity. *Turk J Biochem.* 2012;37(3):287–293. doi:10.5505/tjb.2012.09709
- Kanokratana P, Wongwilaiwalin S, Mhuantong W, Tangphat-sornruang S, Eurwilaichitr L, Champreda V.** Characterization of cellulolytic microbial consortium enriched on Napier grass using metagenomic approaches. *J Biosci Bioeng.* 2018;125(4):439–447. doi:10.1016/j.jbiosc.2017.10.014 Medline
- Kasana RC, Salwan R, Dhar H, Dutt S, Gulati A.** A rapid and easy method for the detection of microbial cellulases on agar plates using gram's iodine. *Curr Microbiol.* 2008;57(5):503–507. doi:10.1007/s00284-008-9276-8 Medline
- Kaur M, Arora S.** Isolation and screening of cellulose degrading bacteria in kitchen waste and detecting their degrading potential. *IOSR J Mech Civ Eng.* 2012;1(2):33–35. doi:10.9790/1684-0123335
- Kyrychenko OV.** Market analysis and microbial biopreparations creation for crop production in Ukraine. *Biotech Acta.* 2015;8(4):40–52.
- Li H, Wu S, Wirth S, Hao Y, Wang W, Zou H, Li W, Wang G.** Diversity and activity of cellulolytic bacteria, isolated from the gut contents of grass carp (*Ctenopharyngodon idellus*) (Valenciennes) fed on Sudan grass (*Sorghum sudanense*) or artificial feedstuffs. *Aquacult Res.* 2016;47(1):153–164. doi:10.1111/are.12478
- Liang YL, Zhang Z, Wu M, Wu Y, Feng JX.** Isolation, screening, and identification of cellulolytic bacteria from natural reserves in the subtropical region of China and optimization of cellulase production by *Paenibacillus terrae* ME27-1. *BioMed Res Int.* 2014; 2014:1–13. doi:10.1155/2014/512497 Medline
- Manabe K, Kageyama Y, Morimoto T, Ozawa T, Sawada K, Endo K, Tohata M, Ara K, Ozaki K, Ogasawara N.** Combined effect of improved cell yield and increased specific productivity enhances recombinant enzyme production in genome-reduced *Bacillus subtilis* strain MGB874. *Appl Environ Microbiol.* 2011;77(23): 8370–8381. doi:10.1128/AEM.06136-11 Medline
- Maughan H, Van der Auwera G.** *Bacillus* taxonomy in the genomic era finds phenotypes to be essential though often misleading. *Infect Genet Evol.* 2011;11(5):789–797. doi:10.1016/j.meegid.2011.02.001 Medline
- Mayrhofer S, Domig KJ, Mair C, Zitz U, Huys G, Kneifel W.** Comparison of broth microdilution, Etest, and agar disk diffusion methods for antimicrobial susceptibility testing of *Lactobacillus acidophilus* group members. *Appl Environ Microbiol.* 2008;74(12): 3745–3748. doi:10.1128/AEM.02849-07 Medline
- McDonald JE, Rooks DJ, McCarthy AJ.** Methods for the isolation of cellulose-degrading microorganisms. In: Gilbert HJ, editor. *Methods in enzymology. Cellulases.* Vol. 510. San Diego (USA): Elsevier Academic Press. 2012; p. 349–374.
- Miller GL.** Use of dinitrosalicylic acid reagent for determination of reducing sugar. *Anal Chem.* 1959;31(3):426–428. doi:10.1021/ac60147a030
- Nicholson WL, Munakata N, Horneck G, Melosh HJ, Setlow P.** Resistance of *Bacillus* endospores to extreme terrestrial and extraterrestrial environments. *Microbiol Mol Biol Rev.* 2000;64(3): 548–572. doi:10.1128/MMBR.64.3.548-572.2000 Medline
- Niranjane AP, Madhou P, Stevenson TW.** The effect of carbohydrate carbon sources on the production of cellulase by *Phlebia gigantea*. *Enzyme Microb Technol.* 2007;40(6):1464–1468. doi:10.1016/j.enzmictec.2006.10.041
- Pastuszewska T, Gryń G.** Cellulolytic activity and virulence of *Clavibacter michiganensis* subsp. *sepedonicus*. *Biuletyn IHAR.* 2013; 270:123–131.
- Pietraszek P, Walczak P.** Characteristic and applications of *Bacillus* strains isolated from soil. *Polish J Agron.* 2014;16:37–44.
- Podpora B, Świdorski F, Sadowska A, Rakowska R, Wasiak-Zys G.** Spent brewer's yeast extracts as a new component of functional food. *Czech J Food Sci.* 2016;34(6):554–563. doi:10.17221/419/2015-CJFS
- Ray AK, Bairagi A, Ghosh KS, Sen SK.** Optimization of fermentation conditions for cellulase production by *Bacillus subtilis* CY5

and *Bacillus circulans* TP3 isolated from fish gut. *Acta Ichthyol Piscat.* 2007;37(1):47–53. doi:10.3750/AIP2007.37.1.07

Ryu JH, Kim H, Beuchat LR. Spore formation by *Bacillus cereus* in broth as affected by temperature, nutrient availability, and manganese. *J Food Prot.* 2005;68(8):1734–1738.

doi:10.4315/0362-028X-68.8.1734 Medline

Shrestha S, Fonoll X, Khanal SK, Raskin L. Biological strategies for enhanced hydrolysis of lignocellulosic biomass during anaerobic digestion: current status and future perspectives. *Bioresour Technol.* 2017;245 Pt A:1245–1257.

doi:10.1016/j.biortech.2017.08.089 Medline

Suau A, Bonnet R, Sutren M, Godon JJ, Gibson GR, Collins MD, Doré J. Direct analysis of genes encoding 16S rRNA from complex communities reveals many novel molecular species within the human gut. *Appl Environ Microbiol.* 1999;65(11):4799–4807. Medline

Toya Y, Hirasawa T, Morimoto T, Masuda K, Kageyama Y, Ozaki K, Ogasawara N, Shimizu H. ¹³C-metabolic flux analysis in heterologous cellulase production by *Bacillus subtilis* genome-reduced strain. *J Biotechnol.* 2014;179(10):42–49.

doi:10.1016/j.jbiotec.2014.03.025 Medline

Upadhyaya SK, Manadhar A, Mainali H, Pokhrel AR, Rijal A, Pradhan B, Koirala B. Isolation and characterization of cellulolytic bacteria from gut of termite. *Rentech Symp Comp.* 2012;1:14–18.

Wesołowska-Trojanowska M, Targoński Z. Cellulases – properties, application and production. *Eng Sci Technol.* 2013; 2(13): 106–121.

Wood TM, Bhat KM. Methods for measuring cellulase activities. In: Wood WA, Kellogg JA, editors. *Methods in Enzymology. Cellulose and Hemicellulose.* Vol. 160. New York (USA): Academic Press. 1998; p. 87–112.

Dengue Outbreaks in Khyber Pakhtunkhwa (KPK), Pakistan in 2017: An Integrated Disease Surveillance and Response System (IDSRS)-Based Report

ABDULLAH¹, SHER ALP², MUHAMMAD SALMAN^{3*}, MISBAHUD DIN¹, KACHKOL KHAN⁴,
MUNIB AHMAD¹, FAISAL HAYAT KHAN¹ and MUHAMMAD ARIF^{1#}

¹Department of Biotechnology, Abdul Wali University, Mardan, Pakistan

²Universidade Federal do Paraná Brazil, Department of Chemistry, Parana, Brazil

³Department of Microbiology and Biotechnology, Abasyn University Peshawar, Pakistan

⁴Tehsil Head Quarter Hospital Dargai, Malakand, Pakistan

Submitted 16 October 2018, revised 16 December 2018, accepted 17 December 2018

Abstract

The current study is a retrospective epidemic report regarding dengue fever (DF) virus infection cases (2017) from fifteen districts of KPK, Pakistan. Medical records of 120 948 patients were reviewed retrospectively for demographic, clinical and laboratory data. The presence of dengue infection was confirmed by NS1-ELISA and RT-PCR, respectively. The total positive cases (of suspected DF samples) were 24 938 (20.6%), whereas seventy cases (0.28%) had a fatal outcome. Mean age \pm SD of the dengue patients was 26 ± 19.8 years, while; the most affected age group was from 16 to 30 years (Chi-square: 12 820.125, p : 0.00). The infected males were 65.3%, and that of the female was 34.7%. All the dengue-infected patients were observed with symptoms of severe fever (100%), body aches (95%), gums and nose bleeding (5%), skin rashes (30%), vomiting (70%). The highest infection rate was found in district Peshawar and that of the lowest was in Bannu, Hungu and Luki Marwat. A high rate of dengue infection was found in post-monsoon months i.e. October (41%) and September (32%) of the year. The results proved that if the dengue outbreaks reveal further in KPK, it could alarmingly increase the mortality rate. Therefore, the Department of Public Health in KPK, Pakistan may take proper measures to avoid and control dengue epidemics in the future.

Key words: Dengue fever, infection, IDSRS, KPK, patients, symptoms, climate

Introduction

Dengue is a mosquito-borne viral ailment which infects over 100 million human population with an annual mortality rate of 30 000 globally (WHO 2013). Dengue virus (DENV) consists of single-stranded positive-sense RNA, belongs to genus Flavivirus, and family Flaviviridae (Durrani et al. 2014; Khan et al. 2018a). Commonly, four antigenically distinct serotypes of DENV have been reported, i.e. DENV 1 to DENV 4 (Durrani et al. 2014; Waseem et al. 2014; Suleman et al. 2017a; Suleman et al. 2017b; Khan et al. 2018b; Shams et al. 2018). According to recent reports from Pakistan, the major serotypes found in Punjab were DENV 2, 3 and 4; however, DENV 2 and 3 were found in Swat area of KPK province in 2013 with a high morbidity as well as mortality rate (Khan et al. 2017; Suleman et al. 2017a;

Suleman et al. 2017b; Khan et al. 2018a). The serotype 3 has always predominated (Koo et al. 2013). Recently, serotype five (DENV 5) has been revealed via neutralization assays (Ghani et al. 2017; Morra et al. 2018).

The aforesaid viruses are transmitted by female of *Aedes* mosquito of order *Diptera* and *Culicidae* family, especially *Aedes aegypti* (primary vector) also known as yellow fever mosquito, and in lesser extent (Nasir et al. 2017; Qsim et al. 2017) *Aedes albopictus* (secondary vector) commonly known as Asian tiger mosquito. There are three main stages of dengue fever (DF): initially mild dengue fever (MDF), followed by severe dengue hemorrhagic fever (DHF), and the life-threatening dengue shock syndrome (DSS).

Dengue fever is endemic in Pakistan; however, highest incidences reported were almost post-monsoon (Rafique et al. 2017; Rafique et al. 2018). Since 2010,

* Corresponding author: M. Salman, Department of Microbiology and Biotechnology, Abasyn University Peshawar, Pakistan; e-mail: s.amazai@yahoo.com

Co-corresponding author: M. Arif, Department of Biotechnology, Abdul Wali Khan University, Mardan, Pakistan; e-mail: arif@awkum.edu.pk

© 2019 Abdullah et al.

This work is licensed under the Creative Commons Attribution-NonCommercial-NoDerivatives 4.0 License (<https://creativecommons.org/licenses/by-nc-nd/4.0/>)

this country is facing some terrible epidemics of dengue accompanied by substantial human health issues and deaths. Local transmission of dengue has been reported since it would also have an important role in the reintroduction of the disease. The recent largest dengue pandemics were recorded for the first time in Lahore (2011) with 22 562 cases and 363 fatalities, and for the second time in Swat (2013) causing 8343 morbidities along with 57 deaths. Recently, in 2017 another huge dengue outbreak has been recorded in Peshawar with 23 541 cases (Hurtado-Díaz et al. 2007; Khan et al. 2018a; Rafique et al. 2018). Therefore, the present study is conducted for the recent outbreaks occurred in Khyber Pakhtunkhwa, Pakistan in 2017.

Experimental

Materials and Methods

Study area. The study was performed in Khyber Pakhtunkhwa (KPK), the Northwest province of Pakistan. According to 2017 census, its total area is 74 521 km² and population is 30.523 million. The province shares boundaries with Afghanistan to the north-west, Gilgit-Baltistan to the north-east, Ex-Federal Administrative Tribal Areas (Ex-FATA) to the west and south, Azad Jammu and Kashmir to the east, Baluchistan to the south, and Islamabad Capital of the Country and Punjab to the South-East. Khyber Pakhtunkhwa is the third highest important populated region of the country (Khan et al. 2017).

Data collection. The study was a retrospective epidemic report regarding DF virus infection cases from fifteen districts of KPK, Pakistan. The data was collected from the Integrated Disease Surveillance and Response System (IDSRS) Directorate General Health Services, Peshawar, KPK, Pakistan with the prior approval of data by the statistical officer of IDSRS.

Clinical manifestations. The indoor patients admitted in different hospitals of the province were investigated for various signs and symptoms e.g. fever, body aches, nausea, vomiting, diarrhea, gum bleeding and bleeding of the nose, skin rashes, animals contact history, and platelet count at admission.

ELISA. The data collected was obtained from medical records. About 120 948 patients were reviewed retrospectively for demographic and clinical as well as laboratory data. The patients' serum was investigated for the presence of non-structural protein-1 (NS1) antigen in order to identify DENV using ELISA, according to the guidelines of the manufacturer (Platelia Biorad Lab, Marnes-la-Coquette, France) (Lutfullah et al. 2017). In case of positive result, the treatment had been started immediately without any delay; however, in case of the

weak positive or ambiguous result of NS1 antigen, the samples were processed with a thermal cyclor.

PCR. To confirm the presence of dengue virus in the samples, the protocol adopted by Khan et al. (2017) was followed. Briefly, RNA was extracted and processed with RT-PCR using type-specific DENV primers (TS1-TS4) (Khan et al. 2018a). Both +ve and -ve controls (DENV-1, 2, 3 and 4) were used, respectively. The resultant amplified DNA products were determined on 2% agarose gels (Salman et al. 2015) (Biotium Inc., USA).

Data analysis. The data obtained in the current study was analyzed on the basis of: 1) geographical distribution in 15 Districts of KPK (Abbottabad, Banu, Buner, Dir lower, Hangu, Haripur, Karak, Kohat, Laki Marwat, Malakand, Mansehra, Mardan, Nowshera, Peshawar and Swabi), 2) month-wise (from July – December 2017), 3) age-wise (1–15, 16–30, 41–45, 46 – 60, and above 60) and 4) sociodemographically (gender-wise and clinical manifestation and outcome basis).

Results

In the current report of 120 948 suspected dengue cases, 24 938 were found positive for DENV that occurred in 15 different districts of Khyber Pakhtunkhwa (KPK) as a result of dengue outbreak in 2017. Preliminarily, out of total positive samples, >90% of the patients were positive with the NS1 antigen ELISA; however, the remaining <10% uncertain cases were confirmed with RT-PCR.

The most numerous cases were found positive in district Peshawar (23 541) with 65 deaths, followed by Mardan (369) with one death, and four death cases were reported from Abbottabad (142) (Table I). Male population was affected in a greater extent (65.33%) when compared to female (34.66%). Mostly, the affected patients were found in the age of 16–30 (45%, Chi-square: 12 820.125, p:0.00), and subsequently of 31–45 (23%), and 1–15 years (20%). On the other hand, patients of age 45–60 and or above 60 years old were less affected (5–7%) (Table III).

Clinical information. All the infected and hospitalized patients were observed with mild to severe fever (100%). The most common symptoms were body aches and pain (95%), followed by vomiting and diarrhea (70%), as well as skin rashes (30%). The patients had also hemorrhagic manifestations in the form of gum bleeding and bleeding from the nose (5%) (Table III).

Monthly distribution of dengue fever. The percentage of dengue viral infection was quite low in July and steadily increased in rainy months and the rate became much high in September and October (Table II). It might be owing to the well-established propagation of *Aedes* (primary and secondary vectors of dengue virus)

Table I
District-wise geographical distribution of dengue cases
in the population.

District	Suspected cases	Positive cases	Male	Female	No. of deaths
Abbottabad	205	142	114	28	4
Banu	6	1	1	0	0
Buner	1102	143	104	39	0
Dir lower	6	6	5	1	0
Hangu	3	1	1	0	0
Hariipur	211	64	42	42	0
Karak	12	9	6	3	0
Kohat	99	17	13	4	0
Laki Marwat	278	1	1	0	0
Malakand	667	240	165	75	0
Mansehra	782	72	49	23	0
Mardan	4295	369	260	109	1
Nowshera	825	199	138	61	0
Peshawar	111979	23541	15302	8239	65
Swabi	478	133	93	40	0
Total	120948	24938	16294	8664	70

Table II
Sociodemographic and clinical presentation of dengue.

Characteristics	DF (n=24938)
Sociodemographic	
Age (years) (Means \pm SD)	26 \pm 19.8
Male	16294 (95.3%)
Female	8664 (34.7%)
Clinical presentation	
Fever	24938 (100%)
Body aches	23691 (95%)
Vomiting/ Nausea	17457 (70%)
Skin rashes	7481 (30%)
Bleeding	1247 (5%)
Outcome	
Death	70 (0.28%)

Table III
Age-based statistical analysis of dengue patients.

Age Group	Frequencies (% age)	Test Statistics	
1 to 15	4987 (20%)	Chi Square	12820.125 ^a
16 to 30	11222 (45%)	Degree of freedom	4
31 to 45	5735 (23%)	Asymptotic significant value	0
45 to 60	1748 (7%)		
Above 60	1246 (5%)		
Total	24938 (100%)		

a - 0 cells (0%) have expected frequencies less than 5. The minimum cell frequency is 4987.6.

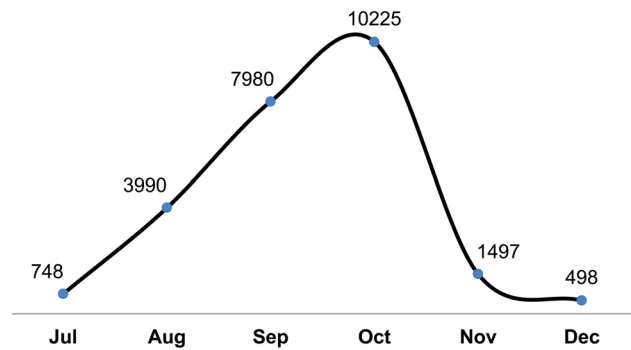


Fig. 1. Month-wise dispersal of dengue infection.

in the monsoon period of the year. In July the infection rate was least (3%) while it slowly increased in August (16%). In September (32%) and October (41%), the infection rate of DF promptly increased owing to the rainy season, while in November (6%) and December (2%) there was a clear decrease again, which was depicted (Fig. 1).

Discussion

Most of the developing world is under high risk of dengue virus; hence, it is becoming a main public health issue, particularly in tropical regions (Hurtado-Díaz et al. 2007; Zafar et al. 2013; Kraemer et al. 2015;). In 2013 different regions of Khyber Pakhtunkhwa (KPK) faced permanent epidemics of DF, and the cases of deaths were also recorded. There were three possible reasons for the greater number of dengue cases reported from Peshawar. First, Peshawar is the capital of KPK province; hence, there are two governmental tertiary hospitals and a medical complex. The major health facilities are also available in this city. Second, in 2017, a dengue outbreak was reported from Peshawar; hence, the larger population was affected. Third, some remote areas, especially the Northern and southern hilly area, may be under-reported for dengue. On the other hand, the current study investigated the rate of dengue infection in other districts of Khyber Pakhtunkhwa (KPK).

When studied in a similar way with the use of the Integrated Disease Surveillance and Response System (IDSRS), there were 24 938 dengue cases including 70 deaths reported from various districts of KPK. In other words, out of 70 death outcomes, 62 (88.6%) were male, while 8 (11.4%) were female.

The dengue cases in the current study were divided into five groups, based on the age of the patients. The highest dengue rate incidence was found in the following sequence; age 16–30 (45%), 31–45 (23%) and 1–15 years (20%), while the patients of the age 45–60 years and above were less affected (7–5%). These results are in correlation with those described in the documented dengue cases (134) in the patients of age 20–30 years (61.77%), and limitedly in children (Zafar et al. 2013). Moreover, some investigations performed in Singapore showed that the majority of infected patients were older (Gadhwal et al. 2016). In this regard, it has been concluded that adults of 16–30 years old in KPK are in the danger region to dengue infection and the risk may depend to the time spend outside (Khan et al. 2017). Simultaneously, in the present study, the infection rate was found the highest in the male population (65.33%) in comparison to female (34.66%). The same results in six Asian countries regarding the dengue infection rate in male-female were recorded (Ahmad et al. 2011; Gadhwal et al. 2016; Zubair et al. 2016). In another report, 71% rates of dengue RNA positive samples were found in male population of KPK and Punjab (Shahid et al. 2013). One study from KPK revealed that male to female ratio of dengue cases was 2:1 (Suleman et al. 2017a). The comparative studies also mentioned the same consequences of the dengue infection relative to male-female patients (> 15 years older) (Durrani et al. 2014; Khan et al. 2018b). The collected data and the results described in this study are compatible to those already documented in the literature (Ali et al. 2013; Hasan et al. 2013; Khalid et al. 2015; Ghani et al. 2017; Iqtadar et al. 2017). The dengue infection in Asian countries could be acquired during both outdoor and indoor activities. Based on outdoor and indoor activities, it has been concluded that male in KPK could be more affected with dengue infection in comparison to female (Khan et al. 2017; Suleman et al. 2017b). The up-to-date study is also scrutinized in a month-wise since the incidences of dengue infection were observed from July – December. The peak incidences were observed for dengue infection in the following periods of time: September – October (32–41%); July – August (16–3%) and November – December (6–2%). The peak incidence of dengue infection was seen in the post-monsoon season – in October (41%). The similar observation was found in the literature, where a steady increase was measured from August to October (Hasan et al. 2013; Khalid et al. 2015; Ghani et al. 2017;). This has also been

previously shown by others (Khan et al. 2006; Khan et al. 2013; Arshad et al. 2015). The main reason for the highest ratio of incidences in post monsoon period may be the water stagnation, what plays a vital role in the reproduction of mosquitoes, vectors of dengue viruses.

Conclusions

From the current report, it may be concluded that DF and DHF are endemic in Khyber Pakhtunkhwa (KPK) in Pakistan; however, Peshawar is under the highest risk of morbidity and mortality. The most affected age group found was from 16 to 30 years. Male to female ratio of the DF was almost 2:1, whereas male to female ratio of mortality was about 9:1. About half of the dengue infection cases reported were in the month of October. In case of negligence of the preventive measures against the dengue outbreak, it may occur an alarming intensification of infections in the future. Therefore, the Department of Public Health in KPK may take a proper consideration to avoid and control dengue epidemics in the future.

The local governments of KPK may play important role in the eradication of dengue fever, therefore, besides the awareness, the proper training given to the teams consisted of young male and female volunteers on union council level is necessary. The emergency response kit may be provided to them and chairperson of the union council may conduct weekly meetings, specifically in monsoon season, in order to combat any disaster on an anticipatory basis. Integrated Disease Surveillance and Response System (IDSRS) with a geographic information system (GIS) are mandatory across the country. IDSRS-GIS will help the health authorities to identify the high-risk area and risk factors, followed by an adaptation of precautionary actions precedent in risk areas.

ORCID

Muhammad Salman [0000-0002-7605-2806](https://orcid.org/0000-0002-7605-2806)

Ethical approval

The study was approved from the ethical committee of Abdul Wali Khan University Mardan, Pakistan.

Conflict of interest

The authors do not report any financial or personal connections with other persons or organizations, which might negatively affect the contents of this publication and/or claim authorship rights to this publication.

Literature

Ahmad N, Fazal H, Ayaz M, Abbasi BH, Mohammad I, Fazal L. Dengue fever treatment with *Carica papaya* leaves extracts. *Asian Pac J Trop Biomed.* 2011;1(4):330–333. doi:10.1016/S2221-1691(11)60055-5 [Medline](https://pubmed.ncbi.nlm.nih.gov/22211691/)

- Ali A, Rehman H, Nisar M, Rafique S, Ali S, Hussain A, Nausheen, Idrees M, Sabri S, Zada H, et al. Seroepidemiology of dengue fever in Khyber Pakhtunkhwa, Pakistan. *Int J Infect Dis*. 2013;17(7):e518–e523. doi:10.1016/j.ijid.2013.01.007 [Medline](#)
- Arshad K, Sheikh S, Naqvi SU, Sarwar I, Javaid S, Asghar M, Butt MA. Frequency of splenomegaly in dengue fever in children. *J Ayub Med Coll Abbottabad*. 2015;27(2):356–359. [Medline](#)
- Durrani MR, Iqbal MD, Munir N, Jamal A. Dengue hemorrhagic fever-epidemic in Karachi, Pakistan (2006–2016) experience at a tertiary care centre. *Pak J Surg*. 2017;33(1):53–58.
- Gadhwal AK, Ankit BS, Chahar C, Tantia P, Sirohi P, Agrawal RP. Effect of *Carica papaya* leaf extract capsule on platelet count in patients of dengue fever with thrombocytopenia. *J Assoc Physicians India*. 2016;64(6):22–26. [Medline](#)
- Ghani E, Mushtaq S, Khan SA. 2017 Multiplex polymerase chain reaction-based serotype analysis of dengue virus during 2015 dengue outbreak in Pakistan. *East Mediterr Heal J*. 2017;23(9):594–597. [Medline](#)
- Hasan SR, Riaz M, Jafri FA. Characteristics and outcome of dengue infection; clinical perspective from a secondary care hospital of Karachi. *Pak J Med Sci*. 2013;29(1):115–118. [Medline](#)
- Hurtado-Díaz M, Riojas-Rodríguez H, Rothenberg SJ, Gomez-Dantés H, Cifuentes E. Short communication: impact of climate variability on the incidence of dengue in Mexico. *Trop Med Int Health*. 2007;12(11):1327–1337. doi:10.1111/j.1365-3156.2007.01930.x [Medline](#)
- Iqtadar S, Akbar N, Mehmood M, Abaidullah S. Clinical audit of dengue related deaths in 2011 at Mayo Hospital Lahore Pakistan. *Pak J Med Sci*. 2017;33(5):1070–1073. doi:10.12669/pjms.335.13051 [Medline](#)
- Khalid B, Ghaffar A. Environmental risk factors and hotspot analysis of dengue distribution in Pakistan. *Int J Biometeorol*. 2015;59(11):1721–1746. doi:10.1007/s00484-015-0982-1 [Medline](#)
- Khan E, Siddiqui J, Shakoor S, Mehraj V, Jamil B, Hasan R. Dengue outbreak in Karachi, Pakistan, 2006: experience at a tertiary care center. *Trans R Soc Trop Med Hyg*. 2007;101(11):1114–1119. doi:10.1016/j.trstmh.2007.06.016 [Medline](#)
- Khan J, Ghaffar A, Khan SA. The changing epidemiological pattern of dengue in Swat, Khyber Pakhtunkhwa. *PLoS One*. 2018a;13(4):e0195706. doi:10.1371/journal.pone.0195706 [Medline](#)
- Khan J, Khan I, Ali I, Iqbal A, Salman M. The role of vertical transmission of dengue virus among field-captured *Aedes aegypti* and *Aedes albopictus* mosquitoes in Peshawar, Khyber Pakhtunkhwa, Pakistan. *Pak J Zool*. 2017;49(3):777–784. doi:10.17582/journal.pjz/2017.49.3.777.784
- Khan J, Khan I, Ghaffar A, Khalid B. Epidemiological trends and risk factors associated with dengue disease in Pakistan (1980–2014): a systematic literature search and analysis. *BMC Public Health*. 2018b;18(1):745. doi:10.1186/s12889-018-5676-2 [Medline](#)
- Khan MI, Anwar E, Agha A, Hassanien NS, Ullah E, Syed IA, Raja A. Factors predicting severe dengue in patients with dengue fever. *Mediterr J Hematol Infect Dis*. 2013;5(1):e2013014. doi:10.4084/mjhid.2013.014 [Medline](#)
- Koo C, Nasir A, Hapuarachchi H, Lee KS, Hasan Z, Ng LC, Khan E. Evolution and heterogeneity of multiple serotypes of dengue virus in Pakistan, 2006–2011. *Virology*. 2013;10(1):275. doi:10.1186/1743-422X-10-275 [Medline](#)
- Kraemer MUG, Perkins TA, Cummings DAT, Zakar R, Hay SI, Smith DL, Reiner RC Jr. Big city, small world: density, contact rates, and transmission of dengue across Pakistan. *J R Soc Interface*. 2015;12(111):20150468. doi:10.1098/rsif.2015.0468 [Medline](#)
- Lutfullah G, Ahmed J, Aftab Khan HI, Ahmad J. Evaluation of Non-Structural Protein-1 (NS1) positive patients of 2013 dengue outbreak in Khyber Pakhtunkhwa, Pakistan. *Pak J Med Sci*. 2017;33(1):172–176.
- Morra ME, Altibi AMA, Iqtadar S, Minh LHN, Elawady SS, Hallab A, Elshafay A, Omer OA, Iraqi A, Adhikari P, et al. Definitions for warning signs and signs of severe dengue according to the WHO 2009 classification: systematic review of literature. *Rev Med Virol*. 2018;28(4):e1979. doi:10.1002/rmv.1979
- Nasir S, Jabeen F, Abbas S, Nasir I, Debboun M. Effect of climatic conditions and water bodies on population dynamics of the dengue vector, *Aedes aegypti* (Diptera: culicidae). *J Arthropod Borne Dis*. 2017;11(1):50–59. [Medline](#)
- Qsim M, Ashfaq UA, Yousaf MZ, Masoud MS, Rasul I, Noor N, Hussain A. Genetically modified *Aedes aegypti* to control dengue: A review. *Crit Rev Eukaryot Gene Expr*. 2017;27(4):331–340.
- Rafique I, Saqib MA, Munir MA, Siddiqui S, Malik IA, Rao MH, Ahmed J, Bashir S, Khan O, Firdous R, et al. Dengue knowledge and its management practices among physicians of major cities of Pakistan. *J Pak Med Assoc*. 2015;65(4):392–396. [Medline](#)
- Rafique I, Saqib MAN, Munir MA, Qureshi H, Taseer IH, Iqbal R, Ahmed W, Akhtar T, Rizwanullah. Asymptomatic dengue infection in adults of major cities of Pakistan. *Asian Pac J Trop Med*. 2017;10(10):1002–1006. doi:10.1016/j.apjtm.2017.09.013 [Medline](#)
- Salman M, Ali A, Jabbar A, Sarwar Y, Rahman M, Iqbal M, Haque A. Simplest identification, O-specific polysaccharide purification and antigenic evaluation of *Salmonella enterica* serovar Typhi Vi negative isolate. *EXCLI J*. 2015;14:1078–1084. [Medline](#)
- Shahid M, Amin I, Afzal S, Fatima Z, Zahid S, Ashraf U, Idrees M. Prevalence and molecular detection of dengue virus in 2013 outbreak in KPK and Punjab, Pakistan. *Pak J Zool*. 2017;49(3):1119–1122. doi:10.17582/journal.pjz/2017.49.3.sc4
- Shams N, Amjad S, Yousaf N, Ahmed W, Seetlani NK, Farhat S. Dengue knowledge in indoor dengue patients from low socioeconomic class; aetiology, symptoms, mode of transmission and prevention. *J Ayub Med Coll Abbottabad*. 2018;30(1):40–44. [Medline](#)
- Suleman M, Faryal R, Alam MM, Khurshid A, Sharif S, Shaikat S, Angez M, Umair M, Sufian MM, Arshad Y, et al. Outbreak of dengue virus type-3 in Malakand, Pakistan 2015; A laboratory perspective. *Acta Trop*. 2017a;169:202–206. doi:10.1016/j.actatropica.2017.02.011 [Medline](#)
- Suleman M, Faryal R, Alam MM, Sharif S, Shaikat S, Aamir UB, Khurshid A, Angez M, Umair M, Sufian MM, et al. Dengue virus serotypes circulating in Khyber Pakhtunkhwa province, Pakistan, 2013–2015. *Ann Lab Med*. 2017b;37(2):151–154. doi:10.3343/alm.2017.37.2.151 [Medline](#)
- Waseem T, Latif H, Shabbir B. An unusual cause of acute abdominal pain in dengue fever. 2014. *Am J Emerg Med*. 32(7):819–3–4.
- WHO. Dengue in Pakistan. *Weekly Epidemiological Monitor*. World Health Organization. 2013 Dec 29;6(52).
- Zafar H, Hayyat A, Akhtar N, Rizwan SF. Prevalence of undifferentiated fever in adults of Rawalpindi having primary dengue fever. *J Pak Med Assoc*. 2013;63(6):770–771. [Medline](#)
- Zubair M, Ashraf M, Ahsan A, Nazir NU, Hanif H, Khan HA. Dengue viral infections in Pakistan and other Asian countries: a comprehensive review. *J Pak Med Assoc*. 2016;66(7):884–888. [Medline](#)

Dependence of Colonization of the Large Intestine by *Candida* on the Treatment of Crohn's Disease

KINGA KOWALSKA-DUPLAGA¹, AGNIESZKA KRAWCZYK², AGNIESZKA SROKA-OLEKSIAK^{2,3},
DOMINIKA SALAMON², ANDRZEJ WĘDRYCHOWICZ¹, KRZYSZTOF FYDEREK¹ and TOMASZ GOSIEWSKI^{2*} 

¹Department of Pediatrics, Gastroenterology and Nutrition, Faculty of Medicine,
Jagiellonian University Medical College, Krakow, Poland

²Department of Molecular Medical Microbiology, Chair of Microbiology, Faculty of Medicine,
Jagiellonian University Medical College, Krakow, Poland

³Department of Mycology, Chair of Microbiology, Faculty of Medicine,
Jagiellonian University Medical College, Krakow, Poland

Submitted 6 November 2018, revised 9 December 2018, accepted 17 December 2018

Abstract

The aim of this study was to determine if there are quantitative differences in *Candida* fungi between pediatric patients with Crohn's disease (before and after exclusive enteral nutrition (EEN), and the biologic therapy with anti-tumor necrosis factor alpha – (IFX)), and healthy controls. DNA was isolated from fecal samples and PCR was used to determine the number of fungal cells. Both therapeutic interventions resulted in a statistically significant decrease in Pediatric Crohn's Disease Activity Index. The numbers of *Candida* decreased during both therapeutic intervention but the difference was statistically significant for the IFX intervention only ($p=0.045$). Moreover, fungi population in both study groups declined during intervention when compared to the control group but the difference was significant before treatment only in the IFX group ($p=0.013$). The total distribution of *Candida* with both IFX and EEN as well as in the control group differed significantly ($p=0.01$) before treatment only. No correlation between the numbers of *Candida* and disease activity as well as the following biochemical parameters: serum iron concentration, protein or glucose level were found. It cannot be ruled out that, in combination with genetic and immunological disorders, fungi can contribute to the initiation of the disease process and perpetuation of active inflammation.

Key words: Crohn's disease; children; gut microbiota; biological treatment

Introduction

Crohn's disease (CD) together with ulcerative colitis belongs to the group of disorders known as inflammatory bowel diseases (IBD). The etiology of Crohn's disease still remains not fully explained, although the changes in the composition and distribution of intestinal microbiome seem to play a crucial role in the development and persistence of inflammation in the gastrointestinal tract (Kostic et al. 2014; Scarpellini et al. 2015). It is still under debate if the changes in the microbiome in IBD are a cause or a consequence of inflammation.

Pediatric-onset CD is on the increase worldwide (Benchimol et al. 2017; Ng et al. 2017). Many young patients present with an extensive and aggressive course

of the disease, which is a real therapeutic challenge. Treatment of CD is a complex, multistage process and depends on the type and clinical activity of the illness. ECCO/ESPGHAN guidelines recommend the usage of exclusive enteral nutrition (EEN) as a first-line therapy to induce remission in pediatric patients with mild to moderate CD (Ruemmele et al. 2014). EEN used as induction therapy should last from six to eight weeks and is usually based on standard, liquid, polymeric formulas. During this period, any other types of food are withdrawn and patients receive liquid diet orally or through a nasogastric tube, which covers full caloric and nutritional demand adjusted to the patient's requirements. Maintenance of remission can be achieved with thiopurines or methotrexate. This therapeutic approach is called conventional therapy.

* Corresponding author: T. Gosiewski, Department of Molecular Medical Microbiology, Chair of Microbiology, Faculty of Medicine, Jagiellonian University Medical College, Krakow, Poland; e-mail: tomasz.gosiewski@uj.edu.pl

© 2019 Kinga Kowalska-Duplaga et al.

This work is licensed under the Creative Commons Attribution-NonCommercial-NoDerivatives 4.0 License (<https://creativecommons.org/licenses/by-nc-nd/4.0/>)

The biologic therapy with anti-tumor necrosis factor alpha (anti-TNF α) is recommended for treatment of patients with moderate to severe CD who didn't respond to conventional treatment (with thiopurines or methotrexate). Infliximab (IFX) is the biologic agent used most often as a first-line treatment in the pediatric population. Induction doses of 5 mg/kg are given intravenously in 0, 2 and 6 weeks mode, followed by maintenance infusions every eight weeks (Hyams et al. 2007).

The majority of IBD therapies are focused on controlling inflammation, but the question of how or whether the clinical status of patients is related to the microbiome remains unanswered. The human gastrointestinal tract contains a wide range of archaea, prokaryota, eukaryota and viruses.

As mentioned above, studies are available in the literature that concern changes in the bacterial flora of the human gastrointestinal tract in the course of IBD; however, there are few articles describing the study of anti-*Candida* antibodies and methods based on the fungi cultures (McKenzie et al. 1990; Standaert-Vitse et al. 2006; Standaert-Vitse et al. 2009). Hence, the primary objective of the present study was to determine if there are quantitative differences in *Candida* fungi (by quantitative real-time PCR (qPCR)) between pediatric patients with CD and healthy controls. Another aim of this study was to compare the quantitative differences in *Candida* fungi in the newly diagnosed CD during EEN and those who were qualified for biologic therapy and to find out whether these differences correlate with the selected biochemical and clinical parameters.

Experimental

Materials and Methods

Patients. We performed a single-center prospective study to examine the *Candida* population in CD patients hospitalized in University Children's Hospital in Krakow, Poland.

Patients aged 2 to 18 years diagnosed with CD according to the revised Porto criteria (Levine et al. 2014) were enrolled into two study groups.

The study protocol was approved by Jagiellonian University Ethics Committee – the decision no. 122.6120.68.2015. The informed consent was signed by patients' parents or legal guardians and by patients themselves if above 16 years of age.

Group 1 consisted of newly diagnosed children, who received EEN for the induction of remission. In this group, we collected two stool samples: the first one (N1) before any therapeutic intervention and the second (N2) 2 to 4 weeks after completing EEN. In a group 2, there were CD patients who failed to respond or stopped

responding to conventional maintenance treatment (with thiopurines or methotrexate) and therefore were qualified for biologic therapy. Stool samples were collected prior to the first dose of IFX (Remsima[®], Celltrion Healthcare, Incheon, Korea) (B1) and then 4 weeks after the 3rd induction dose (B2).

The exclusion criteria comprised the following: 1) age of patient below two years old or above 18 years of age; 2) treatment with antibiotics (including antimycotic antibiotics) and probiotics during the period of 3 months before collecting the stool sample; 3) confirmed infections of the gastrointestinal tract; 4) any active neoplastic diseases (particularly of the gastrointestinal tract); 5) confirmed immunodeficiency.

The control group consisted of healthy children who didn't meet the exclusion criteria. In this group, we collected one stool sample.

Tests. In all CD patients, we routinely checked hematological and biochemical parameters, collected stool samples and calculated the Pediatric Crohn's Disease Activity Index (PCDAI). All these tests were carried out at the University Children's Hospital in Krakow, Poland.

The stool samples were delivered to the Chair of Microbiology of the Jagiellonian University Medical College in deep-freeze conditions (-70°C).

DNA extraction from the stool samples. The frozen samples were thawed, precisely weighed (about 0.1 g of stool sample was used) and homogenized in 0.1 ml of saline. DNA extraction from all samples was performed using the Genomic Mini AX Stool Spin Kit (A&A Biotechnology, Gdańsk, Poland), according to the manufacturer's recommendations, with our own modification (Gosiewski et al. 2014; Salamon et al. 2018). After lysis of bacterial and fungal cells with lysozyme (Sigma-Aldrich, Poznań, Poland) (1 mg/ml) and lysostaphin (Sigma-Aldrich, Poznań, Poland) (0.1 mg/ml), the samples were incubated at 37°C for 20 min. Next, 200 μl 75 mM NaOH (Avantor Performance Materials, Gliwice, Poland) was added and the samples were incubated at 95°C for 10 min. After incubation, the samples were microcentrifuged (12 000 rpm, 10 min), supernatants were removed, and the pellets were resuspended in 500 μl of the buffer supplemented with β -mercaptoethanol (Sigma-Aldrich, Poznań, Poland). For each sample, lyticase (Sigma-Aldrich, Poznań, Poland) was added (0.1 mg/ml). The samples were incubated at 37°C for at least 30 min and microcentrifuged (12 000 rpm, 10 min). The next steps of DNA extraction were carried out according to A&A Biotechnology's procedure.

Quantitative real-time PCR (qPCR). *Candida* spp. in the fecal samples were quantified by qPCR, as described by Gosiewski et al. (2014). To detect specific DNA sequences, ready-to-use JumpStart TaqReadyMix (Sigma-Aldrich, Poznań, Poland) kit, fluorescently

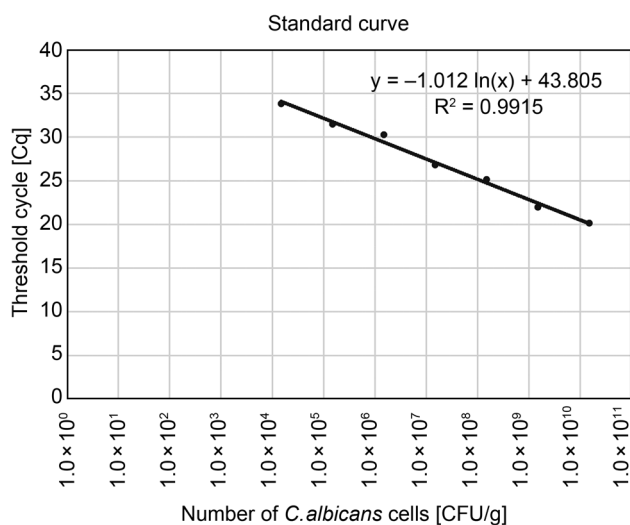


Fig. 1. A RT-PCR standard curve by plotting the threshold cycle (Cq) versus the number of *C. albicans* ATCC10231 (CFU/g). The DNA was amplified with the primers labeled with FAM.

FAM dye labelled probe (FAM-5'-TTAACCTAC-TAAATAGTGCTGCTAGC-3'-BHQ1) and pairs of specific primers (Genomed, Warszawa, Poland): (F) 5'-TTGGTGGAGTGATTTGTCTGCT-3'; (R) 5'-TCTAAGGGCATCACAGACCTG-3' (Genomed) for *Candida* were used (Sugita et al. 2012). A standard curve was prepared. DNA from the given numbers of *C. albicans* ATCC10231 was added in serial dilutions from 10^1 to 10^7 cells (in a volume of 1 ml saline ~ 1 g) to a series of qPCRs. The reactions were carried out in a CFX96 thermocycler (BioRad, California, USA). A standard curve from these data is shown in Fig. 1. Detection and quantitation were linear over the range of the DNA concentrations examined. To determine the number of *Candida* cells, the fluorescent signals detected from DNA of stool samples (in duplicate) in the linear range of the assay were averaged and compared to the standard curve.

Statistical analysis. Descriptive statistics were calculated for quantitative variables. In the case of variables following a normal distribution, means and standard deviations were presented. For variables demonstrating distribution other than normal, medians and interquartile ranges were used. The Mann-Whitney test was used to compare the differences between the two study groups and control. The Kruskal-Wallis test was applied for comparisons for all study groups. In the latter case, multiple comparisons of mean ranks for all groups were performed in order to assess the differences between pairs of groups. The correlation between variables was assessed with Spearman's rank correlation coefficient. Statistical analysis was carried out with the Statistica 13.1 (StatSoft, Inc. Tulsa, Oklahoma, USA) software.

Results

A total of 61 patients were enrolled in this study. Table I contains the baseline patient characteristics. The control group consisted of eight girls and nine boys, aged on average 140.76 months (± 34.58). Both therapeutic interventions resulted in a statistically significant decrease in disease activity assessed according to PCDAI. In group 2, the mean PCDAI was 47.5 points (ranged from 5 to 60 points) before induction therapy and decreased to a mean of 9.04 (ranged from 0 to 20) points ($p=0.00$). In group 1, the mean initial PCDAI was 32.03 points (ranged from 0 to 65) and dropped to a mean of 5.93 (ranged from 0 to 57.5) points ($p=0.00$).

The DNA sequences isolated from all 139 fecal samples were analyzed using qPCR. The presence of *Candida* DNA was assessed quantitatively by qPCR (Fig. 1 and Fig. 2).

The numbers of *Candida* decreased during the therapeutic intervention in both groups (Fig. 2). This

Table I
Baseline patient characteristics.

Characteristics	Biologic therapy - IFX (n=13)	EEN (n=48)	Control group (n=17)
Male:Female, n (%)	7 (54%):6 (46%)	29 (60%):19 (40%)	9 (53%):8 (47%)
Age at diagnosis, months; mean (\pm SD)	137 (± 48.15)	160.27 (± 37.11)	N/A
Age at initial treatment, months; mean (\pm SD)	157.15 (± 45.16)	160.27 (± 37.11)	N/A
Weight, kg; mean (\pm SD)	41.97 (± 16.3)	40.93 (± 14.05)	42.8 (± 17.2)
Height, cm; mean (\pm SD)	149.95 (± 20.31)	155.3 (± 19.1)	148.7 (± 18.8)
BMI, kg/m ² ; mean (\pm SD)	17.89 (± 3.62)	16.4 (± 2.92)	18.3 (± 3.8)
PCDAI-1; mean (\pm SD)	47.5 (± 16.43)	32.03 (± 15.01)	N/A
PCDAI-2; mean (\pm SD)	9.04 (± 6.5)	5.93 (± 11.36)	N/A

EEN - exclusive enteral nutrition; N/A - not applicable; PCDAI (Pediatric Crohn's Disease Activity Index):
1 - prior to therapeutic intervention, 2 - after therapeutic intervention

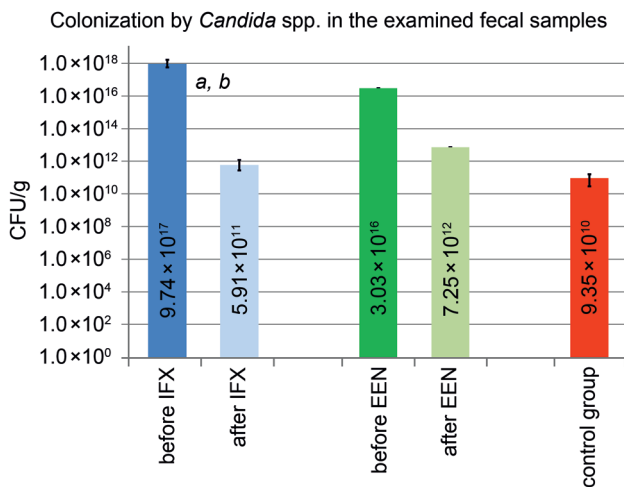


Fig. 2. Quantitative assessment of fungi of the genus *Candida* using qPCR in the stool of patients with CD before and after biologic (IFX) and exclusive enteral nutrition (EEN) treatments and control group.

a – significant differences between children with CD and the control group; b – significant differences between children with CD before and after biologic treatment.

difference was statistically significant in group 2 (IFX intervention) ($p=0.045$) but not in a group 1 (EEN intervention) ($p=0.626$). Additionally, fungi population in both studied groups declined during intervention when compared to the control group but the difference was significant before treatment only in IFX group ($p=0.013$) and in the EEN group, it was close to statistical significance ($p=0.056$) (Fig. 2).

The total distribution of *Candida* in the large intestine contents before treatment with both IFX and EEN as well as in the control group differed significantly ($p=0.01$). The total fungal distribution after treatment in the three groups was statistically insignificant ($p=0.39$).

We didn't find any correlation between the numbers of *Candida* and disease activity as well as with such biochemical parameters as serum iron concentration, protein or glucose level.

Discussion

The increasing occurrence of Crohn's disease and the decreasing age of patients stimulate researchers to find out the causes behind this illness (Benchimol et al. 2017; Ng et al. 2017). Although, until now, it has not been possible to associate a particular microorganism with CD etiology, microbial participation is still considered crucial, besides genetic and immunological disorders, for induction or intensification of inflammation in the gastrointestinal tract (Gosiewski et al. 2012; Wright et al. 2015). However, there is still insufficient knowledge concerning the role of fungi in the course of CD, as well as the impact of the treatment on gastro-

intestinal colonization with fungi of the genus *Candida* in IBD patients.

Research by Sokol et al. (2017) demonstrated a significant increase in the *Candida albicans* population size in patients with IBD in the period of disease exacerbation compared to the period of remission and healthy people. However, the authors did not analyze the influence of the treatment type on the observed change in mycobiota. Similar results were obtained by Standaert-Vitse et al. (2009) where CD patients were more frequently and more heavily colonized by *C. albicans* than the patients in the control group. As it was found in our study, the group undergoing biologic therapy showed significantly higher colonization with *Candida* spp. when compared to healthy children (Fig. 2). Additionally, the patients qualified for biologic therapy exhibited higher numbers of *Candida* fungal cells than the children qualified for nutritional treatment (Table I, Fig. 2); but, the difference between them was not statistically significant. It has to be noted that the clinical activity of the disease in patients qualified for biologic therapy was greater as compared to the group treated with EEN. A further difference was the disease duration, which was longer in the IFX group. It is also telling that these patients stayed longer in the hospital for anti-inflammatory and immunosuppressive treatment and also, in the past, could have undergone antibiotherapy more often. This is an implication that, with the increase in the activity of the disease and its duration, the numbers of *Candida* fungi also increased, which was also confirmed by Li et al. (2014). Moreover, the researchers found that in the inflamed colonic mucosa *Candida* fungi were more numerous than in non-inflamed areas and that the number of fungal cells correlated with overexpression of proinflammatory cytokines, i.e., TNF- α and IFN- γ . It might have been the cause behind the loss of tolerance to commensal fungi among the patients with CD, which resulted in immune disorders as a consequence of continuous induction of an inflammatory response (Li et al. 2014). A confirmation of this hypothesis can be the study by Iliev et al. (2012), which found that mice with Dectin-1 deficiency (it's a receptor responsible for recognition of fungal β -glucan) are substantially more susceptible to developing intestinal inflammation in comparison with mice without the gene knockout encoding this receptor. Furthermore, animals with disorders within Dectin-1 triggered the release of excessive amounts of TNF- α , IFN- γ and IL-17 against fungi within intestinal microbiota, including *Candida* spp. It is also worth noting that administering of antimycotic fluconazole to mice resulted in alleviating the symptoms of the disease (Iliev et al. 2012). These observations could confirm our results, in which the number of *Candida*, before the start of biologic therapy, were significantly higher than

two weeks after its completion ($p=0.045$) (Fig. 2). The strong anti-inflammatory activity of IFX enables the healing of the intestinal mucosa, which has probably reduced the gastrointestinal colonization with fungi. This effect was less visible in the case of EEN treatment when the reduction in the number of fungi was on the borderline of significance ($p=0.056$) (Fig. 2).

Zwolinska-Wcislo et al. (2009) demonstrated, in an animal model, similar observations as regards the effectiveness of treatment of patients with inflammatory bowel diseases using antifungal agents and a significant clinical improvement following treatment with fluconazole.

Our research demonstrated that the IFX therapy translated into a statistically significant reduction in the number of fungi of the genus *Candida*, which following induction therapy was comparable to the number of fungi colonizing the gastrointestinal tract in healthy children (Fig. 2).

A large number of *Candida* fungi in newly diagnosed patients (EEN group) and those with very high disease activity (IFX group) may be the result of a long-term disease process but may also indicate the participation of fungi in the pathogenesis of CD. It cannot be ruled out that in combination with genetic and immunological disorders, fungi can contribute not only to the initiation of the disease process but also play a role in maintaining an active inflammation. None of the applied therapeutic interventions has a documented direct effect on mycobiome. However, both methods of treatment have a proven effect on the so-called mucosal healing. It can be presumed that the reduction in the number of *Candida* is an indicator of recovery and improvement of the defensive role of the mucosal barrier.

This study provides additional information to the multifactorial nature of CD and may contribute to the modification of therapeutic approach.

ORCID

Tomasz Gosiewski [0000-0003-4725-5943](https://orcid.org/0000-0003-4725-5943)

Acknowledgments

The work was supported by Jagiellonian University Medical College in Poland within the framework of project grant no. K/ZDS/007044. Language translation: Catherine Ridgetile.

Conflict of interest

The authors do not report any financial or personal connections with other persons or organizations, which might negatively affect the contents of this publication and/or claim authorship rights to this publication.

Literature

Benchimol EI, Bernstein CN, Bitton A, Carroll MW, Singh H, Otley AR, Vutcovici M, El-Matary W, Nguyen GC, Griffiths AM, et al. Trends in epidemiology of pediatric inflammatory bowel

disease in Canada: Distributed network analysis of multiple population-based provincial health administrative databases. *Am J Gastroenterol.* 2017;112(7):1120–1134. doi:10.1038/ajg.2017.97 Medline

Gosiewski T, Salamon D, Szopa M, Sroka A, Malecki MT, Bulanda M. Quantitative evaluation of fungi of the genus *Candida* in the feces of adult patients with type 1 and 2 diabetes – a pilot study. *Gut Pathog.* 2014;6(1):43. doi:10.1186/s13099-014-0043-z Medline

Gosiewski T, Strus M, Fyderek K, Kowalska-Duplaga K, Wedrychowicz A, Jedynak-Wasowicz U, Sladek M, Pieczarkowski S, Adamski P, Heczko PB. Horizontal distribution of the fecal microbiota in adolescents with inflammatory bowel disease. *J Pediatr Gastroenterol Nutr.* 2012;54(1):20–27. doi:10.1097/MPG.0b013e31822d53e5 Medline

Hyams J, Crandall W, Kugathasan S, Griffiths A, Olson A, Johans J, Liu G, Travers S, Heuschkel R, Markowitz J, et al. REACH Study Group. Induction and maintenance infliximab therapy for the treatment of moderate-to-severe Crohn's disease in children. *Gastroenterology.* 2007;132(3):863–873. doi:10.1053/j.gastro.2006.12.003 Medline

Iliev ID, Funari VA, Taylor KD, Nguyen Q, Reyes CN, Strom SP, Brown J, Becker CA, Fleshner PR, Dubinsky M, et al. Interactions between commensal fungi and the C-type lectin receptor Dectin-1 influence colitis. *Science.* 2012;336(6086):1314–1317. doi:10.1126/science.1221789 Medline

Kostic AD, Xavier RJ, Gevers D. The microbiome in inflammatory bowel disease: current status and the future ahead. *Gastroenterology.* 2014;146(6):1489–1499. doi:10.1053/j.gastro.2014.02.009 Medline

Levine A, Koletzko S, Turner D, Escher JC, Cucchiara S, de Ridder L, Kolho K-L, Veres G, Russell RK, Paerregaard A, et al.; European Society of Pediatric Gastroenterology, Hepatology, and Nutrition. ESPGHAN revised porto criteria for the diagnosis of inflammatory bowel disease in children and adolescents. *J Pediatr Gastroenterol Nutr.* 2014;58(6):795–806. doi:10.1097/MPG.000000000000239 Medline

Li Q, Wang C, Tang C, He Q, Li N, Li J. Dysbiosis of gut fungal microbiota is associated with mucosal inflammation in Crohn's disease. *J Clin Gastroenterol.* 2014;48(6):513–523. doi:10.1097/MCG.000000000000035 Medline

McKenzie H, Main J, Pennington CR, Parratt D. Antibody to selected strains of *Saccharomyces cerevisiae* (baker's and brewer's yeast) and *Candida albicans* in Crohn's disease. *Gut.* 1990;31(5):536–538. doi:10.1136/gut.31.5.536 Medline

Ng SC, Shi HY, Hamidi N, Underwood FE, Tang W, Benchimol EI, Panaccione R, Ghosh S, Wu JCY, Chan FKL, et al. Worldwide incidence and prevalence of inflammatory bowel disease in the 21st century: a systematic review of population-based studies. *Lancet.* 2017;390(10114):2769–2778. doi:10.1016/S0140-6736(17)32448-0 Medline

Ruemmele FM, Veres G, Kolho KL, Griffiths A, Levine A, Escher JC, Amil Dias J, Barabino A, Braegger CP, Bronsky J, et al.; European Crohn's and Colitis Organisation; European Society of Pediatric Gastroenterology, Hepatology and Nutrition. Consensus guidelines of ECCO/ESPGHAN on the medical management of pediatric Crohn's disease. *J Crohn's Colitis.* 2014; 8(10):1179–1207. doi:10.1016/j.crohns.2014.04.005 Medline

Salamon D, Sroka-Oleksiak A, Kapusta P, Szopa M, Mrozińska S, Ludwig-Słomczyńska AH, Wołkow PP, Bulanda M, Klupa T, Małcki MT, et al. Characteristics of the gut microbiota in adult patients with type 1 and 2 diabetes based on the analysis of a fragment of 16S rRNA gene using next-generation sequencing. *Polish Arch Intern Med.* 2018;128:336–343. doi:10.20452/pamw.4246 Medline

Scarpellini E, Ianiro G, Attili F, Bassanelli C, De Santis A, Gasbarrini A. The human gut microbiota and virome: potential

therapeutic implications. *Dig Liver Dis.* 2015;47(12):1007–1012. doi:10.1016/j.dld.2015.07.008 [Medline](#)

Sokol H, Leducq V, Aschard H, Pham HP, Jegou S, Landman C, Cohen D, Liguori G, Bourrier A, Nion-Larmurier I, et al. Fungal microbiota dysbiosis in IBD. *Gut.* 2017;66(6):1039–1048. doi:10.1136/gutjnl-2015-310746 [Medline](#)

Standaert-Vitse A, Jouault T, Vandewalle P, Mille C, Seddik M, Sendid B, Mallet JM, Colombel JF, Poulain D. *Candida albicans* is an immunogen for anti-*Saccharomyces cerevisiae* antibody markers of Crohn's disease. *Gastroenterology.* 2006;130(6):1764–1775. doi:10.1053/j.gastro.2006.02.009 [Medline](#)

Standaert-Vitse A, Sendid B, Joossens M, François N, Vandewalle-El Khoury P, Branche J, Van Kruiningen H, Jouault T, Rutgeerts P, Gower-Rousseau C, et al. *Candida albicans* colonization and ASCA in familial Crohn's disease. *Am J Gastroenterol.* 2009;104(7):1745–1753. doi:10.1038/ajg.2009.225 [Medline](#)

Sugita S, Kamoi K, Ogawa M, Watanabe K, Shimizu N, Mochizuki M. Detection of *Candida* and *Aspergillus* species DNA using broad-range real-time PCR for fungal endophthalmitis. *Graefes Arch Clin Exp Ophthalmol.* 2012;250(3):391–398. doi:10.1007/s00417-011-1819-1 [Medline](#)

Wright EK, Kamm MA, Teo SM, Inouye M, Wagner J, Kirkwood CD. Recent advances in characterizing the gastrointestinal microbiome in Crohn's disease: a systematic review. *Inflamm Bowel Dis.* 2015;21:1. <http://www.ncbi.nlm.nih.gov/pubmed/25844959>. doi:10.1097/MIB.0000000000000382 [Medline](#)

Zwolinska-Wcislo M, Brzozowski T, Budak A, Kwiecien S, Sliwowski Z, Drozdowicz D, Trojanowska D, Rudnicka-Sosin L, Mach T, Konturek SJ, et al. Effect of *Candida* colonization on human ulcerative colitis and the healing of inflammatory changes of the colon in the experimental model of colitis ulcerosa. *J Physiol Pharmacol.* 2009;60(1):107–118. [Medline](#)

Predominance of *Lactobacillus plantarum* Strains in Peruvian Amazonian Fruits

JOHANNA SÁNCHEZ^{1*}, CARLOS VEGAS¹, AMPARO IRIS ZAVALA¹ and BRAULIO ESTEVE-ZARZOSO²

¹Laboratorio de Biología Molecular, Facultad de Farmacia y Bioquímica,
Universidad Nacional Mayor de San Marcos, Lima, Perú

²Departament de Bioquímica i Biotecnologia, Facultat d' Enologia, Universitat Rovira i Virgili, Tarragona, Spain

Submitted 18 October 2018, revised 12 December 2018, accepted 3 January 2019

Abstract

The objective of this research was the identification and characterization of lactic acid bacteria (LAB) isolated from Peruvian Amazonian fruits. Thirty-seven isolates were obtained from diverse Amazonian fruits. Molecular characterization of the isolates was performed by ARDRA, 16S-23S ITS RFLP and rep-PCR using GTG₅ primers. Identification was carried out by sequencing the 16S rDNA gene. Phenotypic characterization included nutritional, physiological and antimicrobial resistance tests. Molecular characterization by Amplified Ribosomal DNA Restriction Analysis (ARDRA) and 16S-23S ITS RFLP resulted in four restriction profiles while GTG₅ analysis showed 14 banding patterns. Based on the 16S rDNA gene sequence, the isolates were identified as *Lactobacillus plantarum* (75.7%), *Weissella cibaria* (13.5%), *Lactobacillus brevis* (8.1%), and *Weissella confusa* (2.7%). Phenotypic characterization showed that most of the isolates were homofermentative bacilli, able to ferment glucose, maltose, cellobiose, and fructose and grow in a broad range of temperatures and pH. The isolates were highly susceptible to ampicillin, amoxicillin, clindamycin, chloramphenicol, erythromycin, penicillin, and tetracycline and showed great resistance to kanamycin, gentamycin, streptomycin, sulfamethoxazole/trimethoprim, and vancomycin. No proteolytic or amylolytic activity was detected. *L. plantarum* strains produce lactic acid in higher concentrations and *Weissella* strains produce exopolymers only from sucrose. Molecular methods allowed to accurately identify the LAB isolates from the Peruvian Amazonian fruits, while phenotypic methods provided information about their metabolism, physiology and other characteristics that may be useful in future biotechnological processes. Further research will focus especially on the study of *L. plantarum* strains.

Key words: Peruvian Amazonian fruits, *Lactobacillus*, *Weissella*, ARDRA, 16S-23S ITS RFLP, GTG₅

Introduction

Lactic acid bacteria (LAB) are Gram-positive, non-sporulating, microaerophilic bacteria that produce mainly lactic acid as a product of carbohydrate fermentation product. LAB are among the most widespread group of microorganisms isolated from various sources in nature, most of which related to the presence of sugar (Liu et al. 2014). LAB isolated from the natural environments may possess special characteristics including phenotypic differences and high intraspecific variability compared with culture collection strains (Fortina et al. 1998).

Previous research has reported the isolation and identification of LAB from different fruits such as ripe mulberries, pineapples, wine grapes, cherries, apples, peaches, prickly pears, bananas and others (Bae et al. 2006; Trias et al. 2008; Chen et al. 2010; Di Cagno et al.

2010; Verón et al. 2017; Abubakr and Al-Adiwish 2017). The most commonly isolated LAB species in these studies were *W. cibaria*, *L. plantarum*, *Leuconostoc mesenteroides*, *Enterobacter* sp. and *Lactococcus* sp. The Peruvian Amazon is a source of a great diversity of fruits which in some cases are consumed by the population as fresh fruits or constitute raw materials for the preparation of different products (juices, ice cream, jams or desserts). They are offered in local markets and provide a great contribution to the regional economy. Peruvian Amazonian fruits grow in conditions of temperature, humidity, and rainfall that differ from those found in the rest of the country. These environmental conditions, in addition to other extrinsic and intrinsic factors, influence fruits microbiology making them an interesting source of microorganisms with unique characteristics of potential use in the industry as starter cultures, probiotics or the production of metabolites such as lactic

* Corresponding author: J. Sánchez, Laboratorio de Biología Molecular, Facultad de Farmacia y Bioquímica, Universidad Nacional Mayor de San Marcos, Lima, Perú; e-mail: jfsanchezdavila@yahoo.com

© 2019 Johanna Sánchez et al.

This work is licensed under the Creative Commons Attribution-NonCommercial-NoDerivatives 4.0 License (<https://creativecommons.org/licenses/by-nc-nd/4.0/>)

acid or exopolysaccharides. Different studies have been performed in order to take advantage of the diversity of Peruvian Amazonian fruits, but there is neither relevant information on the microbiota that colonizes the surface of the fruits nor the potential of these microorganisms.

Selection of biotechnologically useful strains requires accurate identification and characterization. As many LAB show similar nutritional and growth requirements, the biochemical tests for identification sometimes fail, leading to erroneous species identification. Some of the most common physiological tests are included in commercially available systems, such as those specially designed for LAB identification, the API 50CHL (Biomérieux, Marcy l'étoile, France) kit, which tests for 49 carbohydrates and esculin. Other systems designed for Gram-positive or Gram-negative bacteria have been applied to LAB identification, such as the Biolog system, which includes the fermentation of 96 carbohydrates (Moraes et al. 2013). On the other hand, the development of molecular techniques has allowed more accurate identification of LAB. The wide method used for this purpose is based on ribosomal gene sequencing or restriction analysis of the amplified product. These genes are conserved among bacteria but show small variations that allow LAB species identification (Mohania et al. 2008). Using ARDRA of 16S rDNA it is possible to differentiate the main LAB present in wine fermentation (Rodas et al. 2003), but to ensure the identification many authors have used the sequencing of the complete 16S rDNA gene (Reginensi et al. 2013). Although the sequencing of 16S rRNA genes is still con-

sidered the gold standard for bacterial identification, in recent years laser desorption ionization-time of flight mass spectrometry (MALDI-TOF MS) has emerged as a useful technique for microbial identification. It has already been used in different investigations for the identification of pathogenic bacteria, viruses, and fungi. Although the technique has the advantage of being fast and sensitive, its main disadvantage is the high initial cost of equipment and reagents (Singhal et al. 2015).

Although the main phenotypic characteristics of the LAB are common to all strains in a species, the characteristics of interest generally are specific to a strain, and for this reason, a method of strain discrimination should be applied (Kingston et al. 2010). The method most widely used for strain discrimination in LAB has been PCR amplification using the primers M13 (Andrighetto et al. 2001) or GTG₅ (Gevers et al. 2001).

The main focus of the present study was the isolation of LAB from Peruvian Amazonian fruits and their identification and characterization by phenotypic and molecular methods.

Experimental

Materials and Methods

Fruits. Thirteen fresh fruits were collected in July 2016 in a small rustic market of Iquitos, a city located in the Amazonian region of Peru in the northeastern part of the country. The thirteen fruits were chosen for their abundance at the time of sampling. (Table I). Accord-

Table I
Peruvian Amazonian fruits used to isolate lactic acid bacteria. Scientific and Peruvian names have been included together with the LAB species isolated.

Scientific name	Peruvian name	No. LAB strains isolated	LAB Species (No. strains)
<i>Anacardium occidentale</i>	Casho	2	<i>Lactobacillus plantarum</i> (1) <i>Weissella confusa</i> (1)
<i>Averrhoa carambola</i>	Carambola	0	–
<i>Bactris gasipaes</i>	Pijuayo	5	<i>Lactobacillus plantarum</i> (3) <i>Weissella cibaria</i> (2)
<i>Genipa americana</i>	Huito	5	<i>Lactobacillus plantarum</i> (5)
<i>Mauritia flexuosa</i>	Aguaje	0	–
<i>Mauritiella aculeate</i>	Aguajillo	3	<i>Lactobacillus plantarum</i> (3)
<i>Myrciaria dubia</i>	Camu camu	0	–
<i>Oenocarpus bataua</i>	Ungurahui	5	<i>Lactobacillus plantarum</i> (2) <i>Lactobacillus brevis</i> (3)
<i>Passiflora edulis</i>	Maracuyá	4	<i>Lactobacillus plantarum</i> (4)
<i>Passiflora nitida</i>	Granadilla	5	<i>Lactobacillus plantarum</i> (5)
<i>Poraqueiba sericea</i>	Umari	2	<i>Lactobacillus plantarum</i> (2)
<i>Psidium guajava</i>	Guayaba	5	<i>Lactobacillus plantarum</i> (2) <i>Weissella cibaria</i> (3)
<i>Solanum sessiliflorum</i>	Cocona	1	<i>Lactobacillus plantarum</i>

ing to the size, 3 or 4 pieces of each fruit were used to perform the microbiological analysis. After selection of ripe fruits with no apparent spoilage, fruits were placed in sterile plastic bags. Samples were refrigerated and shipped to the laboratory for analysis.

Isolation and presumptive selection of lactic acid bacteria. Surface sampling of the entire fruits was done using swabs wet with 0.85% NaCl. After sampling the cotton part of the swabs were placed in Man Rogosa Sharpe (MRS) (Merck, Darmstadt, Germany) broth in anaerobic conditions at 30°C for 48 h using an Anaerocult system (Merck, Darmstadt, Germany). One hundred microliters of the enriched cultures were spread on MRS agar (Merck, Darmstadt, Germany) and incubated at 30°C for 48 h in anaerobiosis. Five colonies were randomly isolated from each fruit. To check the purity of the isolates, they were streaked out on MRS plates three times, after that, they were kept in 50% glycerol at -20°C. Further cultivation was done in MRS medium.

Cultures of 48 h were used to observe cell morphology of the presumptive LAB strains in a contrast microscope (Beltec Scientific). These cultures were also used to perform Gram staining and catalase activity with 3% hydrogen peroxide. Acid production was performed by adding 2% CaCO₃ to MRS plates. Gram-positive, catalase-negative and acid producer isolates were considered presumptive LAB.

Molecular characterization and identification. From an overnight culture, 1 ml of each culture was used for bacterial DNA extraction according to the procedure of Ausubel et al. (2003). DNA was resuspended in 50 µl of TE and stored at -20°C until use. Identification and characterization of the bacterial isolates were performed by ARDRA, 16S-23S ITS RFLP and rep-PCR using GTG₅ primers. ARDRA was done by amplification and digestion of the 16S rDNA gene, amplification was performed according to Rodas et al. (2003) using a Perkin Elmer 2400 (Norwalk, USA) thermal cycler and *Taq* DNA polymerase (Thermo Scientific, Massachusetts, USA). Digestion was carried out using the restriction enzymes *AluI*, *HaeIII* (Thermo Scientific, Massachusetts, USA) and *MseI* (Biolabs, Massachusetts, USA) according to the manufacturer instructions. PCR products or restriction fragments were run in a 1% or 2.5% (respectively) agarose gels using TBE 1X. A 100 bp Marker (GeneRules 100 bp Plus Ladder) was used to estimate fragment size. Agarose gels were stained with ethidium bromide for 20 min and revealed using a UV transilluminator (UVP Ultra-violet Products). For 16S-23S ITS RFLP, amplification of 16S-23S ITS region was performed using a modification of the procedure of Zavaleta et al. (1996), but we shorten the annealing and elongation steps from 1 min in the original protocol to 45 sec. Then, sequential restriction digestion was performed with enzymes *HaeIII* and *TaqI*

(Thermo Scientific, Massachusetts, USA) according to the manufacturer instructions (first 16 h at 37°C and then 6 h at 65°C after *TaqI* addition). Gel electrophoresis and visualization was performed as described before. Strain characterization by rep-PCR using GTG₅ primer was done as described in Gevers et al. (2001). PCR products were run in 1% agarose gels using TBE 1X, and Lambda/*EcoRI*+*HindIII* was used as a molecular weight marker. LAB identification was performed by 16S rDNA gene sequencing of representative isolates of different profiles obtained by rep-PCR. The 16S rDNA gene sequencing analysis was done at Macrogen Inc. (Seoul, Korea) using an ABI3730 XL DNA sequencer. The sequence homology searching against databases was done using the BLAST software from NCBI database (<http://blast.ncbi.nlm.nih.gov>). Accession numbers were assigned to all the sequences deposited in the GenBank database (Table II). Information available on NCBI of the 16S rDNA nucleotide sequences was used to construct a phylogenetic tree using the Mega version 7.0 program (BioDesign Institute, Tempe, AZ, USA) using the Neighbor-joining method.

The species *L. plantarum*, *L. pentosus* and *L. paraplantarum* were differentiated using the amplification of the *recA* gene as described by Torriani et al. (2001).

Phenotypic characterization. The different assays were in all cases performed at 30°C for 48 h under anaerobic conditions. Methods for LAB identification were used according to Sharpe (1979); in all assays, the inoculum was approximately 1–2 × 10⁸ cells/ml. The growth capacity was evaluated in MRS medium under different conditions of pH (3.5 and 7.5), temperature (10°C and 45°C), and in the presence of NaCl (5%, 10%, and 12.5%). Bacterial growth was evaluated by measurement of the optical density at 620 nm in a Genesys 10S UV-Vis spectrophotometer (Thermo Scientific, Waltham, USA).

The sugar fermentation pattern was done according to MacFaddin (2000) in phenol red broth with 1% of each sugar to be analyzed (glucose, fructose, galactose, maltose, lactose, cellobiose, and sucrose). Positive results were considered after the change from the red color of the medium to yellow. Additionally, only in glucose tubes, an inverted Durham tube was included to test for the production of CO₂. After incubation under the same conditions, a test was considered positive if gas was present inside the Durham tube.

Extracellular enzymes production was also analyzed. Proteolytic activity was measured in MRS with 1% skimmed milk medium (Jini et al. 2011). Positive production was considered when a clear area around a colony was produced. Amyolytic activity was tested on agar MRS after replacement of glucose with 1.5% starch (Díaz-Ruiz et al. 2003). Starch hydrolysis was revealed by Lugol staining.

Table II
Molecular characterization and identification of the representative LAB isolates
from Peruvian Amazonian fruits.

Isolate	ARDRA (<i>AluI</i>) Restriction profile	16S-23S ITS RFLP Restriction profile	GTG ₅ Profile	16S GenBank Accession number	Final identification Species name
LBMBAL1	I	I _R	I.1	KY977384	<i>Lactobacillus plantarum</i>
LBMBAL 2			I.2	KY977388	<i>Lactobacillus plantarum</i>
LBMBAL 3			I.3	KY977397	<i>Lactobacillus plantarum</i>
LBMBAL 4			I.4	KY977386	<i>Lactobacillus plantarum</i>
LBMBAL 5			I.5	KY977393	<i>Lactobacillus plantarum</i>
LBMBAL 6			I.6	KY977394	<i>Lactobacillus plantarum</i>
LBMBAL 7			I.7	KY977399	<i>Lactobacillus plantarum</i>
LBMBAL 8			I.8	KY977398	<i>Lactobacillus plantarum</i>
LBMBAL 9	II	II _R	II.1	KY977400	<i>Lactobacillus brevis</i>
LBMBAL 10	III	III _R	III.1	KY977385	<i>Weissella confusa</i>
LBMBAL 11	IV	IV _R	IV.1	KY977390	<i>Weissella cibaria</i>
LBMBAL 12			IV.2	KY977391	<i>Weissella cibaria</i>
LBMBAL 13			IV.3	KY977392	<i>Weissella cibaria</i>
LBMBAL 14			IV.4	KY977395	<i>Weissella cibaria</i>

Susceptibility against some antimicrobials was tested using commercial paper discs (Oxoid) with the antimicrobial compound, as described in Bauer et al. (1966). According to the criteria of the European Food Safety Authority (EFSA, 2012) the antimicrobials selected were as follows: amoxicillin (10 µg), ampicillin (10 µg), bacitracin (10 µg), clindamycin (2 U), chloramphenicol (30 µg), erythromycin (15 µg), kanamycin (30 µg), gentamicin (10 µg), novobiocin (30 µg), penicillin (10 µg), rifampicin (30 µg), streptomycin (10 µg), sulfamethoxazole/trimethoprim (25 µg), tetracycline (30 µg), and vancomycin (30 µg). The bacterial susceptibility toward antibiotics was analyzed by the agar diffusion test on MRS or Kirby-Bauer disk-diffusion method. According to the presence or absence of bacterial growth around the antimicrobial disc, the colonies were classified as Resistant (R) or Sensitive (S) according to the criteria of Charteris et al. (1998).

Production of lactic acid and exopolymers (EPS) was also tested. Lactic acid production was evaluated according to Wakil and Ajayi (2013). EPS production was analyzed after 5 days of growth at 30°C in anaerobiosis on MRS plates supplemented with 2% of different sugars: glucose, maltose, fructose, and sucrose as described in Smitinont et al. (1999), development of mucoid colonies and precipitation of mucoid substance in cold absolute ethanol were considered positive for EPS production.

All phenotypic tests were carried out in duplicate to evaluate reproducibility according to the method proposed by Sneath and Johnson (1972). For acid lactic production, the mean of two measures was presented.

Results

Sixty-five isolates were obtained from the Amazonian fruits, of which thirty-seven Gram-positive, catalase-negative and acid producer isolates were selected as presumptive LAB (Table I). Colonies from these isolates were very small (1–3 mm), with creamy appearance, convex surface with entire margins and without pigments. Morphologically, 28 isolates were short bacilli and nine isolates were coccobacilli.

Molecular characterization of the LAB isolates by ARDRA showed three restriction profiles using the enzymes *MseI* and *HaeIII* and four profiles when performing the digestion with the enzyme *AluI*. 16S-23S ITS RFLP analysis also showed four restriction profiles, clustering the strains in the same way that it was observed with the ARDRA *AluI* analysis. Based on the 16S rRNA gene sequences, the 37 LAB isolates were identified as *L. plantarum* (28), *W. cibaria* (5), *L. brevis* (3) and *W. confusa* (1) (Table II). Multiplex PCR for *recA* amplification confirmed the identity of *L. plantarum* strains by obtaining amplicons of approximately 318 bp. GTG₅ analysis showed a total of 14 different banding patterns, which corresponded to 14 LAB strains (Fig. 2). Among then, *L. plantarum* and *W. cibaria* strains showed the highest intraspecific diversity with eight and four profiles, respectively. The phylogenetic tree constructed on the basis of the 16S ribosomal gene sequences separated LAB isolates into two large groups, one corresponding to the genus *Lactobacillus* and the other to *Weissella*; additionally, each group consisted of two subgroups correspond-

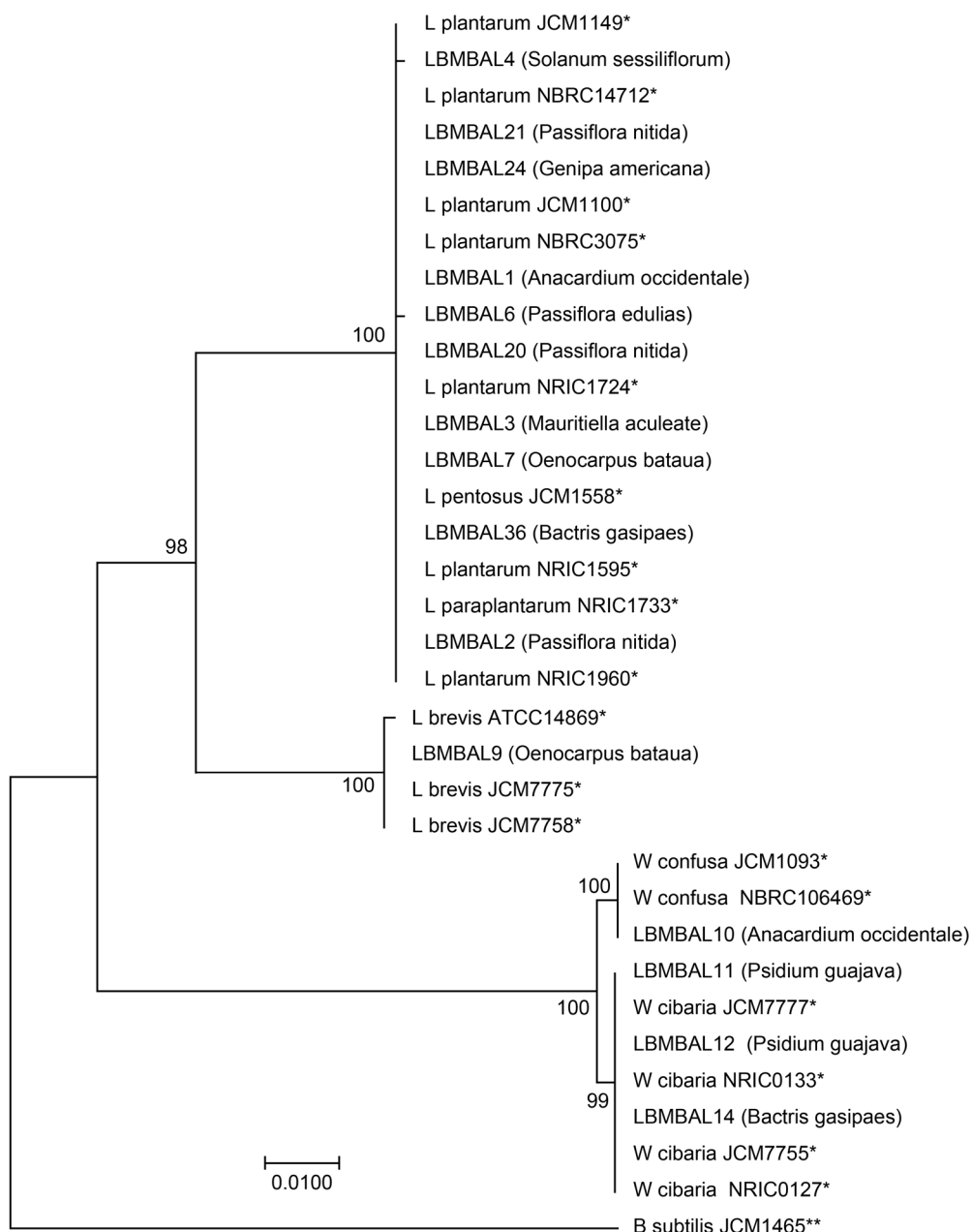


Fig. 1. Phylogenetic tree of LAB isolated from Amazonian Peruvian fruits based on the 16S rDNA sequences. Neighbor-Joining method and bootstrap 1000. Numbers in the nodes correspond to the percentage of bootstrap. The bar represents 1% divergence in the sequences.

* - LAB reference strains. ** - Outgroup. Parentheses include the name of the fruit from which the strain was isolated.

ing to *L. plantarum* and *L. brevis*, and *W. confusa* and *W. cibaria*, respectively. High bootstrap values (98–100) supported these groupings (Fig. 1).

Regarding phenotypic characterization (Table III), most of the isolates (92–100%) fermented glucose, fructose, cellobiose, and maltose but they showed differences in the uptake of the other sugars tested, being galactose and lactose the sugars with minor preference among the isolates. When CO₂ production was analyzed, 25 isolates showed homofermentative metabolism while 12 isolates were heterofermentatives. Growth evaluated at different conditions of temperature, pH

and NaCl showed that 95% to 100% of the isolates were able to grow between 10°C to 45°C, pH 3.5 to 7.5 and 5% NaCl, but only 62% of the isolates grew at 10% NaCl and none of them grew at 12.5% NaCl. No amylolytic or proteolytic activity was detected in the LAB isolates. Concerning antimicrobial susceptibility, the isolates showed high susceptibility (95–100%) to ampicillin, amoxicillin, clindamycin, chloramphenicol, erythromycin, penicillin, and tetracycline, on the contrary, the high resistance (98–100%) was observed against kanamycin, gentamicin, streptomycin, vancomycin, and sulfamethoxazole-thrimethoprim. Only for novobiocin

Table III
Phenotypic characteristics of LAB strains isolated from Peruvian Amazonian fruits.

Specie isolated	<i>Lactobacillus plantarum</i>	<i>Lactobacillus brevis</i>	<i>Weissella confusa</i>	<i>Weissella cibaria</i>
No. strains	28	3	1	5
Cell morphology	Rods	Rods	Cocobacilli	Cocobacilli
Fermentation of:				
Glucose	+	+	+	+
Fructose	+	+	+	+
Galactose	23/5	-	+	-
Sucrose	26/2	-	+	+
Maltose	+	-	+	+
Cellobiose	+	+	+	+
Lactose	24/4	-	-	-
CO₂ from glucose	-	-	+	+
Growth at:				
10°C	+	+	+	+
30°C	+	+	+	+
45°C	+	+	+	3/2
5% NaCl	+	+	+	+
10% NaCl	22/6	1/2	-	-
12.5% NaCl	-	-	-	-
pH 3.5	+	+	+	4/1
pH 7.5	+	+	+	+
Susceptibility to:				
Ampicillin (10 µg)	S	S	S	S
Amoxicillin (10 µg)	S	S	S	S
Bacitracin (10 µg)	R	R	S	S
Clindamycin (2 U)	S	R	S	S
Chloramphenicol (30 µg)	S	S	S	S
Erythromycin (15 µg)	S	S	S	S
Kanamycin (30 µg)	93%	R	R	R
Gentamicin (10 µg)	93%	R	R	R
Penicillin (10 µg)	S	S	R	S
Novobiocin (30 µg)	S	S	R	R
Streptomycin (10 µg)	R	R	R	R
Sulfamethoxazole/ trimethoprim (25 µg)	R	R	R	R
Tetracycline (30 µg)	S	S	S	S
Vancomycin (30 µg)	R	R	R	R
EPS production from:				
Sucrose	-	-	+	+
Glucose	-	-	-	-
Maltose	-	-	-	-
Fructose	-	-	-	-
Lactic acid production (g/l)	20.1 – 23.6	13.1 – 14.6	14.4	14.2 – 16.0

and bacitracin, the differences between bacilli and cocobacilli were observed, while all bacilli were resistant to bacitracin and susceptible to novobiocin, the opposite was observed in cocobacilli.

About EPS production, according to our methodology only isolates belonging to *Weissella* species produce EPS from sucrose but negative results were obtained when glucose, fructose or maltose was used as single

carbon source in the medium. With regard to acid lactic production, a wide range of production was observed (13.1 g/l to 23.6 g/l) being *L. plantarum* strains the higher lactic acid producer (Table III).

Discussion

This research work was interested in the isolation and characterization of LAB from Amazonian Peruvian fruits. Of the 13 fruits studied in three of them (*Myrciaria dubia*, *Averrhoa carambola* and *Mauritia flexuosa*), LAB was not detected on their surfaces. It is possible that the enrichment method used was not appropriate for the development of LAB that inhabit the surface of these fruits or may be the presence of other microorganisms colonizing the fruit surface set up some kind of competence for nutrients available on the surfaces. It is also possible that some intrinsic factors such as the great acidity given by the high vitamin C content, the waxy cuticle or the ripening period of these fruits, were conditions that made LAB survival on the external layer of these fruits difficult (Barrera and Hernández 2004; Leff and Fierer 2013; Azevêdo et al. 2015). As can be seen from Table I, *L. plantarum* was isolated from all the fruits analyzed, while *L. brevis*, *W. cibaria* and *W. confusa* were additionally isolated from only four fruits: *Bactris gasipaes*, *Psidium guajava*, *Anacardium occidentale*, and *Oenocarpus bataua*. Therefore, the predominance of *L. plantarum* over the other LAB species in the Amazonian Peruvian fruits was evident.

In the present study, the presumptive LAB isolates were characterized by ARDRA using the restriction enzymes: *MseI*, *HaeIII*, and *AluI*. *MseI* and *HaeIII* revealed three restriction profiles, while *AluI* showed four restriction profiles demonstrating greater discriminatory power to differentiate the LAB isolates. 16S-23S ITS RFLP analysis also showed four restriction profiles similar to those formed with ARDRA *AluI*, which confirmed the presence of at least four LAB species. These results are in agreement with previous studies which indicate that ARDRA and 16S-23S ITS RFLP are useful techniques for LAB differentiation at species level (Zeng et al. 2013) and agree with the results obtained by Jeyaram et al. (2010) who used both techniques obtained the same number of restriction profiles for LAB species of the genera *Carnobacterium*, *Lactobacillus* and *Enterococcus* isolated from fermented bamboo roots. It is important to bear in mind that the success of ARDRA or 16S-23S ITS RFLP techniques lies in the adequate selection of enzymes for the digestion. Thus, Rachman et al. (2003) showed that the digestion of 16S-23S ITS segment using the *HindIII* enzyme was not efficient to differentiate *L. sakei*, *L. curvatus*, *L. farciminis*, *L. alimentarius*, *L. plantarum* and *L. paraplantarum*; however,

the use of *TaqI* allowed them to obtain different genetic profiles that differentiated most of these species except *L. plantarum* and *L. paraplantarum* due to their phylogenetic closeness. In this study, the discrimination between *W. cibaria* and *W. confusa* was possible by digestion with *AluI* but not when *MseI* or *HaeIII* was used.

ARDRA and 16S-23S ITS RFLP are useful tools to determine the interspecific diversity of LAB; however, it is difficult to detect intraspecific variability when the strains are closely phylogenetically related. Using rep-PCR technique with the GTG₅ primer, it was possible to obtain 14 different patterns which correspond to 14 genotypes or strains demonstrating that among the LAB isolates there was intraspecific diversity that was neither revealed by ARDRA nor 16S-23S ITS RFLP. These results are similar to those reported by Silva et al. (2017) who used the 16S-23S ITS RFLP and the sequencing of the 16S ribosomal genes identified six LAB species from 33 isolates, but using GTG₅ fingerprinting they observed 18 genotypes. Similarly, Kingston et al. (2010) using ARDRA observed similar profiles for 16 LAB isolates identified as *L. paraplantarum* and *L. pentosus*, but using rep-PCR found eight genotypes, demonstrating the existence of intraspecific variability. In this study, the highest intraspecific diversity was observed among isolates of *L. plantarum* (eight patterns). *L. plantarum* is known for its genetic variability, which according to Pisano et al. (2010) is related to the existence of genomic islands composed of groups of the genes destined to the use of carbohydrates that can be acquired, combined, replaced or deleted depending on the characteristics of the medium. The great flexibility of these genomic islands favors the versatility of *L. plantarum* to different substrates and environmental changes. For this reason, Siezen and van Hylckama Vlieg (2011) consider *L. plantarum* a “natural metabolic engineer”.

An interesting fact was the presence of the GTG₅ pattern I.1 in seven fruits analyzed, the imposition of a single strain on those fruits could be attributed to the production of antagonist compounds that limit the survival of other strains (Hibbing et al. 2010).

By sequencing the 16S ribosomal genes, the isolates were identified as *L. plantarum*, *L. brevis*, *W. cibaria* and *W. confusa*, being *L. plantarum* the most abundant LAB isolated from the Amazonian fruits analyzed. These results are in the agreement with different studies which indicates that *L. plantarum* is the most abundant LAB distributed in fruits and vegetables (Naeem et al. 2012, Emerenini et al. 2013, Franquès et al. 2017).

Identification of *L. plantarum*, *L. paraplantarum*, and *L. pentosus* based only on the sequence of the 16S ribosomal genes is not accurate because these species have a similarity greater than 99% in the sequence of these genes (Torriani et al. 2001; Agaliya and

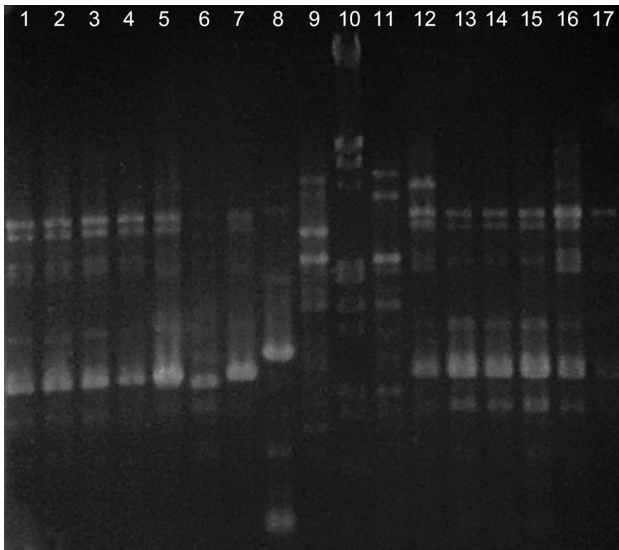


Fig. 2. Different GTG_5 profiles of LAB strains isolated from Peruvian Amazonian fruits. Lines 1–5: *L. plantarum*, 6: *L. brevis*, 7: *L. plantarum*, 8: *W. confusa*, 9: *W. cibaria*, 10: Lambda/EcoRI+HindIII, 11: *W. cibaria*, 12–17: *L. plantarum*.

Jeevaratnam 2013). Their closeness was corroborated when constructing the phylogenetic tree using the 16S rDNA sequences of the *L. plantarum* isolates and reference strains of *L. paraplantarum* and *L. pentosus*, where it was observed that the three species are located in the same group (Fig. 2). Because of this fact, the identity of the *L. plantarum* isolates had to be confirmed by a multiple PCR technique described by Torriani et al. (2001) that used specific primers to amplify the *recA* gene and allows to differentiate the three species according to the amplicons size.

The phenotypic characterization demonstrated that LAB isolates were able to grow in a wide range of pH (3.5–7.5) and temperature (10°C–45°C), and tolerate up to 10% NaCl. These observations are in agreement with the described features of LAB, which indicate that they are robust microorganisms able to survive and adapt to different environmental conditions (Ludwig et al. 2009; Mazzoli et al. 2014). This feature gives LAB a great capacity to be used in diverse industrial processes.

The carbohydrate fermentation test showed that a large percentage of isolated LAB fermented both monosaccharides and disaccharides. As it was described, LAB are microorganisms with high energy requirements being able to obtain the necessary energy from the fermentation of a wide variety of carbohydrates (Mazzoli et al. 2014). Therefore, fruits that contain sugars such as fructose, sucrose, and glucose are favorite sources for LAB development (Serpén 2012). The results also showed that LAB strains belonging to the same species shared a similar carbohydrate fermentation pattern with some differences in the fermentation of galactose, sucrose, and lactose. These metabolic vari-

ations are typical of the intraspecific variation existing in the isolates, especially in *Lactobacillus* strains, such variability is manifested in strains that show atypical characteristics to those usually reported (Pot et al. 1994).

The LAB isolates did not hydrolyze casein or starch. There are different publications that report the isolation of proteolytic and amylolytic LAB from sources rich in proteins (dairy products) or starch (cereal based drinks), respectively (Díaz-Ruiz et al. 2003; Moulay et al. 2006; Hattingh et al. 2015; Kıvanç and Yapıcı 2015). Endo and Dicks (2014) noted that LAB have evolved to adapt to specific niches, gaining specific genes and losing others. In this sense, Kelly et al. (2010) provide evidence that defined dairy starter cultures have arisen from *Lactococcus lactis* strains that have plant origin, such adaptation to the dairy environment involved loss and acquisition of genes (usually plasmid associated) that favor growth in milk. Taking this information into account, it can be explained that LAB isolated from fruits and adapted to this habitat, in which the starch and protein contents are scarce have not developed enzymatic machinery to metabolize these compounds.

Regarding the antimicrobial susceptibility, all the isolates were sensitive to seven of the 14 antimicrobials tested, on the contrary, they were resistant against kanamycin, gentamicin, streptomycin, sulfamethoxazole/trimethoprim, and vancomycin. The high resistance observed, and the results of previous investigations would indicate that the observed resistance is intrinsic among LABs, which means that the possibility of being transferred to other bacteria by horizontal transfer is minimal (Abriouel et al. 2015; Sharma et al. 2016). Intrinsic resistance is typical of all strains of the same species. Some LAB, especially from the genus *Lactobacillus*, are used as probiotics, however a growing concern has arisen over the possibility that LAB may constitute a reservoir of antimicrobial resistance genes that could be transferred horizontally (via plasmids and conjugative transposons, integrons or insertion sequences) to pathogens during their passage through the gastrointestinal tract (Jose et al. 2015). This fact justifies the importance of previously determining antimicrobial resistance patterns before using a LAB strain as a probiotic. Due to their natural origin, LAB isolates from Amazonian fruits could be a safe alternative to be used as probiotics; however, it is necessary to confirm the genetic nature of the observed resistance.

Regarding lactic acid production, the results are in agreement with the type of metabolism observed, being the homofermentative strains (*L. plantarum*) those that produced lactic acid in higher concentrations. They are good candidates to be evaluated for industrial processes where homofermentative strains are preferred to avoid necessary further purification steps if heterofermentative strains are used. One of the advantages of microbial

production of lactic acid by microbial fermentation is that a product of high purity can be obtained when the strains were selected properly, while by chemical synthesis a racemic mixture of D and L lactic acid is obtained (Taskila and Ojamo 2013). Lactic acid is a compound with many industrial applications being one of the most interesting the manufacture of polylactic acid, a biodegradable plastic that can replace similar products derived from petroleum (Ilmen et al. 2007).

EPS production using different carbon sources was also evaluated. *Weissella* strains were able to produce EPS only using sucrose. Similar results were obtained by Smitinont et al. (1999), Van Geel-Schutten et al. (1999) and Di Cagno et al. (2006) who determined that sucrose was the best sugar for EPS production by LAB isolated from different samples. The preference for a particular carbon source has been attributed to the presence of different sugar transport systems in LAB strains or to variations in the activity of the enzymes involved in the precursor synthesis of the repeating units that make up the structure of EPS (Chervaux et al. 2000; Mozzi et al. 2001). LAB strain, medium composition and growth conditions (temperature, agitation, incubation time, pH, oxygen tension) are important factors that influence EPS production (Sanalibaba and Çakmak 2016). EPS production is a distinctive feature of the genus *Weissella* and currently *W. cibaria* and *W. confusa* are two species valued for the production of dextrans, fructans, heteropolysaccharides and non-digestible oligosaccharides, which have a large number of applications in biomedical, cosmetics, food, and feed industries; however, both species have also been reported as human opportunistic pathogens (Fusco et al. 2015). For this reason, the biotechnological use of these strains would have to be evaluated exhaustively.

In this work, 37 LAB isolates from Peruvian Amazon fruits were characterized and identified using molecular and phenotypic methods, which provided complementary information on the genetic diversity and physiology of the isolated strains being necessary to continue the study to determine their usefulness in the future biotechnological processes.

ORCID

Johanna Sánchez [0000-0002-5999-0817](https://orcid.org/0000-0002-5999-0817)

Acknowledgements

This work was supported by INNOVATE-PERU, agreement No. 230-FINCYT-IA-2013 and CIENCIACTIVA, agreement No. 007-FONDECYT-2014.

Conflict of interest

The authors do not report any financial or personal connections with other persons or organizations, which might negatively affect the contents of this publication and/or claim authorship rights to this publication.

Literature

- Abriouel H, Casado Muñoz MC, Lavilla Lerma L, Pérez Montoro B, Bockelmann W, Pichner R, Kabisch J, Cho GS, Franz CMAP, Gálvez A, et al. New insights in antibiotic resistance of *Lactobacillus* species from fermented foods. *Food Res Int.* 2015;78:465–481. doi:10.1016/j.foodres.2015.09.016 [Medline](#)
- Abubakr M, Al-Adiwish WM. Isolation and identification of lactic acid bacteria from different fruits with proteolytic activity. *Int J Microbiol Biotechnol.* 2017;2(2):58–64.
- Agaliya PJ, Jeevaratnam K. Molecular characterization of lactobacilli isolated from fermented idli batter. *Braz J Microbiol.* 2013; 44(4):1199–1206. doi:10.1590/S1517-83822013000400025 [Medline](#)
- Andrighetto C, Knijff E, Lombardi A, Torriani S, Vancanneyt M, Kersters K, Swings J, Dellaglio F. Phenotypic and genetic diversity of enterococci isolated from Italian cheeses. *J Dairy Res.* 2001; 68(2):303–316. doi:10.1017/S0022029901004800 [Medline](#)
- Ausubel FM, Brent R, Kingston RE, Moore DD, Seidman JG, Smith JA, Struhl K. *Current Protocols in Molecular Biology.* London (United Kingdom): John Wiley & Sons Inc. 2003; p. 4410.
- Azevêdo JCS, Borges KC, Genovese MI, Correia RTP, Vatted DA. Neuroprotective effects of dried camu-camu (*Myrciaria dubia* HBK McVaugh) residue in *C. elegans*. *Food Res Int.* 2015;73:135–141. doi:10.1016/j.foodres.2015.02.015
- Bae S, Fleet GH, Heard GM. Lactic acid bacteria associated with wine grapes from several Australian vineyards. *J Appl Microbiol.* 2006;100(4):712–727. doi:10.1111/j.1365-2672.2006.02890.x [Medline](#)
- Barrera JA, Hernández MS. Bases técnicas para el aprovechamiento agroindustrial de las especies nativas de la amazonia. Instituto Amazónico de Investigaciones Científicas SINCHI. Bogotá (Colombia): Editora Guadalupe Ltda. 2004; p. 102.
- Bauer AW, Kirby WMM, Sherris JC, Turck M. Antibiotic susceptibility testing by a standardized single disk method. *Am J Clin Pathol.* 1966;45(4-ts):493–496. doi:10.1093/ajcp/45.4-ts.493 [Medline](#)
- Charteris WP, Kelly PM, Morelli L, Collins JK. Antibiotic susceptibility of potentially probiotic *Lactobacillus* species. *J Food Prot.* 1998; 61(12):1636–1643. doi:10.4315/0362-028X-61.12.1636 [Medline](#)
- Chen Y, Wu H, Yanagida F. Isolation and characteristics of lactic acid bacteria isolated from ripe mulberries in Taiwan. *Braz J Microbiol.* 2010;41(4):916–921. doi:10.1590/S1517-83822010000400010 [Medline](#)
- Chervaux C, Ehrlich SD, Maguin E. Physiological study of *Lactobacillus delbrueckii* subsp. *bulgaricus* strains in a novel chemically defined medium. *Appl Environ Microbiol.* 2000;66(12):5306–5311. doi:10.1128/AEM.66.12.5306-5311.2000 [Medline](#)
- Di Cagno R, Cardinali G, Minervini G, Antonielli L, Rizzello CG, Ricciuti P, Gobbetti M. Taxonomic structure of the yeasts and lactic acid bacteria microbiota of pineapple (*Ananas comosus* L. Merr.) and use of autochthonous starters for minimally processing. *Food Microbiol.* 2010;27(3):381–389. doi:10.1016/j.fm.2009.11.012 [Medline](#)
- Di Cagno R, De Angelis M, Limitone A, Minervini F, Carnevali P, Corsetti A, Gaenzle M, Ciatì R, Gobbetti M. Glucan and fructan production by sourdough *Weissella cibaria* and *Lactobacillus plantarum*. *J Agric Food Chem.* 2006;54(26):9873–9881. doi:10.1021/jf061393+ [Medline](#)
- Díaz-Ruiz G, Guyot JP, Ruiz-Teran F, Morlon-Guyot J, Wachter C. Microbial and physiological characterization of weakly amyolytic but fast-growing lactic acid bacteria: a functional role in supporting microbial diversity in pozol, a Mexican fermented maize beverage. *Appl Environ Microbiol.* 2003;69(8):4367–4374. doi:10.1128/AEM.69.8.4367-4374.2003 [Medline](#)

- Emerenini E, Afolabi OR, Okolie PI, Akintokun K.** Isolation and molecular characterization of lactic acid bacteria isolated from fresh fruits and vegetables using nested PCR analysis. *Br Microbiol Res J.* 2013;3(3):368–377. doi:10.9734/BMRJ/2013/2520
- Endo A, Dicks L.** Physiology of the LAB. In: Holzapfel W, Wood B, editors. *Lactic acid bacteria. Biodiversity and taxonomy.* London (United Kingdom): John Wiley & Sons Ltd. 2014. p. 13–30.
- European Food Safety Authority.** Guidance on the assessment of bacterial susceptibility to antimicrobials of human and veterinary importance. *EFSA J.* 2012;10(6):2740. doi:10.2903/j.efsa.2012.2740
- Fortina MG, Nicasastro G, Carminati D, Neviani E, Manachini PL.** *Lactobacillus helveticus* heterogeneity in natural cheese starters: the diversity in phenotypic characteristics. *J Appl Microbiol.* 1998; 84(1):72–80. doi:10.1046/j.1365-2672.1997.00312.x Medline
- Franquès J, Araque I, Palahí E, Portillo MC, Reguant C, Bordons A.** Presence of *Oenococcus oeni* and other lactic acid bacteria in grapes and wines from Priorat (Catalonia, Spain). *Lebensm Wiss Technol.* 2017;81:326–334. doi:10.1016/j.lwt.2017.03.054
- Fusco V, Quero GM, Cho GS, Kabisch J, Meske D, Neve H, Bockelmann W, Franz CMAP.** The genus *Weissella*: taxonomy, ecology and biotechnological potential. *Front Microbiol.* 2015;6:155. doi:10.3389/fmicb.2015.00155 Medline
- Gevers D, Huys G, Swings J.** Applicability of rep-PCR fingerprinting for identification of *Lactobacillus* species. *FEMS Microbiol Lett.* 2001;205(1):31–36. doi:10.1111/j.1574-6968.2001.tb10921.x Medline
- Hattingh M, Alexander A, Meijering I, Van RCA, Dicks LMT.** Amylolytic strains of *Lactobacillus plantarum* isolated from barley. *Afr J Biotechnol.* 2015;14(4):310–318. doi:10.5897/AJB2014.14149
- Hibbing ME, Fuqua C, Parsek MR, Peterson SB.** Bacterial competition: surviving and thriving in the microbial jungle. *Nat Rev Microbiol.* 2010;8(1):15–25. doi:10.1038/nrmicro2259 Medline
- Ilmén M, Koivuranta K, Ruohonen L, Suominen P, Penttilä M.** Efficient production of L-lactic acid from xylose by *Pichia stipitis*. *Appl Environ Microbiol.* 2007;73(1):117–123. doi:10.1128/AEM.01311-06 Medline
- Jeyaram K, Romi W, Singh TA, Devi AR, Devi SS.** Bacterial species associated with traditional starter cultures used for fermented bamboo shoot production in Manipur state of India. *Int J Food Microbiol.* 2010;143(1-2):1–8. doi:10.1016/j.ijfoodmicro.2010.07.008 Medline
- Jini R, Swapna HC, Rai AK, Vrinda R, Halami PM, Sachindra NM, Bhaskar N.** Isolation and characterization of potential lactic acid bacteria (LAB) from freshwater fish processing wastes for application in fermentative utilisation of fish processing waste. *Braz J Microbiol.* 2011;42(4):1516–1525. doi:10.1590/S1517-83822011000400039 Medline
- Jose NM, Bunt CR, Hussain MA.** Implications of antibiotic resistance in probiotics. *Food Rev Int.* 2015;31(1):52–62. doi:10.1080/87559129.2014.961075
- Kelly WJ, Ward LJH, Leahy SC.** Chromosomal diversity in *Lactococcus lactis* and the origin of dairy starter cultures. *Genome Biol Evol.* 2010;2(1):729–744. doi:10.1093/gbe/evq056 Medline
- Kingston JJ, Radhika M, Roshini PT, Raksha MA, Murali HS, Batra HV.** Molecular characterization of lactic acid bacteria recovered from natural fermentation of beet root and carrot Kanji. *Indian J Microbiol.* 2010;50(3):292–298. doi:10.1007/s12088-010-0022-0 Medline
- Kıvanç M, Yapıcı E.** Kefir as a probiotic dairy beverage: determination lactic acid bacteria and yeast. *ETP Int J Food Eng.* 2015;1(1): 55–60.
- Leff JW, Fierer N.** Bacterial communities associated with the surfaces of fresh fruits and vegetables. *PLoS One.* 2013;8(3):e59310. doi:10.1371/journal.pone.0059310 Medline
- Liu W, Pang H, Zhang H, Cai Y.** Biodiversity of lactic acid bacteria. In: Zhang H, Cai Y, editors. *Lactic acid bacteria: Fundamentals and practice.* New York (USA): Springer. 2014; p. 103–204.
- Ludwig W, Schleifer K-H, Whitman WB.** Orden II. Lactobacillales. In: De Vos P, Garrity GM, Jones D, Krieg NR, Ludwig W, Rainey FA, Schleifer K-H, Whitman WB, editors. *Bergey's Manual of Systematic Bacteriology.* Vol 3. The Firmicutes. 2nd ed. New York (USA): Springer. 2009; p. 464–722.
- MacFaddin JF.** *Biochemical tests for identification of medical bacteria.* Baltimore (USA): Williams & Wilkins. 2000; 928 p.
- Mazzoli R, Bosco F, Mizrahi I, Bayer EA, Pessione E.** Towards lactic acid bacteria-based biorefineries. *Biotechnol Adv.* 2014;32(7): 1216–1236. doi:10.1016/j.biotechadv.2014.07.005 Medline
- Mohania D, Nagpal R, Kumar M, Bhardwaj A, Yadav M, Jain S, Marotta F, Singh V, Parkash O, Yadav H.** Molecular approaches for identification and characterization of lactic acid bacteria. *J Dig Dis.* 2008;9(4):190–198. doi:10.1111/j.1751-2980.2008.00345.x Medline
- Moraes PM, Perin LM, Silva Júnior A, Nero LA.** Comparison of phenotypic and molecular tests to identify lactic acid bacteria. *Braz J Microbiol.* 2013;44(1):109–112. doi:10.1590/S1517-83822013000100015 Medline
- Moulay M, Aggad H, Benmechernene Z, Guessas B, Henni DE, Kihal M.** Cultivable lactic acid bacteria isolated from Algerian raw goat's milk and their proteolytic activity. *World J Dairy Food Sci.* 2006;1(1):12–18.
- Mozzi F, Rollán G, de Giori GS, de Valdez GF.** Effect of galactose and glucose on the exopolysaccharide production and the activities of biosynthetic enzymes in *Lactobacillus casei* CRL 87. *J Appl Microbiol.* 2001;91(1):160–167. doi:10.1046/j.1365-2672.2001.01367.x Medline
- Naem M, Ilyas M, Haider S, Baig S, Saleem M.** Isolation characterization and identification of lactic acid bacteria from fruit juices and their efficacy against antibiotics. *Pak J Bot.* 2012;44:323–328.
- Pisano MB, Patrignani F, Cosentino S, Guerzoni ME, Franz CMAP, Holzapfel WH.** Diversity and functional properties of *Lactobacillus plantarum* – group strains isolated from Italian cheese products. *Dairy Sci Technol.* 2010;91(1):65–76.
- Pot B, Ludwig W, Kersters K, Schleifer K-H.** Taxonomy of lactic acid bacteria. In: De Vuyst L, Vandamme EJ, editors. *Bacteriocins of lactic acid bacteria. Microbiology, Genetics and Applications.* New York (USA): Springer Science+Business Media. 1994; p. 13–90.
- Rachman CN, Kabadjova P, Prévost H, Dousset X.** Identification of *Lactobacillus alimentarius* and *Lactobacillus farciminis* with 16S-23S rDNA intergenic spacer region polymorphism and PCR amplification using species-specific oligonucleotide. *J Appl Microbiol.* 2003;95(6):1207–1216. doi:10.1046/j.1365-2672.2003.02117.x Medline
- Reginensi SM, González MJ, Bermúdez J.** Phenotypic and genotypic characterization of lactic acid bacteria isolated from cow, ewe and goat dairy artisanal farmhouses. *Braz J Microbiol.* 2013;44(2):427–430. doi:10.1590/S1517-83822013000200013 Medline
- Rodas AM, Ferrer S, Pardo I.** 16S-ARDRA, a tool for identification of lactic acid bacteria isolated from grape must and wine. *Syst Appl Microbiol.* 2003;26(3):412–422. doi:10.1078/072320203322497446 Medline
- Sanalibaba P, Çakmak GA.** Exopolysaccharides production by lactic acid bacteria. *Appl Microbiol Open Access.* 2016;2(2): 1000115. doi:10.4172/2471-9315.1000115
- Serpen JY.** Comparison of sugar content in bottled 100% fruit juice versus extracted juice of fresh fruit. *Food Nutr Sci.* 2012;03(11): 1509–1513. doi:10.4236/fns.2012.311196

- Sharma P, Tomar SK, Goswami P, Sangwan V, Singh R.** Antibiotic resistance among commercially available probiotics. *Food Res Int.* 2014;57:176–195. doi:10.1016/j.foodres.2014.01.025
- Sharpe ME.** Identification of the lactic acid bacteria. In: Skinner FA, Lovelock DW, editors. *Identification methods for microbiologists.* London (United Kingdom): Academic Press. 1979; p. 233–259.
- Siezen RJ, van Hylckama Vlieg JET.** Genomic diversity and versatility of *Lactobacillus plantarum*, a natural metabolic engineer. *Microb Cell Fact.* 2011;10 Suppl 1:S3. doi:10.1186/1475-2859-10-S1-S3 Medline
- Silva BC, Sandes SHC, Alvim LB, Bomfim MRQ, Nicoli JR, Neumann E, Nunes AC.** Selection of a candidate probiotic strain of *Pediococcus pentosaceus* from the faecal microbiota of horses by *in vitro* testing and health claims in a mouse model of *Salmonella* infection. *J Appl Microbiol.* 2017;122(1):225–238. doi:10.1111/jam.13339 Medline
- Singhal N, Kumar M, Kanaujia PK, Viridi JS.** MALDI-TOF mass spectrometry: an emerging technology for microbial identification and diagnosis. *Front Microbiol.* 2015;6:791. doi:10.3389/fmicb.2015.00791 Medline
- Smitinont T, Tansakul C, Tanasupawat S, Keeratipibul S, Navarini L, Bosco M, Cescutti P.** Exopolysaccharide-producing lactic acid bacteria strains from traditional Thai fermented foods: isolation, identification and exopolysaccharide characterization. *Int J Food Microbiol.* 1999;51(2–3):105–111. doi:10.1016/S0168-1605(99)00094-X Medline
- Sneath PHA, Johnson R.** The influence on numerical taxonomic similarities of errors in microbiological tests. *J Gen Microbiol.* 1972;72(2):377–392. doi:10.1099/00221287-72-2-377 Medline
- Taskila S, Ojamo H.** The current status and future expectations in industrial production of lactic acid by lactic acid bacteria. In: Kongo JM, editor. *Lactic Acid Bacteria, R&D for food, health and livestock purposes.* London (United Kingdom): IntechOpen. 2013; p. 615–632. doi:10.5772/51282
- Torriani S, Felis GE, Dellaglio F.** Differentiation of *Lactobacillus plantarum*, *L. pentosus*, and *L. paraplantarum* by recA gene sequence analysis and multiplex PCR assay with recA gene-derived primers. *Appl Environ Microbiol.* 2001;67(8):3450–3454. doi:10.1128/AEM.67.8.3450-3454.2001 Medline
- Trias R, Bañeras L, Badosa E, Montesinos E.** Bioprotection of Golden Delicious apples and Iceberg lettuce against foodborne bacterial pathogens by lactic acid bacteria. *Int J Food Microbiol.* 2008; 123(1–2):50–60. doi:10.1016/j.ijfoodmicro.2007.11.065 Medline
- Van Geel-Schutten GH, Faber EJ, Smit E, Bonting K, Smith MR, ten Brink B, Kamerling JP, Vliegenthart JFG, Dijkhuizen L.** Biochemical and structural characterization of the glucan and fructan exopolysaccharides synthesized by the *Lactobacillus reuteri* wild-type strain and by mutant strains. *Appl Environ Microbiol.* 1999;65(7):3008–3014. Medline
- Verón HE, Di Risio HD, Isla MI, Torres S.** Isolation and selection of potential probiotic lactic acid bacteria from *Opuntia ficus-indica* fruits that grow in Northwest Argentina. *LWT.* 2017;84:231–240. doi:10.1016/j.lwt.2017.05.058
- Wakil SM, Ajayi OO.** Production of lactic acid from Starchy-based food substrates. *J Appl Biosci.* 2013;71(1):5673–5681. doi:10.4314/jab.v71i1.98811
- Zavaleta AI, Martínez-Murcia AJ, Rodríguez-Valera F.** 16S-23S rDNA intergenic sequences indicate that *Leuconostoc oenos* is phylogenetically homogeneous. *Microbiology.* 1996;142(8):2105–2114. doi:10.1099/13500872-142-8-2105 Medline
- Zeng YH, Koblížek M, Li YX, Liu YP, Feng FY, Ji JD, Jian JC, Wu ZH.** Long PCR-RFLP of 16S-ITS-23S rRNA genes: a high-resolution molecular tool for bacterial genotyping. *J Appl Microbiol.* 2013;114(2):433–447. doi:10.1111/jam.12057 Medline

Comparison of Performance Characteristics of DxN VERIS System versus Qiagen PCR for HBV Genotype D and HCV Genotype 1b Quantification

MURAT SAYAN^{1,2}, AYSE ARIKAN^{2,3*} and TAMER SANLIDAG^{2,4}

¹Kocaeli University, Faculty of Medicine, Clinical Laboratory, PCR Unit, Kocaeli, Turkey

²Near East University, Research Center of Experimental Health Sciences, Nicosia, Northern Cyprus

³Near East University, Faculty of Medicine, Department of Medical Microbiology,
Nicosia, Northern Cyprus

⁴Celal Bayar University, Faculty of Medicine, Department of Medical Microbiology, Manisa, Turkey

Submitted 17 September 2018, revised 10 November 2018, accepted 14 November 2018

Abstract

The Beckman Coulter DxN VERIS system is a fully automated, closed molecular diagnostic instrument for viral load quantification of hepatitis B virus and hepatitis C virus. In this study, the analytical performance of this new system was compared to routine diagnostic Qiagen PCR kit by using the same clinical samples. The DxN VERIS system demonstrated a high analytical performance. The DxN VERIS allows random access, which means that samples can be uploaded straight on to the system at any time; so, it provides an improvement of workflow, staff productivity and allows faster turn-around of viral load results.

Key words: Hepatitis B virus, hepatitis C virus, real-time PCR, regression analysis, diagnosis

Hepatitis B virus (HBV) and hepatitis C virus (HCV) are hepatotropic, non-cytopathic viruses able to establish a persistent infection that causes different degrees of hepatic inflammation (chronic hepatitis), leading to the development of liver cirrhosis and hepatocellular carcinoma (HCC) (Caccamo et al. 2014; Easterbrook et al. 2017). Today, the main goal of HBV therapy is to prevent the progression of the disease, improving survival and the quality of life; whereas, for the HCV therapy, the aim is to cure the infection to achieve a sustained virological response and consequently, to prevent HCC development (Akhan et al. 2015). Additionally, viral load (VL) monitoring is important in assessing the therapeutic response, monitoring treatment success and detecting drug-resistant viruses (Singh et al. 2017). There are several commercially available HBV-HCV monitoring assays which are mainly based on real-time polymerase chain reaction (RT-PCR); but, using the most effective, the cheapest and the fastest detecting system plays an important role in diagnosing viral infections. Although

these techniques are preferred due to their excellent analytical sensitivity, specificity, accuracy, and broad dynamic range of linear quantification, they require many steps and consumables in the qualified laboratories (Portilho et al. 2015; Wu et al. 2017). VL assays also need to be batched as they arrive in the laboratory. Even a small change in the efficiency of the amplification can lead to striking differences in the amount final product. These reasons indicate the necessity of inventing fully standardized, reproducible and sensitive new assays for monitoring of HBV and HCV infections.

The aim of the study was to compare the analytical performance of random access testing (Beckman Coulter DxN VERIS) with routine diagnostic PCR kit (artus Qiagen).

A total of 67 chronic hepatitis B (CHB) patients with genotype D and 44 chronic hepatitis C (CHC) patients infected with genotype 1b from Kocaeli province in Marmara region of Turkey were analyzed in parallel with the use of DxN VERIS and Qiagen systems

* Corresponding author: A.A. Sarioglu, Near East University, Faculty of Medicine, Medical Microbiology Department, Nicosia, Cyprus;
e-mail: aysearikancy@yahoo.com, ayse.arikansarioglu@neu.edu.tr

© 2019 Murat Sayan et al.

This work is licensed under the Creative Commons Attribution-NonCommercial-NoDerivatives 4.0 License
(<https://creativecommons.org/licenses/by-nc-nd/4.0/>)

Table I
The Qiagen HBV DNA and HCV RNA levels in sampling.

Pattern of HBV sampling	HBV DNA (IU/ml), n/total (%)	Pattern of HCV sampling	HCV RNA (IU/ml), n/total (%)
Negative	12/67 (18%)	Negative	11/44 (25%)
< 10 ¹	14/67 (21%)	> 10 ¹	1/44 (2%)
> 10 ²	9/67 (13%)	> 10 ²	1/44 (2%)
> 10 ³	13/67 (20%)	> 10 ⁴	2/44 (5%)
> 10 ⁴	4/67 (6%)	> 10 ⁵	6/44 (14%)
> 10 ⁵	7/67 (10%)	> 10 ⁶	14/44 (32%)
> 10 ⁶	4/67 (6%)	> 10 ⁷	9/44 (20%)
> 10 ⁸	4/67 (6%)	–	–

synchronously. Qiagen HBV DNA and HCV RNA levels in the samples were in the range from negative to > 10⁸ IU/ml and > 10⁷ IU/ml, respectively, and they are displayed in Table I. The PCR-negative samples were previously diagnosed as taken from the HBV and HCV carriers and their negativities were provided by antiviral treatment. The most predominant genotypes in Turkey are HBV genotype D and HCV genotype 1b; therefore, we have only involved these genotypes in our study (Karatas et al. 2018). The selected blood samples were immediately centrifuged, aliquoted, and then, stored at –80°C until use. The diagnosis of chronic hepatitis B and C was made on the basis of biochemical, serological, virological and histological data according to the EASL guidelines (EASL 2017a, 2017b). The samples were analyzed by using both fully automated DxN VERIS kits (Beckman Coulter DxN VERIS HBV/HCV kits, Nyon, Switzerland) and Qiagen kits (artus HBV/HCV QS RGQ kit, Qiagen, Hilden, Germany) on the same day according to the manufacturer's recommendations. DxN VERIS HBV/HCV assays have quantification ranges from 10–10⁹ IU/ml and 12–10⁸ IU/ml, respectively as it is stated in the package inserts. The relationship between VL quantifications measured by both DxN VERIS and Qiagen assays were analyzed by Passing-Bablok (PB) regression method. Bland Altman plot (BAP) design was used to calculate statistical limits, correlation and standard deviation (SD) of the differences between two types of measurement. To control the distribution of the differences and other properties between quantitative values, a graphical approach was used. Statistical analysis of the study was made with the Analyse-it Software program (Analyse-it Ltd. v 4.60, Microsoft Corp. Leeds, UK).

According to HBV BAP (DxN VERIS combined Qiagen HBV log IU/ml), the specificity resulted in 95% LoA (limits of agreement) [CL (confidence level) 95% = –1.59–0.61], the correlation was equal to 0.97 with SD 0.55 and a mean SD = –0.47. HBV PB indicated DxN VERIS combined = –1.179 + 1.153 Qiagen

log IU/ml with the correlation equal to 0.97. HBV plots for PB and BAP are shown in Fig. 1.

For HCV analysis, BAP (DxN VERIS combined Qiagen HCV log IU/ml) illustrated the specificity of 95% LoA (CL 95% = –1.59–0.72), the correlation of 0.90 with SD 0.59 and a mean SD = –0.43. HCV PB analysis indicated DxN VERIS combined = –0.3394 + 0.8602 Qiagen log IU/ml with the correlation of 0.90. HCV plots for PB and BAP are shown in Fig. 2.

Viral nucleic acid detection is the gold standard for the detection of viral genomes in clinical samples. COBAS Ampliprep, artus Qiagen and Abbott real-time PCR assays are currently the most frequently used platforms worldwide in this field. DxN VERIS systems were mainly compared to COBAS and Abbott systems rather than to Qiagen kits (Saune et al. 2016; Patrick et al. 2017; Park et al. 2019). Studies comparing DxN VERIS HBV to Roche HBV and to Abbott real-time HBV illustrate the average bias that was determined as being equal to –0.26 (95% CI: –0.37 to –0.15) and –0.36 (95% CI: –0.43 to –0.29), respectively in BAP. This was equal to –0.32 log IU/ml in another study (Robert et al. 2014), and respectively to –0.47 log IU/ml in our study (Williams et al. 2014; Park et al. 2019). In the present study, we compared DxN VERIS with Qiagen HBV and HCV and their clinical performances displayed a strong correlation (95%) similar to one another study (Micheli et al. 2016). Currently, the main therapy is based on Peg-IFN and nucleos(t)ide analogues for CHB. However, the main clinical challenge is the development of antiviral resistance, since long-term therapeutic regimens are given to the majority of these patients (EASL 2017b). While monitoring VL, HBV breakthrough that is demonstrated by a sudden increase in DNA level (from > 1 log₁₀ IU/ml to > 1 × 10⁵ IU/ml) can be observed (Braun et al. 2017). Early detection of such viral breakthrough is important because the analysis of the HBV gene mutations responsible for drug resistance is a part of managing clinical treatment. The random access testing can provide effective surveillance

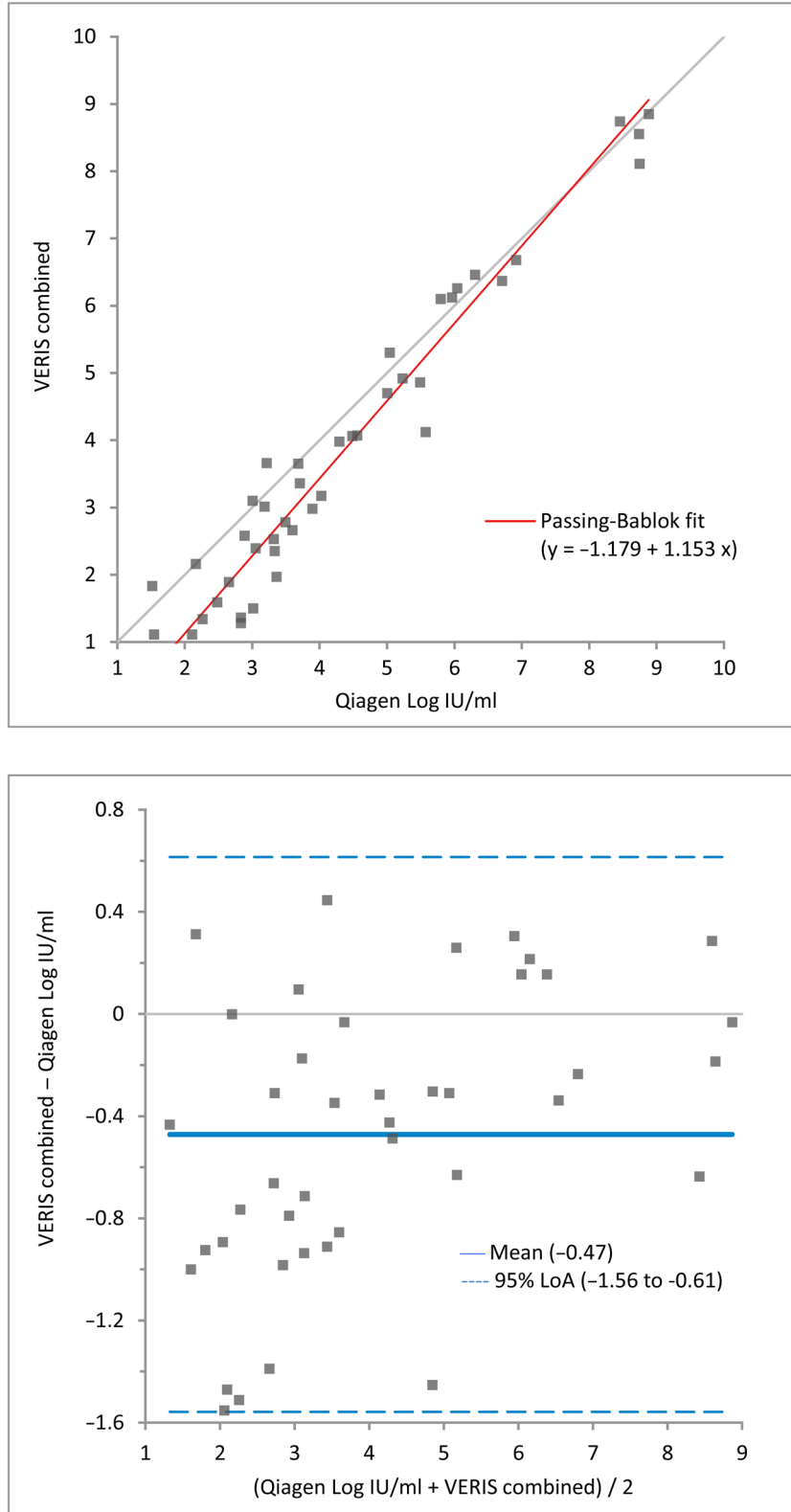


Fig. 1. HBV plots for Passing-Bablok (upper) and Bland Altman analysis (lower).

for CHB treatment. Similarly, monitoring of HCV RNA during treatment is required to assess the success of the treatment and to detect any breakthrough related to viral resistance. As the main goal of therapy for HCV is to cure the infection in order to prevent the

development of HCC and complications related with HCV related liver diseases, random access system enables faster turn-around of VL results to physicians and allows early detection of possible resistance. Therefore, DxN VERIS system may be a new solution as it enables

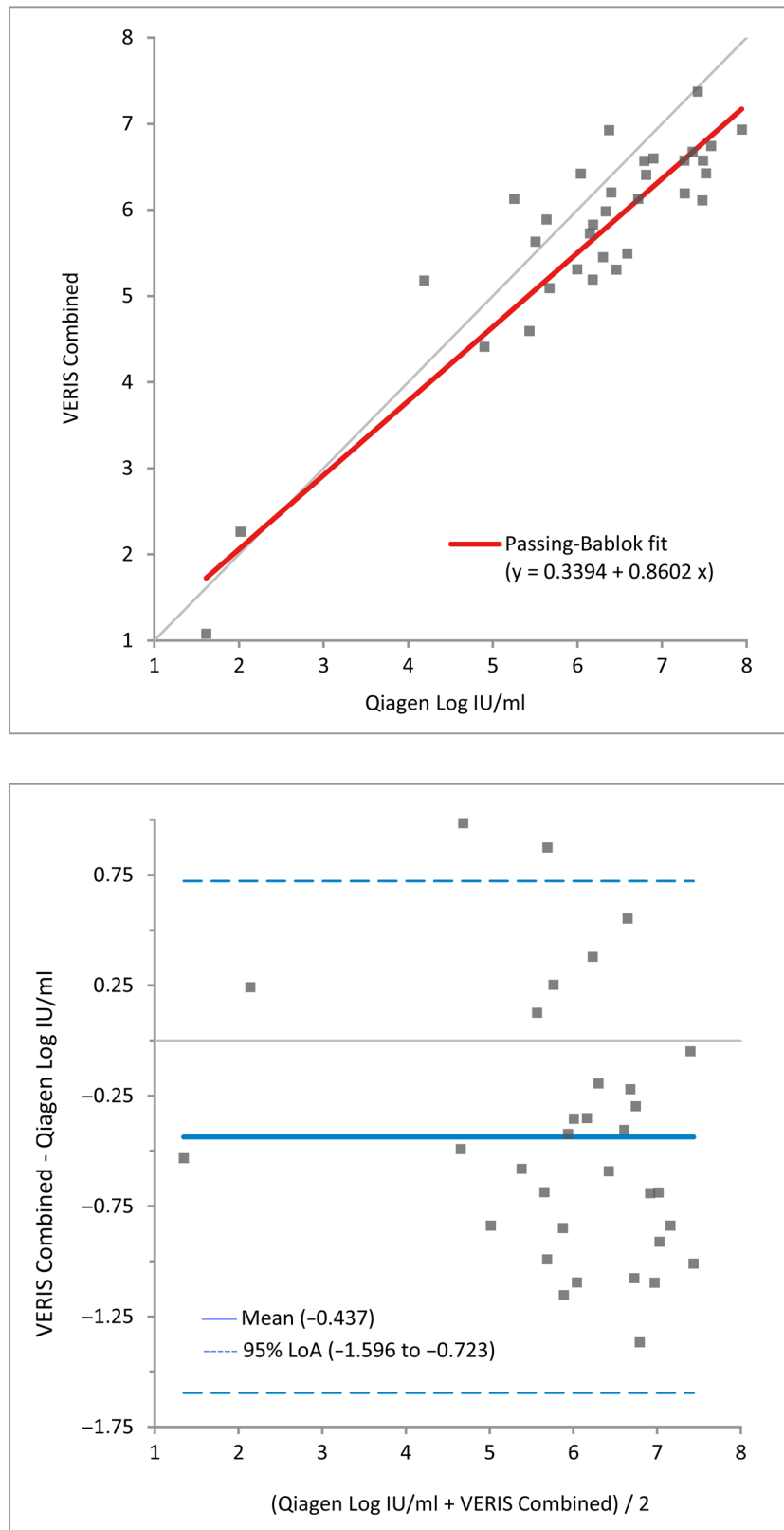


Fig. 2. HCV plots for Passing-Bablok (upper) and Bland Altman analysis (lower).

same-day turn-around results to help the health system improving patient management. None of the other platforms are true single-sample to answer and random-access testing. This is the most important advantage of

DxN VERIS system for us because medical reports can be transformed within a short time to different departments and physicians that could better manage the diseases with antiviral therapy in a short time.

Acknowledgments

The authors are thankful to Dr. Ferdiye Taner for English editing.

Ethical approved

The study has been approved by the Clinical Research Ethics Committee of Kocaeli University (KKAEEK 2011/104).

Conflict of interest

The authors do not report any financial or personal connections with other persons or organizations, which might negatively affect the contents of this publication and/or claim authorship rights to this publication.

Literature

- Akhan S, Aynioglu A, Cagatay A, Gonen I, Gunal O, Kaynar T, Kuruuzum Z, Sayan M, Tunca B, Tulek N, et al.** [Management of chronic hepatitis B virus infection: A consensus report of the study group for viral hepatitis of the Turkish society of clinical microbiology and infectious diseases]. (in Turkish). *Klimik Dergisi/ Klimik J.* 2015;27(1):2–18. doi:10.5152/kd.2014.26
- Braun P, Drago M, Fanti D, Fleury H, Hofmann J, Izopet J, Kühn S, Lombardi A, Micheli V, Sauné K, et al.** A European multicentre study on the comparison of HCV viral loads between VERIS HCV assay and COBAS[®] TaqMan[®] HCV Test and RealTime HCV Assay. *J Clin Virol.* 2017;90:18–25. doi:10.1016/j.jcv.2017.03.006 Medline
- Caccamo G, Saffiotti F, Raimondo G.** Hepatitis B virus and hepatitis C virus dual infection. *World J Gastroenterol.* 2014;20(40):14559–14567. doi:10.3748/wjg.v20.i40.14559 Medline
- Easterbrook PJ, Roberts T, Sands A, Peeling R.** Diagnosis of viral hepatitis. *Curr Opin HIV AIDS.* 2017;12(3):302–314. doi:10.1097/COH.0000000000000370 Medline
- EASL** [European Association for the Study of the Liver]. EASL recommendations on treatment of hepatitis C 2016. *J Hepatol.* 2017a; 66(1):153–194. doi:10.1016/j.jhep.2016.09.001
- EASL** [European Association for the Study of the Liver]. EASL 2017 clinical practice guidelines on the management of hepatitis B virus infection. *J Hepatol.* 2017b;67(2):370–398. doi:10.1016/j.jhep.2017.03.021
- Karatas E, Erensoy S, Akarca US, Sertöz R.** [Analysis of hepatitis B virus (HBV) preS1, preS2 and S gene regions from patient groups infected with HBV genotype D] (in Turkish). *Mikrobiyol Bul.* 2018; 52(1):23–34. Medline
- Micheli V, Lombardi A, Mancon A, Mileto D, Zanchetta N, Magni CF, Milazzo L, Angeli E, Gubertini G, Galli M, et al.** DxN VERIS system for HCV viral load monitoring in the era of second wave direct-acting antiviral agents. *J Hepatol.* 2016;64(2):S627. doi:10.1016/S0168-8278(16)01165-X
- Park J, Cho H, Choi SJ, Lee GD, Sin SH, Ryu JH, Park HS, Lee H, Kim Y, Oh EJ.** Performance evaluation of the Beckman Coulter DxN VERIS hepatitis B virus (HBV) assay in comparison with the Abbott real time HBV assay. *Ann Lab Med.* 2019;39(1):86–90. doi:10.3343/alm.2019.39.1.86 Medline
- Portilho MM, Baptista ML, da Silva M, de Sousa PSF, Lewis-Ximenez LL, Lampe E, Villar LM.** Usefulness of in-house PCR methods for hepatitis B virus DNA detection. *J Virol Methods.* 2015;223:40–44. doi:10.1016/j.jviromet.2015.07.010 Medline
- Sauné K, Abravanel F, Haslé C, Boineau J, Mengelle C, Izopet J.** Analytical performance of the VERIS MDx system HCV assay for detecting and quantifying HCV RNA. *J Clin Virol.* 2016;84:7–11. doi:10.1016/j.jcv.2016.09.003 Medline
- Singh MP, Galhotra S, Saigal K, Kumar A, Ratho RK.** Quantitative nucleic acid amplification methods and their implications in clinical virology. *Int J Appl Basic Med Res.* 2017;7(1):3–9. doi:10.4103/2229-516X.198498 Medline
- Williams JA, Rodriguez J, Wang Z, Lykstad K, Donvito G, Fung J, Howell C, Colinayo VV, Gustafson E, Scholl T.** Quantitative detection of hepatitis B Virus (HBV) on the VERIS MDx System. In: 24th European Congress of Clinical Microbiology and Infectious Diseases, 10–13 May 2014, Barcelona, Spain. [Internet] [cited 2018 September 14];Poster Presentation:P1422. Available from: https://www.escmid.org/escmid_publications/escmid_elibrary/material/?mid=16949
- Wu B, Xiao F, Li P, Du Y, Lin J, Ming K, Chen B, Lei X, Xu B, Liu D.** Ultrasensitive detection of serum hepatitis B virus by coupling ultrafiltration DNA extraction with real-time PCR. *PLoS One.* 2017; 12(2):e0170290. doi:10.1371/journal.pone.0170290 Medline

ERRATUM

Pol J Microbiol. 2018;67(4):455–461. <https://doi.org/10.21307/pjm-2018-053>
Comparison of the Photosensitivity of Biofilms of Different Genera
of Cariogenic Bacteria in Tooth Slices

HOMA DARMANI¹, KHITAM H. TAWALBEH², AHMAD S. AL-HIYASAT³
AND MOHAMMAD-ALI AL-AKHRAS⁴

¹Department of Applied Biology, Faculty of Faculty of Science and Arts, Jordan University of Science and Technology,
Irbid, Jordan

²Department of Biology, College of Medicine, King Saud bin Abdulaziz University for Health Sciences, Riyadh,
Saudi Arabia

³Department of Restorative Dentistry, Faculty of Dentistry, Jordan University of Science and Technology, Irbid, Jordan

⁴Department of Physics, Faculty of Science and Arts, Jordan University of Science and Technology, Irbid, Jordan

On page 455 there is an error in the affiliation.

The affiliation of Khitam H. Tawalbeh is
Department of Applied Biology, Faculty of Faculty of Science and Arts,
Jordan University of Science and Technology, Irbid, Jordan
and
Department of Biology, College of Medicine, King Saud bin Abdulaziz University
for Health Sciences, Riyadh, Saudi Arabia

Z dużą satysfakcją ogłaszamy zakończenie kolejnego etapu rozwoju naszego kwartalnika. Wraz z początkiem bieżącego roku rozpoczęliśmy współpracę ze zlokalizowanym w Nowym Jorku wydawnictwem Exeley, które będzie publikowało nasze czasopismo na swoim portalu. W tym roku będziemy kontynuować projekt tłumaczenia publikacji na wersje angielskie, ponadto spodziewamy się większej liczby artykułów już napisanych w języku angielskim, w tym od Autorów spoza naszego kraju, w związku z czym w dalszym ciągu powiększamy kolegium redakcyjne naszego kwartalnika.

Mamy dużą przyjemność przedstawić nowych członków Redakcji. W pierwszym kwartale bieżącego roku otworzyliśmy dział mikrobiologia molekularna, tworzony przez dwie specjalistki w dziedzinie: dr hab. Adriannę Raczkowską z Uniwersytetu Warszawskiego oraz dr Bożenę Nejman-Faleńczyk z Uniwersytetu Gdańskiego. Do istniejącego już działu biotechnologia dołączyła dr Agnieszka Szczepankowska z Instytutu Biochemii i Biofizyki PAN. Poszerzony został również dział mikrobiologia środowiskowa o redaktor z Uniwersytetu Warszawskiego – prof. Renatę Matlakowską. Dużym zainteresowaniem wśród naszych Czytelników i Autorów cieszą się prace z zakresu mikrobiologii medycznej. Dlatego też utworzyliśmy dział poświęcony tej specjalności, do którego dołączył w tym roku dr hab. n. med. Aleksander Deptuła z Uniwersytetu Mikołaja Kopernika w Toruniu. Obecnie szukamy kandydata na jeszcze jednego redaktora do tego działu, zachęcamy do nadsyłania zgłoszeń do Redakcji. Więcej informacji o aktualnym składzie kolegium redakcyjnego znajdują Państwo w zakładce REDAKCJA na naszej stronie internetowej.



INFORMACJE Z POLSKIEGO TOWARZYSTWA MIKROBIOLOGÓW

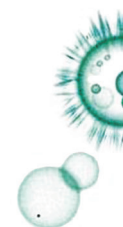
KONFERENCJA POD PATRONATEM PTM



**Konferencja międzynarodowa:
8 Międzynarodowa Konferencja Weiglowska
Łódź, 26–28.06.2019**



**8th International Weigl Conference:
HUMAN WELFARE, CANCERS, SYSTEMIC AND INFECTIOUS DISEASES**
Microorganisms in industrial and medical biotechnology
26-28.06.2019 Venue: Faculty of Management, University of Lodz



**Konferencja organizowana jest przez Instytut Biologii Medycznej PAN,
Uniwersytet Łódzki oraz Uniwersytet Medyczny w Łodzi**

The planned Conference is the eighth conference to commemorate the outstanding Polish microbiologist Prof. Rudolf Weigl, the creator of the first effective vaccine against typhus. The conference is devoted to selected medical, microbiological and biotechnology issues. As part of the conference, thematic sessions will be devoted to (i) gastrointestinal diseases of various etiologies, (ii) skin diseases, (iii) and ophthalmologic cancerous and autoimmune diseases. In addition, there will be (iv) a molecular microbiology session focused on recent developments in microbial virulence, cell metabolism, signal transduction, bacterial biofilm studies and single cell analyzes. The last session (v) will be dedicated to microorganisms in industrial and medical biotechnology. The conference will be a unique platform for meetings and discussions for researchers dealing with the molecular basis of selected diseases, for microbiologists investigating these processes at the level of virulence factor, but also for clinicians involved in everyday diagnostics and treatment of diseases. The conference will also create a unique opportunity to familiarize participants of the session, including students and doctoral students, with different perspectives of research on the same processes, from the human body to pathogenic or saprophytic microorganisms and their mutual interactions.

<http://grupamedica.pl/8th-international-weigl-conference-26-28-06-2019/>
www.twitter/grupamedica; <https://web.facebook.com/8thweiglconferene/>

KONFERENCJA POD PATRONATEM PTM**VII Konferencja Ogólnopolska:
Mikrobiologia Farmaceutyczna 2019
Gdańsk, 22–24 maja 2019 r.**

Konferencja jest kontynuacją rozpoczętego w 2009 roku cyklu spotkań naukowo szkoleniowych, którego celem jest stworzenie Forum Specjalistów zainteresowanych mikrobiologią farmaceutyczną, służącego wymianie wiedzy, poglądów i doświadczeń w obszarach oceny i zapewnienia jakości, badań mikrobiologicznych oraz bezpieczeństwa mikrobiologicznego produktów leczniczych.

Na spotkaniach dążymy do inicjowania szeroko pojętej współpracy między mikrobiologami pracującymi głównie w przemyśle farmaceutycznym, ale też w spożywczym i kosmetycznym.

Patronat Polskiego Towarzystwa Mikrobiologicznego jest dla nas bardzo ważny, to PTM jest organizacją umożliwiającą współpracę, rozwój i kreowanie nowych rozwiązań w dziedzinie Mikrobiologii, a utworzenie sekcji Mikrobiologii Farmaceutycznej umożliwi ciągłe współdziałanie i rozwój Członków.

Podczas naszych konferencji promujemy przynależność do PTM i członkowie PTM już od poprzedniej VI konferencji Mikrobiologia Farmaceutyczna mają zniżkę 100 zł w opłacie konferencyjnej. W konferencjach bierze udział zwykle 80–100 osób z przedsiębiorstw farmaceutycznych, laboratoriów kontrolnych i uczelni.

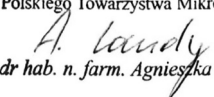
Kontakt do Organizatora:

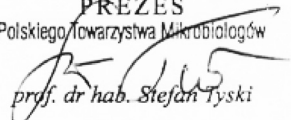
TRANSpharmacia, Pani Barbara Kawałko-Myślińska,
barbara.myslinska@transpharmacia.pl, ul. Bacewiczówny 2/42, 02-786 Warszawa

Poniżej w punktach, w formie skrótowej przedstawiono omawiane sprawy na wirtualnych zebraniach Prezydium ZG PTM oraz spotkaniach z udziałem członków Prezydium.

1. W dniu 10.12.2018 odbyło się kolejne posiedzenie Konferencji Prezesów Towarzystw Lekarskich, w którym wzięli udział przedstawiciele 34 Towarzystw. Polskie Towarzystwo Mikrobiologów reprezentowała Pani prof. dr hab. Ewa Augustynowicz-Kopeć – Wiceprezes PTM. Podczas posiedzenia omówiono następujące punkty:
 - a) Informacja o bieżących pracach w zakresie kształcenia podyplomowego lekarzy – DNiSW MZ oraz Komisja Kształcenia NRL
 - b) Informacja Polskiego Towarzystwa Stomatologicznego o szkoleniach z zakresu umiejętności społecznych oraz propozycje działań, które KPTL mogłaby podjąć
 - c) Propozycja kompleksowego systemu edukacji w zakresie radiologii-diagnostyki obrazowej – Polskie Lekarskie Towarzystwo Radiologiczne
 - d) Wytyczne Polskiego Towarzystwa Bioetycznego dotyczące 7 zagadnień związanych z opracowywaniem i stosowaniem wytycznych postępowania w praktyce medycznej. Dotyczą one adresatów wytycznych, statusu prawnego tych opracowań, zagadnień etycznych, dowodów naukowych na których się opierają, siły formułowanych zaleceń, stosunku do wartości uznawanych przez pacjentów, realiów ekonomicznych.
 - e) Wypalenie zawodowe lekarzy – Polskie Towarzystwo Nefrologiczne przedstawiło wyniki przeprowadzonych wśród nefrologów badań wypalenia zawodowego. Wskazują one, że jest to częsty problem i celowe jest przeprowadzenie badań także wśród innych specjalności.
 - f) Apel w sprawie szczepień – Polskie Towarzystwo Immunologii Doświadczalnej i Klinicznej, przedstawiono apel przyjęty przez Komitet Immunologii i Etiologii Zakażeń Człowieka Polskiej Akademii Nauk oraz Polskie Towarzystwo Immunologii Doświadczalnej i Klinicznej. Pomimo odrzucenia projektu ustawy antyszczepionkowej problem jest nadal aktualny. W Polsce w 2018 roku można spodziewać się nawet około 70000 odmów szczepień i już w 2017 roku nie udało się osiągnąć zalecanego progu 95% wyszczepialności.
 - g) Propozycja stanowiska Polskiego Towarzystwa Medycyny i Techniki Hiperbarycznej w sprawie leczenia tlenem hiperbarycznym i ograniczonej liczby specjalistów, którzy mogą stosować tę terapię w ramach finansowania przez NFZ.
 - h) Informacje o obowiązkach Towarzystw Naukowych wynikających z RODO.
2. Dnia 2 stycznia 2019 r. PTM podpisało trzy letnią umowę z firmą Exeley Inc. w sprawie świadczenia usług wydawniczych dla kwartalnika Postępy Mikrobiologii. Celem jest podniesienie znaczenia czasopisma na światowym rynku czasopism naukowych, pozyskanie czytelników i autorów tekstów w języku angielskim, zwiększenie cytowalności i współczynnika IF. Począwszy od numeru 3/2018 wersja *on-line* zeszytów Postępy Mikrobiologii ukazuje się także w języku angielskim. Teksty tłumaczone są przez pracowników biura tłumaczy z wykorzystaniem środków finansowych uzyskanych z MNiSW na działalność upowszechniającą naukę. Dofinansowane jest także tłumaczenie artykułów w 2019 roku.

3. Na początku stycznia 2019 r. rozpoczęto procedurę przypominania o obowiązku zapłacenia składki członkowskiej PTM za 2018 r. Jeżeli, pomimo dwukrotnego przypomnienia składka nie zostanie wniesiona do końca lutego 2019 r., na zebraniu Zarządu Głównego PTM w marcu 2019 r., zgodnie ze Statutem PTM, osoby bez opłaconej składki za 2018 r. zostaną wykluczone z Towarzystwa.
4. Uregulowaliśmy składki PTM do FEMS (5.455,42 zł) oraz IUMS (4.074,17 zł). Wysokość składek uzależniona jest od liczby członków PTM, dlatego bardzo rygorystycznie podchodzimy do sprawy nieuregulowanych zaległych składek członkowskich.
5. Kancelaria prawna, na wniosek Prezydium PTM i Redakcji czasopism PM i PJM, skierowała do sądu wnioski o uaktualnienie danych dotyczących czasopism PTM znajdujących się w rejestrze sądowym. Tym samym zostały wypełnione wieloletnie zaniedbania w tym obszarze.
6. W dniu 09.01.2019 r. pożegnaliśmy na Cmentarzu Podgórskim w Krakowie Pana dr Andrzeja Kasprowicza, Członka Honorowego PTM, wieloletniego członka Zarządu Głównego PTM, przez szereg kadencji Przewodniczącego Oddziału Terenowego PTM w Krakowie. Doktor Andrzej Kasprowicz był twórcą znanego krakowskiego ośrodka – Centrum Badań Mikrobiologicznych i Autoszczepionek im. dr Jana Bobra, był również współorganizatorem Krajowej Izby Diagnostów Laboratoryjnych i bardzo zaangażowany w jej działalność.
7. Z końcem roku 2018 przekazano do sekretariatu PTM drugi projekt dotyczący opracowania regulaminu wydatkowania i rozliczania funduszy przyznawanych Oddziałom terenowym PTM w kwocie równoważnej 10% opłat członkowskich wnoszonych przez członków PTM z danego Oddziału. Całościowy projekt przekazywania funduszy do Oddziałów został przygotowany w Prezydium, uzyskał aprobatę biura prawnego i Pani księgowej PTM, zostanie przedstawiony na zebraniu ZG PTM.
8. Prezes PTM otrzymał pismo z dnia 17.01.2019 od Rzecznika Praw Obywatelskich w sprawie uprawnień do wykonywania zawodu diagnosty laboratoryjnego. RPO zwraca się do Ministra Zdrowia z prośbą o rozważenie podjęcia działań ustawodawczych skierowanych na przyznanie absolwentom studiów magisterskich na kierunku mikrobiologia uprawnień diagnosty laboratoryjnego i powiadomienie RPO o stanowisku zajęтым w powyższej sprawie.
9. Otrzymaliśmy niepomyślną wiadomość, że firma SCOPUS z końcem 2018 r. przestaje indeksować kwartalnik Postępy Mikrobiologii, przede wszystkim ze względu na niską cytowalność artykułów, które ponadto są jedynie w języku polskim. W PM ukazuje się tylko ok. 40 artykułów rocznie, kwartalnik zajmuje 132 miejsce na 146 światowych czasopism mikrobiologicznych znajdujących się na liście SJR SCIMAGO (<https://www.scimagojr.com/>). Następną oceną jakości czasopisma przez SCOPUS możliwa jest dopiero za 5 lat. Bez przekształcenia PM w czasopismo międzynarodowe wydawane w języku angielskim z udziałem zagranicznych autorów i recenzentów oraz poprawą cytowalności prac nie poprawi się niekorzystnej oceny jakości czasopisma. PTM jako wydawca PM i PJM od 2 lat czyni intensywne wysiłki organizacyjne, łącznie z nakładami finansowymi, aby podnieść kondycję obu naszych czasopism.
10. Otrzymaliśmy pismo od Przewodniczącego Rady Towarzystw Naukowych przy Prezydium Polskiej Akademii Nauk z prośbą o wskazanie kandydata do tej Rady. W wyniku głosowania członków ZG PTM, wybrano Prezesa PTM prof. dr hab. Stefana Tyskiego jako kandydata PTM do RTN przy Prezydium PAN.
11. Rozpoczęliśmy rozmowy z firmą Global Kongres na temat organizacji XXIX Zjazdu PTM w Warszawie we wrześniu 2020 r.
12. W dniu 19.03.2019 r. odbyło się spotkanie Redaktorów Naczelnych PJM i PTM, Z-cy Red. Nacz. PM, Sekretarza PJM, Prezesa i Sekretarz PTM z Panem Dawidem Cecułą Prezesem wydawnictwa Exeley Inc. Omówiono sprawy i problemy związane z wydawaniem *on-line* czasopisma PJM, rozpoczął się drugi rok współpracy oraz rozpoczęto w 2019 r. wydawanie *on-line* PM przez wydawnictwo Exeley Inc. W przypadku PJM podjęto szereg ustaleń zmierzających do przyspieszenia procesu wydawniczego i zwiększenia widoczności artykułów w internecie. **Podjęto decyzję o zwiększeniu opłat redakcyjnych za publikacje w PJM z 250 USD do 350 USD dla autorów korespondencyjnych – członków PTM i z 500 USD do 700 USD dla autorów korespondencyjnych nie będących członkami PTM. Zwiększona opłata dotyczyć będzie manuskryptów przysyłanych do Redakcji PJM po 30.06.2019 r.** W przypadku PM ustalono nowy tytuł czasopisma (**Advancements of Microbiology**), oraz ustalono sposób zamieszczania artykułów PM na stronie wydawnictwa Exeley. W związku z umiędzynarodowieniem, konieczna jest restrukturyzacja czasopisma PM, zwiększenie liczby zagranicznych recenzentów, członków rady redakcyjnej, pozyskanie zagranicznych manuskryptów prac. Ponadto Redakcja PM zobowiązała się do szybszego i bardziej dynamicznego procesowania manuskryptów. PTM uzyskał z MNiSW fundusze na tłumaczenie na język angielski manuskryptów do PM tylko do końca 2019 r.

SEKRETARZ
Polskiego Towarzystwa Mikrobiologów

dr hab. n. farm. Agnieszka E. Laudy

PREZES
Polskiego Towarzystwa Mikrobiologów

prof. dr hab. Stefan Tyski

CZŁONKOWIE WSPIERAJĄCY PTM

Członek Wspierający PTM – Złoty
od 27.03.2017 r.



HCS Europe – Hygiene & Cleaning Solutions
ul. Warszawska 9a, 32-086 Węgrzce k. Krakowa
tel. (12) 414 00 60, 506 184 673, fax (12) 414 00 66
www.hcseurope.pl

Firma projektuje profesjonalne systemy utrzymania czystości i higieny dla klientów o szczególnych wymaganiach higienicznych, m.in. kompleksowe systemy mycia, dezynfekcji, osuszania rąk dla pracowników służby zdrowia, preparaty do dezynfekcji powierzchni dla służby zdrowia, systemy sterylizacji narzędzi.

Członek Wspierający PTM – Srebrny
od 12.09.2017 r.



Firma Ecolab Sp. z o.o. zapewnia: najlepszą ochronę środowiska pracy przed patogenami powodującymi zakażenia podczas leczenia pacjentów, bezpieczeństwo i wygodę personelu, funkcjonalność posiadanego sprzętu i urządzeń. Firma jest partnerem dla przemysłów farmaceutycznego, biotechnologicznego i kosmetycznego.

Członek Wspierający PTM – Srebrny
od 12.12.2017 r.



Od ponad 100 lat siedziba Wodociągów Krakowskich mieści się przy ul. Senatorskiej. Budowę obiektu ukończono w 1913 roku. W 2016 r. do sieci wodociągowej wtłoczono ponad 56 mln m³ wody. Szacuje się, że ponad 99,5% mieszkańców Gminy Miejskiej Kraków posiada możliwość korzystania z istniejącej sieci wodociągowej.

Członek Wspierający PTM – Zwyczajny
od 12.09.2017 r.



Merck Sp. z o.o. jest częścią międzynarodowej grupy Merck KGaA z siedzibą w Darmstadt, Niemcy i dostarcza na rynek polski od roku 1992 wysokiej jakości produkty farmaceutyczne i chemiczne, w tym podłoża mikrobiologiczne.